Behavioural Neurology

Early Detection of Stroke-Initiated Behavioral Disorder

Lead Guest Editor: Hong Lin
Guest Editors: Kamalanand Krishnamurthy and Suresh Chandra Satapathy

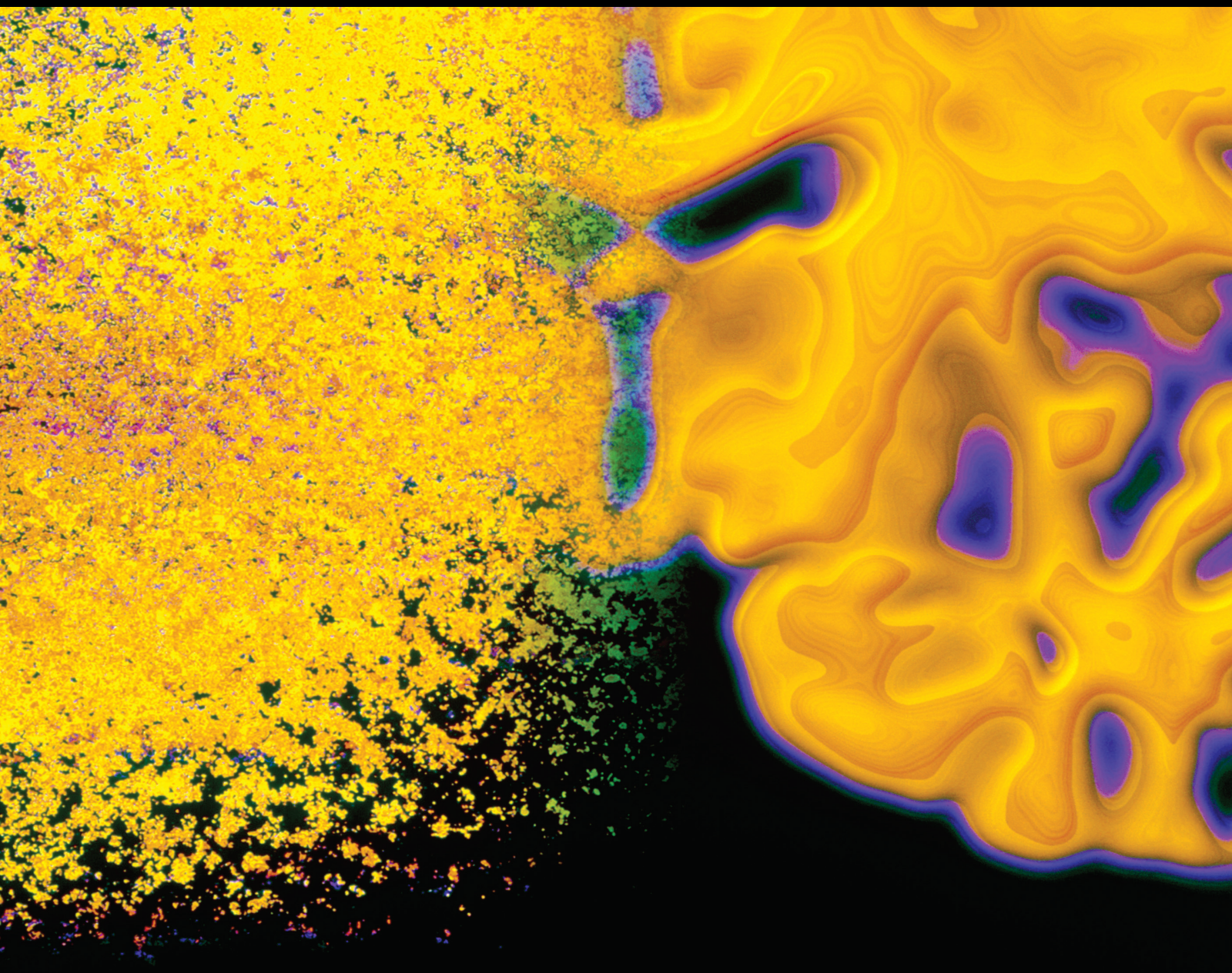

Early Detection of Stroke-Initiated Behavioral Disorder

Behavioural Neurology

Early Detection of Stroke-Initiated Behavioral Disorder

Lead Guest Editor: Hong Lin
Guest Editors: Kamalanand Krishnamurthy and Suresh Chandra Satapathy

Contents

[Retracted] Multimodal Medical Image Fusion of Positron Emission Tomography and Magnetic Resonance Imaging Using Generative Adversarial Networks
R. Nandhini Abirami, P. M. Durai Raj Vincent, Kathiravan Srinivasan, K. Suresh Manic, and Chuan-Yu Chang
Research Article (12 pages), Article ID 6878783, Volume 2022 (2022)

[Retracted] Early Stroke Prediction Methods for Prevention of Strokes
Mandeep Kaur, Sachin R. Sakhare, Kirti Wanjale, and Farzana Akter
Research Article (9 pages), Article ID 7725597, Volume 2022 (2022)

[Retracted] Classification of Myopathy and Amyotrophic Lateral Sclerosis Electromyograms Using Bat Algorithm and Deep Neural Networks
A. Bakiya, A. Anitha, T. Sridevi, and K. Kamalanand
Research Article (9 pages), Article ID 3517872, Volume 2022 (2022)

[Retracted] The Impact of Online Learning System on Students Affected with Stroke Disease
Sobia Wassan, Chen Xi, Tian Shen, Kamal Gulati, Kinza Ibraheem, and Rana M. Amir Latif Rajpoot
Research Article (14 pages), Article ID 4847066, Volume 2022 (2022)

[Retracted] Customer Experience towards the Product during a Coronavirus Outbreak
Sobia Wassan, Tian Shen, Chen Xi, Kamal Gulati, Danish Vasan, and Beenish Suhail
Research Article (18 pages), Article ID 4279346, Volume 2022 (2022)

[Retracted] A Rapid Artificial Intelligence-Based Computer-Aided Diagnosis System for COVID-19 Classification from CT Images
Hassaan Haider Syed, Muhammad Attique Khan, Usman Tariq, Ammar Armghan, Fayadh Alenezi, Junaid Ali Khan, Seungmin Rho, Seifedine Kadry, and Venkatesan Rajinikanth
Research Article (13 pages), Article ID 2560388, Volume 2021 (2021)

[Retracted] Ensemble Classification Approach for Sarcasm Detection
Jyoti Godara, Isha Batra, Rajni Aron, and Mohammad Shabaz
Research Article (13 pages), Article ID 9731519, Volume 2021 (2021)

[Retracted] Transcranial Electrical Motor Evoked Potential in Predicting Positive Functional Outcome of Patients after Decompressive Spine Surgery: Review on Challenges and Recommendations towards Objective Interpretation
Mohd Redzuan Jamaludin, Khin Wee Lai, Joon Huang Chuah, Muhammad Afiq Zaki, Yan Chai Hum, Yee Kai Tee, Maheza Irna Mohd Salim, and Lim Beng Saw
Review Article (16 pages), Article ID 2684855, Volume 2021 (2021)

Patient Behavioral Analysis with Smart Healthcare and IoT
Anurag Tiwari, Viney Dhiman, Mohamed A. M. Iesa, Haider Alsarhan, Abolfazl Mehbodniya, and Mohammad Shabaz
Research Article (9 pages), Article ID 4028761, Volume 2021 (2021)

Hindawi
Behavioural Neurology
Volume 2023, Article ID 9893564, 1 page
https://doi.org/10.1155/2023/9893564

Retraction

Retracted: Multimodal Medical Image Fusion of Positron Emission Tomography and Magnetic Resonance Imaging Using Generative Adversarial Networks

Behavioural Neurology

Received 19 December 2023; Accepted 19 December 2023; Published 20 December 2023

This article has been retracted by Hindawi following an investigation undertaken by the publisher [1]. This investigation has uncovered evidence of one or more of the following indicators of systematic manipulation of the publication process:

(1) Discrepancies in scope

(2) Discrepancies in the description of the research reported

(3) Discrepancies between the availability of data and the research described

(4) Inappropriate citations

(5) Incoherent, meaningless and/or irrelevant content included in the article

(6) Manipulated or compromised peer review

The presence of these indicators undermines our confidence in the integrity of the article's content and we cannot, therefore, vouch for its reliability. Please note that this notice is intended solely to alert readers that the content of this article is unreliable. We have not investigated whether authors were aware of or involved in the systematic manipulation of the publication process.

Wiley and Hindawi regrets that the usual quality checks did not identify these issues before publication and have since put additional measures in place to safeguard research integrity.

We wish to credit our own Research Integrity and Research Publishing teams and anonymous and named external researchers and research integrity experts for contributing to this investigation.

The corresponding author, as the representative of all authors, has been given the opportunity to register their agreement or disagreement to this retraction. We have kept a record of any response received.

References

[1] R. Nandhini Abirami, P. M. Durai Raj Vincent, K. Srinivasan, K. S. Manic, and C. Y. Chang, "Multimodal Medical Image Fusion of Positron Emission Tomography and Magnetic Resonance Imaging Using Generative Adversarial Networks," *Behavioural Neurology*, vol. 2022, Article ID 6878783, 12 pages, 2022.

Hindawi
Behavioural Neurology
Volume 2023, Article ID 9879352, 1 page
https://doi.org/10.1155/2023/9879352

Retraction

Retracted: Transcranial Electrical Motor Evoked Potential in Predicting Positive Functional Outcome of Patients after Decompressive Spine Surgery: Review on Challenges and Recommendations towards Objective Interpretation

Behavioural Neurology

Received 19 December 2023; Accepted 19 December 2023; Published 20 December 2023

This article has been retracted by Hindawi following an investigation undertaken by the publisher [1]. This investigation has uncovered evidence of one or more of the following indicators of systematic manipulation of the publication process:

(1) Discrepancies in scope

(2) Discrepancies in the description of the research reported

(3) Discrepancies between the availability of data and the research described

(4) Inappropriate citations

(5) Incoherent, meaningless and/or irrelevant content included in the article

(6) Manipulated or compromised peer review

The presence of these indicators undermines our confidence in the integrity of the article's content and we cannot, therefore, vouch for its reliability. Please note that this notice is intended solely to alert readers that the content of this article is unreliable. We have not investigated whether authors were aware of or involved in the systematic manipulation of the publication process.

In addition, our investigation has also shown that one or more of the following human-subject reporting requirements has not been met in this article: ethical approval by an Institutional Review Board (IRB) committee or equivalent, patient/participant consent to participate, and/or agreement to publish patient/participant details (where relevant).

Wiley and Hindawi regrets that the usual quality checks did not identify these issues before publication and have since put additional measures in place to safeguard research integrity.

We wish to credit our own Research Integrity and Research Publishing teams and anonymous and named external researchers and research integrity experts for contributing to this investigation.

The corresponding author, as the representative of all authors, has been given the opportunity to register their agreement or disagreement to this retraction. We have kept a record of any response received.

References

[1] M. R. Jamaludin, K. W. Lai, J. H. Chuah et al., "Transcranial Electrical Motor Evoked Potential in Predicting Positive Functional Outcome of Patients after Decompressive Spine Surgery: Review on Challenges and Recommendations towards Objective Interpretation," *Behavioural Neurology*, vol. 2021, Article ID 2684855, 16 pages, 2021.

Hindawi
Behavioural Neurology
Volume 2023, Article ID 9784791, 1 page
https://doi.org/10.1155/2023/9784791

Retraction

Retracted: Early Stroke Prediction Methods for Prevention of Strokes

Behavioural Neurology

Received 19 December 2023; Accepted 19 December 2023; Published 20 December 2023

This article has been retracted by Hindawi following an investigation undertaken by the publisher [1]. This investigation has uncovered evidence of one or more of the following indicators of systematic manipulation of the publication process:

(1) Discrepancies in scope

(2) Discrepancies in the description of the research reported

(3) Discrepancies between the availability of data and the research described

(4) Inappropriate citations

(5) Incoherent, meaningless and/or irrelevant content included in the article

(6) Manipulated or compromised peer review

The presence of these indicators undermines our confidence in the integrity of the article's content and we cannot, therefore, vouch for its reliability. Please note that this notice is intended solely to alert readers that the content of this article is unreliable. We have not investigated whether authors were aware of or involved in the systematic manipulation of the publication process.

Wiley and Hindawi regrets that the usual quality checks did not identify these issues before publication and have since put additional measures in place to safeguard research integrity.

We wish to credit our own Research Integrity and Research Publishing teams and anonymous and named external researchers and research integrity experts for contributing to this investigation.

The corresponding author, as the representative of all authors, has been given the opportunity to register their agreement or disagreement to this retraction. We have kept a record of any response received.

References

[1] M. Kaur, S. R. Sakhare, K. Wanjale, and F. Akter, "Early Stroke Prediction Methods for Prevention of Strokes," *Behavioural Neurology*, vol. 2022, Article ID 7725597, 9 pages, 2022.

Hindawi
Behavioural Neurology
Volume 2023, Article ID 9769130, 1 page
https://doi.org/10.1155/2023/9769130

Retraction

Retracted: Classification of Myopathy and Amyotrophic Lateral Sclerosis Electromyograms Using Bat Algorithm and Deep Neural Networks

Behavioural Neurology

Received 19 December 2023; Accepted 19 December 2023; Published 20 December 2023

This article has been retracted by Hindawi following an investigation undertaken by the publisher [1]. This investigation has uncovered evidence of one or more of the following indicators of systematic manipulation of the publication process:

(1) Discrepancies in scope

(2) Discrepancies in the description of the research reported

(3) Discrepancies between the availability of data and the research described

(4) Inappropriate citations

(5) Incoherent, meaningless and/or irrelevant content included in the article

(6) Manipulated or compromised peer review

The presence of these indicators undermines our confidence in the integrity of the article's content and we cannot, therefore, vouch for its reliability. Please note that this notice is intended solely to alert readers that the content of this article is unreliable. We have not investigated whether authors were aware of or involved in the systematic manipulation of the publication process.

Wiley and Hindawi regrets that the usual quality checks did not identify these issues before publication and have since put additional measures in place to safeguard research integrity.

We wish to credit our own Research Integrity and Research Publishing teams and anonymous and named external researchers and research integrity experts for contributing to this investigation.

The corresponding author, as the representative of all authors, has been given the opportunity to register their agreement or disagreement to this retraction. We have kept a record of any response received.

References

[1] A. Bakiya, A. Anitha, T. Sridevi, and K. Kamalanand, "Classification of Myopathy and Amyotrophic Lateral Sclerosis Electromyograms Using Bat Algorithm and Deep Neural Networks," *Behavioural Neurology*, vol. 2022, Article ID 3517872, 9 pages, 2022.

Hindawi
Behavioural Neurology
Volume 2023, Article ID 9842478, 1 page
https://doi.org/10.1155/2023/9842478

Retraction

Retracted: Customer Experience towards the Product during a Coronavirus Outbreak

Behavioural Neurology

Received 8 August 2023; Accepted 8 August 2023; Published 9 August 2023

This article has been retracted by Hindawi following an investigation undertaken by the publisher [1]. This investigation has uncovered evidence of one or more of the following indicators of systematic manipulation of the publication process:

(1) Discrepancies in scope

(2) Discrepancies in the description of the research reported

(3) Discrepancies between the availability of data and the research described

(4) Inappropriate citations

(5) Incoherent, meaningless and/or irrelevant content included in the article

(6) Peer-review manipulation

The presence of these indicators undermines our confidence in the integrity of the article's content and we cannot, therefore, vouch for its reliability. Please note that this notice is intended solely to alert readers that the content of this article is unreliable. We have not investigated whether authors were aware of or involved in the systematic manipulation of the publication process.

Wiley and Hindawi regrets that the usual quality checks did not identify these issues before publication and have since put additional measures in place to safeguard research integrity.

We wish to credit our own Research Integrity and Research Publishing teams and anonymous and named external researchers and research integrity experts for contributing to this investigation.

The corresponding author, as the representative of all authors, has been given the opportunity to register their agreement or disagreement to this retraction. We have kept a record of any response received.

References

[1] S. Wassan, T. Shen, C. Xi, K. Gulati, D. Vasan, and B. Suhail, "Customer Experience towards the Product during a Coronavirus Outbreak," *Behavioural Neurology*, vol. 2022, Article ID 4279346, 18 pages, 2022.

Hindawi
Behavioural Neurology
Volume 2023, Article ID 9820206, 1 page
https://doi.org/10.1155/2023/9820206

Retraction

Retracted: Ensemble Classification Approach for Sarcasm Detection

Behavioural Neurology

Received 8 August 2023; Accepted 8 August 2023; Published 9 August 2023

This article has been retracted by Hindawi following an investigation undertaken by the publisher [1]. This investigation has uncovered evidence of one or more of the following indicators of systematic manipulation of the publication process:

(1) Discrepancies in scope

(2) Discrepancies in the description of the research reported

(3) Discrepancies between the availability of data and the research described

(4) Inappropriate citations

(5) Incoherent, meaningless and/or irrelevant content included in the article

(6) Peer-review manipulation

The presence of these indicators undermines our confidence in the integrity of the article's content and we cannot, therefore, vouch for its reliability. Please note that this notice is intended solely to alert readers that the content of this article is unreliable. We have not investigated whether authors were aware of or involved in the systematic manipulation of the publication process.

Wiley and Hindawi regrets that the usual quality checks did not identify these issues before publication and have since put additional measures in place to safeguard research integrity.

We wish to credit our own Research Integrity and Research Publishing teams and anonymous and named external researchers and research integrity experts for contributing to this investigation.

The corresponding author, as the representative of all authors, has been given the opportunity to register their agreement or disagreement to this retraction. We have kept a record of any response received.

References

[1] J. Godara, I. Batra, R. Aron, and M. Shabaz, "Ensemble Classification Approach for Sarcasm Detection," *Behavioural Neurology*, vol. 2021, Article ID 9731519, 13 pages, 2021.

Hindawi
Behavioural Neurology
Volume 2023, Article ID 9802476, 1 page
https://doi.org/10.1155/2023/9802476

Retraction

Retracted: The Impact of Online Learning System on Students Affected with Stroke Disease

Behavioural Neurology

Received 8 August 2023; Accepted 8 August 2023; Published 9 August 2023

This article has been retracted by Hindawi following an investigation undertaken by the publisher [1]. This investigation has uncovered evidence of one or more of the following indicators of systematic manipulation of the publication process:

(1) Discrepancies in scope

(2) Discrepancies in the description of the research reported

(3) Discrepancies between the availability of data and the research described

(4) Inappropriate citations

(5) Incoherent, meaningless and/or irrelevant content included in the article

(6) Peer-review manipulation

The presence of these indicators undermines our confidence in the integrity of the article's content and we cannot, therefore, vouch for its reliability. Please note that this notice is intended solely to alert readers that the content of this article is unreliable. We have not investigated whether authors were aware of or involved in the systematic manipulation of the publication process.

In addition, our investigation has also shown that one or more of the following human-subject reporting requirements has not been met in this article: ethical approval by an Institutional Review Board (IRB) committee or equivalent, patient/participant consent to participate, and/or agreement to publish patient/participant details (where relevant).

Wiley and Hindawi regrets that the usual quality checks did not identify these issues before publication and have since put additional measures in place to safeguard research integrity.

We wish to credit our own Research Integrity and Research Publishing teams and anonymous and named external researchers and research integrity experts for contributing to this investigation.

The corresponding author, as the representative of all authors, has been given the opportunity to register their agreement or disagreement to this retraction. We have kept a record of any response received.

References

[1] S. Wassan, C. Xi, T. Shen, K. Gulati, K. Ibraheem, and R. M. Amir Latif Rajpoot, "The Impact of Online Learning System on Students Affected with Stroke Disease," *Behavioural Neurology*, vol. 2022, Article ID 4847066, 14 pages, 2022.

Hindawi
Behavioural Neurology
Volume 2023, Article ID 9878720, 1 page
https://doi.org/10.1155/2023/9878720

Retraction

Retracted: Effects of Acupuncture and Rehabilitation Training on Limb Movement and Living Ability of Patients with Hemiplegia after Stroke

Behavioural Neurology

Received 8 August 2023; Accepted 8 August 2023; Published 9 August 2023

This article has been retracted by Hindawi following an investigation undertaken by the publisher [1]. This investigation has uncovered evidence of one or more of the following indicators of systematic manipulation of the publication process:

(1) Discrepancies in scope

(2) Discrepancies in the description of the research reported

(3) Discrepancies between the availability of data and the research described

(4) Inappropriate citations

(5) Incoherent, meaningless and/or irrelevant content included in the article

(6) Peer-review manipulation

The presence of these indicators undermines our confidence in the integrity of the article's content and we cannot, therefore, vouch for its reliability. Please note that this notice is intended solely to alert readers that the content of this article is unreliable. We have not investigated whether authors were aware of or involved in the systematic manipulation of the publication process.

In addition, our investigation has also shown that one or more of the following human-subject reporting requirements has not been met in this article: ethical approval by an Institutional Review Board (IRB) committee or equivalent, patient/participant consent to participate, and/or agreement to publish patient/participant details (where relevant).

Wiley and Hindawi regrets that the usual quality checks did not identify these issues before publication and have since put additional measures in place to safeguard research integrity.

We wish to credit our own Research Integrity and Research Publishing teams and anonymous and named external researchers and research integrity experts for contributing to this investigation.

The corresponding author, as the representative of all authors, has been given the opportunity to register their agreement or disagreement to this retraction. We have kept a record of any response received.

References

[1] J. Zhang, Y. Mu, and Y. Zhang, "Effects of Acupuncture and Rehabilitation Training on Limb Movement and Living Ability of Patients with Hemiplegia after Stroke," *Behavioural Neurology*, vol. 2022, Article ID 2032093, 10 pages, 2022.

Hindawi
Behavioural Neurology
Volume 2023, Article ID 9876194, 1 page
https://doi.org/10.1155/2023/9876194

Retraction

Retracted: A Rapid Artificial Intelligence-Based Computer-Aided Diagnosis System for COVID-19 Classification from CT Images

Behavioural Neurology

Received 8 August 2023; Accepted 8 August 2023; Published 9 August 2023

This article has been retracted by Hindawi following an investigation undertaken by the publisher [1]. This investigation has uncovered evidence of one or more of the following indicators of systematic manipulation of the publication process:

(1) Discrepancies in scope

(2) Discrepancies in the description of the research reported

(3) Discrepancies between the availability of data and the research described

(4) Inappropriate citations

(5) Incoherent, meaningless and/or irrelevant content included in the article

(6) Peer-review manipulation

The presence of these indicators undermines our confidence in the integrity of the article's content and we cannot, therefore, vouch for its reliability. Please note that this notice is intended solely to alert readers that the content of this article is unreliable. We have not investigated whether authors were aware of or involved in the systematic manipulation of the publication process.

In addition, our investigation has also shown that one or more of the following human-subject reporting requirements has not been met in this article: ethical approval by an Institutional Review Board (IRB) committee or equivalent, patient/participant consent to participate, and/or agreement to publish patient/participant details (where relevant).

Wiley and Hindawi regrets that the usual quality checks did not identify these issues before publication and have since put additional measures in place to safeguard research integrity.

We wish to credit our own Research Integrity and Research Publishing teams and anonymous and named external researchers and research integrity experts for contributing to this investigation.

The corresponding author, as the representative of all authors, has been given the opportunity to register their agreement or disagreement to this retraction. We have kept a record of any response received.

References

[1] H. H. Syed, M. A. Khan, U. Tariq et al., "A Rapid Artificial Intelligence-Based Computer-Aided Diagnosis System for COVID-19 Classification from CT Images," *Behavioural Neurology*, vol. 2021, Article ID 2560388, 13 pages, 2021.

Hindawi
Behavioural Neurology
Volume 2023, Article ID 9878720, 1 page
https://doi.org/10.1155/2023/9878720

Retraction

Retracted: Effects of Acupuncture and Rehabilitation Training on Limb Movement and Living Ability of Patients with Hemiplegia after Stroke

Behavioural Neurology

Received 8 August 2023; Accepted 8 August 2023; Published 9 August 2023

This article has been retracted by Hindawi following an investigation undertaken by the publisher [1]. This investigation has uncovered evidence of one or more of the following indicators of systematic manipulation of the publication process:

(1) Discrepancies in scope

(2) Discrepancies in the description of the research reported

(3) Discrepancies between the availability of data and the research described

(4) Inappropriate citations

(5) Incoherent, meaningless and/or irrelevant content included in the article

(6) Peer-review manipulation

The presence of these indicators undermines our confidence in the integrity of the article's content and we cannot, therefore, vouch for its reliability. Please note that this notice is intended solely to alert readers that the content of this article is unreliable. We have not investigated whether authors were aware of or involved in the systematic manipulation of the publication process.

In addition, our investigation has also shown that one or more of the following human-subject reporting requirements has not been met in this article: ethical approval by an Institutional Review Board (IRB) committee or equivalent, patient/participant consent to participate, and/or agreement to publish patient/participant details (where relevant).

Wiley and Hindawi regrets that the usual quality checks did not identify these issues before publication and have since put additional measures in place to safeguard research integrity.

We wish to credit our own Research Integrity and Research Publishing teams and anonymous and named external researchers and research integrity experts for contributing to this investigation.

The corresponding author, as the representative of all authors, has been given the opportunity to register their agreement or disagreement to this retraction. We have kept a record of any response received.

References

[1] J. Zhang, Y. Mu, and Y. Zhang, "Effects of Acupuncture and Rehabilitation Training on Limb Movement and Living Ability of Patients with Hemiplegia after Stroke," *Behavioural Neurology*, vol. 2022, Article ID 2032093, 10 pages, 2022.

Hindawi
Behavioural Neurology
Volume 2022, Article ID 2032093, 10 pages
https://doi.org/10.1155/2022/2032093

Research Article

Effects of Acupuncture and Rehabilitation Training on Limb Movement and Living Ability of Patients with Hemiplegia after Stroke

Juhua Zhang, Yingmei Mu, and Yunxia Zhang

Neurosurgery, Shandong Yuhuangding Hospital, Yantai, 264000 Shandong, China

Correspondence should be addressed to Yunxia Zhang; 2011010111@st.btbu.edu.cn

Received 20 November 2021; Accepted 14 March 2022; Published 26 April 2022

Academic Editor: Kamalanand Krishnamurthy

Stroke is a disease with a high disability rate, having a serious impact on that patient's working and daily survival quality and bringing economic burden to the family and society. Patients with stroke hemiplegia are mostly tetraplegic and have difficulty regulating their balance, and their long-term symmetry has been destroyed. The application in the rehabilitation process of acupuncture in patients with hemorrhagic stroke may produce unexpected effects. It is very effective to study the effect of acupuncture combined with rehabilitation training on limb movement and patient survival. It is very helpful in improving normal motor function and normal life, increasing joint mobility and muscle strength, and reducing muscle tension. In this paper, it is found that the observational group has a complication rate of 2.13%, in contrast to 17.02% as in the group of control, and the pin-prick combined with a rehabilitative training makes a significant improvement to the patients. This study provides suggestions for the study to investigate acupuncture combined with recovery exercise on limb movement and living capacities of people with stroke paraparesis.

1. Introduction

Acupuncture is a rehabilitation treatment for acute cerebrovascular diseases in recent years. It achieves the goal of "Internal Diseases and External Treatments," by stimulating the meridian, promoting blood circulation and eliminating veins in the blood, and fully providing local and comprehensive treatment. At present, scalp acupuncture and hemispherical acupuncture are common in clinical treatment. Traditional Chinese medical theory believes that the head is where the IQ and the meridian merge. Through scalp acupuncture, IQ is adjusted to improve local microcirculation and increase brain blood. Cerebral edema flow and relief using different acupuncture points and different stimulating forces can lead to brain cell stimulation or inhibition of two-way regulation, stimulating the central dynamic nervous system, improving the signal input to the dynamic area of the cerebral cortex, and thereby promoting recovery.

Because the central nervous system is damaged, the patient's dynamic function is also reduced. If the patient does not receive systematic rehabilitation training, it will have serious consequences, which will greatly reduce the quality of life and put more burden on the patient's family. According to related research, when the central nervous cells of the human body are damaged, their adjacent brain cells are stimulated, and a part of their damaged nerve functions is distinguished and compensated. Control patients benefited from standard therapy only, with associated medications to restore neurological function in the patients. In contrast, it was found that acupuncture integrated with rehabilitation traveled far and above conventional therapy.

The Hachisuka A. et al. study found that pituitary stroke is usually the result of a hemorrhagic infarction of pituitary adenomas. Clinical manifestations are diverse, including asymptomatic cases, typical pituitary stroke, and even sudden death. Cerebral ischemia caused by pituitary stroke is very rare. It may be caused by vasospasm or tumor directly compressing the cerebral blood vessels [1]. The Satyarthee and Sharma study found the diagnostic value of DD and coagulation indicators for stroke, providing clinical basis

for diagnosis (40 cases) and hemorrhagic stroke group (observation group 2, 20 cases), using a coagulometer to detect DD, PT, APTT, FIB, and AT-III. The results of Satyarthee and Sharma showed significantly higher levels of DD and FIB compared to the development of the controlled group ($p < 0.01$). In the observation subjects 1 and 2, the levels were significantly higher, APTT was significantly prolonged, and AT-III was significantly lower, with striking statistically significant differences ($p < 0.05$). Detecting indicators 1 and 2 were not significantly different ($p < 0.05$), and APTT and FIB were positively correlated with stroke ($r = 0.422$, 0.138, 0.171, p 0.05) [2].

Acquisitions of comorbid rehabilitation training combined with acupuncture can often have unexpected effects on limb movements and life skills in stroke patients with hemiplegia. In this paper, 94 stroke patients admitted from December 2019 to January 2020 were selected and compared with the reference. The rehabilitation status of the two groups of patients who received "acupuncture incorporating rehabilitation training and no acupuncture combing training" was observed. A better recovery effect with the combination of acupuncture and moxibustion training was observed than that without the combination of needle and moxibustion training. However, these studies still need to be more improved in experiments, especially to pay attention to the innovation of experimental methods.

2. Proposed Method

2.1. Acupuncture. It is the general term for acupuncture and exercise. With guidance from Chinese medical theory, moxibustion refers to the insertion of needles (often called pins) into a specific angle into a patient's torso. Particular areas will be stimulated to achieve a disease treatment goal. This puncture point is known as a point on the body and is called an acupuncture point. The most current acupuncture manual numbers 361 acupuncture spots throughout the entire body. It is done by rubbing or kneading, fumigation, ironing, and the application of heat stimulation to a "point" on the upper surface of the body to prevent and treat disease. There are also other methods such as moxibustion, moxibustion, core moxibustion, and mature moxibustion. In addition, there are other methods such a moxibustion, osier moxibustion, core moxibustion, and mature moxibustion. It includes "moxibustion" and "moxibustion with medicine," as an important part of Oriental medicine, including acupuncture theory, the points, acupuncture techniques, and related equipment. During its formation, application, and preparation, the unique Chinese culture and regional characteristics are the result of the valuable heritage of Chinese cultural and social traditions, and in 2006, the school of Chinese medicine announced with the State Council that acupuncture was included in the first inscription of national intake of intangible cultural property [3, 4]. Therefore, there is also more and more clinical research on acupuncture.

In China, acupuncture can be used as a unique treatment for diseases. It is a medicine for internal and external treatment. Which is accomplished by guiding meridians and acupoints and applying certain methods to treat systemic diseases. Acupuncture is used to diagnose the causes of TCM and identify the methods that belong to nature, meridians, and injured organs according to the TCM practice and confirmed as belonging to the TCM category. Discussions are followed by respective prescriptions for acute treatment. Through the channeling of meridians and the regulation of hemoplasm, the functions of yin and yang are rendered relatively balanced for the preventing of diseases. It is part of the ancestral medical heritage and a unique and ethnic Chinese medical approach. Over the centuries, it has made outstanding contributions to the protection of national well-being and reproduction. It remains his task up until now and has won the popular trust [5].

The function of the meridian is to keep the meridian unblocked and exercise its normal physiological functions. This is the most basic and direct treatment method of acupuncture [6]. The meridian is the internal organs of the viscera and external limbs, and Qi and blood surgery are one of its main physiological functions. The meridian is not connected, the blood is not connected, and the clinical manifestations are pain, deafness, swelling, eczema, and other symptoms. Acupuncture chooses appropriate acupuncture methods and triangle needles to keep the meridians free and qi and blood normal [7].

2.2. Stroke Rehabilitation Training

2.2.1. Guidance on Training Essentials

(1) Provide good psychological care for patients and their families: patients and their families should be patiently informed about the purpose, methods, effects, and training of medical physical rehabilitation before rehabilitation training. Rehabilitation cannot be replaced by drugs. Only through early training can the remaining functions be restored in accordance with the "progressive" rehabilitation training plan and cannot be rushed. Only with the active participation of patients and the strong support of family members can rehabilitation training be successfully completed [2, 8, 9]

(2) Maintain the correct position of good limbs: good limbs are not the same as functional limbs. This is a temporary location, designed from a therapeutic perspective. Most of the affected limbs in the acute phase of hemiplegia are now relaxed. Not only can it not move, but it can also lead to subluxation of the joints and damage to the soft tissues around the joints and even contracture due to abnormal posture for a long time. Good limb placement can play a role in inhibiting spasm patterns, preventing shoulder bruises and early separation movements. Play is an important measure to prevent many complications and improve rehabilitation [10, 11]

2.2.2. Training Method

(1) Posterior method: place your head on the pillow, tilt it slightly to the healthy side, refer to the affected

side, the height of the pillow should be sufficient, and the thoracic spine should not be bent. Place a cushion below the patient's hip to move the affected pelvis forward to prevent hip flexion and external rotation. Place a small pillow under the patient's shoulder joint to push the scapula forward. Stretch your upper elbows on your pillow, and stretch your wrists backwards and your fingers. Place a sandbag on the outside of the thigh and the middle of the thigh to prevent hip dislocation and external rotation and a small pillow in the sleeping area to prevent knee joint extension

(2) The lateral position below the affected side: the affected side's shoulder belt stretches forward, shoulder reflexes, elbows straight, wrists straight, and fingers straight. The affected limb is straightened, and the knee joint is slightly bent. The hips and knees of the lower limbs on the healthy side are bent, and a cushion is placed below to prevent the affected lower limbs from being squeezed together. A pillow is pressed against the back, and the upper body can be leaned on to obtain a relaxed posture [12, 13]

(3) Above the affected side: the upper limb of the affected side is extended forward, and the shoulder joint is bent about 90 degrees. The floor is supported by cushions, and the healthy upper limbs can be placed freely. Hip and knee joints of the affected lower limbs are bent and placed on a cushion. The left hip is stretched, the knees are slightly bent, and the back is pressed against the pillow to relax the trunk. In order to prevent joint contraction and to maintain pressure in a specific position for too long, you must change the position in time according to the situation and generally reverse it every two hours. When changing positions, special care should be taken to protect the shoulder joints and do not pull the affected joints to prevent shoulder injuries [14–16]

2.2.3. Problems to Pay Attention to during Training

(1) Avoid intravenous amputation where possible: some patients and family members believe that the affected limb will not move this way, or that it is an intravenous infusion. I do not know that a healthy limb is free, but it does bring the repair of a damaged limb. Side effect. Due to insufficient blood return of the affected limb, coupled with sweating and limited movement, it is easy to cause hand swelling and tissue adhesion, increase the risk of shoulder-hand syndrome, and provide guidance and cooperation for rehabilitation nursing staff to facilitate patient limb repair [17, 18]

(2) Academic practice should be avoided in limb rehabilitation training: limb paralysis is a common symptom of stroke patients, and joint training for the ability of amputated limbs is an important rehabilitation measure. The principle is to train in pain, and rehabilitation nurses must have stable knowledge in various fields such as neuroscience, anatomy, psychology, and medicine. Restore. On this basis, they should be processed manually to prevent rough handling. For patients with pain, you can take hot packs or painkillers before training to avoid shoulder dislocation, shoulder joint syndrome, and epilepsy during exercise; exercise should be slow and rhythmic, and the patient should be clearly explained before training. The purpose, content, function, and correct action items of the action inform the patient of the active part, direction, and regular muscles, and then, slowly perform passive activities 2-3 times so that the patient can feel the movement and gradually decrease in this case. Auxiliary active exercise volume [19, 20]

(3) Pay attention to the scale and intensity of training during physical rehabilitation: patients often feel anxious when freely moving. Excessive exercise can cause modern compensatory exercise or pain and fatigue, which increases spasm and affects exercise results. Rehabilitation nurses should explain to patients and their families different training methods used at different rehabilitation stages, as well as monitor the general situation of patients, follow small- and long-term nursing principles, and gradually increase education, that is, to complete the total training and avoid the negative effects of overtraining from overtraining. Each time you train an action, you must maintain a precise attitude and focus your brain's thoughts on this action and the main part of your training body to "control" this behavior of the brain. Power is always a passive activity and cannot achieve the purpose of education. Training the passive activity in one's own active action is the real problem of training [21, 22]

(4) Attention to the systemic and follow-up of rehabilitation training: to achieve a good training effect and in order to achieve the expected purpose of restoring physical function, it is necessary to carry out serious training at the prescribed time in accordance with the established plan. Classes and holidays should be avoided. Interrupted training is interrupted because the trainee cannot experience specific repetitive stimuli, cannot produce adaptive responses, and has no value to avoid focusing on any training. Although these sections ignore other sections, they must fully consider different joints, muscles, and different functions. Therefore, the restoration of limb function requires some persistence and family supervision

(5) When performing physical rehabilitation training, care should be taken to avoid premature walking: some patients and their families are concerned about the slight mobility of the affected limbs. They want to achieve this. They cannot wait for intensive education of many people. Hold on and hold your hand to walk or climb the stairs. It is necessary to know that

"not enough speed" does not focus on the training of basic movements and ignore the stages of the patient's movement pattern

(6) Be careful when dealing with recovery after rejection: some patients become sensitive and vulnerable after illness, overreliance on doctors and their families, lack of initiative in rehabilitation education, and think that the doctor's technology is the treatment of fact. In effect, active training is much better than passive training [23]. Some failures tend to last longer and some even last a lifetime. Therefore, we should not only be interested in the training of patient care, we should pay attention to education or social education after the patients are repatriated, and fully guide family members to teach patients the knowledge and skills to maintain health and daily life. The patients have recovered to a good society and family status. After refusing treatment, the rehabilitation nurse must conduct a telephone return visit to understand the patient's self-service ability and training home guidance after treatment [24]

2.3. Application of Acupuncture in Stroke. Heme is the main manifestation of limb dysfunction in stroke patients, and the main reason is the neuron damage and transplantation abnormality. An implant includes impaired coordination between muscle groups, increased muscle tone, and limited joint mobility. Since joint motion is controlled by the contraction and relaxation of related muscle groups, joint mobility can be improved by strengthening the function of related muscle groups. Traditional Chinese medicine can promote local muscle blood circulation and alleviate the symptoms of edema and pain while improving muscle and neurotrophy, eliminate the pressure of neuroedema, and achieve the effects of promoting functional recovery and inhibiting muscle atrophy. The damage of the upper motor neurons prevents the release of the retroreflector in the lower center, which is the cause of hemophilic contraction, but the effect of simply applying traditional Chinese medicine to repair the damaged neurons is average. Acupuncture can select the puncture site according to the anatomy of the patient's limbs or muscles, stimulate nerve muscles, correct excitement imbalance and inhibit nerves, and promote nerve recovery. Medical aspects. Acupuncture can promote the movement of the affected limb, use and regulate the body's reflexes, strengthen central stimulation, and improve coordinated control of the affected limb. Limited joint mobility is a common manifestation of dyskinesia. Improving joint mobility is the main purpose of rehabilitation for semidisabled patients. Hip and knee joints are important joints that control the movement of the lower limbs, and it is not necessary to increase the effect of Chinese medicine on joint mobility. Muscle failure is the leading cause of stiff limbs. The enhancement of muscle strength after acupuncture combined with Chinese medicine is related to the improvement of muscle strength and the reconstruction of acupuncture function. In addition, the reduction of muscle tension after acupuncture with Chinese medicine is also the basis for increasing joint mobility.

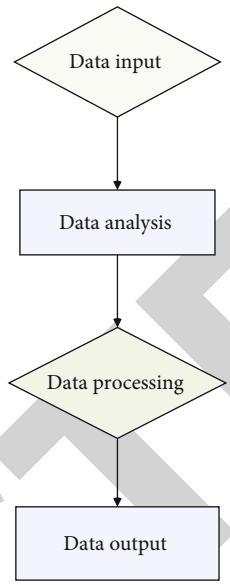

Figure 1: Data processing process.

3. Experiments

3.1. Materials and Methods

(1) General information: from December 2019 to January 2020, 94 stroke patients were selected and treated. Inclusion criteria are as follows: all patients met the diagnostic criteria in the 2016 American Heart Association/American Heart Association Brain Repair Guidelines. Depressive symptoms, signed informed consent, agreed to receive research training, no surgery or thrombolytic therapy, all patients appeared for the first time, and the course of disease was less than two weeks

(2) There was an observation group and a control group divided into 47 cases in each group by the contact ball method. The observer group had 26 cases of males and 21 cases of females, aged 54-76 years, meaning 65.2-1.4 years, including 23 cases of mongrel, 24 cases of right hemizygous, and 25 cases of male. The control group consisted of 22 females and 55 females, ~76 years old, mean age 65.3~1.3) years old, in which 24 cases of left hematoma and 23 cases of right hematoma

(1) First of all, it is necessary to correctly position and transform the limbs, try to keep the limbs in an anatomical functional position, and often move the limbs to prevent the pressure of ulcers

(2) Active and passive movements on the bed, such as upper arm abduction, elbow extension, lower limb extension, and back twist of knees and ankles

Table 1: Comparison of the incidence of complications between the two groups (n).

Group	Number of cases	Intracranial hypertension	Glycemic change	Pneumonia	Total incidence (%)
Observation group	47	1	0	0	2.13%
Control group	47	3	3	2	17.02%
X^2 value	0	0	0	0	4.424%
p value	0	0	0	0	0.035%

Table 2: Comparison of neurological deficit score and mental health score between the two groups ($x \pm s$).

Group	Number of cases	Neurological deficit score	Mental health score
Observation group	47	2.36 ± 0.26	36.65 ± 2.32
Control group	47	4.56 ± 0.22	78.25 ± 1.98
t value		44.284	93.505
p value		<0.05	<0.05

(3) To perform a certain massage repair, it is necessary to regularly massage the affected joints and muscles of the patient to accelerate the blood circulation of the limbs. Seated training

(4) Continuous balance training

(5) Stairs for walking and climbing

(6) Life skills training (including food, laundry, dressing, etc.)

(7) Resistance training: the above active and passive exercises are trained once a day in the morning. The total training time is 2~3 h/d for a total of 3 months. During the training, the patient can endure without feeling tired

(8) Get some psychological treatment

(2) Both groups of patients received conventional neurological treatment, and the nurses evaluated the patient's symptoms, combined with the cause to give the patient general treatment, assisted to actively fight the disease, and established a correct and good treatment mentality; the observation group was supplemented with rehabilitation training interventions. The specific content is as follows: the medical staff sets up a rehabilitation training intervention group consisting of the attending doctor, rehabilitation physician, and nurse and conducts training work around the content of rehabilitation training to actively improve its self-cognition level and comprehensive ability and develop rehabilitation training based on the patient's condition and actual situation. The plan mainly includes correct posture placement, changes, active and passive joint activities, early seated adaptive training, stance changes, and body center of gravity shifts and monitoring the patient's quality of life and mental state throughout the process. For patients with sexual psychology, the nurses carry out health training work around them in a timely manner, inform the patients of stroke, depression, treatment, and prognosis, improve the patient's self-cognition level, and enable them to actively cooperate with treatment and nursing work to ensure intervention effect. Acupuncture treatment was given, and patients were instructed to take the supine position and take acupuncture points such as Sanyinjiao, Shenmen, Sishencong, and Baihui to get Qi for 30 min, 1 time/d, with 10 d as a course of treatment; for patients with liver qi stagnation, Taichong and Hegu points can be added; those with phlegm fever can be added to the inner court and Fenglong acupoints, and the liver and fire are strong, and those with yin deficiency can be added with acupuncture points such as Taichong, Yongquan, and Taixi. Acupoint, rest 3 d after the end of the treatment course, and proceed to the next course according to the actual situation of the patient. Treatment group rehabilitation content: in addition to the same rehabilitation training as the control group, acupuncture was also used for functional rehabilitation. Acupuncture is mainly based on acupuncture points of the large intestine and stomach, supplemented by acupoints of the bladder and bile. At the beginning of the disease, only the affected side is punctured. After a long course of disease, the healthy side can be punctured first, and then, the affected side can be punctured. Mainly take ring jump, Yanglingquan, Zusanli, and Kunlun, and can take turns to Fengshi, Juegu, Yaoyangguan and other points. Acupuncture points with symptoms: Taiyang and Taichong with liver yang and hyperthyroidism; Fenglong and Hegu with wind and phlegm resistance; varus correction with foot inversion and Qiuxu through the sea; valgus with Zhongfeng, Taixi, and correction of eversion; foot droop with Jiexi and Taichong; and constipation with Fenglong and ditch. Acupoints and needles are routinely disinfected. In the acute phase, twist and diarrhea was used, and the needle was continuously applied for 10-15 minutes. During the recovery period, the needle was used for 20-30 minutes, and moxibustion was performed on the acupuncture points. Once a day, 10 d is a course of treatment, rest 3 d, and continue treatment

3.2. Research Indicators. Observe the effects after the intervention, including the occurrence of complications,

Table 3: Comparison of depression scores between the two groups before and after intervention ($x \pm s$).

Group	Number of cases	Before intervention	Prognosis after intervention	t value	p value
Observation group	47	14.65 ± 3.21	3.20 ± 0.13	24.434	>0.05
Control group	47	14.66 ± 3.22	6.625 ± 0.25	17.066	<0.05
t value		0.015	83.205		
p value		>0.05	<0.05		

Table 4: Comparison of Barthel index in daily living ability.

Group	n	Before rehabilitation	After rehabilitation
Treatment group	30	25.12 ± 9.13	65.41 ± 13.55
Control group	30	22.83 ± 8.32	42.24 ± 12.08

neurological deficit scores, mental health scores, and changes in depression scores before and after the intervention. The NIHSS scoring system was used to assess the degree of neurological deficits. The score was 100 points. The smaller the score, the smaller the neurological deficit, and vice versa. The SCL-90 symptom self-assessment scale was used to assess the mental health of patients. The scale items are as follows: thinking, living habits, consciousness, interpersonal relationships, emotions, feelings, behaviors, diet and sleep, etc., from none, very light, medium, biased, and severely corresponding 1 to 5 grades; scale score is 450 points; the lower the score, the better the mental health. The psychiatric class A PHQ-9 score was used to assess depression, and the questionnaire survey was used. The normal score was 0 to 4 points, with depressive symptoms; 5 to 9 points, the obvious depressive symptoms; and 10 to 14 points, severe depressive symptoms: 15~27 minutes. Efficacy criteria are as follows: Barthel index of daily living ability, FAC lower limb walking function score, Fugl-Meyer score, and other treatment effects were evaluated. The statistical data of the statistical method was expressed as $z \pm 5$.

3.3. Data Processing. Data processing was performed using the statistical software SPSS21.0. The calculation data was described by $x \pm s$ and t test; count data was expressed by rate and χ^2 test; $\alpha = 0.05$ was used as the test criterion. The entire data processing process is shown in Figure 1.

4. Discussion

4.1. Control Group. Higher levels of complications in the two groups are presented in Table 1.

Table 1 shows that the complication rate in both groups was 2.13% (1/47) compared against the observation group, being 17.02% (8/47) lower than that in the control group, for which the variation was of statistical relevance ($p = 0.035$).

The score of neurological deficits and mental health ratings of the two groups is compared in Table 2.

As seen in Table 2, the neurological deficit rating and mental health score in both groups with statistically significant differences ($p < 0.05$) were lower on the control group.

Comparison of before and after interventions for both groups is shown in Table 3.

The depression scores of the two groups before and after the intervention were compared according to Table 3. With the observation group, depression scores were lower when compared to the control group after the intervention, and differences were observed which was statistically important ($p < 0.05$).

From Tables 1–3 before and after the comparison, we can know that poststroke depression is one of the common sequelae of patients with clinical stroke, and the incidence is 31.2%~63.1%, which is at a very high level. After the occurrence of depression sequelae, the patient's mental state is in a deep and depressed state for a long time, and he loses attention to life. Some severely depressed people may even ignore life and give up life, which seriously affects their prognosis and health. Moreover, in the clinic, most patients with stroke have language dysfunction, which makes it impossible to detect the depressive symptoms in time, so it is necessary to strengthen the observation of patients' mental and emotional states. Rehabilitation training intervention is a clinical intervention measure applied in recent years. It mainly implements interventions for patients with limb dysfunction, evaluates their limbs and emotions early, and implements guidance based on their characteristics to promote their limb function recovery as soon as possible. The results showed that in the observation group, the risk of complications after rehabilitation intervention was effectively reduced. After the intervention, the patients' neurological function and psychology and depression scores were in a good range, which further confirmed the significant effect of rehabilitation intervention in clinical. The clinical application of rehabilitation training in poststroke depression patients helps to alleviate and enlighten the patient's negative psychology and adverse emotions, enabling them to face treatment and rehabilitation training with a good attitude and to maximize their impact on the disease. Implementing acupuncture interventions can effectively improve the patient's own tolerance, improve their physical condition through dredging channels and channels, and promote the improvement of the intervention effect.

Table 4 shows the Barthel index of the two groups after rehabilitation.

This is seen in Table 4, the Barthel index was significantly higher in both groups after rehabilitation than before rehabilitation, and the difference was dramatically significant ($p < 0.05$). It also shows that the Barthel index of the control group was higher than that of the treatment group on rehabilitation, and there was a significant difference ($p < 0.05$).

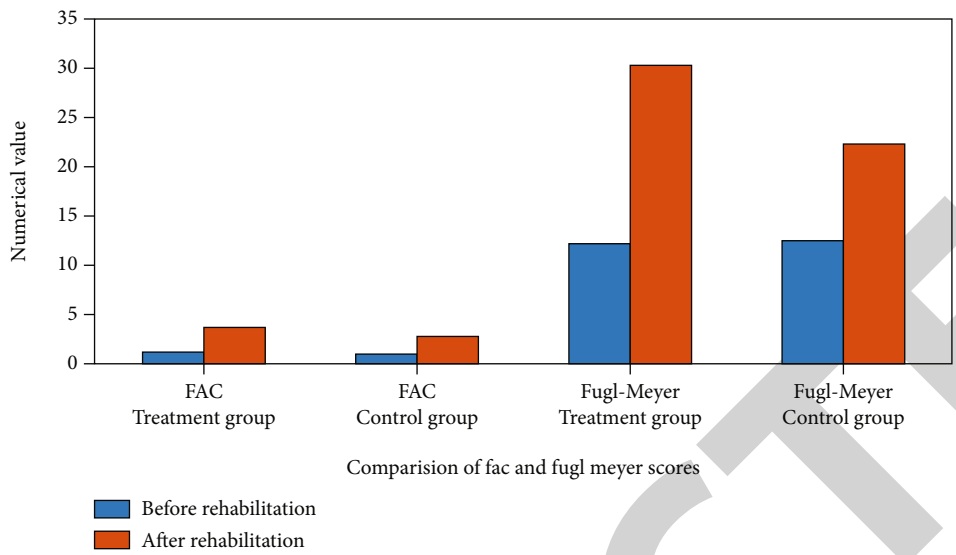

Figure 2: Comparison of FAC and Fugl-Meyer scores.

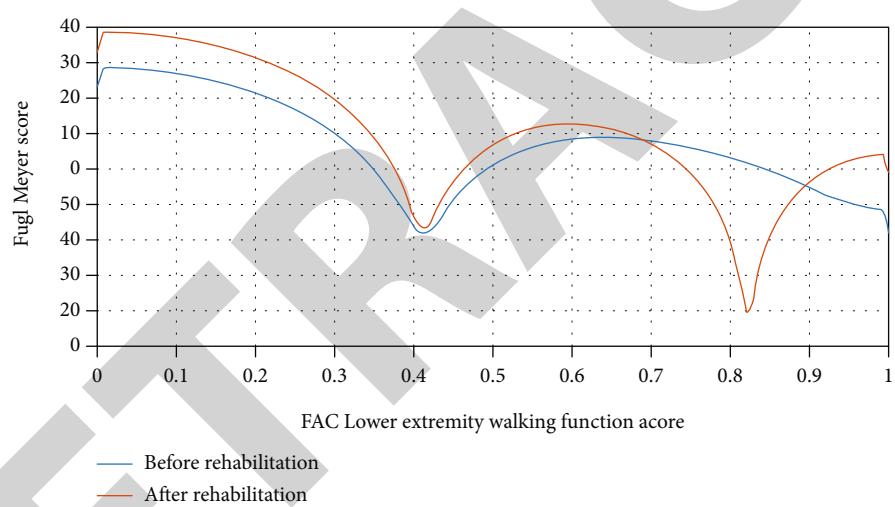

Figure 3: Comparative analysis of FAC and Fugl-Meyer before and after rehabilitation.

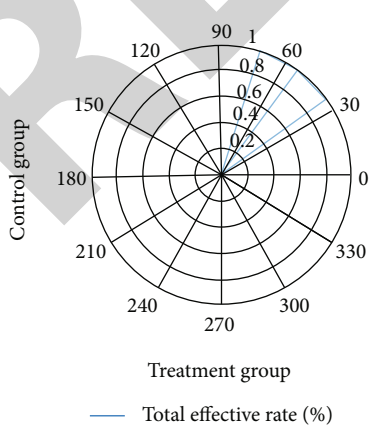

Figure 4: Comparison of total effective rate between the two groups (example).

Table 5: NIHSS scores of the two groups before and after treatment.

Group	Reciprocal	Before treatment	After treatment
Treatment group	40	28.53 ± 6.2	11.12 ± 0.25
Control group	40	28.64 ± 5.5	19.5 ± 3.25
P		>0.05	<0.05

4.2. Comparison of FAC and Fugl-Meyer Scores. The FAC and Fugl-Meyer lower limb basic motor function scores of the two groups of patients after rehabilitation are shown in Figure 2.

As seen in Figure 2, the FAC results after recovery were significantly higher than those before recovery in both groups, with a remarkable variance ($p < 0.01$). After recovery, the FAC scores in the treatment oriented group were

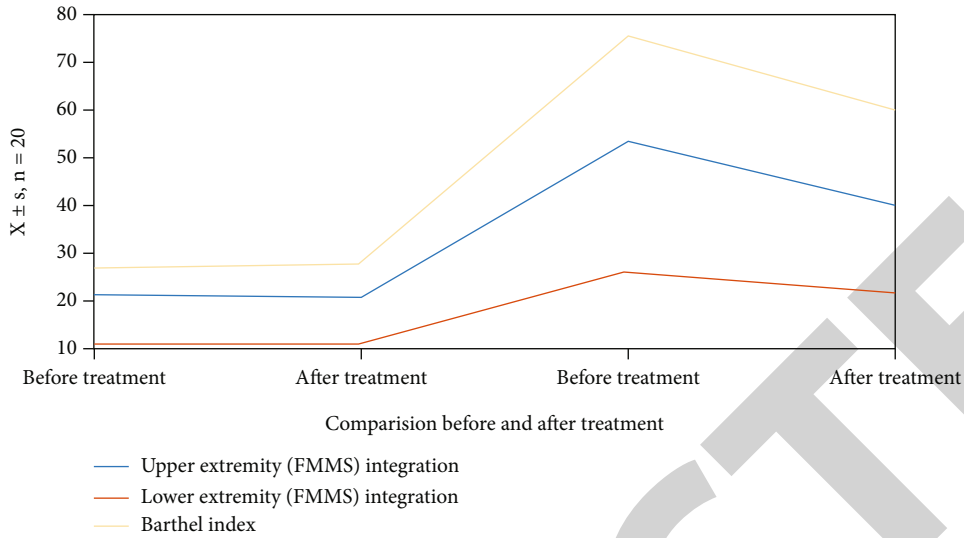

Figure 5: Comparison of the functions of the two groups before and after treatment (x ± s, n = 20).

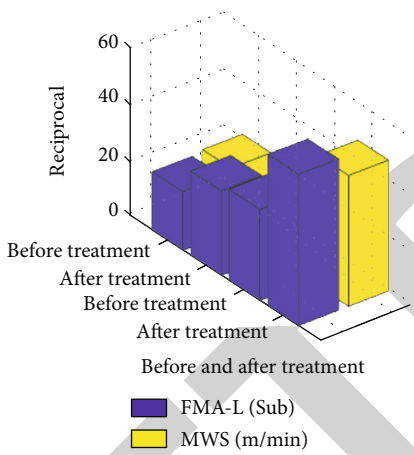

Figure 6: Comparison of FMA-Ll and MWS between the two groups before and after treatment ($x \pm s$).

significantly higher from the control group ($p < 0.05$). It can also be seen from Figure 1 that the degree of basic motor function of Fugl-Meyer's lower limbs was significantly higher after rehabilitation than before rehabilitation ($p < 0.01$). For the basic motor function score, difference was significantly more than control group ($p < 0.05$).

Acupuncture and rehabilitation both advocate early treatment, and early patient position care is the main link of limb rehabilitation. Acupuncture or modern rehabilitation treatment as soon as possible after the vital signs of stroke patients are stable can effectively improve the symptoms of motor function and neurological deficits and improve their daily activities. Figure 3 is a comparison of FAC's lower limb walking function score.

The lower extremity FAC score is an evaluation of the lower limb walking ability of a half-life patient, and the Fugl-Meyer score is an assessment of the underlying dynamics of surgical treatment of the lower extremity of a hemiplegia patient. Figure 3 shows that the results of rehabilitation training in the two groups of patients are significantly higher than before, indicating that there is a significant difference between before rehabilitation and before acupuncture, and that traditional rehabilitation methods and acupuncture have a certain rehabilitation effect. According to the literature, acupuncture can stimulate the excitement of motor neurons, promote the formation of new high-level centers and peripheral transportation routes, and mutually promote rehabilitation training. However, it can be seen from Figure 2 that the FAC and Fugl-Meyer scores of the treatment group are significantly higher than those of the control group, and it shows that acupuncture combined with traditional repair methods has a better ability to recover walking. For a long time, traditional recognition in the field of neurological interventions considered spasm to be the most important factor limiting motor function recovery. Treatment strategies focus on normalizing muscle tone and promoting the formation of normal forms of exercise. Patients with hemiplegia are predominantly spasm of the sixth muscle of the knee, which leads to irregular bending of the knee joint. Acupuncture is mainly based on acupuncture points near the muscles of the affected limbs, which can reduce reflex tension and muscle tension. Combined with techniques that promote confrontation and nerves in rehabilitation training, it can improve the motor function of the affected limb and the overall physical performance of the body. It is not necessary to have a promotion effect similar to or better than promotion. Acupuncture stimulates active muscles, which is basically a regional sensory input that can stimulate motor neurons, stimulate the production and strengthening of muscle tension, and stimulate motor neurons to promote traffic shunting.

The effective rates of the treatment group and control group are shown in Figure 4 and Table 5.

The clinical efficacy can be seen in Figure 4 and Table 5: according to the evaluation criteria, there was an overall

effective rate of 97.5% in the treated group and 75.0% in the control group. It was better in the treatment group with a lower neurological deficit score after treatment than in the control group compared to the control group.

In the treatment group together with the controls, the limb motor function scores and daily living ability are shown in Figure 5.

As seen in Figure 5, the limb motor function scores and daily living ability in the treating group improve significantly compared to the control group, and the difference is statistically significant ($p < 0.01$) when comparing the two groups. There was a statistically significant difference compared with that before treatment ($p < 0.01$). In the treatment period, no adverse events and side effects occurred. There was no significant change in heart rate and blood pressure before and after treatment in the treatment group. The rehabilitation of patients with stroke hemiplegia can be divided into different stages (including soft paralysis, spasticity, and recovery), and the different acupuncture treatments at different stages are satisfactory.

The difference between FMA-L and MWS before and after treatment in the two groups is shown in Figure 6.

As seen in Figure 6, the differences in FMA-L and MWS before and after treatment in both groups were not significant ($p > 0.05$) compared to FMA.L and MWS for both groups before treatment. There were elevated FMA-L and MWS in both groups after treatment, but the differences were statistically significant ($p < 0.05$). Both indices were higher than the control group after of the treatment, and the difference was statistically significant ($p < 0.01$). Time-dependent parameters of gait of the two groups before and after treatment were compared. There was an increase in gait frequency, stride length, affected and habilitation side stride length, gait cycle, and leg bolstering time after treatment, and the differences were statistically significant ($p < 0.05$). Each indicator was better than the core group with statistically meaningful differences after treatment ($p < 0.05$).

5. Conclusions

Stroke is a common disease in clinical neurology. It is mainly caused by the sudden rupture or blockage of blood vessels in the brain. After the illness, patients may experience dizziness, numbness, vomiting, and hemiplegia. In some severe cases, neurological and motor functions may be impaired, which may threaten their normal life and health. Acupuncture combined with rehabilitation training is effective in treating poststroke interventions. It can improve patients' mental state, depression, and neurological function and effectively reduce the impact of other complications on their prognosis.

This article uses a comparative experiment to compare acupuncture and rehabilitation training in patients with stroke. The first group did not use acupuncture combined with rehabilitation training, with the last group which employed acupuncture combined with restoration training, which was found to improve muscle strength. Limb function improves balance and coordination between muscle groups. During recovery, convulsions in the affected limb were relieved. This treatment is mainly based on acupuncture and antidiarrhea, which is beneficial to improve blood circulation in the extremities, increase tissue stimulation, and gradually recover from separated, thin, and controllable surgery, which significantly improves the patient's limb function and daily life. Therefore, the flexible use of acupuncture at different stages in patients with hemistroke is beneficial to functional recovery.

This article establishes comparative experiments and shows that a large number of patient rehabilitation training data show that acupuncture has a great effect on the rehabilitation training of stroke patients. The research in this article is limited to the analysis of clinical manifestations and prognosis of patients, and the mechanism of its impact is not clear. Therefore, it is still necessary to conduct analysis and research around the core theories of this study in order to contribute to the further improvement of clinical intervention. This article studies the effects of acupuncture combined with rehabilitation training on the physical activity and living capacity of stroke patients with hemiplegia.

This study found that lower limb motor operation, walking ability, and daily life in the observation group were significantly improved, and acupuncture combined with rehabilitation training significantly improved limb motion and survival evidence for stroke patients and intermission. Acupuncture can promote the movement of the affected limb, utilize and regulate the body's reflexes, strengthen central stimulation, and strengthen coordinated control of the affected limb. In combination with rehabilitation for improved limb circulation and limb survival, needles can have an improving action on stroke and hemiplegic patients. We studied the effect of acupuncture combined with convalescent training on limb movement and living capacity in stroke hemiplegic patients. This paper provides guidance for the study of needles combined with rehabilitation training on limb motion and living capabilities in stroke patients with paraplegia.

Data Availability

No data were used to support this study.

Conflicts of Interest

The author states that this article has no conflict of interest.

Authors' Contributions

Juhua Zhang and Yingmei Mu contributed equally to this work.

References

[1] A. Hachisuka, Y. Matsushima, K. Hachisuka, and S. Saeki, "A case of apoplexy attack-like neuropathy due to hereditary neuropathy with liability to pressure palsies in a patient diagnosed with chronic cerebral infarction," *Journal of Stroke & Cerebrovascular Diseases the Official Journal of National Stroke Association*, vol. 25, no. 6, pp. e83–e85, 2016.

Hindawi
Behavioural Neurology
Volume 2023, Article ID 9893564, 1 page
https://doi.org/10.1155/2023/9893564

Retraction

Retracted: Multimodal Medical Image Fusion of Positron Emission Tomography and Magnetic Resonance Imaging Using Generative Adversarial Networks

Behavioural Neurology

Received 19 December 2023; Accepted 19 December 2023; Published 20 December 2023

This article has been retracted by Hindawi following an investigation undertaken by the publisher [1]. This investigation has uncovered evidence of one or more of the following indicators of systematic manipulation of the publication process:

(1) Discrepancies in scope

(2) Discrepancies in the description of the research reported

(3) Discrepancies between the availability of data and the research described

(4) Inappropriate citations

(5) Incoherent, meaningless and/or irrelevant content included in the article

(6) Manipulated or compromised peer review

The presence of these indicators undermines our confidence in the integrity of the article's content and we cannot, therefore, vouch for its reliability. Please note that this notice is intended solely to alert readers that the content of this article is unreliable. We have not investigated whether authors were aware of or involved in the systematic manipulation of the publication process.

Wiley and Hindawi regrets that the usual quality checks did not identify these issues before publication and have since put additional measures in place to safeguard research integrity.

We wish to credit our own Research Integrity and Research Publishing teams and anonymous and named external researchers and research integrity experts for contributing to this investigation.

The corresponding author, as the representative of all authors, has been given the opportunity to register their agreement or disagreement to this retraction. We have kept a record of any response received.

References

[1] R. Nandhini Abirami, P. M. Durai Raj Vincent, K. Srinivasan, K. S. Manic, and C. Y. Chang, "Multimodal Medical Image Fusion of Positron Emission Tomography and Magnetic Resonance Imaging Using Generative Adversarial Networks," *Behavioural Neurology*, vol. 2022, Article ID 6878783, 12 pages, 2022.

Hindawi
Behavioural Neurology
Volume 2022, Article ID 6878783, 12 pages
https://doi.org/10.1155/2022/6878783

Research Article

Multimodal Medical Image Fusion of Positron Emission Tomography and Magnetic Resonance Imaging Using Generative Adversarial Networks

R. Nandhini Abirami,[1] P. M. Durai Raj Vincent,[1] Kathiravan Srinivasan,[2] K. Suresh Manic,[3] and Chuan-Yu Chang[4,5]

[1]*School of Information Technology and Engineering, Vellore Institute of Technology, Vellore 632014, India*
[2]*School of Computer Science and Engineering, Vellore Institute of Technology, Vellore, 632 014 Tamil Nadu, India*
[3]*Department of Electrical and Communication Engineering, National University of Science and Technology, Muscat, Oman*
[4]*Department of Computer Science and Information Engineering, National Yunlin University of Science and Technology, Yunlin 64002, Taiwan*
[5]*Service Systems Technology Center, Industrial Technology Research Institute, Hsinchu, Taiwan*

Correspondence should be addressed to P. M. Durai Raj Vincent; pmvincent@vit.ac.in and Chuan-Yu Chang; chuanyu@yuntech.edu.tw

Received 25 November 2021; Accepted 27 March 2022; Published 14 April 2022

Academic Editor: Hong Lin

Multimodal medical image fusion is a current technique applied in the applications related to medical field to combine images from the same modality or different modalities to improve the visual content of the image to perform further operations like image segmentation. Biomedical research and medical image analysis highly demand medical image fusion to perform higher level of medical analysis. Multimodal medical fusion assists medical practitioners to visualize the internal organs and tissues. Multimodal medical fusion of brain image helps to medical practitioners to simultaneously visualize hard portion like skull and soft portion like tissue. Brain tumor segmentation can be accurately performed by utilizing the image obtained after multimodal medical image fusion. The area of the tumor can be accurately located with the information obtained from both Positron Emission Tomography and Magnetic Resonance Image in a single fused image. This approach increases the accuracy in diagnosing the tumor and reduces the time consumed in diagnosing and locating the tumor. The functional information of the brain is available in the Positron Emission Tomography while the anatomy of the brain tissue is available in the Magnetic Resonance Image. Thus, the spatial characteristics and functional information can be obtained from a single image using a robust multimodal medical image fusion model. The proposed approach uses a generative adversarial network to fuse Positron Emission Tomography and Magnetic Resonance Image into a single image. The results obtained from the proposed approach can be used for further medical analysis to locate the tumor and plan for further surgical procedures. The performance of the GAN based model is evaluated using two metrics, namely, structural similarity index and mutual information. The proposed approach achieved a structural similarity index of 0.8551 and a mutual information of 2.8059.

1. Introduction

The process of image fusion combines the unique features and spatial attributes to generate single fused image using images from single or multiple modalities [1]. This is performed to improve the results of medical image analysis. The ultimate aim of multimodal medical image fusion is to retain the spatial feature of the image and to make the medical image analysis and disease diagnosis accurate and less time consuming [2]. Medical image fusion is found to be successful in multivarious fields, namely, image enhancement, medical image analysis, and surveillance. Medical

image fusion helps in diagnosing and classifying disease with high accuracy [3]. The classical approach of medical image fusion is to perform medical image registration, which aligns the images obtained from multiple sources resulting in single enhanced output image obtained from two or more input images [4]. The ultimate goal in combining the multimodal images is to transform the images into highly informative and classifiable image. Some of its applications are classification of disease, weather prediction, and other operations related to military. Deep learning is found to be successful in many applications [5] like image fusion, segmentation [6], facial expression recognition [7], and other medical-related application [8]. Abbreviations presents the full forms used in this work.

With the advancement in technology highly reliable medical imaging tools and techniques like Magnetic Resonance Image, Positron Emission Tomography, and Computed Tomography, they have come up making the diagnoses of diseases accurate and less time consuming [9]. Positron Emission Tomography is not involved in the introduction of any medical instruments into the human body. Rather, it utilizes Positron Emitting Radioisotopes to generate multiple images based in tissue concentrations [10]. However, considering PET image alone has several drawbacks. The spatial resolution of PET images is very low making the medical diagnoses difficult. However, pathological and molecular information can be obtained from PET. Similarly, MRI provides regional change details in physiology, tissue composition, and hemodynamics functional information. Hence, performing the fusion of images from different or same modalities has become inevitable to obtain accurate results [11]. Figure 1 shows some of the medical diagnostic images used in recent times. Combining these images makes the resulting image information rich with features integrated from multiple modalities. Image fusion adds advantage of using combining all the important information from different images into one single fused image making the process of image analysis easier, quicker, and accurate. Also, image fusion technique enhances the spatial clarity of the fused image. The space occupied for storing individual images is greatly reduced when multiple images are fused together into single image.

MRI and CT images are structural images with higher resolution and anatomical structure [12]. PET and SPECT are functional images with lower resolution and functional information [13]. Several research works have already been proposed related to multimodal medical image fusion to overcome the drawbacks of single images from various modalities [14]. However, the existing approaches have their own advantages and disadvantages. Wavelet transform was one of the frequently used approaches for performing medical image fusion [15]. Few other approaches used to perform medical image fusion are discrete wavelet transform [16], stationary wavelet transform [17], redundancy wavelet transform, average method, principal component analysis, brovey method, and curvelet transform. However, technically, combining PET images with MRI images is challenging because of the existing incompatibility between magnetic field and the PET detectors. Also, some of the existing image fusion approaches presume that distortions follow Gaussian distribution leading to model mismatch problem. These issues are handled by using generative adversarial networks for combing PET and MRI images. Yet another challenge in combining PET and MRI images is that MRI image is a grey scale image while the PET image is a pseudocolored image. Figure 2 shows various existing approaches adopted to perform image fusion. These approaches have several advantages and disadvantages. The main disadvantages of the existing approaches are the actual chromaticity of the diagnostic images which are not preserved. In order to overcome these drawbacks, medical image fusion is proposed using generative adversarial networks. Combining medical images has been proven successful for scientific and medical purposes especially oncology, cardiology, and neurology.

Combining PET and MRI images into a single image allows simultaneous acquisitions, though instinctively simple; it is technically more challenging than it appears to be [18]. It has been impossible to combine these two diagnostic images for several years because of their incompatibility between photomultiplier tube of PET and powerful magnetic field of MRI [4]. As a solution to this issue, it has been proposed to perform sequential PET-MRI scans for the patient and subsequent merging of this bimodality system for accurately fusing these diagnostic images. However, the process was complex and time-consuming. In order to overcome these issues and make the process simpler and less time-consuming deep learning-based approaches have been proposed to perform multimodal image fusion for medical diagnostics.

Brain tumor is collection of anomalous cells in a human brain affecting more than 15 million people every year [19]. It is considered a global health problem; timely prediction is necessary to prevent a medical condition to save lives [20]. Hence, detecting brain tumor at an early phase is necessary to provide timely medical intervention and prevent further complications [21]. The outcome can be improved by taking appropriate action on the warning signs of brain tumor. In recent times, brain images in modalities like computed tomography, MRI, and PET are used to evaluate the intensity of the stroke [22]. Deep learning models have proven successful in many medical applications. Hence, a deep learning-based robust model is proposed to utilize multimodal medical images to detect a brain tumor. Here, the proposed model performs multimodal medical image fusion to detect a brain tumor. Fusion of PET and MRI images are performed using generative adversarial networks to detect a brain tumor.

Behavioral disorder involves disorderly behavior in childhood or adolescence. Some of the frequently seen behavioral disorder in children are bipolar disorder, anxiety disorder, depression, bipolar disorder, learning disorder, conduct disorder, attention deficit hyperactivity disorder, oppositional defiant disorder, and autism spectrum disorder. Some of the childhood issues are related with family history and gender. The children with behavioral disorder express inability to obey rules, arguing recurrently, seeking revenge, and deliberately annoying others. The child may also express difficulty in concentrating, difficulty making friends, low self-esteem, and persistent negativity. The children with behavioral disorder may be given family therapy by a child psychiatrist.

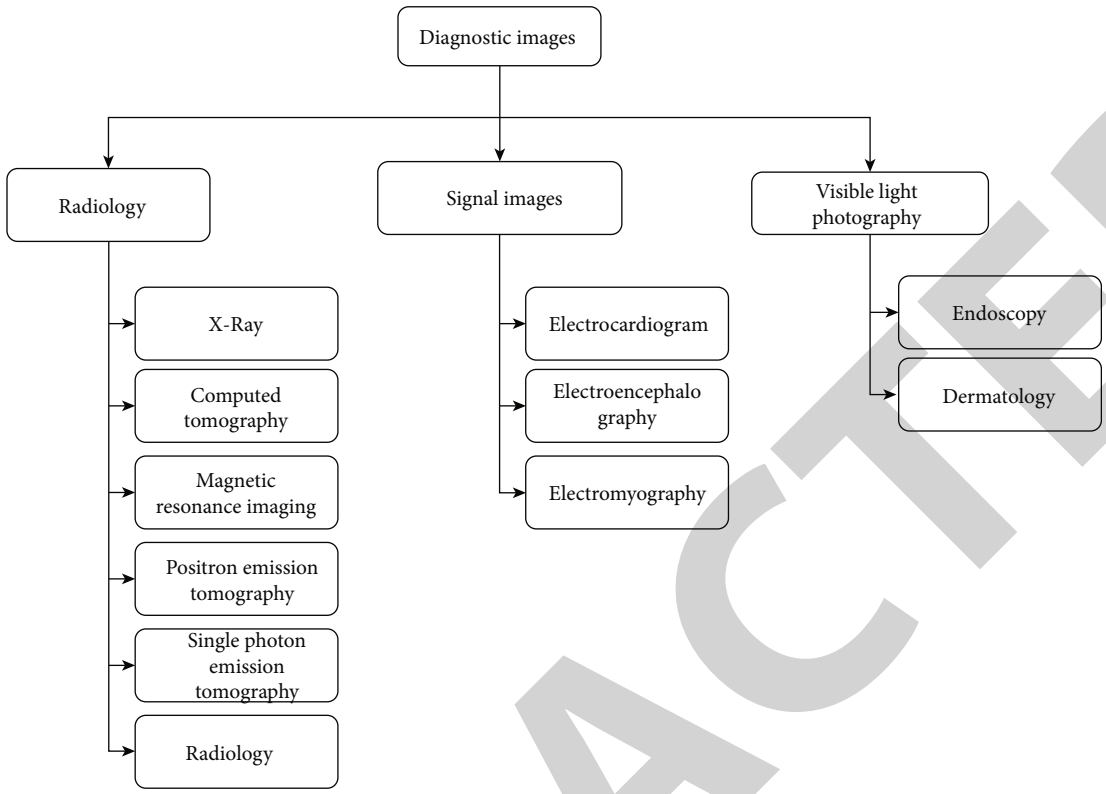

Figure 1: Medical image modalities.

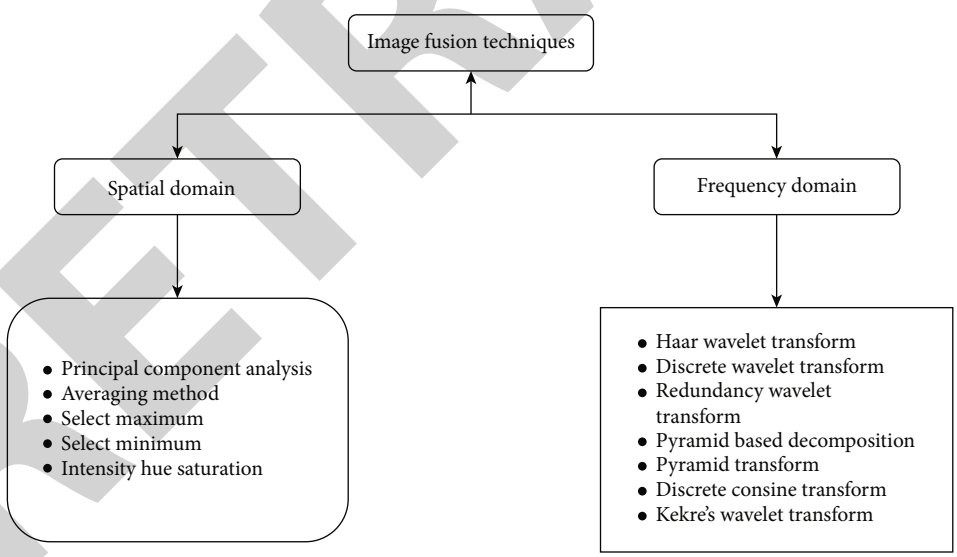

Figure 2: Methods adopted to perform image fusion.

The main contribution of the proposed work is that it models an effective image fusion technique using generative adversarial networks. The proposed approach adopts a novel dual discriminator approach to perform multimodal medical image fusion. The results display that the proposed approach is superior to the existing medical image fusion approaches in preserving the anatomical and functional information of the input images.

In this paper, the proposed model performs multimodal medical image fusion for combining multimodal brain images, namely, PET and MRI using generative adversarial network. The working flow of the paper in the following fashion. Section 2 describes other works that are related to medical image fusion. Section 3 describes the materials and methods adopted to perform medical image fusion, network architecture, and the loss function used in the proposed

work. Section 4 discusses about the experiments and the result. Section 5 concludes the proposed work.

2. Literature Review

Multimodal medical image fusion acts as a potential tool for performing medical diagnosis and provide timely treatment for the diagnosed disease [23]. PET and MRI images are considered to be one of the most advanced imaging techniques in the medical field. A detailed and accurate assessment of a human subject can be made bringing together the molecular data presented by PET and the functional and morphological data presented by MRI. The fused image is capable of simultaneously providing high-resolution molecular, anatomic, and functional data allowing brain tumor analysis and segmentation in a single image examination. This fusion technique has also brought a massive progress in diagnosing cancer, its stages, and the response to the treatment [23]. Multimodal image fusion has made the detection of metastases easier, which was complex with individual image modalities.

Haddadpour et al. proposed an approach to combine PET and MRI images. The authors used a 2-dimensional HT and IHS to perform multimodal image fusion. The performance of the model is tested using performance metrics. Discrepancy evaluates the performance of the model in retaining the spectral features in the fused image. A higher spectral resolution is achieved with lower value of discrepancy. The discrepancy obtained using this method is minimum resulting in retaining spectral features. Also, the method achieved good average gradient resulting in retaining spatial features. The difference between overall performance and discrepancy represents the overall performance. Lower value of overall performance indicates a better fusion quality. The combination of 2-dimensional HT and HIS resulted in low overall performance [24].

Shahdoosti and Mehrabi proposed PET-MRI image fusion using dual ripplet II transform. Ripplet II transform suffers from shift variance problem. In order to overcome this issue, the authors proposed dual repplet II transform. The color and spatial information of the image is preserved using a weighing matrix. Dual ripplet transform is advantageous over ripplet II transform as traditional wavelet is used in ripplet II transform and complex wavelet is used in dual ripplet II transform. Also, dual ripplet II transform uses generalized radon transform. The proposed approach decomposes the input image into low-pass bands and then to high-pass bands. The proposed method used MRI images of good resolution and PET images that are colored images. The size of PET images was not the same as that of MRI images. MRI images were of size 256×256 while PET images where of size 128×128. So to match the size of PET and MRI images to perform fusion of images, PET images were upscaled to 256×256 pixels. The images were obtained from Harvard University website. The experiment used images of different disease categories, namely, coronal and Alzheimer's disease. The parameter settings were 0.03 for λ, 0.005 for β, and 0.001 for ε. The proposed approach preserved the functional features of PET image and anatomical details of MRI image. The model is evaluated using normalized weighted performance metric. The proposed model achieved 0.8771 normalized weighted performance metric [25].

Ouerghi et al. performed a fusion of PET-MRI images based on shearlet transform and a NN model. The proposed approach converted the input PET image into independent components. Both MRI and the transformed independent components of PET images are broken up into two bands, namely, the low frequency and high frequency. The nonsubsampled shearlet transform combines the low-frequency components. A simplified pulse coupled neural network model combined high-frequency components. The proposed model initially performed MRI and PET image registrations. The registered images are further normalized and then transformed into independent components. This is performed to separate the chromatic information and the illuminance of the input. The model is compared with other models using fusion quality index [26]. Du et al. performed the fusion of PET-MRI images using intrinsic image decomposition approach to decompose the images into 2 different components. It used two algorithms; one algorithm extracted the anatomical information of the image while keeping the noise level from the input low. Another approach performed summing up of the color details obtained from input image. The signal-to-noise ratio obtained from the proposed approach is very less in comparison with other models. The implementation of the model is compared with Bonferroni-Dunn and Friedmann tests. Though the proposed work performed reasonably good in combining the PET and MRI images, the proposed approach expressed dependencies of intrinsic image decomposition [27].

Liu et al. proposed a model to fuse medical image using multiresolution and nonparametric density models. The space registered input images are first generalized and then broke into different frequency components using contourlet transform. The model is evaluated using average cross entropy that calculates the difference between the input and the output. Lower value of average cross entropy results in better fusion. The clarity and spatial resolution of the resultant image is assessed using average gradient. When the value of average gradient high, it implies better spatial clarity. The proposed approach is compared quantitatively and qualitatively with six fusion methods on three classes of images, namely, Alzheimer's, normal, and neoplastic images of brain. The quality of the final fused image is assessed using five different metrics, namely, mutual information, edge intensity, average gradient, average cross entropy, and entropy. The proposed approach achieved 0.1558 cross entropy, 90.5 edge intensity, 9.166 average gradient, and 3.9 mutual information [28]. Tang et al. [29] obtained the neighborhood information to realize the focused and defocused pixels of the input image. Prabhakar et al. proposed medical image fusion using unsupervised deep learning model. Multimodal image fusion is performed using a generative adversarial network [30–32]. Table 1 shows the existing approaches in performing multimodal medical image fusion.

Table 1: Medical image fusion—existing approaches.

Modality	Work	Organ	Fusion technique	Approach
PET and MRI	[24]	Brain	2D Intensity Hue Saturation and Hilbert transform	PET and MRI image fusion using 2D Hilbert transform and Intensity Hue Saturation Fourier Transform is calculated for each of the input signals.
PET and MRI	[25]	Brain	Dual ripplet II transform	The proposed approach uses dual ripplet II transform as it uses complex wavelet transform. The color and spatial information of the images are preserved using weight matrix.
PET and MRI	[27]	Brain	Intrinsic image decomposition	Model based on intrinsic image decomposition are proposed to extract structural information from MRI and for obtaining color details from PET.
PET and MRI	[26]	Brain	Non-subsamples shearlet transform	The input images are registered and normalized and then transformed into independent components. Pulse coupled neural network is used to obtain useful information from the image.
MRI and CT	[33]	Brain	Hybrid image fusion	The image fusion is performed using principal component analysis and independent component analysis.
MRI and CT	[34]	Brain	Adolescent Identity Search Algorithm	The proposed approach decomposes the input image into high and low frequency component using nonsubsampled shearlet transform.
MRI and PET	[35]	Brain	Spectral Total Variation Transform	The proposed method decomposes the source image into base components and then combined using spatial frequency dual channel model.

Input:
$\boldsymbol{I_{mri}}$: MRI image
$\boldsymbol{I_{pet}}$: PET image
$\boldsymbol{I_{fu}}$: Generated fused image
$\boldsymbol{D_m}$: Discriminator 1
$\boldsymbol{D_P}$: Discriminator 2
Train discriminator $\boldsymbol{D_m}$ and $\boldsymbol{D_P}$
Concatenate $\boldsymbol{I_{mri}}$ and $\boldsymbol{I_{pet}}$
$\boldsymbol{Generator}, \boldsymbol{G} : \{\boldsymbol{I_{mri}}\, \boldsymbol{I_{pet}}\} \longrightarrow \boldsymbol{I_{fu}}$
Output:
$\boldsymbol{I_{fu}}$:Fused image
Update discriminator parameters
Update generator parameters
Repeat until an output image with less distortion and high structural information is obtained.

Algorithm 1.

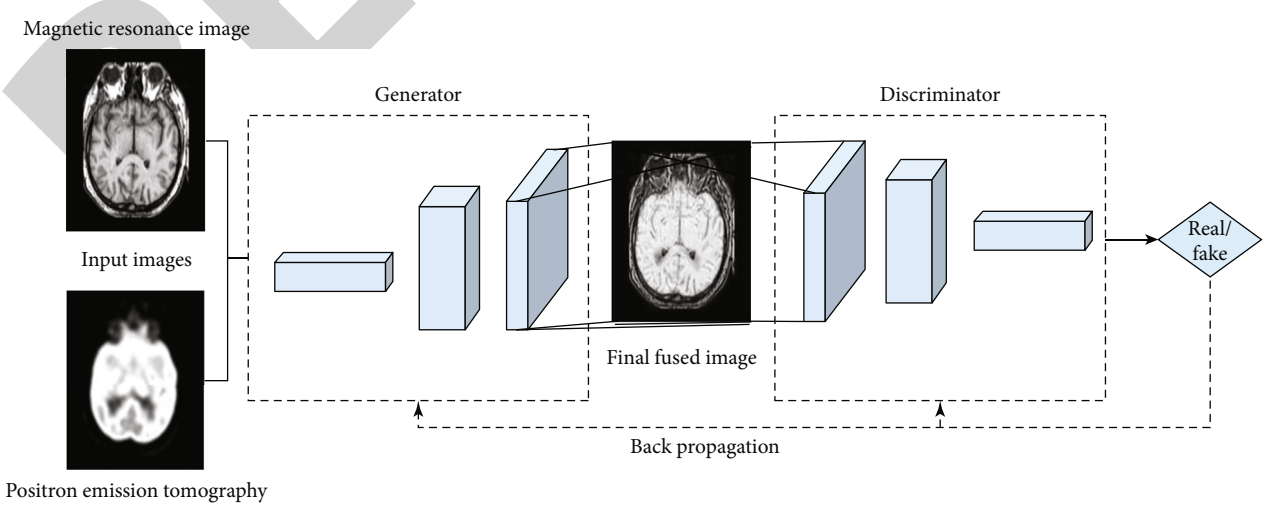

Figure 3: Architecture of the proposed approach for image fusion.

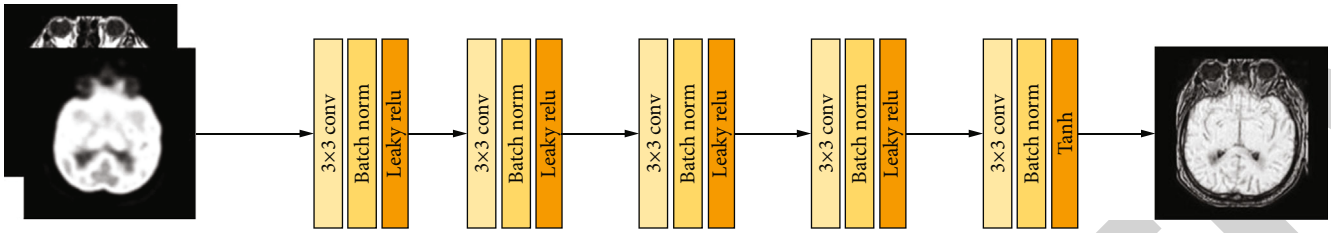

Figure 4: Generator architecture.

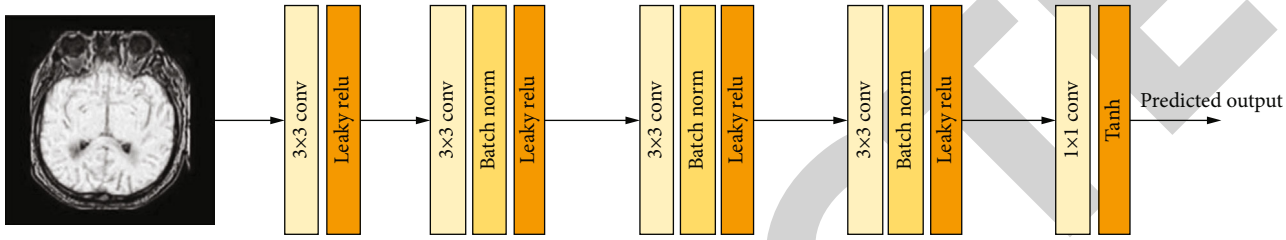

Figure 5: Discriminator architecture.

3. Materials and Methods

PET images are of low spatial resolution depicting the brain function. MRI images depicts the anatomy of brain and does not possess any functional details of the brain. Obtaining the necessary clinical information from a single image is practically not possible. Hence, to get accurate results of diagnosis, the diagnostic image should depict both spatial characteristics and functional information with no distortions. Hence, combining PET and MRI images would be a highly reliable diagnostic tool to perform image analysis. The image fusion should be performed in a way that the fused image retains the anatomic, functional, and structural details of the input images.

The primary goal of the proposed work is to combine the MRI image and PET image. The goal of generator in GAN is to generate the data distribution same as that of the input data. The goal of discriminator is to differentiate the output image from the original image. When the discriminator is not capable of differentiating the output image from the actual image, the generator has learnt the data. The goal of the GAN proposed in this model is to selectively retain the information present in the input images, namely, MRI and PET. The details retained are controlled by the hyperparameters. Algorithm 1 represents the workflow of the proposed model in generating the fused image.

Given the input images PET and MRI, the whole process of image fusion is represented in Figure 3. To retain the functional details of PET and anatomical details of MRI, we formulated a novel model using GAN to fuse the given input images. The input images are concatenated and sent to the network generator. The output generated from the generator is a fused image I_{fu}. The generated image I_{fu} represents the structural information of MRI I_{mri} and functional details of PET I_{pet}. Followed by this, the output image I_{fu} and the input image is compared. The proposed approach establishes a min max game between generator and discriminator, and with more number of iterations the I_{fu} will contain more and more details from the input image. During the process of training, if the discriminator fails to distinguish between the actual and the generated samples, the generator is trained well. The generated image is then passed as input to the dual discriminator. One discriminator receives MRI image and combined image as the input and the other discriminator receives PET image and the fused image as the

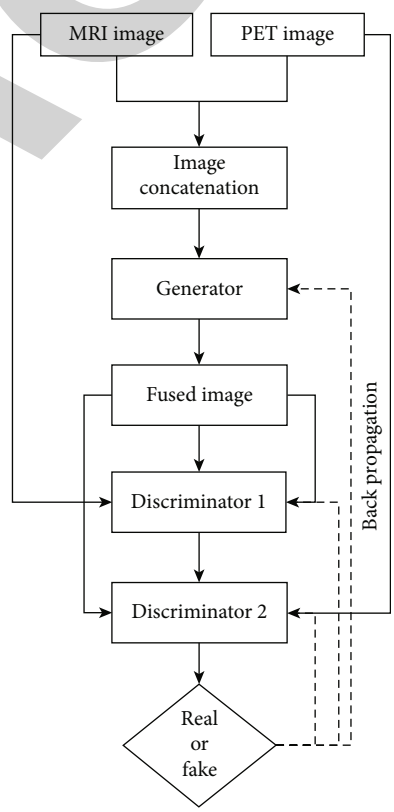

Figure 6: Flowchart of the proposed approach.

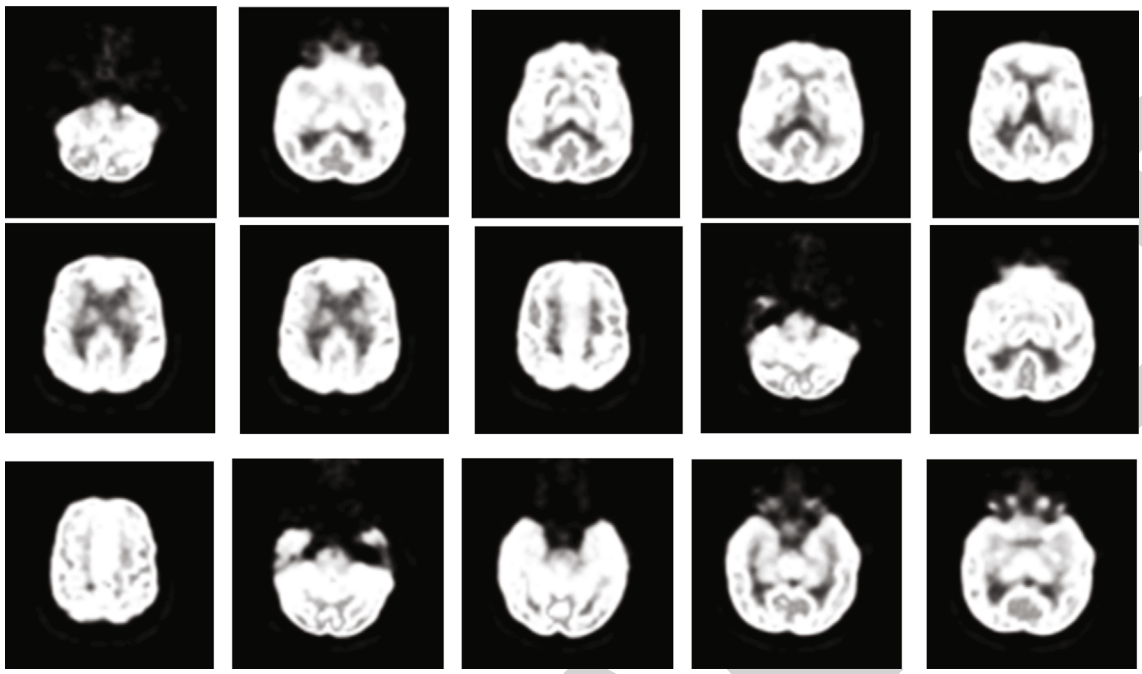

Figure 7: Sample PET images from the dataset.

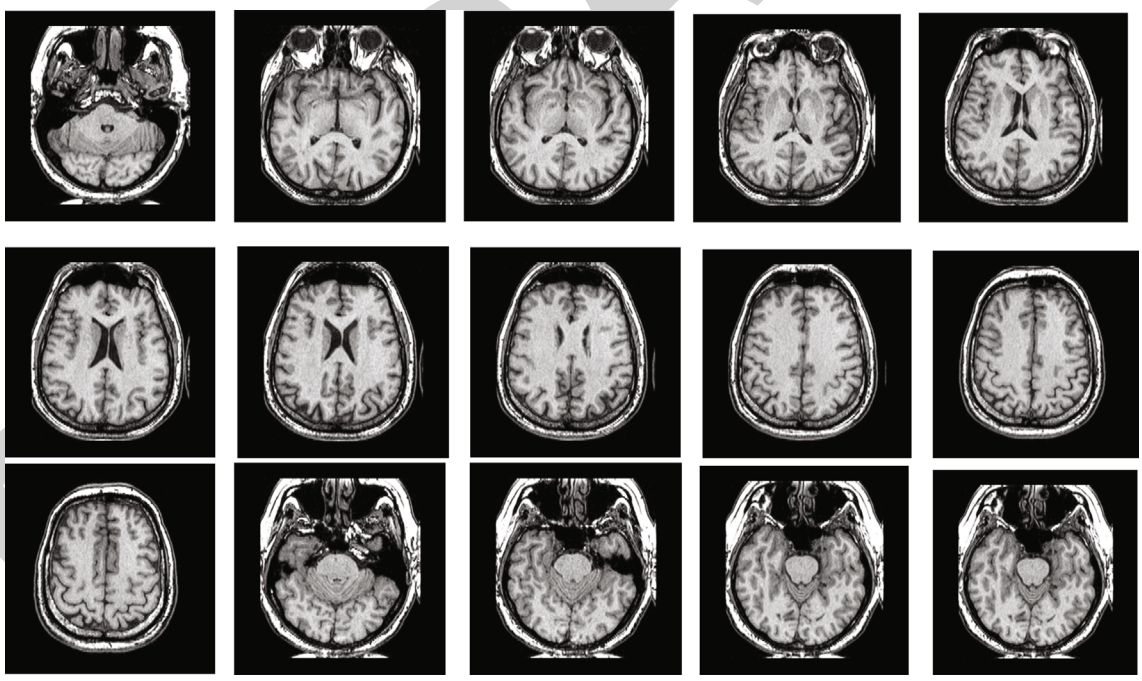

Figure 8: Sample MRI images from the dataset.

input. The discriminator D_m is trained to differentiate the generated image from the MRI image, while the discriminator D_P is trained to differentiate the output image from the PET image. The generator training with two discriminators is formulated as

$$\begin{aligned}\min\ G\ \max\ D_M D_P\,(G,D) = {} & E[\log\ D_M(I_{\mathrm{mri}})] + E\left[\log\left(1 - D_M\left(G\left(I_{\mathrm{mri}}, I_{\mathrm{pet}}\right)\right)\right)\right] \\ & + E\left[\log\ D_P\left(I_{\mathrm{pet}}\right)\right] \\ & + E\left[\log\left(1 - D_P\left(G\left(I_{\mathrm{mri}}, I_{\mathrm{pet}}\right)\right)\right)\right].\end{aligned} \tag{1}$$

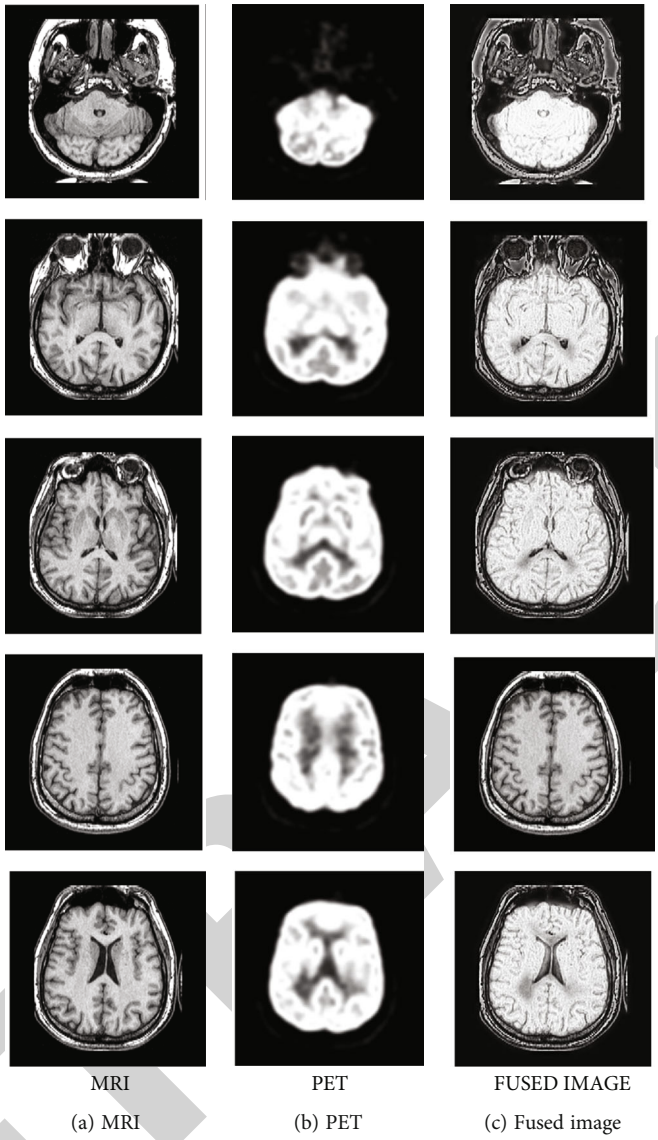

Figure 9: Result obtained from the proposed approach.

According to equation (1), the generator is trained to minimize the above equation and discriminator is trained to maximize the above equation.

The loss function of the proposed model is composed of two losses. One loss is from the generator, and the other loss is from the discriminator. The generator loss L_G represented by equation (1) is again composed of two components. The first component is the adversarial loss, which is the loss between the generator and the discriminator.

$$L_G = L_{\text{Adv}} + \gamma L_{\text{Inf}}. \tag{2}$$

The second component in the generator loss L_G represents the information loss. Since the MRI image I_g has information related to anatomical details of brain and PET image, I_q has information related to function; it is enforced that the fused image I_f to represent similar functional and anatomical information as I_q and I_g. γ is the parameter controlling the tradeoff between adversarial loss and information loss.

The architecture of generator in GAN is represented in Figure 4. The generator has five layer CNN with 3×3 filters in each of the layers. The value of stride in each of these five convolutional layers is set to one. The input to the generator is a PET-MRI concatenated image. The convolutional layers extract feature maps of input image. Batch normalization is used in generator architecture to make the model more stable. Leaky Relu is used in all the layers of the generator before the last layer, and tanh activation function is used in the last layer. Leaky Relu and Tanh are represented as follows:

$$\text{Leaky Relu} = \max\,(0.1x, x), \tag{3}$$

$$\text{tanH} = \tanh\,(x). \tag{4}$$

The architecture of the discriminator of GAN is

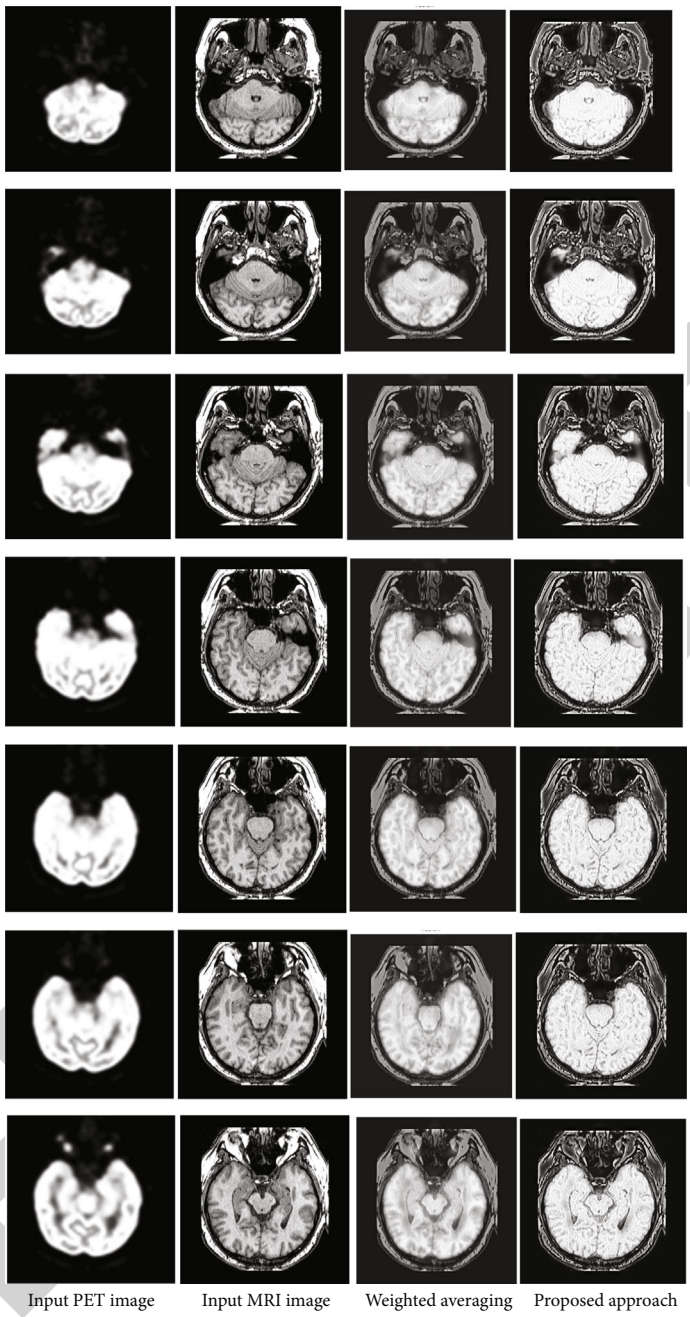

Figure 10: Comparison of obtained fusion results with existing approach.

represented in Figure 5. The discriminator has five layer CNN with 3×3 filters in the first four layers and 1×1 filter in the last layer. The value of stride in each of these five convolution layers is set to two. The discriminator is basically a classifier which first performs feature extraction and then performs classification. Batch normalization is used in the layers between the first and the last layers. Leaky Relu is used as the activation function in all the layers before the last layer, and tanh is used in the last layer. The last layer performs the classification which classifies the image as real or generated image. The flowchart of the proposed approach is represented in Figure 6.

4. Experiments and Results

The data for the proposed approach is obtained from the medical library of Harvard University, (http://www.med.harvard.edu/AANLIB/home.html). Pairs of MRI and PET data were obtained from the database. The database had MRI images of high resolution with size 256×256 and the PET images with size 128×128. In order to perform the fusion of images, PET images were resized to 256×256. Some of the sample PET images obtained from the database are represented in Figure 7, and sample MRI images obtained from the database are shown in Figure 8.

Table 2: Performance evaluation of the proposed approach.

Fusion technique	Average structural similarity	Mutual information
Shift-invariant shearlet transform [37]	0.7104	2.2583
Wavelet transform [38]	0.6725	2.3171
Nonsubsampled shearlet transform [39]	0.8051	2.4336
Multilevel local extrema [40]	0.8175	2.5377
Proposed method	0.8551	2.8059

The result obtained from the proposed approach is represented in Figure 8. Figure 9(a) shows the input MRI image, Figure 9(b) shows the input PET image, and Figure 9(c) shows the generated fused image. From the results obtained, it is clearly visible that the anatomical structure of MRI and functional details of PET are preserved in the resulting fused image. Figure 10 shows the comparison of results obtained from the proposed approach and weighted averaging technique [36].

Table 2 shows the performance of the proposed approach in comparison with other existing approaches in performing medical image fusion. The performance of the proposed model is estimated using average structural similarity and mutual information. Average structural similarity is a metric that determines the similarity between two images and estimates the quality degradation after performing the image fusion. Mutual information is the metric that assesses the quantity of information that is being transferred from the input images and the source image.

$$\text{Mutual information, } I(X\,;Y) = \Sigma_{x\epsilon X}\,\Sigma_{y\epsilon Y} p(x,y)\,\log\,\frac{p(x,y)}{p(x)p(y)}, \tag{5}$$

where $p(x)$ and $p(y)$ are the marginal probability distribution functions of both the margins and $p(x,y)$ is the marginal probability distribution.

$$\text{Structural similarity index, } = \frac{1}{M}\sum_{J=1}^{M} Q(\{i_k(j)\}, F), \tag{6}$$

where Q is the correlation coefficient between the ground truth image and the fused image.

5. Conclusion

In the past few years, image fusion has been immensely used for several image-processing applications in various fields, particularly medical applications like retinopathy and brain tumor segmentation. The work presented a novel approach in performing medical image fusion using generative adversarial networks. The proposed approach efficiently captured the functional information from PET images and anatomical structure from MRI images and transformed them to the resulting fused image. The proposed approach generates fused images with less distortion and better structural information when compared to the existing approaches. The advantages of the proposed approach over the other existing approaches are that it can retain the textural information from the MRI image and the metabolic information from the PET image without losing pixel intensity. The performance of the proposed approach is evaluated using two metrics, namely, structural similarity index and mutual information. The proposed approach achieved a structural similarity index of 0.8551 and a mutual information of 2.8059. The results display that the proposed approach is superior to the existing medical image fusion approaches in preserving the anatomical and functional information of the input images. The work can be extended in performing the fusion of multimodal images with color. Also, the future work can incorporate other deep learning techniques and evaluate the performance using various other metrics. The work still needs to be improved to handle images with more noise.

Abbreviations

MRI: Magnetic Resonance Image
PET: Positron Emission Tomography
GAN: Generative adversarial network
SPECT: Single-Photon Emission Computed Tomography
CT: Computed Tomography
HT: Hilbert Transform
IHS: Intensity Hue Saturation
CNN: Convolutional Neural Network
NN: Neural network.

Data Availability

The original contributions generated for this study are included in the article; further inquiries can be directed to the corresponding author.

Conflicts of Interest

The authors declare that they have no conflicts of interest to report regarding the present study.

Acknowledgments

This research was partially funded by "Intelligent Recognition Industry Service Research Center" from The Featured Areas Research Center Program within the framework of the Higher Education Sprout Project by the Ministry of Education (MOE) in Taiwan and Ministry of Science and Technology in Taiwan (Grant No. MOST 109-2221-E-224-048-MY2).

References

[1] B. Rajalingam, F. Al-Turjman, R. Santhoshkumar, and M. Rajesh, "Intelligent multimodal medical image fusion with deep guided filtering," *Multimedia Systems*, pp. 1–15, 2020.

[2] J. Du, W. Li, and H. Tan, "Three-layer medical image fusion with tensor-based features," *Information Sciences*, vol. 525, pp. 93–108, 2020.

[3] S. Shehanaz, E. Daniel, S. R. Guntur, and S. Satrasupalli, "Optimum weighted multimodal medical image fusion using particle swarm optimization," *Optik*, vol. 231, article 166413, 2021.

[4] B. Huang, F. Yang, M. Yin, X. Mo, and C. Zhong, "A review of multimodal medical image fusion techniques," *Computational and mathematical methods in medicine*, vol. 2020, Article ID 8279342, 16 pages, 2020.

[5] R. Nandhini Abirami, P. M. D. R. Vincent, K. Srinivasan, U. Tariq, and C.-Y. Chang, "Deep CNN and deep GAN in computational visual perception-driven image analysis," *Complexity*, vol. 2021, Article ID 5541134, 30 pages, 2021.

[6] N. Abirami, D. R. Vincent, and S. Kadry, "P2P-COVID-GAN," *International Journal of Data Warehousing and Mining*, vol. 17, no. 4, pp. 101–118, 2021.

[7] R. N. Abiram, P. D. R. Vincent, and School of Information Technology, Vellore Institute of Technology, Vellore, Tamilnadu, India, "Identity preserving multi-pose facial expression recognition using fine tuned VGG on the latent space vector of generative adversarial network," *Mathematical Biosciences and Engineering*, vol. 18, no. 4, pp. 3699–3717, 2021.

[8] A. Esteva, A. Robicquet, B. Ramsundar et al., "A guide to deep learning in healthcare," *Nature Medicine*, vol. 25, no. 1, pp. 24–29, 2019.

[9] M. A. Khan, K. Muhammad, M. Sharif, T. Akram, and S. Kadry, "Intelligent fusion-assisted skin lesion localization and classification for smart healthcare," *Neural Computing and Applications*, pp. 1–16, 2021.

[10] V. P. Sudarshan, G. F. Egan, Z. Chen, and S. P. Awate, "Joint PET-MRI image reconstruction using a patch-based joint-dictionary prior," *Medical Image Analysis*, vol. 62, article 101669, 2020.

[11] M. A. Khan, M. I. Sharif, M. Raza, A. Anjum, T. Saba, and S. A. Shad, "Skin lesion segmentation and classification: a unified framework of deep neural network features fusion and selection," *Expert Systems*, no. article e12497, 2019.

[12] M. Nazir, M. A. Khan, T. Saba, and A. Rehman, "Brain tumor detection from MRI images using multi-level wavelets," in *2019 international conference on Computer and Information Sciences (ICCIS)*, pp. 1–5, Sakaka, Saudi Arabia, 2019.

[13] A. A. Khan and R. T. de Rosales, "Radiolabelling of extracellular vesicles for PET and SPECT imaging," *Nanotheranostics*, vol. 5, no. 3, pp. 256–274, 2021.

[14] F. Gao, "Integrated positron emission tomography/magnetic resonance imaging in clinical diagnosis of Alzheimer's disease," *European Journal of Radiology*, vol. 145, article 110017, 2021.

[15] V. A. Rani and S. Lalithakumari, "Efficient medical image fusion using 2-dimensional double density wavelet transform to improve quality metrics," *IEEE Instrumentation and Measurement Magazine*, vol. 24, no. 4, pp. 35–41, 2021.

[16] K. Brahmbhatt and M. Joshi, "Image fusion in discrete wavelet transform: a review," *Aut Aut Research Journal*, vol. 11, no. 12, pp. 483–486, 2020.

[17] M. A. Khan, T. Akram, M. Sharif, S. Kadry, and Y. Nam, "Computer decision support system for skin cancer localization and classification," *Computers, Materials & Continua*, vol. 68, no. 1, pp. 1041–1064, 2021.

[18] M. A. Khan, M. Rashid, M. Sharif, K. Javed, and T. Akram, "Classification of gastrointestinal diseases of stomach from WCE using improved saliency-based method and discriminant features selection," *Multimedia Tools and Applications*, vol. 78, no. 19, pp. 27743–27770, 2019.

[19] A. Addeh and M. Iri, "Brain tumor type classification using deep features of MRI images and optimized RBFNN," *Engineering Transactions*, vol. 2, pp. 1–7, 2021.

[20] A. Rehman, M. A. Khan, T. Saba, Z. Mehmood, U. Tariq, and N. Ayesha, "Microscopic brain tumor detection and classification using3D CNNand feature selection architecture," *Microscopy Research and Technique*, vol. 84, no. 1, pp. 133–149, 2021.

[21] M. Attique Khan, M. Sharif, T. Akram, S. Kadry, and C.-H. Hsu, "A two-stream deep neural network-based intelligent system for complex skin cancer types classification," *International Journal of Intelligent Systems*, pp. 1–29, 2021.

[22] F. Grosse, F. Wedel, U. W. Thomale et al., "Benefit of static FET PET in pretreated pediatric brain tumor patients with equivocal conventional MRI results," *Klinische Pädiatrie*, vol. 233, no. 3, pp. 127–134, 2021.

[23] R. Matthews and M. Choi, "Clinical utility of positron emission tomography magnetic resonance imaging (PET-MRI) in gastrointestinal cancers," *Diagnostics*, vol. 6, no. 3, p. 35, 2016.

[24] M. Haddadpour, S. Daneshvar, and H. Seyedarabi, "PET and MRI image fusion based on combination of 2-D Hilbert transform and IHS method," *Biomedical journal*, vol. 40, no. 4, pp. 219–225, 2017.

[25] H. R. Shahdoosti and A. Mehrabi, "MRI and PET image fusion using structure tensor and dual ripplet-II transform," *Multimedia Tools and Applications*, vol. 77, no. 17, pp. 22649–22670, 2018.

[26] H. Ouerghi, O. Mourali, and E. Zagrouba, "Non-subsampled shearlet transform based MRI and PET brain image fusion using simplified pulse coupled neural network and weight local features in YIQ colour space," *IET Image Processing*, vol. 12, no. 10, pp. 1873–1880, 2018.

[27] J. Du, W. Li, and H. Tan, "Intrinsic image decomposition-based grey and pseudo-color medical image fusion," *IEEE Access*, vol. 7, pp. 56443–56456, 2019.

[28] Z. Liu, Y. Song, V. S. Sheng et al., "MRI and PET image fusion using the nonparametric density model and the theory of variable-weight," *Computer Methods and Programs in Biomedicine*, vol. 175, pp. 73–82, 2019.

[29] H. Tang, B. Xiao, W. Li, and G. Wang, "Pixel convolutional neural network for multi-focus image fusion," *Information Sciences*, vol. 433-434, pp. 125–141, 2018.

[30] J. Ma, W. Yu, P. Liang, C. Li, and J. Jiang, "FusionGAN: a generative adversarial network for infrared and visible image fusion," *Information Fusion*, vol. 48, pp. 11–26, 2019.

[31] H. Xu, P. Liang, W. Yu, J. Jiang, and J. Ma, "Learning a generative model for fusing infrared and visible images via conditional generative adversarial network with dual discriminators," in *Proceedings of the Twenty-Eighth International Joint Conference on Artificial Intelligence*, pp. 3954–3960, Macao, China, 2019.

[32] J. Ma, P. Liang, W. Yu et al., "Infrared and visible image fusion via detail preserving adversarial learning," *Information Fusion*, vol. 54, pp. 85–98, 2020.

[33] S. P. Yadav and S. Yadav, "Image fusion using hybrid methods in multimodality medical images," *Medical & Biological Engineering & Computing*, vol. 58, no. 4, pp. 669–687, 2020.

[34] J. Jose, N. Gautam, M. Tiwari et al., "An image quality enhancement scheme employing adolescent identity search algorithm in the NSST domain for multimodal medical image

Hindawi
Behavioural Neurology
Volume 2023, Article ID 9784791, 1 page
https://doi.org/10.1155/2023/9784791

Retraction

Retracted: Early Stroke Prediction Methods for Prevention of Strokes

Behavioural Neurology

Received 19 December 2023; Accepted 19 December 2023; Published 20 December 2023

This article has been retracted by Hindawi following an investigation undertaken by the publisher [1]. This investigation has uncovered evidence of one or more of the following indicators of systematic manipulation of the publication process:

(1) Discrepancies in scope

(2) Discrepancies in the description of the research reported

(3) Discrepancies between the availability of data and the research described

(4) Inappropriate citations

(5) Incoherent, meaningless and/or irrelevant content included in the article

(6) Manipulated or compromised peer review

The presence of these indicators undermines our confidence in the integrity of the article's content and we cannot, therefore, vouch for its reliability. Please note that this notice is intended solely to alert readers that the content of this article is unreliable. We have not investigated whether authors were aware of or involved in the systematic manipulation of the publication process.

Wiley and Hindawi regrets that the usual quality checks did not identify these issues before publication and have since put additional measures in place to safeguard research integrity.

We wish to credit our own Research Integrity and Research Publishing teams and anonymous and named external researchers and research integrity experts for contributing to this investigation.

The corresponding author, as the representative of all authors, has been given the opportunity to register their agreement or disagreement to this retraction. We have kept a record of any response received.

References

[1] M. Kaur, S. R. Sakhare, K. Wanjale, and F. Akter, "Early Stroke Prediction Methods for Prevention of Strokes," *Behavioural Neurology*, vol. 2022, Article ID 7725597, 9 pages, 2022.

Hindawi
Behavioural Neurology
Volume 2022, Article ID 7725597, 9 pages
https://doi.org/10.1155/2022/7725597

Research Article

Early Stroke Prediction Methods for Prevention of Strokes

Mandeep Kaur,[1] **Sachin R. Sakhare**,[2] **Kirti Wanjale**,[2] **and Farzana Akter**[3]

[1]*Department of Computer Science, Savitribai Phule Pune University, Pune, India*
[2]*Computer Engineering Department, Vishwakarma Institute of Information Technology, Kondhwa (Bk), Pune, India*
[3]*Department of ICT, Bangabandhu Sheikh Mujibur Rahman Digital University, Bangladesh*

Correspondence should be addressed to Farzana Akter; farzana@ict.bdu.ac.bd

Received 26 November 2021; Revised 2 March 2022; Accepted 21 March 2022; Published 11 April 2022

Academic Editor: Suresh Satapathy

The emergence of the latest technologies gives rise to the usage of noninvasive techniques for assisting health-care systems. Amongst the four major cardiovascular diseases, stroke is one of the most dangerous and life-threatening disease, but the life of a patient can be saved if the stroke is detected during early stage. The literature reveals that the patients always experience ministrokes which are also known as transient ischemic attacks (TIA) before experiencing the actual attack of the stroke. Most of the literature work is based on the MRI and CT scan images for classifying the cardiovascular diseases including a stroke which is an expensive approach for diagnosis of early strokes. In India where cases of strokes are rising, there is a need to explore noninvasive cheap methods for the diagnosis of early strokes. Hence, this problem has motivated us to conduct the study presented in this paper. A noninvasive approach for the early diagnosis of the strokes is proposed. The cascaded prediction algorithms are time-consuming in producing the results and cannot work on the raw data and without making use of the properties of EEG. Therefore, the objective of this paper is to devise mechanisms to forecast strokes on the basis of processed EEG data. This paper is proposing time series-based approaches such as LSTM, biLSTM, GRU, and FFNN that can handle time series-based predictions to make useful decisions. The experimental research outcome reveals that all the algorithms taken up for the research study perform well on the prediction problem of early stroke detection, but GRU performs the best with 95.6% accuracy, whereas biLSTM gives 91% accuracy and LSTM gives 87% accuracy and FFNN gives 83% accuracy. The experimental outcome is able to measure the brain waves to predict the signs of strokes. The findings can certainly assist the physicians to detect the stroke at early stages to save the lives of the patients.

1. Introduction

Nowadays, due to technological advancements, life expectancy of human being is rising day by day. The lifestyle has been changed from active lifestyle to sedentary lifestyle due to the advent of technical gadgets such as laptops, smart phones, and portable devices. Not only the aging society but the young generation is also facing many health problems such as cardiovascular diseases, diabetes, hypertension, and strokes due to inactive lifestyle. There is a need of smart health-care devices to monitor the health of individuals by using some biomarkers and noninvasive smart techniques. The studies in the exiting literature produce evidences of bad impact of sedentary lifestyle on human health [1–3]. In this paper, we are focusing on the problem of strokes, and an attempt is made to devise a system which uses bioelectrical images to predict the strokes. The major cause behind stroke is disruption of blood supply due to clotting in the blood to the nerves in the brain. The stroke can be major or minor. In minor stroke, the blood supply to some parts of the brain is hampered, and in major stroke, the person can lose life. Stroke is an emergency health condition which has to be dealt with carefully. The common symptoms include trouble in movement, confusions, improper verbal communication, and difficulty in understanding. Stroke causes long-term neurological damage and death.

There are two categories of stroke, ischemic embolic and hemorrhagic. Ischemic embolic stroke occurs when there is a blood lump at heart and not in the brain, and it narrows the brain arteries. In hemorrhagic stroke, there is blood leakage

at the artery in the brain due to the damage. For elderly generation, stroke can be lethal. The heart gets damage during the heart attack and stroke damage the brain in a similar manner. Once a person is diagnosed with stroke disease, it needs continuous health monitoring. The stroke starts with a ministroke which is known as transient ischemic attacks (TIA). It is the condition which reveals that the person will face stroke within a couple of days from the occurrence of the ministroke. The World Health Organization (WHO) claims that there are frequent deaths due to stroke [4]. If stroke is detected or diagnosed early, the loss of death and severe damage to brain can be prevented in 85% cases [5]. Extra care is needed for senior citizens as it is more lethal for the aging community. A disease like stroke needs continuous monitoring and observation. The rate of stroke cases is increasing day by day due to stress, inactivity, consumption of drugs, and bad dietary habits [6].

Stroke causes dysfunctionalities at some parts of the brain locations which results into problems in the brain blood vessels [6]. In 2016, WHO has published one report which reveals that stroke is the second most growing reason of disability in the current population worldwide. In the past 40 years, it has been observed that the number of cases of stroke doubled with the passage of each decade [7]. There is no specific treatment in medical science for handling strokes; therefore, early diagnosis is the key to handle strokes. The early detection can prevent disabilities, loss of deaths, and other brain-related severe ailments [8]. In most of the stroke identification-existing studies, magnetic resonance imaging (MRI) and computed tomography (CT) are used, but these techniques expose the patients to radiations or probable allergic reactions. Secondly, MRI or CT scans are very expensive methods for diagnosis, and people in underdeveloped countries cannot take advantage of these techniques due to excessive cost. Nowadays, noninvasive techniques such as EEG (electroencephalogram) are getting popularity which is also cost-effective or nonexpensive technique [9, 10]. COVID-19 has also increased the cases of strokes. Many authors have investigated the correlation between the history of strokes and deaths of the hospitalized patients with COVID-19 [4]. From the comprehensive study of 3248 patients, it is found that history of stroke is significantly associated with the deaths of hospitalized patients. The clinical course of COVID-19 patients with the history of stroke is examined. Even in COVID-19 patients, the noninvasive techniques have played a great role in identification of strokes. The studies are also correlating stress and depression with strokes [11].

1.1. Related Work. This subsection discusses the exiting works in the area of the proposed research.

The study presented in [6] is also devising a software-based model where screening of depression is performed with deep learning and EEG signals are used to distinguish between normal brain signals and abnormal brain signals which induce strokes. The authors also found that right hemisphere signals are more idiosyncratic during depression as compared to the left hemisphere. In [12], the authors have invented one device for detection of stroke along with time and duration. In [7], the authors have combined EEG with galvanic skin response (GSR) signals for the diagnosis of strokes, but the accuracy is 73.8%. In [9], the authors have used EEG data without using the frequency characteristics of EEG. Real-time data is gathered from EEG sensors to develop and train the stroke detection model. In [10], the authors have combined the bioelectrical signals with natural language processing, and then, machine learning is used for classification of strokes and normal signals. In [11], a bidirectional deep neural network is used for EEG-based image classification. The information of signals is processed at various regions to distinguish between right and left hemispheres of the brain. Finally, the classification is made between abnormal and normal signals. Paper [13] uses sparse representation (SR) and CNN for classification of MRI images to detect strokes. In [14], the deep learning-based classification is utilized that learns from end-to-end information without extracting handcrafted features and considers multiple bioelectrical signals for classification.

In [15], the authors have used time series concept for classification of brain signals by transforming single-dimensional time series to a double-dimensional image classification problem. In [16], the authors have devised a prediction model that shows stepwise improvement in the correct prediction of brain signals to detect the early stages of strokes. In article [17], the authors have utilized EEG signal-based classification, and prior to applying classification techniques, the signals are transformed into images, and then, neural networks are applied for detection of strokes. The aim of [18] is to use deep neural network for decoding the EEG signals. The authors have examined the methods for single-trial and multitrial EEG classification. The researchers have proposed many approaches [19–23] for dealing with strokes to minimize the damage of brain tissues. The existing techniques have certain flaws such as time complexity for producing the results, expensive data generated by using MRI or CT scans, and space complexity where finding solution is difficult to determine the difference between ministroke (TIA) and actual stroke. In order to overcome these problems, this paper is proposing a noninvasive technique for identifying the bioelectrical signals (specifically EEG) with deep learning models to predict the strokes at early stage.

The highlights of the stroke prediction strategy are as follows:

(a) The strategy is using deep learning-based predictors to predict the strokes. Three deep learning models are devised to test the efficacy of three different models because accurate prediction plays important role in predicting the results

(b) The first phase collects the raw data based on EEG bioelectrical signals

(c) The next phase extracts the features from the data and the characteristics of the frequency of signals

(d) The stored signal-based data is consumed as an input to the deep learning-based modules

(e) Then, the time series-based prediction module is invoked which predicts whether the patient can have stroke or TIA

(f) The predicted stroke outputs are compared with the actual outputs to judge the efficacy of the time series-based deep learning models

The paper is organized into four sections. The next section highlights the methods used in the research study. The results and inferences are presented in the third section of the paper. The last part is summarizing the paper work.

2. Proposed Methods

The methods proposed in this paper are based on time series prediction methods. The steps of the proposed method are described below and also shown in Figure 1.

(a) The first phase collects the raw data based on EEG bioelectrical signals

(b) The next phase extracts the features and the important characteristics of the frequency of signals

(c) The next phase prepares the model based on deep learning-based predictors

(d) The stored signal-based data is consumed as an input to the deep learning-based modules

(e) Then, the time series-based prediction module is invoked which predicts whether the patient can have stroke or TIA

2.1. Collection of Bioelectrical Signals (EEG, ECG, and EMG) through Smart Sensing Devices. The bioelectrical signals such as EEG (electroencephalography) are collected through sensors as in our research work. We have made use of noninvasive technique. EEG is preferred over other two techniques, ECG (electrocardiography) and EMG (electromyography), as other methods are invasive methods. The easiest method is adopted to collect the RAW data as bioelectrical signals. The bioelectrical signals can help in diagnosis of strokes as the sequence of signals reveal whether everything is normal or there are some abnormalities in terms of TIA or strokes. Figure 2 is depicting the bioelectrical signal-based collection of data where brain signals are recorded to reveal the conditions of strokes in earlier stages.

2.2. Porting of RAW Data to the Server. The EEG data is gathered by using six channels at predetermined frequency of 1000 Hz. The data is collected in the form of bioelectrical signals, and the collected data is ported to the server. The server prepares the database of the collected raw data. The data is then prepared for preprocessing, and then, the features are extracted. The signals of EEG are categorized into five types of signals as shown in Figure 3. The categories include alpha, beta, gamma, theta and delta. It is very important to use these categories of the signals to detect normal people and stroke affected people.

2.3. Stroke Forecasting Module. The next is our stroke forecasting module which is based on deep neural networking techniques. The series of processes contribute in this module where we have taken up four algorithms for checking the viability of the algorithms on the problem statement of detection of early strokes. The first algorithm is FFNN which is feeding the neural network in a forward manner, the next is LSTM (a better version of recurrent neural network), an attempt is made to try with bidirectional LSTM (biLSTM), and then finally, GRU has been tried to produce the more accurate results. The deep learning methods get the input as raw data of EEG signals, the waveline analysis is learned from an offline data, and then, the trained algorithms are tried on the actual data to analyze the wave signals. In order to learn from the offline data, the neural networks are trained against all types of possible signals of brain to identify strokes. Since the patterns are almost fixed and almost all the signals find their similar signals in the offline dataset for training, the testing results are quite promising. The trained and tuned module can certainly predict whether the signals belong to a person who is having stroke or to a normal person.

The LSTM algorithm forecasts the next stage by keeping historical and futuristic information as LSTM has forget gates to remember more data. The biLSTM overcomes the shortcomings of LSTM by incorporating a backward processing layer in normal LSTM. The biLSTM is more powerful than LSTM in providing accuracy as biLSTM can infer from the historical data for the future and also perform the reverse inference from future to history. The GRU is also tried as GRU is less complex and delivers the results in lesser span of time. While LSTM has three gates, GRU has two gates, reset and update. Feed forward is also tried with the EEG data to make the comparison of the deep learning techniques and to evaluate the output accuracy.

2.3.1. Prediction Framework. To predict the early strokes on the basis of symptoms recorded in terms of data fields, the neural network-based predictors are proposed as transfer learning models which learn from the offline data and can be applied on the online quick data for predicting the likely chances of strokes. The predictors are designed into threefold strategy: Processing of data during training, to train the model from offline stroke-based data, and transfer phase where offline training is applied on online data for prediction of strokes.

(1) Data Processing. The data has to be processed after receiving the offline data to train the stroke prediction model, and when the data is collected online, then the collected data is transformed in discrete units. The discrete units are then supplied to the predictor in a sequence.

(2) Module Preparation. The stroke predictor requires building of the model based on the input data, and this phase is very important; the second phase is of prime importance which builds the model. We have adopted three-layered structures to minimize the time complexity and to keep the model simple for usage of physicians. Layer one is the input

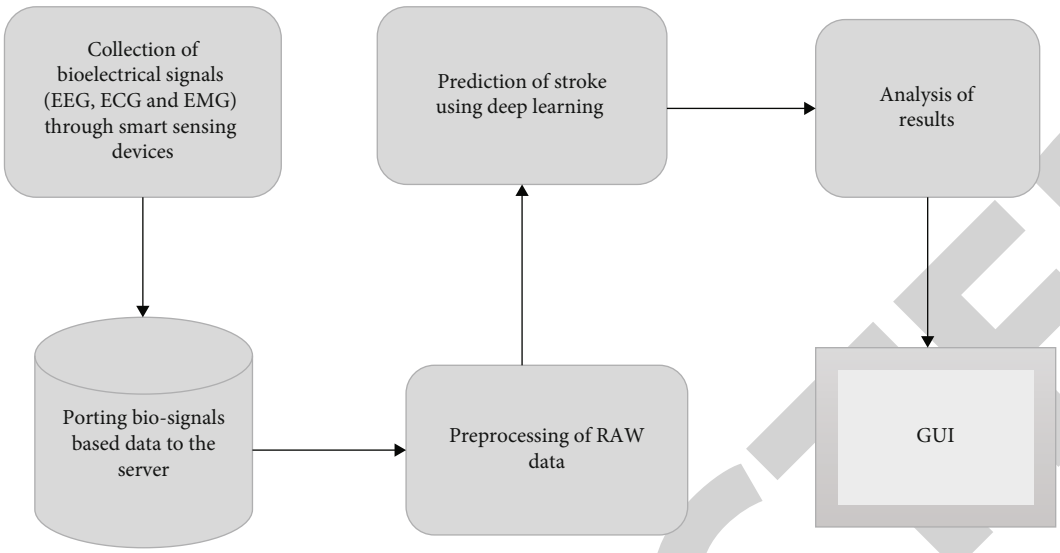

Figure 1: Architecture diagram of the proposed work.

Figure 2: Collection of bioelectrical signals using EEG.

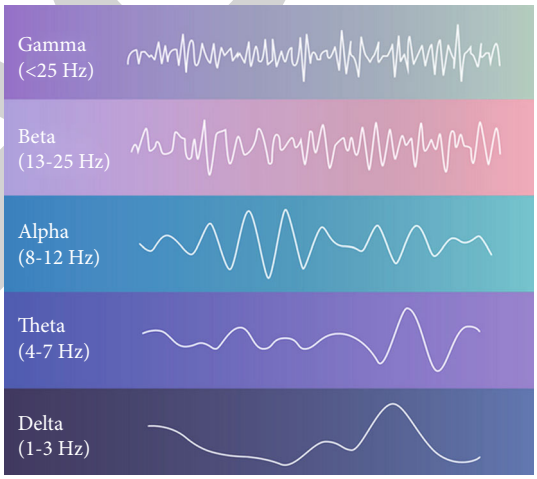

Figure 3: Types of EEG waves found in human brain.

layer, and it contains neurons which represents dimension of the stroke-based data. The hidden or intermediate layer is decided by the empirical study to get the more accurate results. The output layer predicts whether the patient can have strokes or not.

(3) Training Phase. The training phase begins with the module training on offline stroke-based data. This phase optimizes the loss function value to retain the information intact between the layers and to help the model to converge at global optima solution. In biLSTM and GRU, ion filter is adopted to escape the model from converging at local optima.

(4) Testing Phase. The predictors are tested on the online or real-time data to check the efficacy of the models. It is found that GRU-based predictor gives the most accurate stroke prediction results, followed by biLSTM and FFNN methods.

2.3.2. Analysis of the Outcome. Once the output is received from the proposed methods, the outcome is evaluated against the statistical performance evaluators to check whether the proposed algorithms are predicting with accuracy whether the person is normal or can have ministroke (TIA) or actual stroke. The analysis is made on the basis of RMSE score (root mean square error), MAE (mean absolute error), MSE (mean squared error), MRE (mean relative error), and time consumption for producing output.

2.3.3. GUI-Based Output. The final module is graphically presenting the results to the user whether the input data shows abnormality in the wavelines and a person can experience stroke in the near future or everything is normal.

3. Results and Inferences

3.1. Experimental Results. In this subsection, the performance is evaluated on the basis of statistical metrics. We

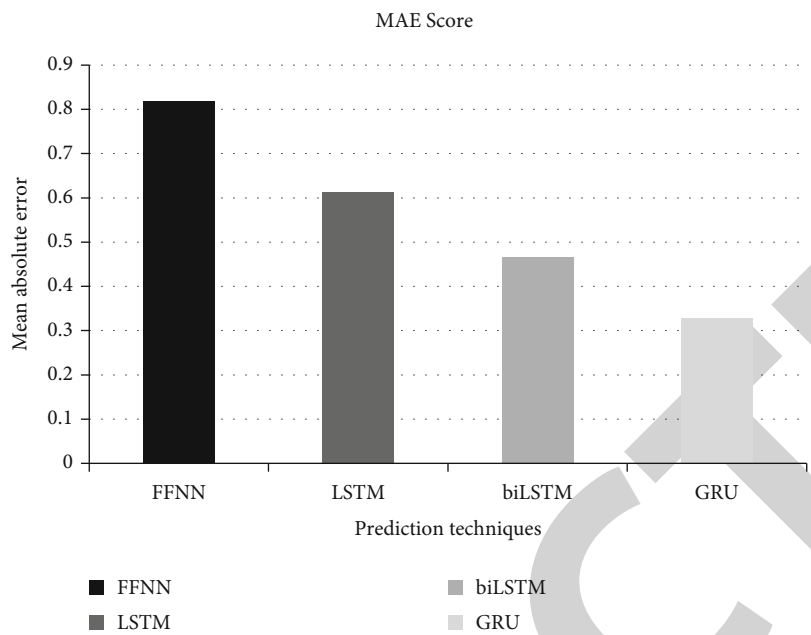

Figure 4: MAE values obtained by the proposed and other models.

have used statistical error analysis to predict the capability of proposed techniques. To evaluate the prediction capability of the proposed GRU, biLSTM, and other prediction methods, the statistical error analysis methods are used. In order to obtain the results, the machines with special configuration capabilities are used to train the models such as 16 GB RAM, GPU—NVIDIA GeForce GTX 940, and Microsoft Windows 10 (64-bit) platform. GPUs are required to train the deep neural networks, and after training, testing is also performed on the same machines.

(1) Mean absolute error (MAE) represents median of all the absolute errors and formulae is expressed below in Equation (1).

$$\mathrm{MAE} = \frac{1}{m}\sum_{a=1}^{m}|X_a - X|, \tag{1}$$

where the number of errors is represented by m, $\sum$ represents addition of all values, and $|X_a - X|$ is the absolute errors

In the following chart (Figure 4), the mean absolute error value for each technique is displayed. It is obtained for all the prediction methods (GRU, biLSTM, LSTM, and FFNN) reflected in the proposed work section. The results demonstrate that for proposed GRU method has achieved highest accuracy with minimal error, the MAE score for biLSTM is also better than other techniques considered in the study such as LSTM and FFNN. It is found that biLSTM is performing far better than the conventional LSTM as it has ability to work in a forward as we all backward direction. The feed forward method is not performing well in the time series problem.

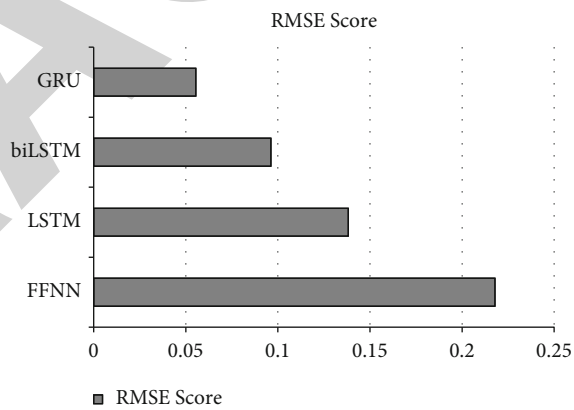

Figure 5: RMSE score obtained by the applied algorithms.

(2) Root mean square error (RMSE) depicts the standard deviation of the predicted errors. The formula for it is expressed in Equation (2).

$$\mathrm{RMSE} = \sqrt{\frac{\sum_{a=1}^{m}\left(X_a - \widehat{X}_a\right)^2}{M}}, \tag{2}$$

where M is equal to the number of nonmissing data points, a is the variable, X_a is the actual observations of time series and $\widehat{X}_a$ represents forecasted time series

In the chart (Figure 5), RMSE values are presented for all the applied algorithms. Proposed GRU algorithm gives excellent results with respect to RMSE score and beats other algorithms considered for study.

(3) Mean squared error (MSE) is a summary of the prediction ability and accuracy predicted for the

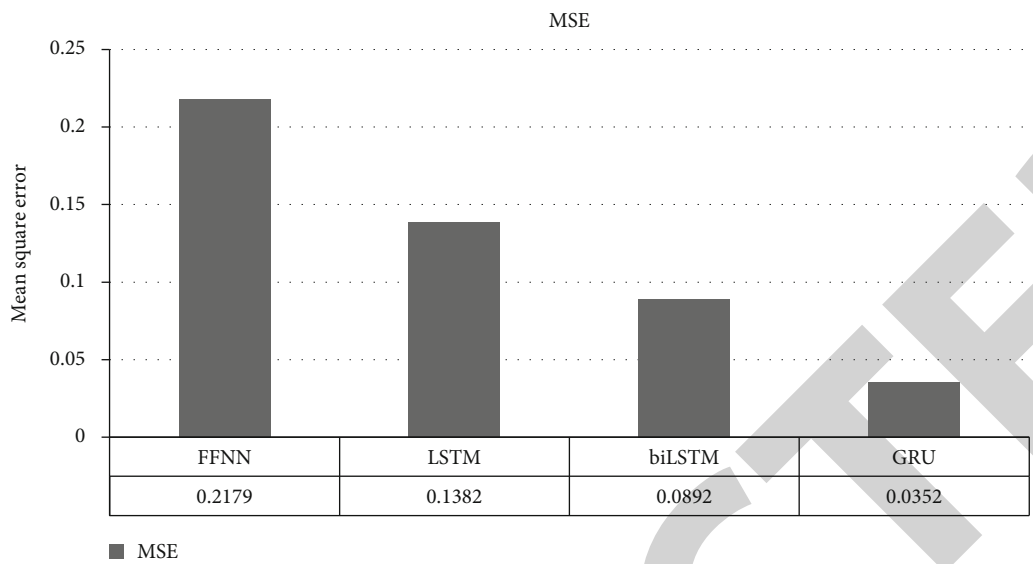

Figure 6: Presenting MSE values found by applied algorithms.

proposed GRU model. A formula for it is given in Equation (3).

$$\mathrm{MSE} = \frac{1}{m} * \sum (\mathrm{actual} - \mathrm{predicted})^2 \quad (3)$$

The results of MSE scores are given in Figure 6. It can be inferred that GRU gives the best accuracy, followed by biLSTM, LSTM, and FFNN. In this paper, we have compared proposed GRU-based prediction algorithm with three comparative algorithms which are benchmarked methods for the prediction of the stroke. When we compare GRU with the LSTM and FFNN stroke prediction algorithm, performance of the GRU is best. It also has ability to predict by retaining relevant information in its layers. The biLSTM is capable to process short-term time series, whereas GRU can consider long-term series also. It is observed from statistical continuity that LSTM does not support nonlinear fitting capability. Performance of the LSTM is good in the diagnosis of strokes diseases, but sometimes, the relevant information is lost in the hidden layers. Accuracy of GRU is more as compared to LSTM.

To verify the time complexity and efficiency of convergence of the algorithms, the iterations for training set are defined similarly for the algorithms considered for the research, and it is observed from Figure 7 that the GRU outperforms other techniques with respect to MRE scores. However, the beginning relative error of the proposed GRU is higher, and gradually, it decreases. The other techniques also behave in the same manner, but GRU shows the best performance with respect to the MRE scores.

(4) Specificity and sensitivity scores are used to measure the accuracy in the results produced by the implemented algorithms

Figure 8 demonstrates the sensitivity and specificity scores obtained by the various methods. All the methods work well for classifying the strokes, but the proposed GRU stroke identification or forecasting method outperforms other forecasting models. The time series-based models, LSTM and biLSTM, also perform well and provide quite accurate results. Timely forecasting is very important to save the life of the patient. Delay in prediction may lead to fatal outcomes. The specificity allows the correct identification of patients who can have strokes in the near future. The sensitivity specifies how often the proposed forecasting models can correctly generate the positive results for the patients who can definitely have problem of strokes in the near future.

3.2. Analysis. Stroke is related to the serious brain condition which can give rise to severe problems like reduction in blood perfusion, decrease in glucose supply, and decrease in oxygen supply in the brain. It may lead to paralysis attack or may lead to death as well. The brain's electrical activity in case of ischemic stroke is associated with hypoperfusion of cerebral tissues. An ischemic stroke is a serious condition which hampers the blood supply to the brain, and it prevents the tissues of the brain from getting enough oxygen for proper functioning of the brain. In this case, brain cells start dying in minutes. The hemorrhagic stroke occurs due to a burst or permeable blood vessels that bleed into the brain. The reduction in blood supply to the brain damages tissues and causes paralysis, numbness in arm, face, or leg, slurred speech, behaviour changes, loss of balance, dizziness, nausea, or severe headache. The damage caused by stroke is irreversible. Hence, this paper attempts to bring a solution in the form of early stroke prediction model which can reveal whether the person can have stroke in the future on the basis of biomarkers study, EEG signals, and the characteristics of the frequency of signals. We have made use of deep learning models in this research study for accurate predictions of the

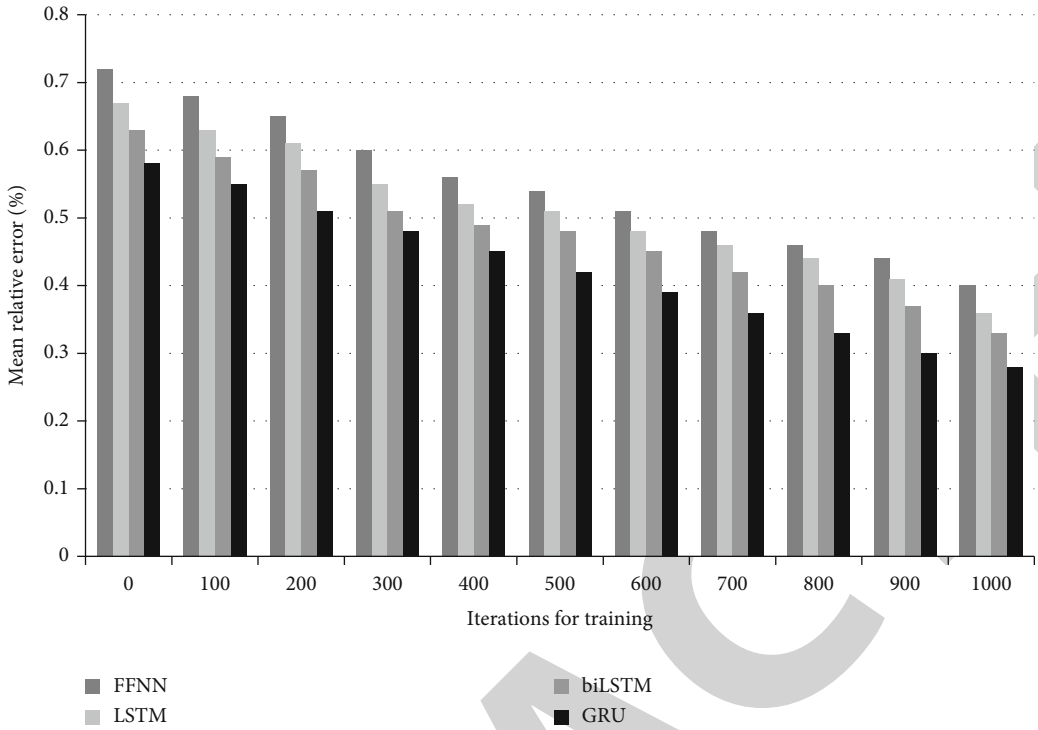

Figure 7: MRE values obtained by diverse techniques in defined iterations.

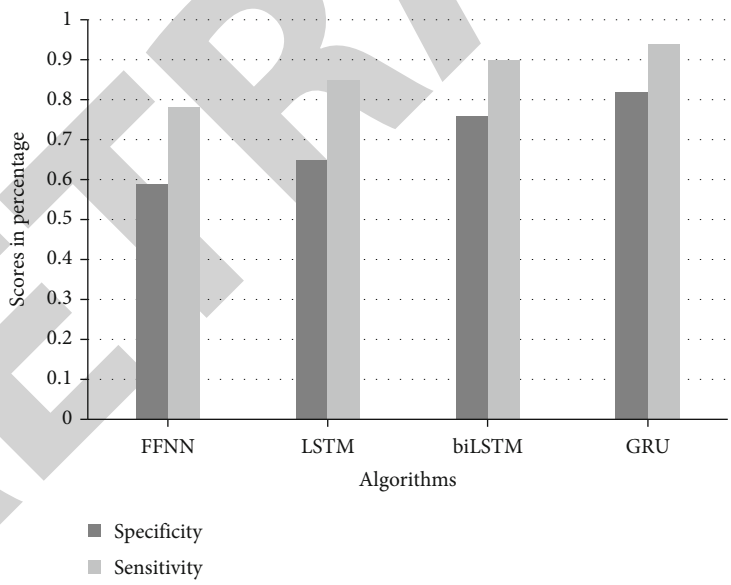

Figure 8: Specificity and sensitivity scores obtained by various techniques.

early stroke conditions. The four deep learning models are tried, and their respective results are compared in this section to judge the accuracy and viability of the proposed models. The results show that GRU performs the best in terms of accurate predictions and biLSTM and LSTM also perform well in predicting the early strokes. By adopting the proposed model, physicians can certainly identify the patients who may likely suffer from strokes in the future. The early detection can assist the doctors for treating the patients on time. Prevention is always better than cure, and timely forecasting of strokes can save many lives.

4. Conclusion

In this paper, a framework for identification of bioelectrical signals with the aid of deep learning is proposed that enables the early detection and prediction of stroke disease. The prediction model is capable of learning from offline data and

then make predictions on the online data quickly for early detection of strokes. Nowadays, ministrokes/TIA also signifies that the person may get stroke sooner or later. Early detection of signals can certainly assist the physicians to start quick treatments for the prevention of strokes. The damage of stroke is irreversible, and prevention is the only cure for strokes. Hence, this paper is presenting a quick technique based on noninvasive method which uses EEG signals as raw data to train the framework and then to predict whether the person can have stroke in the near future or the signals are normal. The proposed framework uses four different deep learning techniques to check the versatility of the deep neural networks for prediction of strokes, and it is found that all the deep learning techniques can work well for detecting strokes from the biosignals, but GRU and biLSTM outperform the conventional LSTM and FFNN. The accuracy is better with GRU and biLSTM; the prediction error rates are minimal for GRU and biLSTM as compared to LSTM and FFNN. The specificity score obtained by GRU is 0.82, biLSTM is 0.76, LSTM is 0.65, and FFNN is 0.59, whereas the sensitivity score obtained by GRU is 0.94, biLSTM is 0.90, LSTM is 0.85, and FFNN is 0.78. It is a remarkable research outcome that reveals that the stroke could be detected so easily by using the proposed noninvasive framework. In the future, more methods will be considered along with EEG such as ECG and CT scan images for better prediction and prevention of strokes.

Data Availability

The data gathered online can be made available, but offline data which is used for training the module is restricted to share as per the norms of data provider.

Conflicts of Interest

The authors declare that they have no conflicts of interest.

References

[1] V. L. Feigin, M. H. Forouzanfar, R. Krishnamurthi et al., "Global and regional burden of stroke during 1990-2010: findings from the Global Burden of Disease Study 2010," *Lancet*, vol. 383, no. 9913, pp. 245–255, 2014.

[2] G. A. Roth, G. A. Mensah, C. O. Johnson et al., "Global burden of cardiovascular diseases and risk factors, 1990-2019: update from the GBD 2019 study," *Journal of the American College of Cardiology*, vol. 76, no. 25, pp. 2982–3021, 2020.

[3] N. M. Mule, D. D. Patil, and M. Kaur, "A comprehensive survey on investigation techniques of exhaled breath (EB) for diagnosis of diseases in human body," *Informatics in Medicine Unlocked*, vol. 26, article 100715, 2021.

[4] L. Zhang, W. Sun, Y. Wang et al., "Clinical course and mortality of stroke patients with coronavirus disease 2019 in Wuhan, China," *China Stroke*, vol. 51, no. 9, pp. 2674–2682, 2020.

[5] M. Lee, J. Ryu, and D. Kim, "Automated epileptic seizure waveform detection method based on the feature of the mean slope of wavelet coefficient counts using a hidden Markov model and EEG signals," *ETRI Journal*, vol. 42, no. 2, pp. 217–229, 2020.

[6] U. R. Acharya, S. L. Oh, Y. Hagiwara, J. H. Tan, H. Adeli, and D. P. Subha, "Automated EEG-based screening of depression using deep convolutional neural network," *Computer Methods and Programs in Biomedicine*, vol. 161, pp. 103–113, 2018.

[7] Y. H. Kwon, S. B. Shin, and S. D. Kim, "Electroencephalography based fusion two-dimensional (2D)-convolution neural networks (CNN) model for emotion recognition system," *Sensors*, vol. 18, no. 5, p. 1383, 2018.

[8] B. Kim, N. Schweighofer, J. P. Haldar, R. M. Leahy, and C. J. Winstein, "Corticospinal tract microstructure predicts distal arm motor improvements in chronic stroke," *Journal of Neurologic Physical Therapy*, vol. 45, no. 4, pp. 273–281, 2021.

[9] H. A. Adhi, S. K. Wijaya, C. Badri, and M. Rezal, "Automatic detection of ischemic stroke based on scaling exponent electroencephalogram using extreme learning machine," *Journal of Physics: Conference Series*, vol. 820, pp. 12005–12013, 2017.

[10] E. C. Djamal, R. I. Ramadhan, M. I. Mandasari, and D. Djajasasmita, "Identification of post-stroke EEG signal using wavelet and convolutional neural networks," *Bulletin of Electrical Engineering and Informatics*, vol. 9, no. 5, pp. 1890–1898, 2020.

[11] A. Fares, S. H. Zhong, and J. Jiang, "EEG-based image classification via a region-level stacked bi-directional deep learning framework," *BMC Medical Informatics and Decision Making*, vol. 19, no. 268, pp. 1–11, 2019.

[12] S. Chambon, V. Thorey, P. Arnal, E. Mignot, and A. Gramfort, "DOSED: a deep learning approach to detect multiple sleep micro-events in EEG signal," *Journal of Neuroscience Methods*, vol. 321, pp. 64–78, 2019.

[13] A. K. Saenger and R. H. Christenson, "Stroke biomarkers: progress and challenges for diagnosis, prognosis, differentiation, and treatment," *Clinical Chemistry*, vol. 56, no. 1, pp. 21–33, 2010.

[14] S. Chambon, M. N. Galtier, P. J. Arnal, G. Wainrib, and A. Gramfort, "A deep learning architecture for temporal sleep stage classification using multivariate and multimodal time series," *IEEE Transactions on Neural Systems and Rehabilitation Engineering*, vol. 26, no. 4, pp. 758–769, 2018.

[15] A. M. Anwar and A. M. Eldeib, "EEG signal classification using convolutional neural networks on combined spatial and temporal dimensions for BCI systems," in *2020 42nd Annual International Conference of the IEEE Engineering in Medicine & Biology Society (EMBC)*, pp. 434–437, Montreal, QC, Canada, 2020.

[16] W. Fadel, C. Kollod, M. Wahdow, Y. Ibrahim, and I. Ulbert, "Multi-class classification of motor imagery EEG signals using image-based deep recurrent convolutional neural network," in *2020 8th Int. Wint. Confe. on Brain-Computer Interface (BCI)*, pp. 1–4, Gangwon, Korea (South), 2020.

[17] L. A. Boyd, K. S. Hayward, N. S. Ward et al., "Biomarkers of stroke recovery: consensus-based core recommendations from the stroke recovery and rehabilitation roundtable," *International Journal of Stroke*, vol. 12, no. 5, pp. 480–493, 2017.

[18] N. Hasan, P. McColgan, P. Bentley, R. J. Edwards, and P. Sharma, "Towards the identification of blood biomarkers for acute stroke in humans: a comprehensive systematic review," *British Journal of Clinical Pharmacology*, vol. 74, no. 2, pp. 230–240, 2012.

[19] T. J. Kleinig and R. Vink, "Suppression of inflammation in ischemic and hemorrhagic stroke: therapeutic options," *Current Opinion in Neurology*, vol. 22, no. 3, pp. 294–301, 2009.

Hindawi
Behavioural Neurology
Volume 2023, Article ID 9769130, 1 page
https://doi.org/10.1155/2023/9769130

Retraction

Retracted: Classification of Myopathy and Amyotrophic Lateral Sclerosis Electromyograms Using Bat Algorithm and Deep Neural Networks

Behavioural Neurology

Received 19 December 2023; Accepted 19 December 2023; Published 20 December 2023

This article has been retracted by Hindawi following an investigation undertaken by the publisher [1]. This investigation has uncovered evidence of one or more of the following indicators of systematic manipulation of the publication process:

(1) Discrepancies in scope

(2) Discrepancies in the description of the research reported

(3) Discrepancies between the availability of data and the research described

(4) Inappropriate citations

(5) Incoherent, meaningless and/or irrelevant content included in the article

(6) Manipulated or compromised peer review

The presence of these indicators undermines our confidence in the integrity of the article's content and we cannot, therefore, vouch for its reliability. Please note that this notice is intended solely to alert readers that the content of this article is unreliable. We have not investigated whether authors were aware of or involved in the systematic manipulation of the publication process.

Wiley and Hindawi regrets that the usual quality checks did not identify these issues before publication and have since put additional measures in place to safeguard research integrity.

We wish to credit our own Research Integrity and Research Publishing teams and anonymous and named external researchers and research integrity experts for contributing to this investigation.

The corresponding author, as the representative of all authors, has been given the opportunity to register their agreement or disagreement to this retraction. We have kept a record of any response received.

References

[1] A. Bakiya, A. Anitha, T. Sridevi, and K. Kamalanand, "Classification of Myopathy and Amyotrophic Lateral Sclerosis Electromyograms Using Bat Algorithm and Deep Neural Networks," *Behavioural Neurology*, vol. 2022, Article ID 3517872, 9 pages, 2022.

Hindawi
Behavioural Neurology
Volume 2022, Article ID 3517872, 9 pages
https://doi.org/10.1155/2022/3517872

Research Article

Classification of Myopathy and Amyotrophic Lateral Sclerosis Electromyograms Using Bat Algorithm and Deep Neural Networks

A. Bakiya,[1] A. Anitha,[2] T. Sridevi,[3] and K. Kamalanand[4]

[1]*Department of Electronics and Communication Engineering, Vel Tech Rangarajan Dr. Sagunthala R&D Institute of Science and Technology, Chennai 600062, India*
[2]*PG Department of Computer Science, Dwaraka Doss Goverdhan Doss Vaishnav College, Chennai-600106, India*
[3]*PG and Research Department of MCA, Dwaraka Doss Goverdhan Doss Vaishnav College, Chennai-600106, India*
[4]*Department of Instrumentation Engineering, MIT Campus, Anna University, Chennai-600044, India*

Correspondence should be addressed to K. Kamalanand; kamalanand@mitindia.edu

Received 17 November 2021; Revised 12 February 2022; Accepted 5 March 2022; Published 4 April 2022

Academic Editor: Nicola Tambasco

Electromyograms (EMG) are a recorded galvanic action of nerves and muscles which assists in diagnosing the disorders associated with muscles and nerves. The efficient discrimination of abnormal EMG signals, myopathy and amyotrophic lateral sclerosis, engage crucial role in automatic diagnostic assistance tools, since EMG signals are nonstationary signals. Hence, for computer-aided identification of abnormalities, extraction of features, selection of superlative feature subset, and developing an efficient classifier are indispensable. Initially, time domain and Wigner-Ville transformed time-frequency features were extracted from abnormal EMG signals for experiments. The selection of substantial characteristics from time and time-frequency features was performed using bat algorithm. Extensively, deep neural network classifier is modelled for selected feature subset using bat algorithm from extracted time and time-frequency features. The performance of deep neural network exerting selected features from bat algorithm was compared with conventional artificial neural network. Results demonstrate that the deep neural network modelled with layers 2 and 3 (neurons = 2 and 4) using time domain features is efficient in classifying the abnormalities of EMG signals with an accuracy, sensitivity, and specificity of 100% and also exhibited finer performance. Correspondingly, the developed conventional single layer artificial neural network (neurons = 7) with time domain features has shown an accuracy of 83.3%, sensitivity of 100%, and specificity of 71.42%. The work materializes the significance of conventional and deep neural network using time and time-frequency features in diagnosing the abnormal signals exists in neuromuscular system using efficient classification.

1. Introduction

The arrangement of human neuromuscular structure in human anatomy is a complex aggregation of muscular and nervous system [1]. The structure of neuromuscular (NMR) system is influenced by NMR disorders. Myopathies, multiple sclerosis, myasthenia gravis, and progressive neurodegenerative disease such as amyotrophic lateral sclerosis (ALS) are various distinct disorders which affects the neuromuscular system [2]. The NMR disorder is principally classified into two categories, namely, myopathy and neuropathy [3]. Myopathies are the ailments in connection to muscles and its fiber, which are further grouped into types, inherited and acquired myopathies. Myopathies can be manifested from several symptoms which include muscle weakness, fatigue, muscle atrophy, and myotonia [4]. Similarly, disorders related to nerves are termed as neuropathy, i.e., Lou Gehrig's disease also known as ALS. ALS is an incessant disease which affects motor neurons, causing injury to neuron cell, and respiratory system failure leading to death [5, 6]. ALS is categorized into two types, the sporadic and hereditary ALS.

Electromyography is a technique for documenting the galvanic activity of neuromuscular structure [7]. Neuromuscular diseases can be identified by analyzing the recorded EMG signals [8]. The abnormal signals are acquired either using noninvasive electrodes or invasive electrodes. Hence, efficient investigation of EMG signals needs automatic computer assisted diagnostic systems employing techniques such as attribute extraction, feature reduction, and modelling appropriate classifiers [9]. Feature extraction is the technique to obtain important dominant features from the collected biosignals and the features extricated define the properties and characteristics of original biosignals [10].

Time domain techniques are used to convert signal information that varies with respect to time [11]. Time domain features are simple and rapid to deploy since it does not necessitate transformation and can extracted directly from prototypical signals. The combined information of time and frequency signals is referred as time frequency techniques, and its transformations provide highly nonstationary information of the signals [12]. Earlier studies have incorporated the time-domain and time-frequency features for building finer classification model [13, 14].

Torres-Castillo et al. (2022) [15] have used the machine learning algorithms with decomposition techniques for detection of neuromuscular disorders using Hilbert transformed time-frequency features. The authors have concluded that the ensemble empirical mode decomposition (EEMD) has exhibited a best result in identifying the normal and abnormal signals. Bhattacharjee and Singh (2021) [16] have deployed the ensemble machine learning models to classify the different hand gestures using time domain features. The authors have culminated that the XG-boost classifier attained higher accuracy than the other classifier models. Lee et al. (2022) [17] built various classifiers for EMG signals from hand gesture movements, in which eighteen-time domain features were fetched. From the classifiers modelled, the author has revealed that artificial neural network exhibited greater performance.

Although features can be extracted from different domains, time domain takes the advantage of its simplicity and its wide application in EMG signal processing whereas time-frequency domain needs transformation for extracting the features [17]. In order to assess the performance, both domains were employed in this work and the results have been analyzed.

Feature selection technique [18] is deployed for selecting relevant efficient features from the extracted features which facilitate to build an accurate classification model with less computational complexity.

Recently, many researchers focus on building the model for classifying EMG signals using computational and knowledge engineering techniques such as linear discriminant analysis, logistic regression, K-means, KNN classifiers, support vector machine, extreme learning machines, artificial neural network, and deep learning methods [19, 20].

Deep learning techniques are more constructive and effective in terms of memorization and generalization capabilities which are employed for developing intelligent tool for biomedical signal processing applications such as pattern recognition, classification of image, speech recognition, and computer vision [21, 22].

The main intent of this work is to extract the time and time-frequency (TF-f) features of abnormal (Myopathy and ALS) electromyographic signals. Further, most relevant features are selected using bat algorithm (BA). Finally, the performance measures were compared for selected time and time-frequency features using developed deep neural network (DNN) and conventional artificial neural network (CANN) classifiers.

The paper is organized with the sections: methodology, result discussion, and conclusion. Methodology section comprises of acquisition of EMG signals, overall framework of the work, feature extraction and selection, brief description of bat algorithm, and constructed classification model. Further, subsequent section is extended to discuss the results obtained using the built classification model, and the last section concludes the results obtained.

2. Methodology

2.1. EMG Signal Acquisition. In this work, vastus medialis muscle region was chosen for the acquiring myopathy and ALS electromyographic signals. In total, 60 signals were employed for analysis. From the total signals, exclusively, 30 signals from myopathy and 30 signals from ALS were utilized for the work. The electromyographic signals were procured from standard open-source database EMGLAB [23]. The signal sampling rate is 23437.5 Hz, and total time period for each signal is 11.8 seconds [23]. Figures 1(a) and 1(b) manifest the typical myopathy and ALS electromyogram signals for a period of 0.5 seconds.

2.2. Feature Extraction and Selection in EMG. Feature extraction is the process of extracting the relevant information or features from the original biological signals [24]. Feature extraction techniques for biosignals are categorized as time domain, frequency domain, and conjunction of time with frequency techniques [25]. From the context of signal processing, time domain methods provide the information of signals with respect to time. In addition, the time frequency techniques provide the information of signals concerning both time and frequency. Generally, the time-frequency techniques require reconstruction of single dimensional signals into two dimensional images. Reconstruction techniques, namely, wavelet transform, stock-well transform, and discrete cosine transform, were widely used for biosignal applications [26]. In this work, seventeen time features [27] and nineteen time-frequency features were extracted from reconstructed images. The time and time-frequency feature subsets were selected using bat algorithm which is further used to investigate and analyze the EMG signals. Finally, DNN and CANN were built to diagnose the abnormalities of signals, and their performances were compared. The overview for classifying the abnormalities exist in the EMG signals is depicted in Figure 2.

2.3. Wigner-Ville Transform (WVT). The Wigner-Ville time-frequency transform was developed by Eugene Wigner

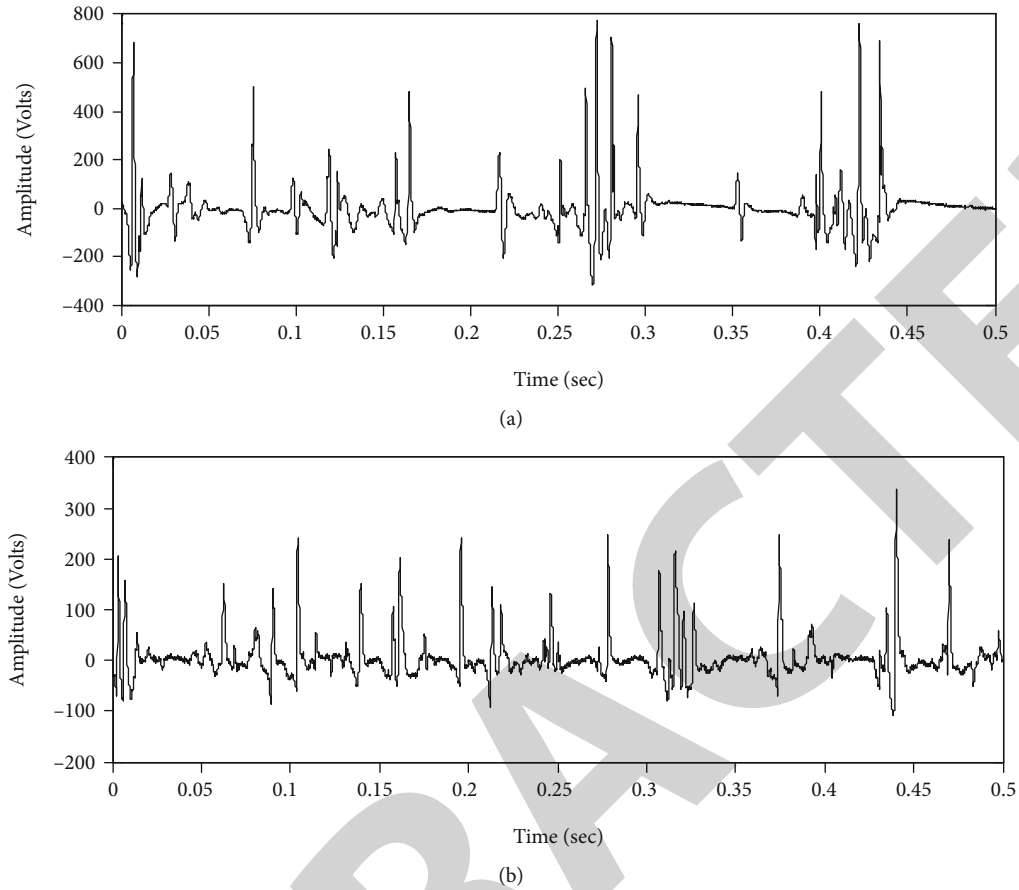

Figure 1: Typical myopathy and ALS EMG signals.

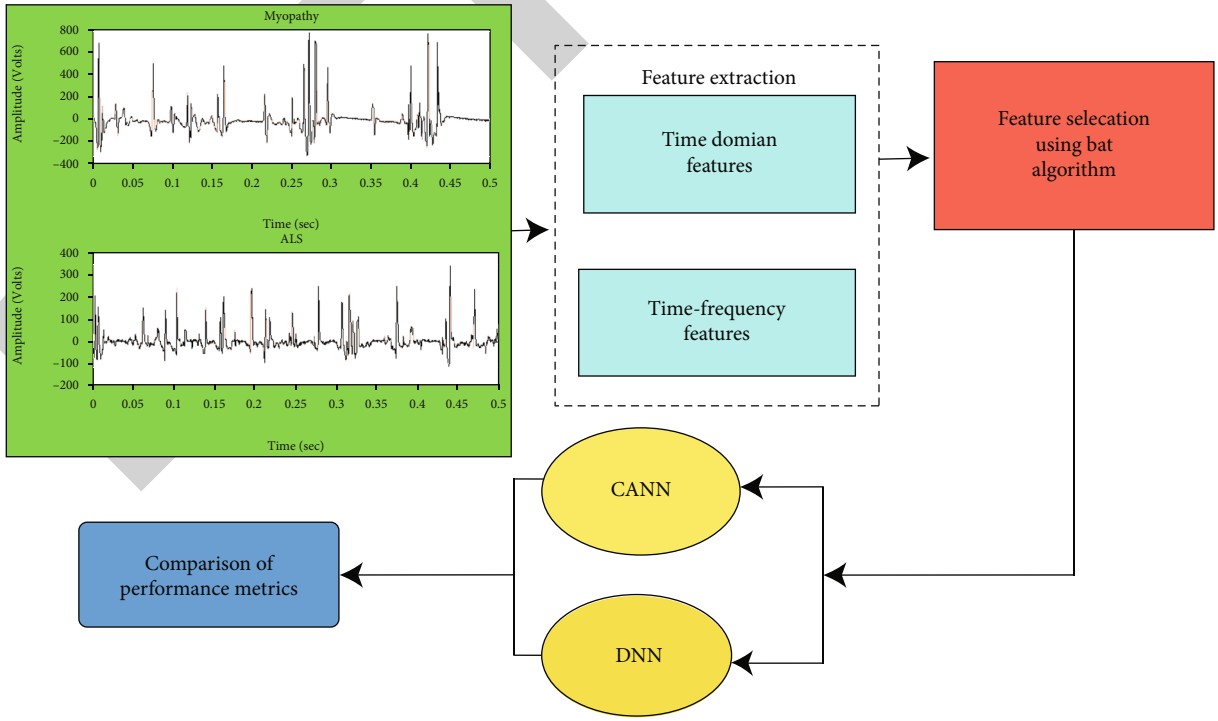

Figure 2: Overview of classification of abnormalities in EMG signals.

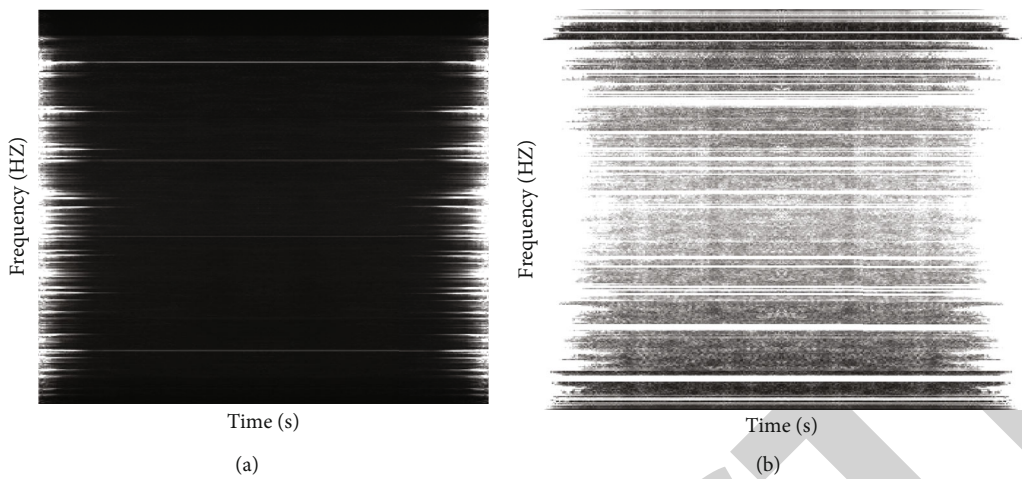

Figure 3: Representative time-frequency images obtained using WVT (a) myopathy and (b) ALS.

(1932), which was derived from the Gabor transformation. Mathematically, WVT can be applied to time, frequency, and discrete signals [28]. Figures 3(a) and 3(b) show the reconstructed time-frequency images using WVT of abnormal EMG signals, respectively.

The formulation of WVT [29, 30] is expressed with real component $G(t)$ and complex component $G^*(t)$ signals by the following equation

$$W_{wvt}(t,f) = \int_{-\infty}^{\infty} e^{-j2\pi f\tau} G^*\left(t - \frac{1}{2}\tau\right) G\left(t + \frac{1}{2}\tau\right) d\tau. \quad (1)$$

For this work, WVT reconstruction technique is utilized to extract nineteen well-established time-frequency attributes from abnormal EMG signals.

2.4. Bat Algorithm. Attribute selection is the mechanism of selecting the optimal attributes from the comprehensive features excluding unnecessary and redundant features, which assist in establishing efficient classification systems [31]. Bat algorithm is used for this work to select the best features from the extracted time and time-frequency feature sets.

Yang proposed bat algorithm by perceiving the characteristics and functional behaviors of the microbat in early 2010. The Yang's algorithm identifies the three primary characteristics of the microbat and rules which enacted to contrive the fundamental structure [32] are

(1) Microbats identify the prey using its echolocation characteristics, but few bats do not adapt to this behavior

(2) Microbats employ precise wavelength, frequency, and loudness to track the prey

(3) Emulating the difference in loudness and pulse emission rates in searching

In Yang's bat algorithm, the virtual microbat movement is simulated with the following equation

$$\begin{aligned} f_{yj} &= f_{y(\min)} + \left(f_{y(\max)} - f_{y(\min)}\right).\beta, \\ v_j^t &= v_j^{t-1} + \left(p_j^t - p_{\text{best}}\right).f_{yj}, \\ p_j^t &= p_j^{t-1} + v_j^t, \end{aligned} \quad (2)$$

where the bat searches for its prey in the frequency f_y, in the range (min, max). p_j represents the jth bat position in the solution space, v_j signifies the bat's velocity, j denotes the present iteration, β is the vector chosen randomly from a uniform distribution where $\beta \in [0, 1]$ and p_{best} designate the near-best global solution computed so far found around the whole population.

The training variables for bat algorithm used in this work were number of bat is 20 and iteration is 100. The prominent time and time-frequency (TF-f) features were selected using BA algorithm from the extracted features.

2.5. Classification of EMG Signals Using DNN and CANN. Deep neural network and conventional artificial neural network classifiers were used to identity abnormal (myopathy and ALS) EMG signals. Classifier efficiency was compared for the feature set (both time and time-frequency) determined using the BA optimization algorithm. CANN models are commonly used for biomedical applications such as classification, regression, clustering, and identification of pattern. To classify the abnormal EMG signal, the CANN consists of three (input, output, and hidden) layers, activation (tan sigmoid) functions, and back-propagation learning technique [33]. Using different number of hidden neurons, the network was trained, and the performance of CANN was analyzed.

An extension of CANN is the DNN which has input, output, and minimum of two hidden layers. DNN is widely adopted to solve the complex nonlinear problems which require more memory and greater generalization capabilities. The DNN models were used in biomedical problems for image classification [34], segmentation [35], and biosignal classification [36] and for the development of diagnostic systems [37].

Table 1: P value of extracted features from abnormal EMG signals.

Extracted time domain features	P value	Extracted time-frequency feature	WVT P value	SPWVT P value
Enhanced mean absolute value	0.0001*	Autocorrelation	0.0001*	0.27
Enhanced wavelength	0.002*	Cluster prominence	0.0191*	0.2675
Mean absolute value	0.0001*	Cluster shade	0.0897	0.268
Wavelength	0.0186	Contrast	0.0057*	0.2611
Zero crossing	0.0001*	Correlation	0.1465	0.3197
Slope sign change	0.0023*	Difference entropy	0.0099*	0.2301
Root mean square	0.0001*	Difference variance	0.0007*	0.2248
Average amplitude change	0.0186	Dissimilarity	0.0442	0.2611
Difference absolute standard deviation error	0.3737	Energy	0.0083*	0.2031
Log detector	0.37	Entropy	0.1577	0.2002
Modified mean absolute value	0.0001*	Homogeneity	0.0946	0.261
Modified mean absolute value 2	0.0018*	Information measure of correlation 1	0.9769	0.101
Myopulse percentage rate	0.0001*	Information measure of correlation 2	0.4707	0.0891
Simple square integral	0.0346	Inverse difference	0.1315	0.261
Variance of EMG	0.0346	Maximum probability	0.0007*	0.2196
Willison amplitude	0.022	Sum average	0.0001*	0.1934
Maximal fractal length	0.0599	Sum entropy	0.0899	0.1862
		Sum of squares variance	0.0469*	0.198
		Sum variance	0.0368*	0.1572

*Statistically significant features.

In this work, CANN was constructed with the selected time and time-frequency feature subsets with varied hidden neurons for the classification of myopathy and ALS electromyograms. Further, DNN is developed for varied hidden layers with hidden neurons. Both the networks were trained using feed-forward back propagation algorithm. The training parameters used in this work to build classifier models were tan sigmoid activation layer, number of hidden layers: 1 to 4, data split: 80% training data, and 20% test data; and maximum iteration: 100. The results of the constructed classifiers were quantified using standard performance measures [38].

3. Results and Discussion

In this segment, the results attained from the experiments using MATLAB software were summarized. The extracted time domain and time-frequency (TF-f) domain features of abnormal EMG signals are presented in Table 1. From Table 1, it is evident that most of the time domain features are highly statistically significant. Further, it is observed that the features obtained using Wigner-Ville transform are more statistically significant than from the smoothed pseudo-Wigner-Ville transform (SPWVT). Hence, the Wigner-Ville transform is a suitable tool for extraction of time-frequency features from myopathy and ALS EMG signals.

From the extracted features, the highly significant feature subsets were selected from BA optimization technique. The features selected using BA algorithm for time and time-frequency (TF-f) features were listed in Table 2.

Figure 4 Shows the accuracy of CANN and DNN classifiers for features (time and TF-f) in classifying abnormal vastus medialis muscle signals. Analyzing the performance of CANN, it is discerned that classification accuracy of time domain EMG features with neurons ($N = 2$ and 4) is higher when compared with the accuracy using time-frequency features with neurons ($N = 2$ and 4). Concurrently, the accuracy of CANN classifier using time and TF-f features with neurons ($N = 7$) is identical. Consequently, the accuracy of the constructed DNN by varying the hidden layers 2, 3, and 4 with distinct neurons ($N = 2$, 4, and 7), respectively, were compared for time and TF-f features. The evaluation of DNN classifier using time domain features with two hidden layers ($L = 2$) with neurons ($N = 2$, 4, and 7) has exhibited higher accuracy with respect to the other hidden layers ($L = 3$ and 4).

Figures 5 and 6 depict the sensitivity and specificity of the developed CANN and DNN classifiers using both time and TF-f features, respectively. The sensitivity and specificity of CANN and DNN using time domain features exhibited better performance were noted when compared to performance of both the classifiers using time-frequency features.

Figures 7 and 8 demonstrate the positive and negative predictive values (PPV and NPV) of the developed CANN and DNN classifiers using time and TF-f features, respectively. The PPV and NPV values of CANN and DNN using time domain features attained better performance when

Table 2: Features selected using bat algorithm.

Time domain features	Selected features
Enhanced wavelength	Cluster prominence
Myopulse percentage rate	Cluster shade
Simple square integral	Correlation
Variance of EMG	Entropy
Maximal fractal length	Homogeneity
	Information measure of correlation 2
	Sum entropy

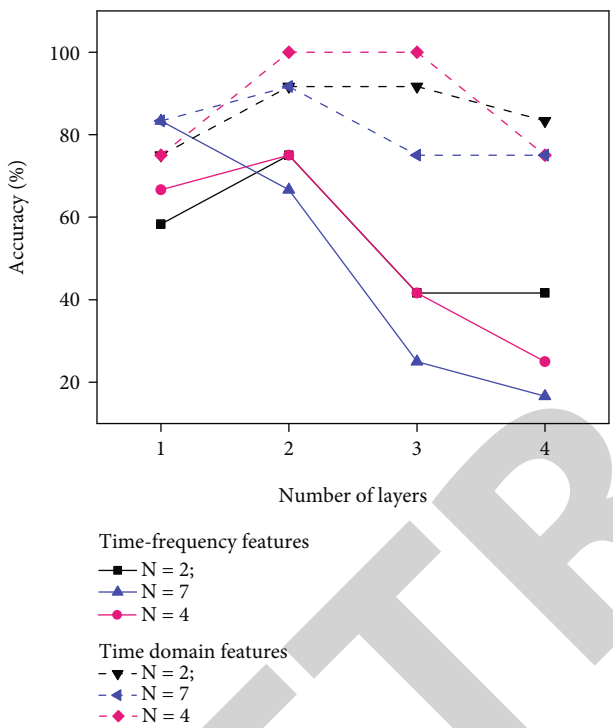

Figure 4: Accuracy of CANN and DNN classifiers of different hidden layers and hidden neurons for time and time-frequency features.

compared to performance of both the classifiers using time-frequency features.

Figure 9 depicts the computational time taken by the classifiers CANN and DNN using time and TF-f features. In examining the performance of CANN classifier using time and TF-f features, the computational time taken by the network for classification with distinct neurons ($N = 4$ and 7) is lesser in contrast to neuron $N = 2$. Further, it is noted that, with respect to CANN performance, there is a decrease in computational time while increasing the number of neurons.

Adversely, in the modelled DNN classifier using time features, it is observed that, if the number of hidden layers is increased, computational time also increases. Consequently, in modelled DNN classifier using time-frequency features, if the number of hidden layers is increased, there is a reduction in computational time.

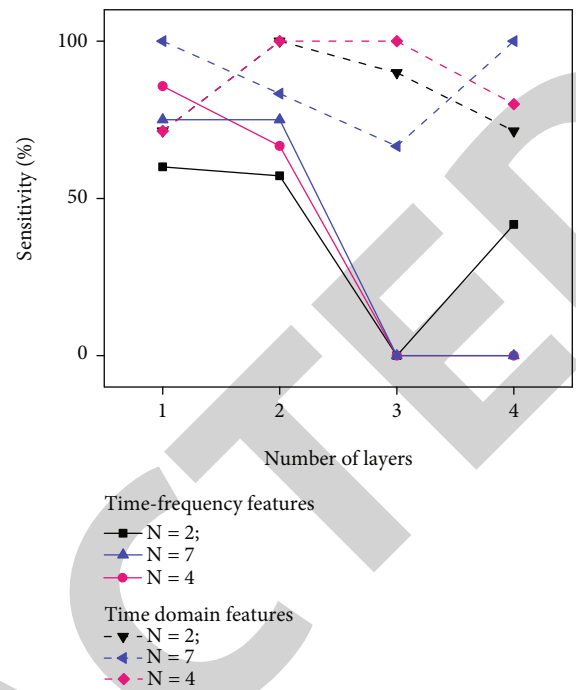

Figure 5: Sensitivity of CANN and DNN classifiers of different hidden layers and hidden neurons for time and time-frequency features.

Exploring the results obtained by Torres-Castillo et al. (2022) [15], it is noted that the authors have developed various machine learning models with decomposition techniques for classifying normal and abnormal EMG signals using time-frequency features. From the developed models, the authors revealed that the ensemble empirical mode decomposition (EEMD) with K-nearest neighbor has shown the best accuracy, sensitivity, and specificity of 99.5%, 99.6%, and 99.2%, respectively. Similarly, Bhattacharjee and Singh (2021) [16] experimented with different classifiers for classification of normal and abnormal EMG signals. The XGBoost (gblinear) has exhibited the maximum accuracy of 98.33%. Consequently, Lee et al. (2022) [17] has signified that the modelled ANN for EMG signal classification manifested with an accuracy of 94.0%.

However, in this work, classifiers DNN and CANN have been modelled using both time and TF-f features and results affirmed that the constructed DNN classifier using time domain features has shown a highest accuracy, sensitivity, and specify of 100% in classifying the abnormalities in the EMG signals. It is also found from the studies that the adopted techniques can be focused on classifying normal and abnormal EMG signals. Further, the developed DNN and CANN models using time and TF-f features instigate the classification of different types of abnormal EMG signals rather than normal/abnormal EMG signal classification. Interestingly, it is also observed that if the number of hidden layers in DNN is increased with varied neurons, accuracy of DNN decreases for both time and time-frequency features.

Globally, a prevalence of ALS has been reported between 4.1 and 8.4 per 100000 individuals, and particularly, 5 per

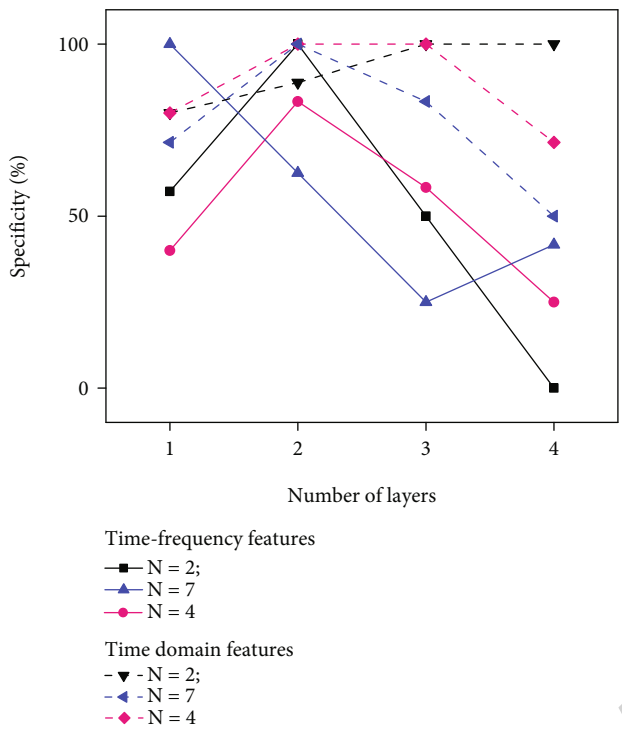

Figure 6: Specificity of CANN and DNN classifiers of different hidden layers and hidden neurons for time and time-frequency features.

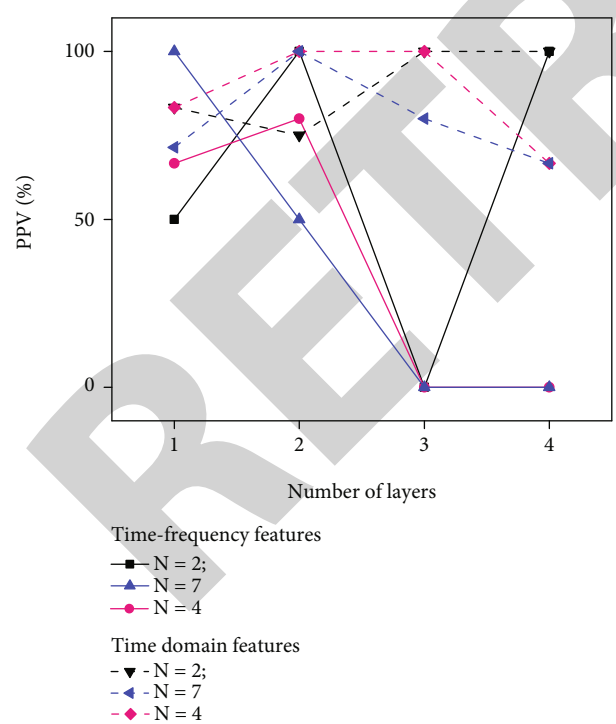

Figure 7: PPV of CANN and DNN classifiers of different hidden layers and hidden neurons for time and time-frequency features.

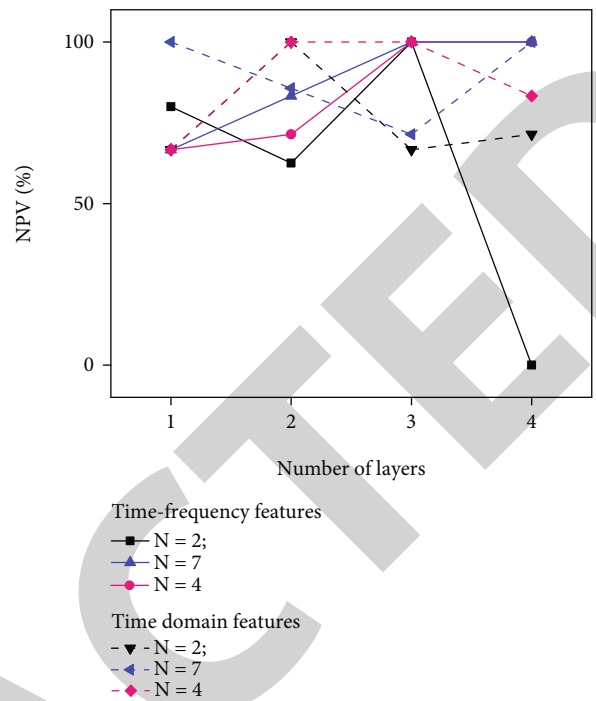

Figure 8: NPV of CANN and DNN classifiers of different hidden layers and hidden neurons for time and time-frequency features.

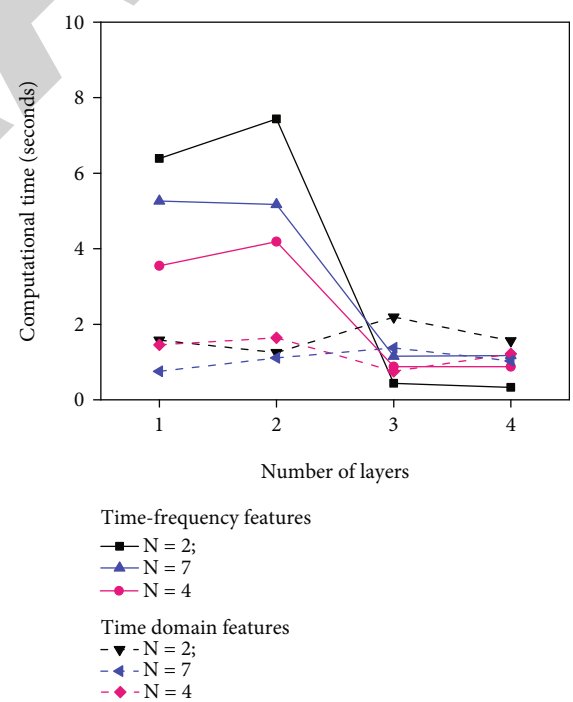

Figure 9: Computational time (in seconds) of CANN and DNN classifiers of different hidden layers and hidden neurons for time and time-frequency features.

100000 have been reported in USA [39]. National Institute of Neurological Disorders and Stroke have reported that 20 to 40% of affected individuals from one of sub category of ALS disorders, namely, "Familial cases," which are affected from C90RF72 gene and 12 to 20% of familial cases are caused from S0D1 gene. Further, the NIH researcher's team and uniformed universities Services University declared that

the exclusive genetic ALS affects the children as early as age 4 years [40].

Early diagnosis of ALS is still a challenging task for researchers as well as clinicians. Currently, there are no long-lasting clinical treatments exiting for the affected individuals, in extending their life expectancy. The developed model facilitates the early discrimination of neuromuscular abnormalities (myopathy and ALS) using EMG signals efficiently.

4. Conclusion

Electromyography is a distinguished method for registering the galvanic activities in human NMR system. The procured signals were exceptionally useful for assisting the impairment exists in human muscular and nervous system. A highly efficient classification system is essential to identify the abnormal vastus medialis muscle EMG signals. The complexity of signals necessitates the efficient extraction accompanied with selection of superlative feature subsets for constructing effective discriminating systems. Further, seventeen-time domain features and nineteen WVT transformed TF-f of ALS and myopathy EMG signals were extracted. Further, two separate feature subsets from the extracted time and TF-f were selected using BA optimization algorithm. The DNN and CANN classification system were constructed using the selected features of BA algorithm. The performance of the developed DNN classifier ($L = 2$ and 3) using time domain features for classification of abnormal signals (ALS and myopathy) were found to be higher with accuracy of (100%) when compared to the DNN classifiers ($L = 2$, 3, and 4) using time-frequency features. Similarly, the constructed CANN classifier with neuron ($N = 7$) using both time domain and TF-f has shown an identical accuracy of 83.3%. Results also reveal that the time taken for computation by DNN classifier using TF-f decreases when the hidden layers are incremented. Alternatively, the computational time taken by classifier using time domain features increases when the hidden layers are incremented. Finally, the CANN and DNN using time domain features have shown superior performance for the classification of abnormal EMG signals in comparison with time-frequency features.

Data Availability

The myopathic and ALS electromyograms were obtained from open-source database [http://www.emglab.net].

Conflicts of Interest

The authors have no conflicts of interest.

References

[1] S. M. Reed, W. M. Bayly, and D. C. Sellon, *Equine Internal Medicine-E-Book*, Elsevier Health Sciences, 2017.

[2] D. Blottner, M. Salanova, D. Blottner, and M. Salanova, "Skeletal Muscle," in *In The Neuro Muscular System: From Earth to Space Life Science*, pp. 9–62, Springer International Publishing, 2015.

[3] P. Artameeyanant, S. Sultornsanee, K. Chamnongthai, and K. Higuchi, "Classification of electromyogram using vertical visibility algorithm with support vector machine," in *In Asia-Pacific Signal and Information Processing Association, 2014 Annual Summit and Conference (APSIPA)*, pp. 1–5, Siem Reap, Cambodia, 2014.

[4] D. C. Preston and B. E. Shapiro, "Electromyography and neuromuscular disorders E-book," in *Clinical-Electrophysiologic Correlations. Elsevier Health Sciences*, Elsevier Health Sciences, 2013.

[5] L. P. Rowland and N. A. Shneider, "Amyotrophic lateral sclerosis," *New England Journal of Medicine*, vol. 344, no. 22, pp. 1688–1700, 2001.

[6] M. J. Greenway, P. M. Andersen, C. Russ et al., "ANG mutations segregate with familial and 'sporadic' amyotrophic lateral sclerosis," *Nature Genetics*, vol. 38, no. 4, pp. 411–413, 2006.

[7] F. Sadikoglu, C. Kavalcioglu, and B. Dagman, "Electromyogram (EMG) signal detection, classification of EMG signals and diagnosis of neuropathy muscle disease," *Procedia Computer Science*, vol. 120, pp. 422–429, 2017.

[8] C. J. G. Duque, L. D. Muñoz, J. G. Mejía, and E. D. Trejos, "Discrete Wavelet Transform and K-Nn Classification in EMG Signals for Diagnosis of Neuromuscular Disorders," in *In Image, Signal Processing and Artificial Vision (STSIVA)*, pp. 1–5, Armenia, Colombia, 2014.

[9] A. Phinyomark, P. Phukpattaranont, and C. Limsakul, "Feature reduction and selection for EMG signal classification," *Expert Systems with Applications*, vol. 39, no. 8, pp. 7420–7431, 2012.

[10] N. Nazmi, M. Abdul Rahman, S. I. Yamamoto, S. Ahmad, H. Zamzuri, and S. Mazlan, "A review of classification techniques of EMG signals during isotonic and isometric contractions," *Sensors*, vol. 16, no. 8, p. 1304, 2016.

[11] P. Geethanjali, Y. K. Mohan, and J. Sen, "Time domain feature extraction and classification of EEG data for brain computer interface," in *In 2012 9th International Conference on Fuzzy Systems and Knowledge Discovery*, pp. 1136–1139, Chongqing, China, 2012.

[12] M. A. Oskoei and H. Hu, "Myoelectric control systems–a survey," *Biomedical Signal Processing and Control*, vol. 2, no. 4, pp. 275–294, 2007.

[13] S. M. Vasanthi and T. Jayasree, "Performance evaluation of pattern recognition networks using electromyography signal and time-domain features for the classification of hand gestures," *Proceedings of the Institution of Mechanical Engineers, Part H: Journal of Engineering in Medicine*, vol. 234, no. 6, pp. 639–648, 2020.

[14] R. R. Sharma, M. Kumar, and R. B. Pachori, "Classification of EMG signals using eigenvalue decomposition-based time-frequency representation," in *Biomedical and Clinical Engineering for Healthcare Advancement*, pp. 118–196, IGI Global, 2020.

[15] J. R. Torres-Castillo, C. O. López-López, and M. A. Padilla-Castañeda, "Neuromuscular disorders detection through time-frequency analysis and classification of multi-muscular EMG signals using Hilbert-Huang transform," *Biomedical Signal Processing and Control*, vol. 71, article 103037, 2022.

[16] D. Bhattacharjee and M. Singh, *Time-Domain Feature and Ensemble Model Based Classification of EMG Signals for Hand Gesture Recognition*, 2021.

Hindawi
Behavioural Neurology
Volume 2023, Article ID 9802476, 1 page
https://doi.org/10.1155/2023/9802476

Retraction

Retracted: The Impact of Online Learning System on Students Affected with Stroke Disease

Behavioural Neurology

Received 8 August 2023; Accepted 8 August 2023; Published 9 August 2023

This article has been retracted by Hindawi following an investigation undertaken by the publisher [1]. This investigation has uncovered evidence of one or more of the following indicators of systematic manipulation of the publication process:

(1) Discrepancies in scope

(2) Discrepancies in the description of the research reported

(3) Discrepancies between the availability of data and the research described

(4) Inappropriate citations

(5) Incoherent, meaningless and/or irrelevant content included in the article

(6) Peer-review manipulation

The presence of these indicators undermines our confidence in the integrity of the article's content and we cannot, therefore, vouch for its reliability. Please note that this notice is intended solely to alert readers that the content of this article is unreliable. We have not investigated whether authors were aware of or involved in the systematic manipulation of the publication process.

In addition, our investigation has also shown that one or more of the following human-subject reporting requirements has not been met in this article: ethical approval by an Institutional Review Board (IRB) committee or equivalent, patient/participant consent to participate, and/or agreement to publish patient/participant details (where relevant).

Wiley and Hindawi regrets that the usual quality checks did not identify these issues before publication and have since put additional measures in place to safeguard research integrity.

We wish to credit our own Research Integrity and Research Publishing teams and anonymous and named external researchers and research integrity experts for contributing to this investigation.

The corresponding author, as the representative of all authors, has been given the opportunity to register their agreement or disagreement to this retraction. We have kept a record of any response received.

References

[1] S. Wassan, C. Xi, T. Shen, K. Gulati, K. Ibraheem, and R. M. Amir Latif Rajpoot, "The Impact of Online Learning System on Students Affected with Stroke Disease," *Behavioural Neurology*, vol. 2022, Article ID 4847066, 14 pages, 2022.

Hindawi
Behavioural Neurology
Volume 2022, Article ID 4847066, 14 pages
https://doi.org/10.1155/2022/4847066

Research Article

The Impact of Online Learning System on Students Affected with Stroke Disease

Sobia Wassan,[1] **Chen Xi**,[1] **Tian Shen**,[2] **Kamal Gulati**,[3,4] **Kinza Ibraheem**,[5] **and Rana M. Amir Latif Rajpoot**[5]

[1]*Business School, Nanjing University, China*
[2]*School of International Education, Nanjing University of CM, China*
[3]*Amity University, Noida, Uttar, Pradesh, India*
[4]*Stratford University, Virginia, USA*
[5]*Department of Computer Science COMSATS University Islamabad, Sahiwal Campus, Pakistan*

Correspondence should be addressed to Chen Xi; chenx@nju.edu.cn and Tian Shen; shentian025@aliyun.com

Received 31 October 2021; Revised 24 December 2021; Accepted 28 December 2021; Published 7 February 2022

Academic Editor: Hong Lin

Stroke, also known as a cerebrovascular accident, is a medical emergency that causes temporary or permanent behavioral dysfunction in people. Sleep deprivation affects our brains in a variety of ways. The advantages of sleep much justify the risks of not having enough sleep. Sleep deprivation (SD) includes a variety of factors, including prolonged awake. Neuroimaging investigates SD's impact on attention, working memory, mood, and hippocampal learning. We analyzed how this data enriches our mechanistic understanding of these alterations and the clinical illnesses linked with sleep disruption. We have used Cronbach's alpha to test the reliability of a scale, so we then have 19 individual attributes responding to 174 participants via survey. The evaluated result shows the reliability statistics; the value for Cronbach's alpha is .962, which is very excellent as it reaches 1. So, there is very strong reliability. If the value falls under .6, we look back to the mean and standard deviation table and remove the attribute with low values for mean or standard deviation and try the remaining attributes. Cronbach's alpha tells us which attribute or item to delete to increase the reliability, and we also have analyzed the correlation among the class students while watching the same video lecture. We have collected data for at least ten students watching the same video using a webcam. Once the data is collected, we then have applied some correlation techniques to determine the class students' behavior towards the same video lecture. This way, we can see the overall behavior of the class upon a specific video lecture. The study further reveals that subjective happiness is influenced by its efficiency, entertainment value, and effectiveness. Does the research offer an original emphasis on analyzing how does lack of sleep affect our brains? Sleep loss frameworks are minimal compared to the benefits of sleep.

1. Introduction

Our cognitive and emotional capacities are negatively affected when we do not get enough sleep. What alterations in the brain are causing these abnormalities? In this article, the authors [1] explained what do these changes reveal about the widespread relationship between sleep disturbance and a variety of neurological and mental disorders? [1]. The authors [2] explained that there are at least three reasons to accurately describe how SD impacts the human brain. One must first determine whether brain networks are prone or resistant to the special effects of sleep deprivation and how SD-induced changes in activities or functional connections justify the deleterious changes in behavior related with SD. Sleep deprivation does not only refer to sleeplessness and the associated behavior's, though. Rather, sleep deprivation is a combination of several harmful causes, including prolonged alertness and lack of sleep. It is thus inadequate to learn about the functional advantages of sleeping and then learn about the neurological and behavioral alterations that occur when sleep is lacking. Second, all significant neurological, including schizophrenia, Alzheimer's disease, and other serious neuropsychiatric

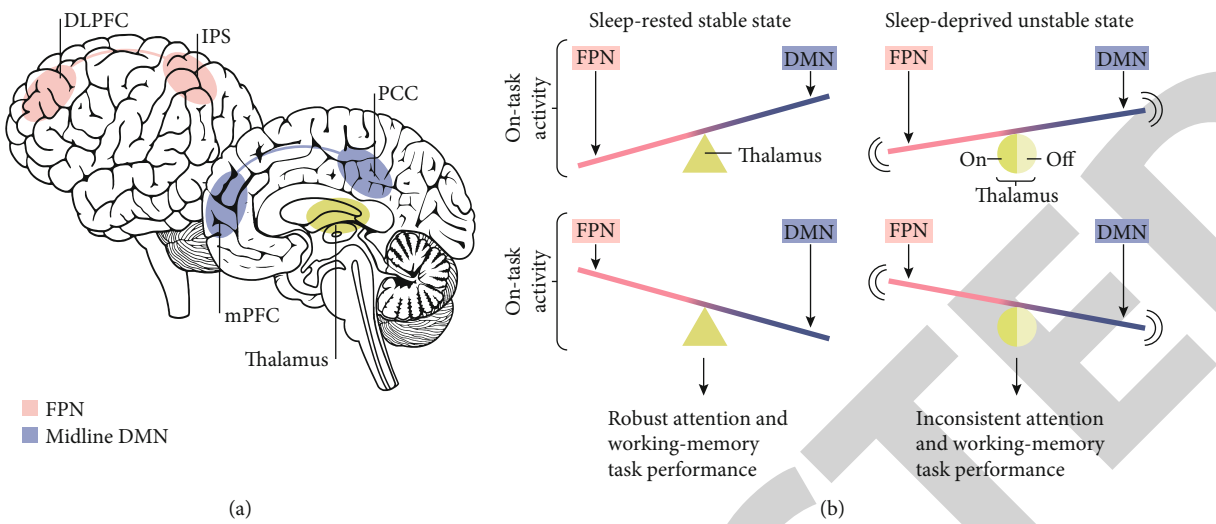

Figure 1: Sleep rested vs. sleep-deprived.

disorders, and anxiety disorders have concomitant sleep disturbance. Attention, which is required for continuous goal-directed behavior, is one cognitive capacity that is particularly vulnerable to sleep deprivation. Due to increased sleep pressure, attentional activities decline in a dose-dependent way as the sum of time spent wakeful grows [3]. In this article, the authors state that "lapses" or "microsleep" is a prototypic deficit on such tasks that entail reaction failure that reflect errors and omissions [4]. The authors explained that increased sleep propensity and instability of waking neurobehavioral processes are connected to poor cognitive performance and severe social, economic, and health-related implications. Sleep deprivation has been shown to impair a variety of cognitive processes, including attention, memory, and learning [5]. In this article, the aim of this analysis is on sleep loss; it is worth noting that daily clock alertness signals interact with SD to cause attentional impairment that increases exponentially with increasing awake time [6, 7]. The behavioral repercussions of these brain alterations include difficulties focusing on a single input while disregarding distractions [8, 9]. It is less clear why some people are more or less susceptible to these attentional problems after SD than others. A clearer understanding of how severe SD affects brain function linked to attentional activities is developing. When performing attentional tasks, SD reduces fMRI signals in the DLPFC and temporoparietal sulcus [10]. Reduced activity in the DLPFC and temporal and parietal sulcus has a role in attentional performance failure once again [11]. Nonetheless, the authors state that the total time spent awake predicted attention deficits in both acute and chronic partial sleep deprivations [2].

1.1. Awakening with Sleep Deprivation. SD enhances amygdala activity (red) and decreases amygdala–MPFC connectivity (blue). SD alters the salience-detection network's sensitivity to emotional signals ranging from adversely (red) to neutrally (blue) to positively (green) (red). The capacity to discriminate between emotion (red vertical line) and neutral (blue vertical line) stimuli is enhanced during sleep (left graph). Reducing one's capacity to discern between emotion

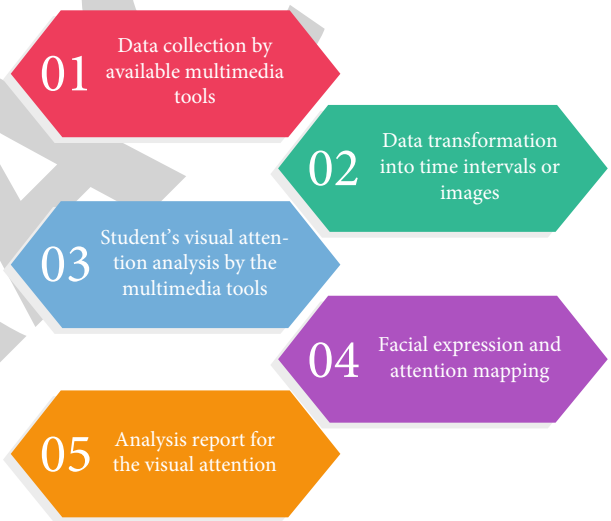

Figure 2: Research technique for students' visual focus.

salience levels may be reduced by using SD (right graph) (short vertical difference line). The salience-detection network misidentifies a seemingly neutral input (blue line) as emotional, leading to skewed emotional judgments of neutral stimuli. These central brain alterations, together with impaired peripheral cardiac nervous system input of visceral bodily information, may result in erroneous or missing emotional expression. Experiments reveal that people who are sleep deprived cannot recognize emotive faces on a computer and so cannot correctly duplicate their emotional expressions. Part A is from REF with permission [12] (Elsevier).

Under SD circumstances, adequate persistence of DMN activity is seen throughout working-memory task execution [13]. On the other hand, the amount of abnormal, on-task DMN activity predicted the intensity of sleep-deprived people's working memory deficits [14] (Figure 1). A common process causing SD-induced attentiveness and memory issues might be insufficiently gated on-task vs. off-task network control. Because the thalamus is involved in cortical arousal, changes

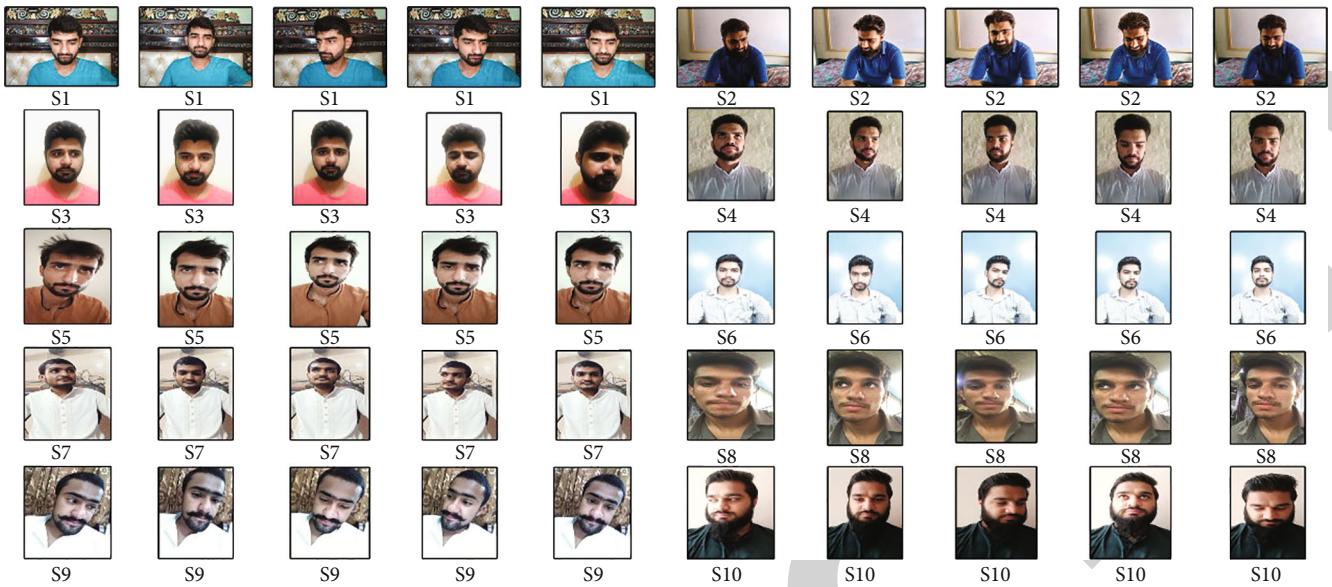

Figure 3: The sample pictures of 10 students while watching the lecture.

1	numberOfFaces	actualEyes	detectedEyes	openedEyes	closedEyes	eyesDetectionError	pfps	attentiveness	attentionLevel	TimeStamp
2	1	2	0	0	0	2	0	0.5	sleepy	2:18:14 PM
3	1	2	0	0	0	2	0	0.5	sleepy	2:18:15 PM
4	1	2	0	0	0	2	0	0.5	sleepy	2:18:15 PM
5	1	2	0	0	0	2	0	0.5	sleepy	2:18:15 PM
6	1	2	0	0	0	2	0	0.5	sleepy	2:18:15 PM
7	1	2	0	0	0	2	0	0.5	sleepy	2:18:15 PM
8	1	2	0	0	0	2	0	0.5	sleepy	2:18:15 PM
9	1	2	0	0	0	2	0	0.5	sleepy	2:18:15 PM
10	1	2	0	0	0	2	0	0.5	sleepy	2:18:15 PM
11	1	2	0	0	0	2	9	0.5	sleepy	2:18:15 PM
12	1	2	0	0	0	2	9	0.5	sleepy	2:18:15 PM
13	1	2	0	0	0	2	9	0.5	sleepy	2:18:15 PM
14	1	2	0	0	0	2	9	0.5	sleepy	2:18:16 PM
15	1	2	0	0	0	2	9	0.5	sleepy	2:18:16 PM
16	1	2	0	0	0	2	9	0.5	sleepy	2:18:16 PM
17	1	2	0	0	0	2	9	0.5	sleepy	2:18:16 PM
18	1	2	0	0	0	2	9	0.5	sleepy	2:18:16 PM
19	1	2	0	0	0	2	9	0.5	sleepy	2:18:16 PM
20	1	2	0	0	0	2	9	0.5	sleepy	2:18:16 PM

Figure 4: The sample screenshot of student1 for measuring the attentiveness while taking the online lecture.

in thalamic activity and connectivity can calculate memory losses under stressful conditions (SDS). An improved link between the thalamic DMN and the hippocampus is associated with increased subjective exhaustion in sleep deprivation, as well as a worse performance in working memory tasks [15].

A literature review appears in Section 2, a methodology appears in Section 3, the results and discussion appear in Section 4, and the conclusion and future research appear in Section 5.

2. Literature Review

Cognitive changes are quite prevalent (80%). The most prevalent issues are as follows: memory focus processor speed changes in selective attention and visual-spatial/perceptual processing are common. It might be evident (aphasia, neglect) or subtle (e.g. intellectual underfunctioning and visuoperceptual difficulties). In contrast, a higher thalamus-precuneus connection predicts better working-memory recovery in SD than in sleep-rested. This data supports the concept that in SD, partially recovering specific behaviors is possible due to compensation neural activity in the brain [16]. The authors explained that during concentration activities, thalamic activity fluctuates [17]. The combined impact of nap times and nocturnal sleep on stroke risk is unknown. The authors' study used data from the large cross-sectional and cohort investigation to corroborate this association [18]. Sleep efficiency declines with age, affecting the quality

1	S1	S2	S3	S4	S5	S6	S7	S8	S9	S10
2	0.5	0.5	0.5	0.5	0.5	0.75	0.5	0.5	0.5	0.5
3	0.5	0.5	0.5	0.75	0.5	0.5	0.5	0.5	0.5	0.5
4	0.5	0.75	0.5	0.5	0.5	0.5	0.5	1	0.5	0.5
5	0.5	0.5	0.5	0.5	0.5	0.75	0.5	0.5	0.5	0.5
6	0.5	0.5	0.5	0.5	0.5	0.5	0.5	1	0.75	0.5
7	0.5	0.5	0.5	0.5	0.5	0.5	0.5	1	0.75	0.5
8	0.75	0.5	0.5	0.5	0.5	0.5	0.5	0.75	0.5	0.5
9	1	0.5	0.5	0.75	0.75	0.5	0.5	0.5	0.5	0.5
10	0.5	0.5	0.5	0.5	0.5	0.5	0.5	0.5	0.5	0.5
11	0.5	0.5	0.5	0.5	0.5	0.5	0.5	0.75	0.5	0.5
12	1	0.5	0.5	0.5	0.5	0.5	0.5	0.75	0.5	0.5
13	1	0.5	0.5	0.5	0.5	0.5	0.5	0.75	0.5	0.5
14	1	0.5	0.5	0.75	0.5	0.5	0.5	0.5	0.5	0.5
15	1	0.75	0.5	0.5	0.5	0.5	0.5	0.75	0.5	0.5
16	1	0.75	0.5	0.5	0.5	0.5	0.5	0.75	0.5	0.5
17	1	0.5	0.5	0.5	0.5	0.5	0.5	0.75	0.5	0.5
18	1	0.5	0.75	0.5	0.5	0.5	0.5	0.75	0.5	0.5
19	1	1	0.5	0.5	0.5	0.5	0.5	0.5	0.5	0.5
20	1	1	0.75	0.5	0.5	0.5	0.5	0.5	0.5	0.5

Figure 5: The attentiveness level of the ten students while taking the online lecture.

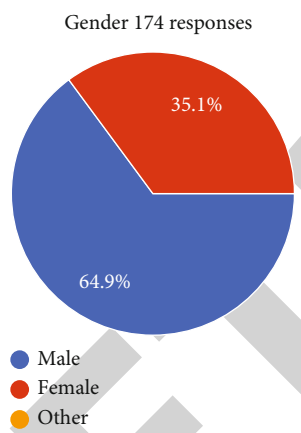

Figure 6: The percentage of the population involved in the survey.

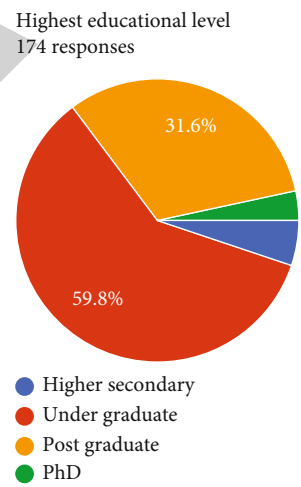

Figure 7: The percentage of the education level of the population involved in the survey.

of life. Also, a stroke that occurs while sleeping might be fatal to an aged person. So, real-time health monitoring is critical for stroke detection. Material(s)/Method: Smart IoT sensors integrated into mattresses, wearable gadgets, and clothing record and physiological factors such as brainwaves, sleep movement, and muscle activation. Sleep monitoring devices assess sleep quality and detect sleep disorders [19]. To address the influence of continuous sleep on cerebral apoplexy in Chinese people, the authors' research demonstrates that persons with durative somnipathy have more adverse occurrences [20]. Poststroke tiredness is a typical consequence of stroke that affects the quality of life. Although numerous therapy techniques have been investigated in the past decade, the risks for PSF remain unclear. This meta-analysis sought to identify PSF risk factors, particularly clinical and social associated with an increased risk, that may be prevented [21]. After a stroke, up to two-thirds of individuals develop OSA. These individuals had poorer short-term sickness, cognitive and functional recovery, and long-term death rates than those without OSA. Detecting OSA and controlling it with positive airway pressure (PAP) are key therapeutic aims after a stroke [22]. People who have had a stroke often have trouble sleeping. Poor sleep is linked to a worse quality of life, and more research is required on the long-term effects of stroke on sleep. This study compared the sleep habits of chronic stroke patients with those of non-survivors. The authors looked at mood and activity as possible sleep correlations [23]. At the beginning of the study, 95,023 Chinese volunteers who had never had a stroke were surveyed (2006-2007). The authors explained that based on sleep duration, the Cox proportional models were used to calculate stroke hazard ratios and confidence intervals [24]. Stroke rehabilitation patients in Canada were monitored

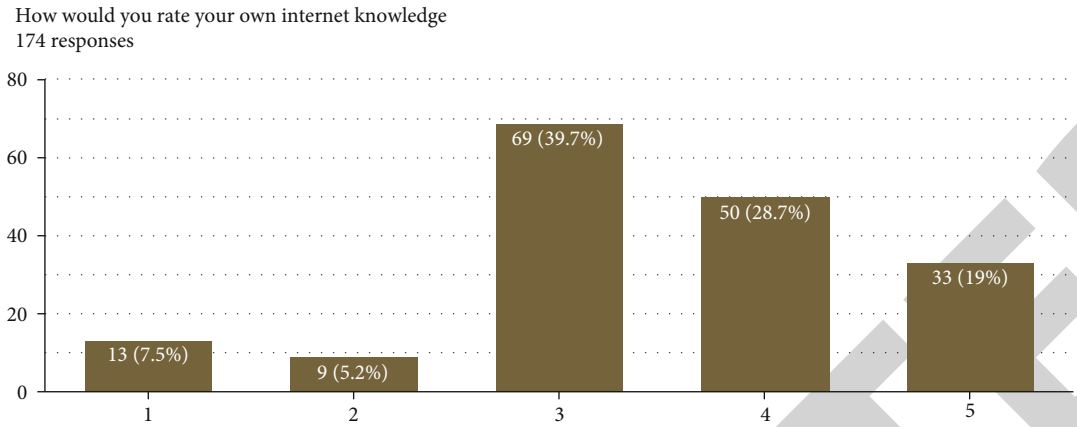

Figure 8: The percentage of the knowledge rate population involved in the survey.

for two weeks to determine their activity levels and sedentary time [25]. The results of a study published in the *Journal of Sleep Research* suggest that chronic sleep deprivation can lead to cumulative waking neurobehavioral impairments [3]. An attack on the brain known as a stroke occurs when the "unexpectedly disruption of blood supply." The blood flow to a portion of the brain may have been unexpectedly halted or a cardiovascular system ruptured. The term "wake-up stroke" refers to a condition in which a patient wakes up with symptoms that have never been seen before they went to sleep [26]. The results of their study were published in the *Journal Sleep Research*, where they describe how awake neurobehavioral and physiological processes are measured and compared to those of people who do not sleep at all [2]. The purpose of this research is to examine if post-stroke urine incontinence (UI) affects one-year outcomes in terms of attention and cognitive processing speed [27]. Physical therapists who treat persons with chronic stroke in the community were the focus of the research. Professionals caring for long-term stroke survivors may benefit from the findings of this research in [28]. In this article, the authors stated that three teaching hospitals in the United Kingdom conducted a study comparing aged care, general medical care, and stroke care [29]. Deglutition seems to be more significant than swallowing postischemic impairment. A prompt swallowing rehabilitation may enhance and speed up the recovery of patients with apparent clinical, psychological, and economic benefits. An Italian rehabilitation center has already been treating a patient with ischemic illness and stroke at Udine Civil Hospital since 1989 [30]. Tissue plasminogen activator (TPA) injections and thrombectomy were previously restricted to 4.5 and 6 hours, respectively [31]. What happens to our brains when we do not get enough sleep? Frameworks for assessing sleep loss are few in comparison to the positive effects of sleep. Sleep deprivation (SD) is not only about the lack of sleep and the associated advantages; rather, it is also about a variety of other things, including prolonged awake. Neuroimaging studies are used to examine the special effects of SD on attention and working memory, positively and negatively reaction, and hippocampal learning. There are recognized changes in cognition and emotion related to sleep disturbance, This

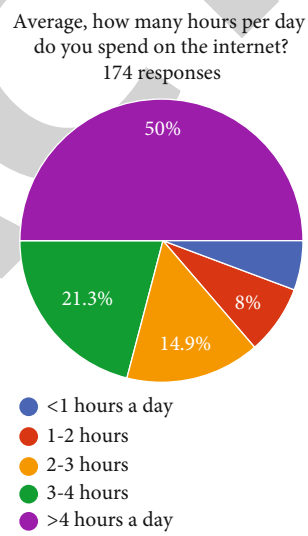

Figure 9: The percentage of how much time students spend on the Internet in a day.

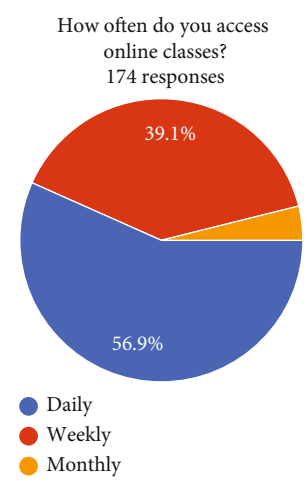

Figure 10: The percentage of how often students take online classes.

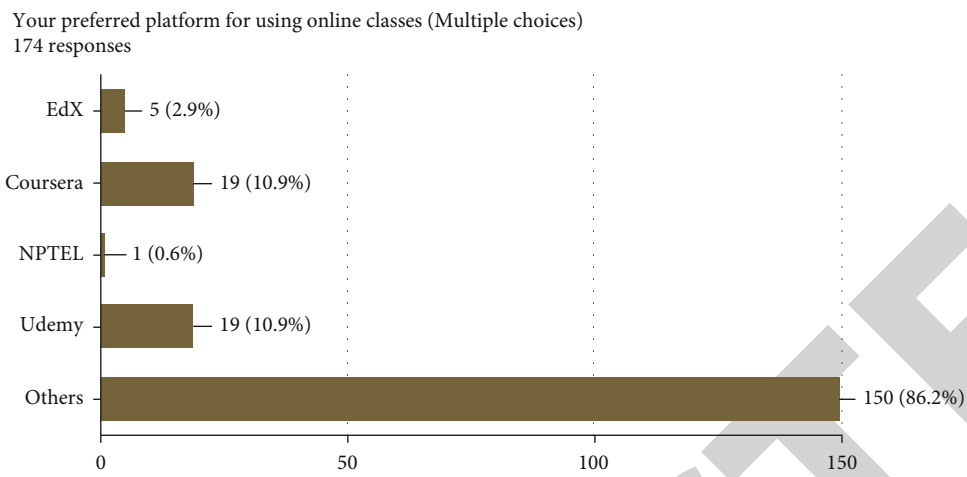

Figure 11: The percentage of the ratio of the top-rated online platforms.

data can help us develop a mechanistic understanding of these changes, in addition to understanding how sleep disruptions cause clinical disorders. We have used the Cronbach's alpha to test the reliability of a scale, so we have 19 individual attributes that have been responded by 174 participants via survey. The evaluated result shows the reliability statistics; the value for Cronbach's alpha is .962, which is very excellent as it reaches 1.

3. Methodology

A stroke often causes cognitive and memory damage. A year after a stroke, 30% of people acquire dementia. Stroke impairs attention, cognition, language, and direction. The suggested research approach includes phases of data collection and analysis. Comparison of existing work and a comparison of why we have selected this topic will also be elaborated in detail. The research methodology for visual attention is presented in Figure 2. These data were collected through the use of multimedia software and instruments within the e-learning environment. During the data collecting time, we focus on student attention scores by capturing the face, the eyes opened and the eyes closed in the form of photographs to assess students' interest. After collecting data in the form of photographs, we analyze students' comprehensibility using the developed app. To assess the results' validity and correctness, a comparison is made between the software and manual observation of students in the e-learning environment. The methodology steps are as follows:

(i) Firstly, the data is collected as a CSV file whenever the student watches the lecture using the C# application's webcam, and it is logged in the system

(ii) The study of datasets based on attentiveness scores shall be retained

(iii) The correlation will be made among all the students of the class with some graphical representation

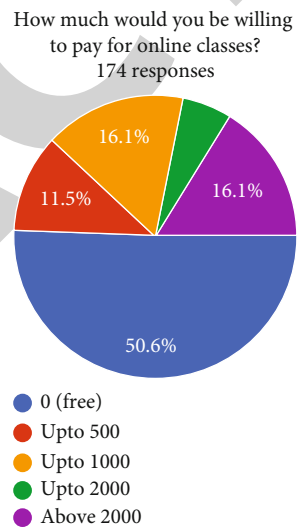

Figure 12: The percentage of how much fee students want to spend for online classes.

Whenever we want to assess the students' attention, we collect the student data from the webcam in the first step. The information is gathered while the student watched the lecture. We are going to give an example of the method for collecting data. Let us imagine S1 is a student viewing a video lecture, and we want to gauge S1's attention using facial expressions. S1 viewed the video lecture for this purpose; meanwhile, his/her computer's webcam is on. Our C# application runs behind the scene and collects each image where the student's face is in front of the webcam. When a webcam sensor detects a face or a C# application sensor detects a student's facial features, the C# app saves the photo to the computer system.

Later, we develop the results and experimentations, the C# application converts a large picture to a small 64×64 -dimensional image, transformed into a 96 dpi 8-bit grayscale image. Switching the image to grayscale, after that on, helps to identify facial expressions more easily and quickly.

The C# program also enhances the image quality before saving it to a computer system. The front is, however,

1	InternetH	OnlineCla	OnlineCla	PersonalS	OnlineCla	OnlineCla	OnlineCla	Favorable	OnlineCla	OnlineCla	IntendToL	IncreaseO	OnlineCla	OnlineCla	SystemUs	OnlineCla	TryAnyFur	IknowBefo	TryTechnologyToEvaluate
2	5	2	1	-1	0	2	0	-2	-1	0	1	-2	-1	0	2	2	0	-2	-2
3	4	0	0	0	0	0	0	0	0	0	0	0	0	0	0	0	0	0	0
4	4	-2	-2	-1	0	-1	-1	-1	-1	-1	-1	-1	-1	-1	-1	-1	-1	1	1
5	5	1	1	1	0	-1	1	1	0	-1	0	-1	0	-1	0	-1	-1	1	1
6	4	-1	-2	1	-2	1	-2	-1	0	-2	-1	-1	-2	1	1	-1	1	-1	-1
7	1	-2	-2	-2	-2	-2	-2	-2	-2	-2	-2	-2	-2	-2	-2	-2	-2	-2	-2
8	1	-2	-2	-2	-2	-2	-2	-2	-2	-2	-2	-2	-2	-2	-2	-2	-2	-2	-2
9	4	0	0	-1	0	-1	-1	-2	-2	-2	0	0	-1	0	0	-1	-1	0	-2
10	3	-1	-1	1	1	0	-1	0	0	-2	-1	-2	-2	-1	-1	0	2	2	1
11	3	-1	-1	0	-1	0	-1	-1	-1	1	-1	0	-1	-2	-1	-1	-1	-1	0
12	5	1	0	1	0	1	1	2	0	0	1	0	-1	1	0	0	0	0	0
13	4	1	1	0	1	1	1	1	1	1	1	1	1	1	1	1	1	1	1
14	3	1	0	0	0	1	1	1	0	1	0	0	0	1	1	-1	1	1	1
15	4	0	-1	0	-1	-1	-1	-1	-1	0	-1	-1	-1	-1	-1	-2	-2	-2	0
16	4	-2	-2	0	-2	-2	-2	-2	-2	-2	-2	-2	-2	-2	-2	-2	-2	0	2
17	4	-2	-2	-2	-1	-1	-1	-2	-2	-1	-2	-2	-1	-2	-2	-1	-2	-2	-2
18	3	-1	-1	-1	-1	-1	-1	-1	-1	0	-1	-1	-1	0	-1	-1	0	0	0
19	3	-1	-2	0	-2	-1	-1	-1	-2	-1	-1	-2	-2	-2	-1	-1	-1	-2	0
20	3	-1	-1	-1	-2	-2	-2	-2	-2	0	-2	-2	-2	-1	-1	-2	-2	1	1

Figure 13: The sample screenshot of the dataset for student behavior related to the online classes.

detected by the Haar Cascade Classifier accessible in C#. We can see in the image below how the images look when they are stored on the system. Figure 3 shows sample photos of 10 students watching the lecture.

We are implementing the detection and saving of the face. Meanwhile, we are preparing a column that has been saved to a CSV file that the C# framework can generate automatically. ScoringDataNumber.csv is the name of the file, and the number reflects the user ID who is watching the same video lecture. Figures 4 and 5 display a preview of the dataset file.

3.1. Number of Faces. This section specifies the number of faces in the webcam image. For detecting the number of faces within a picture, the C# app uses the Haar Cascade Classification.

4. Actual Eyes

For example, when two sides are detected in the actual picture frame, the values in this column are 4. But if only one face is identified in the current image frame, the value is two. The attentiveness of the current face will later be determined exactly.

4.1. Detected Eyes. This column reflects the current image's eyes; its value maybe 0, 1, or 2.

4.2. Opened Eyes. For example, if one eye is opened on the detected face, the value is 1; if both eyes are opened, then the value is 2.

4.3. Closed Eyes. This column tracks the closed column's reverse values, because if one eye is closed in the current face recognition, the value is 1 and, when both eyes are closed, the value is 0, etc.

4.4. Eye Detection Error. This column records the eye-tracking error; for example, if multiple faces were observed in the existing frame and the numbers of eyes identified were one or null, the eye identification error would be 1 and 2, so if one eye were spotted, the number of eyes detected would be 2. The detection error method is seen below.

$$\text{Eye detection error} = \text{actual eyes} - \text{detected eyes}. \quad (1)$$

4.5. PFPS. This column shows the number of frames per second processed.

4.6. Attentiveness. This column records the score of attention using the formula given:

```
if (numberOfFaces != 0)
attentiveness = ((0.5 * numberOfFaces * 2 / actual Eyes) + (opened Eyes / actual Eyes * 0.5));
else
attentiveness =0;
```

While using the above formulas, the value remains o.5 or 0.75 or 1 for attention.

4.7. Attention Level. This attribute is very important as it tells us how sleepy a student is if the attention value is 0.5, 0.75, or 1, this value is considered satisfying. This value is considered an attention level in this column.

5. Validating the Student's Behavior towards Online Learning

Personalized learning is part of learning for hundreds of years. In the past, when the facilities in the education field were so less, the number of schools was too less; people learn their prior knowledge from home or any intellectual person from the family. After this, thousands of schools open, and students get their education by themselves. They go to school and get an education, but many students cannot afford the fees and expenses. For this, they go for a job and mostly prefer online learning or personalized learning. This type of education they can get when they are free from their jobs. In online learning, the student's attention level is how much he is attentive when he takes the lecture. Due to the coronavirus (COVID-19) worldwide, a pandemic situation spread in today's time. More or less, everything has been stopped worldwide; as per condition, all schools, colleges, and universities are helpless. They all are intended to give online education, as the big issue is that our students are not used to taking online classes because their reflexes and attentional level are not as high. So, in this research work, we measure the student's attention level; we will check the student's behavior. For this, we will generate a survey for the students of Pakistan. Because in Pakistan, the literacy

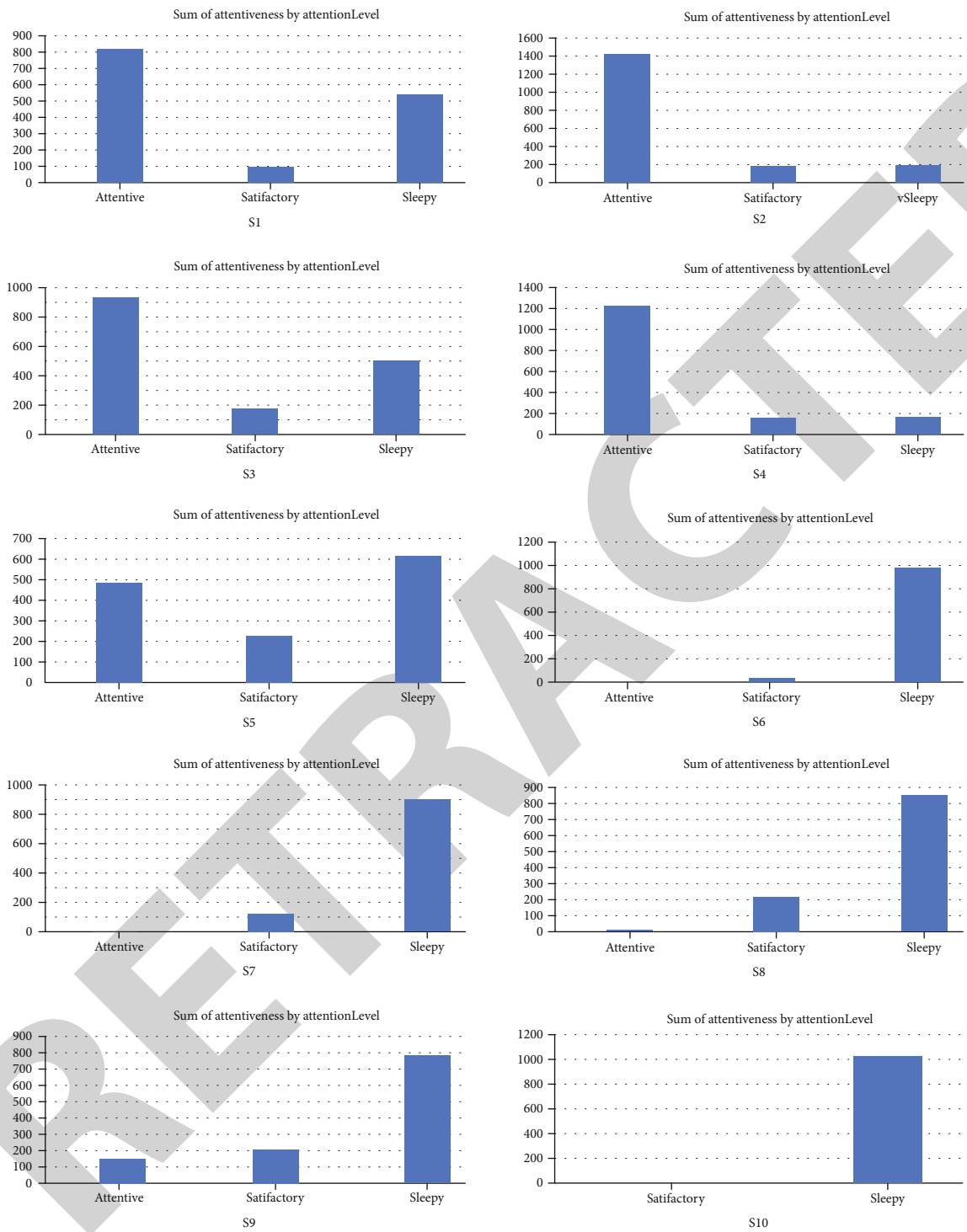

Figure 14: Visualization of 10 students' attentiveness by attention level.

rate is almost half of the population; also, they are not used to online leering and search for things from the Internet and research work.

5.1. Google Analytics Visualization. In this section, we have visualized the population's detail, which is involved in the survey. We have to take the survey from 174 genders from Pakistan. The ratio of male and female is as shown in Figure 6, where the 64.9% population from the male side and 35.1% are females.

In Figure 7, we have shown the educational level of the population involved in this survey. There are four major categories: higher secondary, undergraduate, postgraduate, and Ph.D.

Figure 8 shows the ratio of the prior information of the population relating to knowledge about the Internet. As in online learning, the knowledge related to the Internet is

more important. So, we have seen that 39.7% have good knowledge and 5.2% have less knowledge about the Internet.

Figure 9 displays the average rate that how much time in a day you have spent on the Internet. So, we have analyzed half of the population spends more than four hours on the Internet in a day.

Figure 10 shows how many students are taking online classes in a day, week, and month. Our analysis showed that 56.9% have taken online classes daily.

In Figure 11, we have asked students which platform they have mostly used for online learning: our query regarding the most rated online learning platform like EdX, Coursera, NPTEL, or Udemy. We have evaluated that 86.2% population is not encouraging these all-top-rated platforms. They want to learn online from their institutes or the Internet [32].

Figure 12 shows that 50.6% of the population prefer to learn from the Internet, and they do not want to pay their institutes or coaching centers, because they want to learn free of cost [33].

Figure 13 shows the sample screenshot of the dataset which we used in our analysis; in the dataset, we have asked multiple question from the students. Therefore, in our analysis, we cannot use these questions as it is in SPSS tool. Thus, we have converted them in a short form variable that can easily generate the results. So the short form abbreviated questions are as follows: Internet Hours, OnlineClassesHelpLongRun, OnlineClassesWillImproveLearning, PersonalSuccessByOnlineClasses, OnlineClassesHelpBoostSkills, OnlineClassesAreSimpleToUse, OnlineClassesMoreFlexible, FavorableAttitudeTowardsOnlineClasses, OnlineClassesImpactsPositivityOnMe, OnlineClassesUseIsTrend, IntendToUseOnlineClasses, IncreaseOccurracneOfOnlineClasses, OnlineClassesWillEnhance, OnlineClassesConsistentWithDevices, SystemUseWillBoostMyLearning, OnlineClassesMatchesWithOldSystem, TryAnyFunction, IknowBefore, and TryTechnologyToEvaluate.

6. Results and Discussion

6.1. Overview. Our results from the extracted dataset that we discussed earlier were presented in this section; so there are three levels of attention:

(i) Sleepy

(ii) Satisfactory

(iii) Attentiveness

Image 14 showed the attentiveness and attention level results of the ten students. In this figure, we tested the 10 students' attentiveness and attention level, which is the display with the name S1 to S10.

6.2. Student1 Attentiveness and Attention Level. Student1 (S1) remains the most attentive when the sleepy attention level is the second-highest in the graph. And then, the student's attention level turns to be satisfactory for very little time compared to the attentive attention level.

Table 1: Descriptive statistics.

	Mean	Std. deviation	*N*
S1	.8772	.21086	851
S2	.9239	.18474	851
S3	.8481	.21810	851
S4	.5247	.07845	851
S5	.5320	.08872	851
S6	.6366	.19230	851
S7	.5400	.09166	851
S8	.5138	.06207	851
S9	.5006	.01211	851
S10	.5000	.00000	851

Table 2: Correlations[d] (a).

		S1	S2	S3	S4	S5	S6
S1	Pearson correlation	1	.077*	.086*	.032	-.045	.006
	Sig. (2-tailed)		.025	.012	.347	.189	.857
S2	Pearson correlation	.077*	1	.058	.013	.041	.123**
	Sig. (2-tailed)	.025		.092	.705	.230	.000
S3	Pearson correlation	.086*	.058	1	.108**	-.011	.010
	Sig. (2-tailed)	.012	.092		.002	.758	.779
S4	Pearson correlation	.032	.013	.108**	1	.087*	.044
	Sig. (2-tailed)	.347	.705	.002		.011	.196
S5	Pearson correlation	-.045	.041	-.011	.087*	1	.118**
	Sig. (2-tailed)	.189	.230	.758	.011		.001
S6	Pearson correlation	.006	.123**	.010	.044	.118**	1
	Sig. (2-tailed)	.857	.000	.779	.196	.001	
S7	Pearson correlation	-.027	.080*	-.093**	.006	.123**	.061
	Sig. (2-tailed)	.425	.020	.006	.864	.000	.074
S8	Pearson correlation	-.016	-.101**	-.068*	-.055	-.014	-.023
	Sig. (2-tailed)	.633	.003	.049	.109	.692	.509
S9	Pearson correlation	-.087*	-.111**	-.078*	-.015	-.018	-.034
	Sig. (2-tailed)	.011	.001	.024	.656	.610	.315
S10	Pearson correlation	.b	.b	.b	.b	.b	.b
	Sig. (2-tailed)	.	.	.	.	.	.

6.3. Student2 Attentiveness and Attention Level. Student2 (S2) seems very attentive, as we can see in the picture; attentive attention is much higher than satisfactory and sleepy.

6.4. Student3 Attentiveness and Attention Level. Student3 (S3) is attentive, and then, its graph is a little bit satisfactory; then the student is sleepy. Therefore, we can say the student has almost 60% of attention to be attentive here.

Table 3: Correlations [d] (b).

		S7	S8	S9	S10
S1	Pearson correlation	-.027	-.016	-.087*	.b
	Sig. (2-tailed)	.425	.633	.011	.
S2	Pearson correlation	.080*	-.101**	-.111**	.b
	Sig. (2-tailed)	.020	.003	.001	.
S3	Pearson correlation	-.093**	-.068*	-.078*	.b
	Sig. (2-tailed)	.006	.049	.024	.
S4	Pearson correlation	.006	-.055	-.015	.b
	Sig. (2-tailed)	.864	.109	.656	.
S5	Pearson correlation	.123**	-.014	-.018	.b
	Sig. (2-tailed)	.000	.692	.610	.
S6	Pearson correlation	.061	-.023	-.034	.b
	Sig. (2-tailed)	.074	.509	.315	.
S7	Pearson correlation	1	.006	-.021	.b
	Sig. (2-tailed)		.854	.537	.
S8	Pearson correlation	.006	1	.380**	.b
	Sig. (2-tailed)	.854		.000	.
S9	Pearson correlation	-.021	.380**	1	.b
	Sig. (2-tailed)	.537	.000		.
S10	Pearson correlation	.b	.b	.b	.b
	Sig. (2-tailed)	.	.	.	

*Correlation is significant at the 0.05 level (2-tailed). **Correlation is significant at the 0.01 level (2-tailed). [b]It cannot be computed because at least one of the variables is constant. [d]List wise $N = 851$.

Table 4: Case processing summary.

		N	%
Cases	Valid	170	99.5
	Excluded[a]	4	.5
	Total	174	100.0

Table 5: Reliability statistics.

Cronbach's alpha	Cronbach's alpha based on standardized items	N of items
.962	.962	18

6.5. Student4 Attentiveness and Attention Level. This student is sleepy, and very little proportion seems to be satisfactory. Therefore, we can say this student has very low interest in the lecture.

6.6. Student5 Attentiveness and Attention Level. Student5 (S5) is like student4 (S4); this student is also sleepy almost all the time, so the student seems the least interested in the lecture, or he/she is sleeping and not watching the lecture properly.

6.7. Student6 Attentiveness and Attention Level. Student6's (S6) behavior is almost the same as student5's because this student is almost sleepy and satisfactory for a very short interval.

Table 6: Item statistics.

	Mean	Std. deviation	N
OnlineClassesHelpLongRun	-0.51	1.198	170
OnlineClassesWillImproveLearning	-0.55	1.162	170
PersonalSuccessByOnlineClasses	-0.44	1.181	170
OnlineClassesHelpBoostSkills	-0.61	1.132	170
OnlineClassesAreSimpleToUse	-0.39	1.212	170
OnlineClassesMoreFlexible	-0.62	1.166	170
FavorableAttitudeTowardsOnlineClasses	-0.48	1.198	170
OnlineClassesImpactsPositivityOnMe	-0.55	1.182	170
OnlineClassesUseIsTrend	-0.24	1.237	170
IntendToUseOnlineClasses	-0.43	1.191	170
IncreaseOccurracneOfOnlineClasses	-0.49	1.142	170
OnlineClassesWillEnhance	-0.54	1.255	170
OnlineClassesConsistentWithDevices	-0.35	1.204	170
SystemUseWillBoostMyLearning	-0.35	1.148	170
OnlineClassesMatchesWithOldSystem	-0.64	1.164	170
TryAnyFunction	-0.19	1.250	170
IknowBefore	-0.22	1.266	170
TryTechnologyToEvaluate	-0.08	1.285	170

6.8. Student7 Attentiveness and Attention Level. Student7's (S7) graph shows that he/she is a little bit satisfactory, and most of the time, the attentiveness level is sleepy, so we

Table 7: Interitem correlation matrix.

	Online Classes Help LongRun	Online Classes WillImprove Learning	Personal SuccessBy Online Classes	Online Classes HelpBoost Skills	Online Classes AreSimple ToUse	Online Classes More Flexible	Favorable Attitude Towards Online Classes	Online Classes Impacts Positivity OnMe	Online Classes UseIs Trend	Intend ToUse Online Classes	Increase Occurracne OfOnline Classes	Online Classes Will Enhance	Online Classes Consistent With Devices	SystemUse WillBoost MyLearning	OnlineClasses Matches WithOld System	TryAny Function	Iknow Before	Try Technology ToEvaluate
OnlineClasses HelpLongRun	1	0.789	0.757	0.683	0.577	0.633	0.590	0.614	0.526	0.656	0.588	0.712	0.626	0.605	0.547	0.470	0.454	0.415
OnlineClassesWill ImproveLearning	0.789	1	0.744	.714	0.599	0.552	0.575	0.614	0.564	0.653	0.607	0.697	0.660	0.629	0.568	0.425	0.421	0.437
PersonalSuccess ByOnlineClasses	0.757	0.744	1	.731	0.611	0.581	0.670	0.716	0.459	0.672	0.607	0.682	0.651	0.657	0.580	0.480	0.592	0.522
OnlineClassesHelp BoostSkills	0.683	0.714	0.731	1	0.568	0.579	0.653	0.629	0.510	0.656	0.605	0.626	0.605	0.607	0.612	0.491	0.555	0.462
OnlineClassesAre SimpleToUse	0.577	0.599	0.611	0.568	1	0.564	0.569	0.545	0.594	0.626	0.576	0.559	0.603	0.547	0.556	0.545	0.469	0.470
OnlineClasses MoreFlexible	0.633	0.552	0.581	0.579	0.564	1	0.697	0.665	0.546	0.624	0.618	0.640	0.576	0.550	0.588	0.439	0.42	0.329
FavorableAttitude TowardsOnline Classes	0.590	0.575	0.670	0.653	0.569	0.697	1	0.722	0.603	0.723	0.724	0.613	0.650	0.591	0.590	0.552	0.528	0.544
OnlineClasses ImpactsPositivity OnMe	0.614	0.614	0.716	0.629	0.545	0.665	0.722	1	0.547	0.677	0.651	0.699	0.604	0.677	0.629	0.551	0.58	0.457
OnlineClasses UseIsTrend	0.526	0.564	0.459	0.51	0.594	0.546	0.603	0.547	1	0.622	0.555	0.517	0.544	0.483	0.437	0.511	0.413	0.565
IntendToUse OnlineClasses	0.656	0.653	0.672	0.656	0.626	0.624	0.723	0.677	0.622	1	0.785	0.700	0.715	0.654	0.662	0.522	0.460	0.534
IncreaseOccurracne OfOnlineClasses	0.588	0.607	0.607	0.605	0.576	0.618	0.724	0.651	0.555	0.785	1	0.646	0.662	0.576	0.617	0.499	0.528	0.477
OnlineClasses WillEnhance	0.712	0.697	0.682	0.626	0.559	0.640	0.613	0.699	0.517	0.700	0.646	1	0.665	0.591	0.590	0.528	0.447	0.464
OnlineClasses Consistent WithDevices	0.626	0.660	0.651	0.605	0.603	0.576	0.650	0.604	0.544	0.715	0.662	0.665	1	0.757	0.568	0.612	0.559	0.544
SystemUse WillBoost MyLearning	0.605	0.629	0.657	0.607	0.547	0.550	0.591	0.677	0.483	0.654	0.576	0.591	0.757	1	0.679	0.588	0.614	0.586
OnlineClasses Matches WithOldSystem	0.547	0.568	0.580	0.612	0.556	0.588	0.590	0.629	0.437	0.662	0.617	0.590	0.568	0.679	1	0.502	0.410	0.447
TryAnyFunction	0.470	0.425	0.48	0.491	0.545	0.439	0.552	0.551	0.511	0.522	0.499	0.528	0.612	0.588	0.502	1	0.595	0.705
IknowBefore	0.454	0.421	0.592	0.555	0.469	0.420	0.528	0.580	0.413	0.460	0.528	0.447	0.559	0.614	0.410	0.595	1	0.596
TryTechnology ToEvaluate	0.415	0.437	0.522	0.462	0.470	0.329	0.544	0.457	0.565	0.534	0.477	0.464	0.544	0.586	0.447	0.705	0.596	1

Table 8: Scale item-total statistics.

	Mean if item deleted	Variance if item deleted	Corrected item Total correlation	Squared multiple correlations	Cronbach's alpha if item deleted
OnlineClassesHelpLongRun	-7.16	251.760	0.771	0.738	0.959
OnlineClassesWillImproveLearning	-7.12	252.661	0.771	0.756	0.959
PersonalSuccessByOnlineClasses	-7.23	250.817	0.809	0.780	0.959
OnlineClassesHelpBoostSkills	-7.06	253.298	0.775	0.672	0.959
OnlineClassesAreSimpleToUse	-7.28	253.257	0.720	0.572	0.960
OnlineClassesMoreFlexible	-7.05	254.341	0.720	0.646	0.960
FavorableAttitudeTowardsOnlineClasses	-7.19	250.714	0.800	0.730	0.959
OnlineClassesImpactsPositivityOnMe	-7.12	251.174	0.799	0.739	0.959
OnlineClassesUseIsTrend	-7.44	254.354	0.674	0.604	0.961
IntendToUseOnlineClasses	-7.24	249.924	0.827	0.768	0.958
IncreaseOccurracneOfOnlineClasses	-7.18	252.907	0.779	0.709	0.959
OnlineClassesWillEnhance	-7.14	249.893	0.782	0.692	0.959
OnlineClassesConsistentWithDevices	-7.32	250.514	0.801	0.731	0.959
SystemUseWillBoostMyLearning	-7.32	252.526	0.785	0.744	0.959
OnlineClassesMatchesWithOldSystem	-7.03	254.443	0.719	0.625	0.960
TryAnyFunction	-7.48	253.92	0.678	0.649	0.961
IknowBefore	-7.45	254.746	0.647	0.611	0.961
TryTechnologyToEvaluate	-7.59	254.551	0.641	0.671	0.961

can say this person is sleepy as well and not interested or not watching the lecture properly.

6.9. Student8 Attentiveness and Attention Level. Student8 (S8) is a little bit satisfactory and, most of the time, sleepy, so this student is also not watching the lecture properly, or we may say that the student is not interested in the lecture.

6.10. Student9 Attentiveness and Attention Level. Student9 (S9) is a little bit interested in the lecture because some of the graphs show satisfactory and attentive behavior. Again, the student gets sleepy for almost half of the time than satisfactory and attentive attention.

6.11. Student10 Attentiveness and Attention Level. Student10 has mixed behavior like in [34]. As we can see, the graph has a considerable bar for being attentive and satisfactory now. Comparing both attention levels with the sleepy attention level is also very strong; this may conclude that student10 S10 and was about 0% interested in the lecture. Before we conclude overall behavior, we might consider that our eyes get closed after a specific time interval, so every graph has some kind of natural biases. However, by considering that face, we can even then see considerable sleepy behavior. We can conclude here that the lecture topic is boring, or the students are not interested in watching this specific lecture for some reason. Now it is up to the teacher; he/she should take some feedback from the students to improve the lecture or ask them to watch the lecture more attentively if there is no problem with the lecture content or video quality, as shown in Figure 14.

6.12. Correlations. The following table shows the correlations among the ten students. So, any significant value, which is less than 0.05, shows a strong relationship. The significance value of S1and S2 is 0.025, so S1 and S2 have a strong relationship, and we have also seen it above in the graph analytics.

If we compare the correlation between s4 and s2, then the significance value S4 is .705, which is very large than 0.05, so there is no good relation between s4 and s2, which is also seen well in the graph analytics above. Likewise, we can check all the pairs, and every pair will support the graph analytics results discussed above and shown in Tables 1–3.

6.13. Reliability Scale: All Variables by Cronbach's Alpha Using SPSS. Cronbach's alpha is a test of the reliability of a scale, we have 19 attributes so we have 19 individual attributes responding to participants via survey. Cronbach's alpha can be used to test the reliability of the scale when we have a series of items/attributes; in this case, we have 19 attributes. We can see only 4 rows are excluded or miss some values while there are 170 cases considered for the results, as shown in Table 4.

6.13.1. The Procedure Is Deleted List-Wise Based on All Variables. Table 4 shows the mean and standard deviation of the attributes used for further interpretations. The following table is very important as it shows the reliability statistics; the value for Cronbach's alpha is .962, which is very excellent as it reaches 1. Thus, there is very strong reliability. If the value falls under 6, we look back to the mean and standard deviation table and remove the attribute with low values for mean or standard deviation and try the test for the remaining attributes, as shown in Tables 5–7.

The total item statistics 2nd column tells us the value for Cronbach's alpha if a specific item or attribute is deleted. For

Table 9: Scale Statistics.

Mean	Variance	Std. deviation	*N* of items
-7.67	282.494	16.808	18

example, if we delete the first attribute and apply Cronbach's alpha on the remaining items, the reliability scale value will be 7.16. In this way, we can highlight each attribute's significance. Hence, if an attribute does not affect the value of reliability, we can go ahead and delete that attribute. So, Cronbach's alpha tells us which attribute or item to delete to increase the reliability. Still, in our case, we have luckily chosen the attributes which are best already, so we will not delete any attribute, as shown in Tables 8 and Table 9.

7. Conclusion

Medical emergencies such as strokes, which are also known as cerebrovascular accidents, can induce behavioral dysfunction in people. Sleep deprivation affects our brains in several different ways. When compared to the advantages of sleep, sleep loss frameworks are minimal. Many factors contribute to sleep deprivation (SD), including being awake for an extended period. Neuroimaging studies the effects of SD on attention, working memory, mood, and hippocampus-based learning. To assess biosignaling/bioimaging data acquired from the patient, automated diagnostic techniques are generally favored. In this research, we explored the association between watching the same lecture and students' results. For ten students watching the same video, we collected data via a webcam. We also implemented graph analysis and correlation methodology after the data was collected to determine the class students' behavior towards the same video lecture. We noticed that most students were not interested in this video lecture. Still, the teacher can ask the students to view the lecture more carefully. If there is any problem with the lecture's quality or the topic is confusing or boring, the teacher can give the lecture to the students again and maybe take some necessary action. The alpha of Cronbach showed a strong correlation between the attributes/questions that we asked in our survey, and we will use this survey to prepare for online class evaluations.

8. Future Work Limitations

The purpose of usage may have been determined by certain considerations, such as prior experience required to take a specific course, not included in the analysis. There will also be further variables in prospective experiments, and the connections between them should be established or the indirect influence of the variables included in the current model tested. This work is limited to survey data in the future.

Data Availability

We are attaching dataset files that are used in this paper (dataset link: https://github.com/sobiawassan/The-Impact-of-Online-Learning-System-on-Students-Who-Affected-with-Stroke-Disease-main.git).

Conflicts of Interest

The authors declare that they have no conflicts of interest.

Acknowledgments

The work was supported in part by the National Social Science Foundation of China under Grant No. 21ZDA033 and 21BGL223, by the National Natural Science Foundation of China under Grant Nos. 71771118 and 72071104, by the Ministry of Education Humanities and Social Sciences Foundation of China under Grant No.18YJCZH146, and by the Key Project of Social Science Foundation of Jiangsu Province under Grant No. 20GLA007.

Supplementary Materials

The impact of online learning system on students who affected with stroke disease. *(Supplementary Materials)*

References

[1] A. J. Krause, E. B. Simon, B. A. Mander et al., "The sleep-deprived human brain," *Nature Reviews Neuroscience*, vol. 18, no. 7, pp. 404–418, 2017.

[2] H. P. A. Van Dongen, G. Maislin, J. M. Mullington, and D. F. Dinges, "The cumulative cost of additional wakefulness: dose-response effects on neurobehavioral functions and sleep physiology from chronic sleep restriction and total sleep deprivation," *Sleep*, vol. 26, no. 2, pp. 117–126, 2003.

[3] H. P. A. Van Dongen and D. F. Dinges, "Sleep debt and cumulative excess wakefulness," *Sleep*, vol. 26, no. 3, pp. 249–249, 2003.

[4] J. S. Durmer and D. F. Dinges, "Neurocognitive consequences of sleep deprivation," *Seminars in Neurology*, vol. 25, no. 1, pp. 117–129, 2005.

[5] N. Goel, H. Rao, J. S. Durmer, and D. F. Dinges, "Neurocognitive consequences of sleep deprivation," *Seminars in Neurology*, vol. 29, no. 4, pp. 320–339, 2009.

[6] A. A. Borbely, "Sleep, sleep deprivation and depression. A hypothesis derived from a model of sleep regulation," *Human Neurobiology*, vol. 1, no. 3, pp. 205–210, 1982.

[7] N. Goel, M. Basner, H. Rao, and D. F. Dinges, "Circadian rhythms, sleep deprivation, and human performance," *Progress in Molecular Biology and Translational Science*, vol. 119, pp. 155–190, 2013.

[8] M. W. L. Chee and J. C. Tan, "Lapsing when sleep deprived: neural activation characteristics of resistant and vulnerable individuals," *NeuroImage*, vol. 51, no. 2, pp. 835–843, 2010.

[9] M. W. L. Chee, J. C. Tan, S. Parimal, and V. Zagorodnov, "Sleep deprivation and its effects on object-selective attention," *NeuroImage*, vol. 49, no. 2, pp. 1903–1910, 2010.

[10] M. W. L. Chee, C. S. F. Goh, P. Namburi, S. Parimal, K. N. Seidl, and S. Kastner, "Effects of sleep deprivation on cortical activation during directed attention in the absence and presence of visual stimuli," *NeuroImage*, vol. 58, no. 2, pp. 595–604, 2011.

Hindawi
Behavioural Neurology
Volume 2023, Article ID 9842478, 1 page
https://doi.org/10.1155/2023/9842478

Retraction

Retracted: Customer Experience towards the Product during a Coronavirus Outbreak

Behavioural Neurology

Received 8 August 2023; Accepted 8 August 2023; Published 9 August 2023

This article has been retracted by Hindawi following an investigation undertaken by the publisher [1]. This investigation has uncovered evidence of one or more of the following indicators of systematic manipulation of the publication process:

(1) Discrepancies in scope

(2) Discrepancies in the description of the research reported

(3) Discrepancies between the availability of data and the research described

(4) Inappropriate citations

(5) Incoherent, meaningless and/or irrelevant content included in the article

(6) Peer-review manipulation

The presence of these indicators undermines our confidence in the integrity of the article's content and we cannot, therefore, vouch for its reliability. Please note that this notice is intended solely to alert readers that the content of this article is unreliable. We have not investigated whether authors were aware of or involved in the systematic manipulation of the publication process.

Wiley and Hindawi regrets that the usual quality checks did not identify these issues before publication and have since put additional measures in place to safeguard research integrity.

We wish to credit our own Research Integrity and Research Publishing teams and anonymous and named external researchers and research integrity experts for contributing to this investigation.

The corresponding author, as the representative of all authors, has been given the opportunity to register their agreement or disagreement to this retraction. We have kept a record of any response received.

References

[1] S. Wassan, T. Shen, C. Xi, K. Gulati, D. Vasan, and B. Suhail, "Customer Experience towards the Product during a Coronavirus Outbreak," *Behavioural Neurology*, vol. 2022, Article ID 4279346, 18 pages, 2022.

Hindawi
Behavioural Neurology
Volume 2022, Article ID 4279346, 18 pages
https://doi.org/10.1155/2022/4279346

Research Article

Customer Experience towards the Product during a Coronavirus Outbreak

Sobia Wassan,[1] **Tian Shen**,[2] **Chen Xi**,[1] **Kamal Gulati**,[3,4] **Danish Vasan**,[5] **and Beenish Suhail**[6]

[1]*Business School, Nanjing University, China*
[2]*School of International Education, Nanjing University of CM, China*
[3]*Amity University, Noida, Uttar Pradesh, India*
[4]*Stratford University, Virginia, USA*
[5]*School of Software, Tsinghua University Beijing, China*
[6]*School of Economics, Shanghai University, China*

Correspondence should be addressed to Tian Shen; shentian025@aliyun.com and Chen Xi; chenx@nju.edu.cn

Received 9 October 2021; Accepted 10 December 2021; Published 2 February 2022

Academic Editor: Kamalanand Krishnamurthy

Nowadays, sentimental analysis of consumers' review is becoming much crucial in the marketing world. It is not just giving ideas to the firms that how consumers like their product or service, but it would also help them make their service better. In this article, the statistical method identifies the relationship of many factors in consumer feedback. It introduces a deep-based learning method called DSC (deep sentiment classifier) to determine whether or not to recommend the reviewed product thoroughly. Our suggested method also investigates the effect sizes of the feedback, such as positives, negatives, and neutrals. We used the women's clothing review dataset containing 22,642 records after preprocessing of the results. Experimental studies show that the recommendations are an excellent positive sentiment indicator. In comparison, ratings become fuzzy performance metrics in product reviews. The 10-fold cross-validation analysis shows that the recommended form has the top F1 score (93.56%) in the sentimental classification on average and the recommended classification (88.32%) on average. A comparative description of other classifiers focused on machine learning, for example, KNN, random forest, logistic regression, decision tree, support vector machine multilayer perceptron, and naïve Bayes, also demonstrates that DSC gives the best possible result. We have tested DSC on the dataset IMDB (Internet Video Database), which includes the sentiment of the 50,000 movie reviews (25000 for training and 25000 for testing). In comparison to other baseline methods, DSC obtained an excellent classification score for this experiment.

1. Introduction

The study of emotions is a tactic of understanding the ideas, feelings, and expectations expressed in the text feature or the level of a sentence in a given text [1]. Today, enterprises use sites such as Twitter, forums, and blogs as reliable platforms to understand their consumers' expectations and improve their services. Sentiment analysis has become an attractive research field for collecting and assessing thoughts, feelings, and behaviours from sources of language, expression, and datasets that tally to how people respond to a given problem or event [2, 3]. Understanding consumer preferences based on the results of sentiment analysis will boost the industry world [4].

Nowadays, text mining is one of the most considered problems in the area defined above, a technique used to manually or automatically classify text. To address this gap, many studies have been investigated using sentiment analysis to interpret the comments found in chat forums, social media, and review pages [5–7]. Companies have frequently used the task described above to understand investors through their social media customer service teams.

In particular in e-commerce review analyses, there are three crucial approaches for assessing sentimental analysis:

Table 1: Features available with description and data type in the women's clothing dataset.

Feature	Description	Type
Clothing's ID	Unique ID	int64
Ages	Reviewer ages	(int64)
Titles	Review titles	(Object)
Reviews	Reviews	(Object)
Rating	Reviewer rating on the product	(int64)
Recommended ID	Product is recommended or not	(int64)
Positive feedback count	Number of positive feedbacks	(int64)
Division name	Division name of the product	(Object)
Department name	Department name of the product	(Object)
Class name	Product type	(Object)

(i) Lexical analysis

(ii) Machine learning-based analysis

(iii) Hybrid analysis

Lexical analysis: this method of categorizing the words of the response stream in their sections of expression and their reciprocal tagging, well known as POS tagging, is lexical analysis. It is a pretrained lexicon that is prepared for the method [8, 9].

Machine learning-based analysis: artificial intelligence is a subset of machine learning [10, 11] that is used for intelligent algorithms to train a correct classifier model. The research comprises preprocessing data, feature extraction, feature selection, testing, and labelling of the test dataset [12–14]. Deep learning methods are classified into three main classes: unsupervised learning, supervised learning, and semisupervised learning [1, 15, 16].

Hybrid analysis: hybrid methodology is a grouping of classification and regression problems. This methodology is more rapid and more precise than the other methods stated above.

In this article, on this dataset, we established a DSC for sentimental analysis and concentrated on the relationship of different factors in consumer reviews using statistical analysis, which included multivariate distributions, univariate distributions, multivariate analysis, and descriptive statistics [17]. During the first phase, we scrutinized the not-text feedback features (e.g., clothing, department name, ages, classes, and names) and the consumer references present in this dataset to analyze their relationship. We used a deep learning technique [18] to identify customer reviews' feelings about the products and assess whenever a positive review has been done for the purchased items. Generally, the main contributions of the present research work are as follows:

(i) Have a critical overview of similar studies on the study of sentimental analysis of consumer product review

(ii) The way to examine the correlation between the different variables in the consumer product review depends on the four statistical research methods, containing multivariate distribution, univariate distribution, multivariate statistical analysis, and descriptive analysis

(iii) Create a new deep learning algorithm called a deep sentiment classifier that accepts binary forms of text mining problems, such as a recommendation classification and a sentimental analysis on consumer review of purchased products

(iv) Our method can automate the mining and selection of features. This methodology differentiates our contribution from that of [19–21] utilizing handcrafted features

(v) Doing a comprehensive survey by performing several machine learning and conventional natural language and deep learning methods on these complex data to provide businesses with an understanding of how consumers like their goods and amenities

Table 2: Frequency distribution in women's apparel datasets of selected features.

Features	Unique counts
Clothing's ID	1173
Ages	78
Titles	13985
Text review	22622
Ratings	4
Recommended ID	3
Positive feedback counting	83
Division names	4
Department names	7
Class names	20

This paper is structured into sections: Section 2 presents the related work, Section 3 provides a list of the dataset used in this research, Section 4 set out realistic scientific work, Section 5 presents the conclusions as well as the discussions, and Section 6 concludes with several recommendations for future research.

Table 3: Description of statistical analysis for women's data of clothes.

Feature	Mean	Std	Min	25%	50%	75%	Max
Clothing's ID	921.685909	203.683805	1.01	862.0	936.01	1078.0	1205.01
Ages	44.292881	13.328177	18.1	35.1	42.1	53.0	98.01
Ratings	42193093	1.125912	1.01	4.1	5.1	5.1	5.1
Recommended ID	0.828765	0.395223	0.01	1.1	1.1	1.0	1.01
Positive feedback count	2.641785	5.797521	0.01	0.1	1.1	3.0	123.01
Word counts	60.221951	28.543054	2.1	37.1	59.1	88.0	116.01
Character counts	308.771535	143.944127	9.1	187.1	302.1	459.0	509.01
Labels	0.885264	0.307223	0.1	1.0	1.0	1.0	1.0

2. Literature Work

Sentimental analysis is a type of data mining. We relied on predictive analysis and machine learning customer reviews of women's apparel e-commerce datasets. Some traditional methods focus on complex feature models or hand-crafted dictionary-based approaches for predictive analysis and sentiment analysis. In this article, we discussed the previous work on sentiment analysis. Authors [22] performed a hypothetical level of sentimental analysis. The researchers' focus is on three different lexicon techniques, supervised learning and unsupervised learning. At this time, we implemented supervised learning since we had access to supervised machine learning approaches and supervised data. That performed better than the unsupervised ones. Authors [23] addressed the tree-CRF approach to support binary and sparse function presentations. This methodology was a comprehensive and dynamic model of information.

In other words, [24] recommended a stacked denoising autoencoder technique that used a distributed feature to use such distributed word representations. That methodology outperformed tree-CRF as it could not provide a dynamic future structure and can be applied to many other domains. Tang et al.'s [25, 26] sentiment classification was implemented on microblog. Previously, authors used distributed word presentation as polarization, and scholars including [27] applied deep learning approaches. Their implementation was built using a single-layer CNN, while our method includes RNN and addresses two kinds of textual classification problems.

In some researchers [28, 29], a recursive autoencoder approach has been used to embed lexical information into deep learning. [8] proposed a Japanese emotion classification method that used a bidirectional long-term memory (LSTM) RNN network. After, it would be seen that integrating POS tag, word embedding, and Japanese polarization dictionary features strongly affected classification accuracy.

Authors [30] used the long-term memory system (LSTM) bidirectional recurrent neural network (RNN) to suggest and identify sentiments on datasets of e-commerce review. The results have shown that the recommendation is now a high positive sentiment metric. The bidirectional LSTM model mentioned above obtained an F1 score of 89% for the recommendation classified and 94% for the sentimental analysis. At the same time, our proposed model gained an F1 score of 89.32% for classifying recommendations and of 94.52% for classifying emotions.

Much like our proposed methods, Mousa and Schuller and Song et al. [31, 32] have built approaches using a bidirectional LSTM model to produce high-level information through expression and Asian consumer review datasets. In our study, we found actual consumer reviews on women's apparel for dataset analysis and used a deep learning method for sentimental analysis. This research applies natural language and machine learning methods to define large patterns in customer behaviour in text. In the data collection, the total number of unique words is 9811.

Our crucial objective existed to find out what consumers like and do not like about their purchasing. To accomplish this goal, we have performed observational analyses on this massive dataset. Firstly, we used to have to identify the features of the selected attributes and accelerate the difficulty of the analysis until a proper objective had been envisaged. And after that, through our research, we have shown that our statistical experiments are conducted using natural language methods. The results of sentiment analysis provided by state-of-the-art deep learning techniques have been considerable and helpful to e-commerce.

3. Material

(i) We used two distinct types of data sources in this analysis

(ii) The sentiment of women's clothe e-commerce product review

(iii) Movie review thought (IMBD) (Internet Movie Database)

(iv) The sentiment of the women's clothe e-commerce product review dataset [17] is made by actual customers and is thus anonymized; i.e., brand names are replaced by suppliers and customer names are exempted. The data consisted of 22,641 user reviews with 9 supporting attributes, such as age, department, class name, and positive feedback count. Table 1 describes the additional features with the titles, and Table 2 describes the frequency

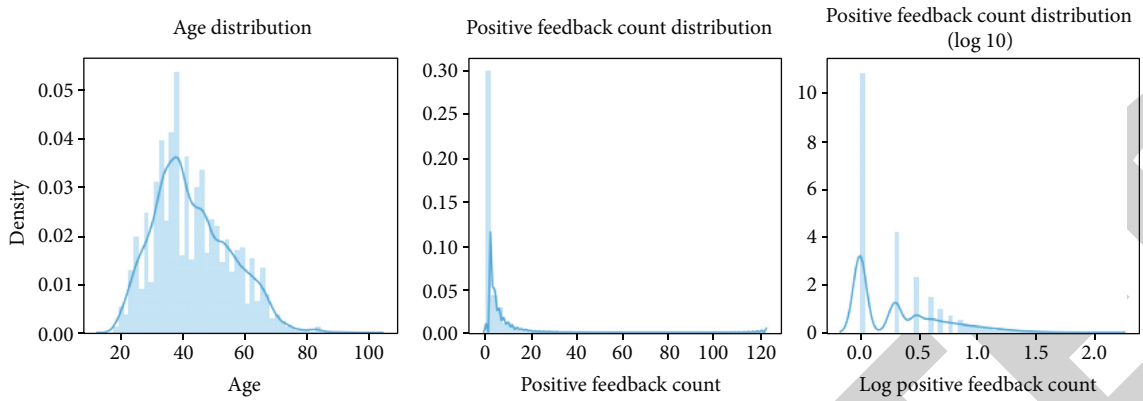

Figure 1: Customer age frequency distributions and positive feedback.

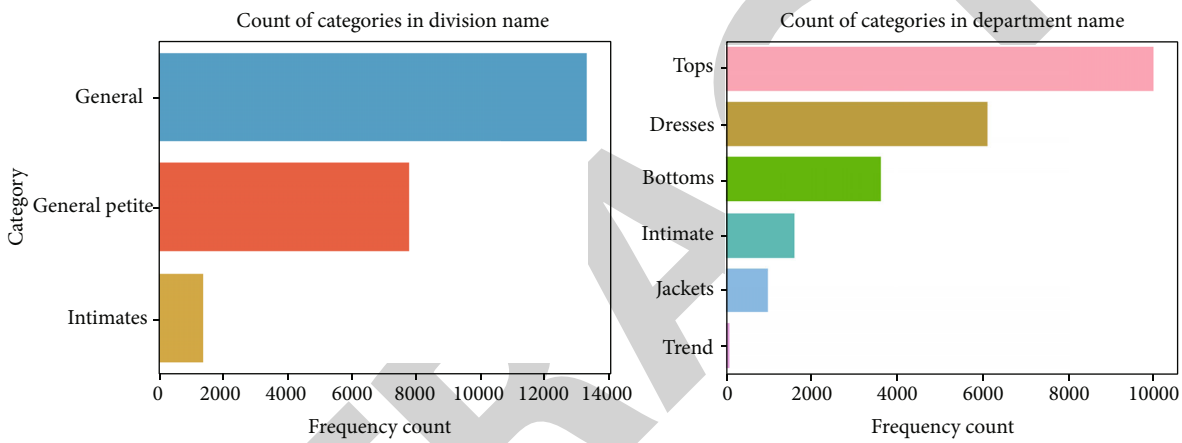

Figure 2: The frequency distribution per department and division of customer feedback.

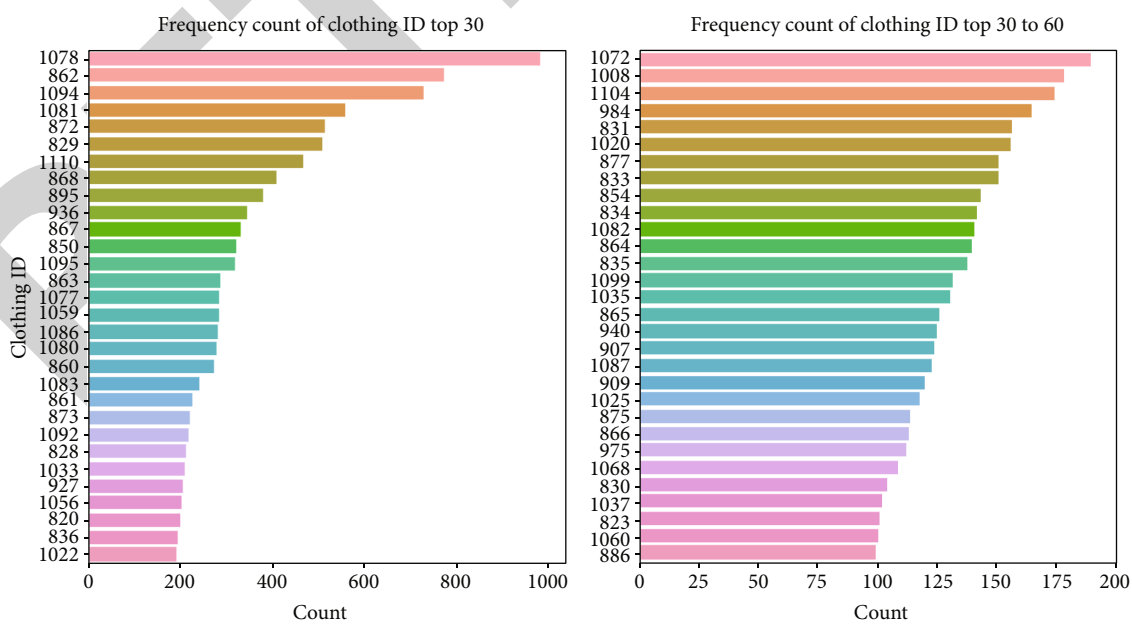

Figure 3: Clothing IDs among the top 60 e-commerce apparel reviews.

Table 4: A clothing ID summary of statistical descriptions (1078, 1094, and 862).

Feature	Mean	Std	Min	25%	50%	75%	Max
Clothing's ID	1016.4849	104.396023	863.0	8623.0	1079.0	1095.0	1095.0
Ages	43.7249	13.150428	19.0	35.0	42.0	52.0	98.0
Ratings	04.1893	01.104307	01.0	04.0	05.0	6.0	6.0
Recommendation IND	00.8185	01.385593	0.0	2.0	01.0	01.0	1.00
Positive feedback counts	02.8625	06.773022	0.0	0.0	01.0	4.0	99.0
Word counts	060.5913	29.731487	2.00	37.0	61.0	88.0	116.0
Character counts	311.8605	145.836159	17.00	188.0	306.0	468.00	505.0
Labels	00.9025	01.296833	0.0	1.0	1.0	1.0	1.0

Class name distribution: as we can see in Figure 4, in the frequency of distributions, the top 3 clothing types (skirts, knits, and blouses) have been the most reported.

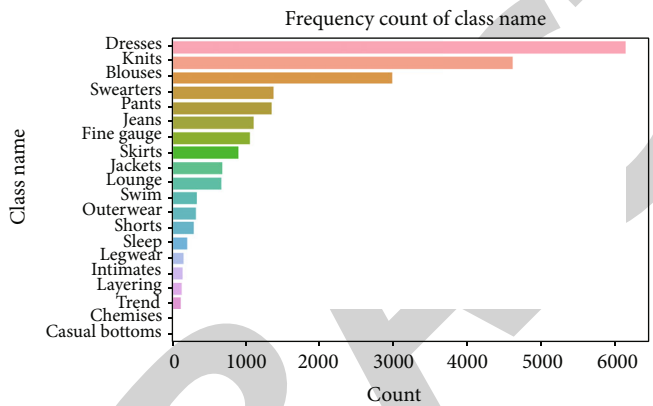

Figure 4: The distribution of the frequency of the most tested classes of clothing.

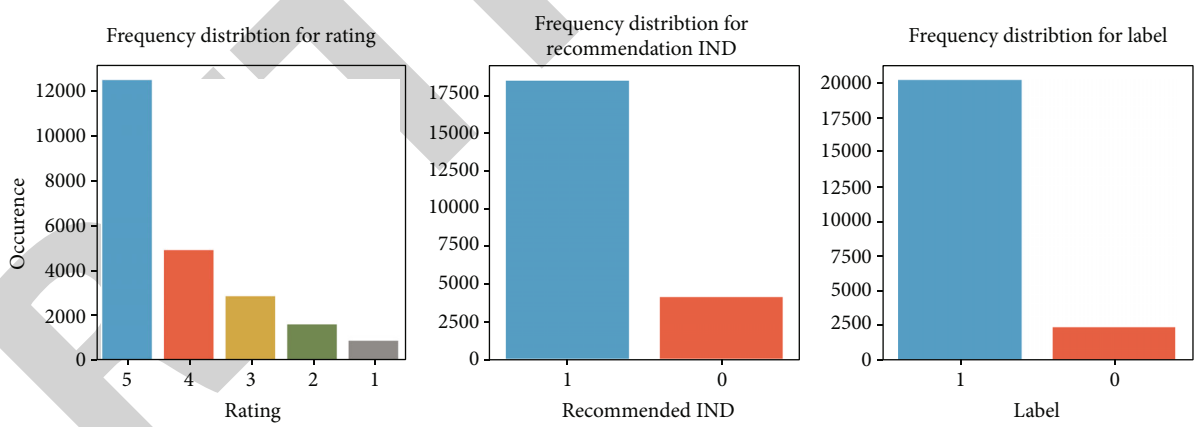

Figure 5: The frequency distribution of rating, recommended IND, and label.

distribution and labelling of the features present in the dataset, such as age and recommendation ID

An analysis of IMDB's (50,000) movie reviews was performed using two positive features, text analysis, and sentiment analysis [5]. Compared to the previous benchmark functions, this framework gives considerably more information about quantitative emotion classification. The dataset includes a collection of 25,000 vastly polarized film reviews for preparation and 25,000 for analysis.

4. Technical Method

The computational method is distributed about three portions to evaluate the classification of sentiments: statistical analysis, deep learning, and machine learning analysis.

4.1. Statistical Analysis. The statistical analysis describes the computational relationship among variables using equations or models [33]. In this part, the dataset was analyzed using four statistical analysis methods, such as univariate

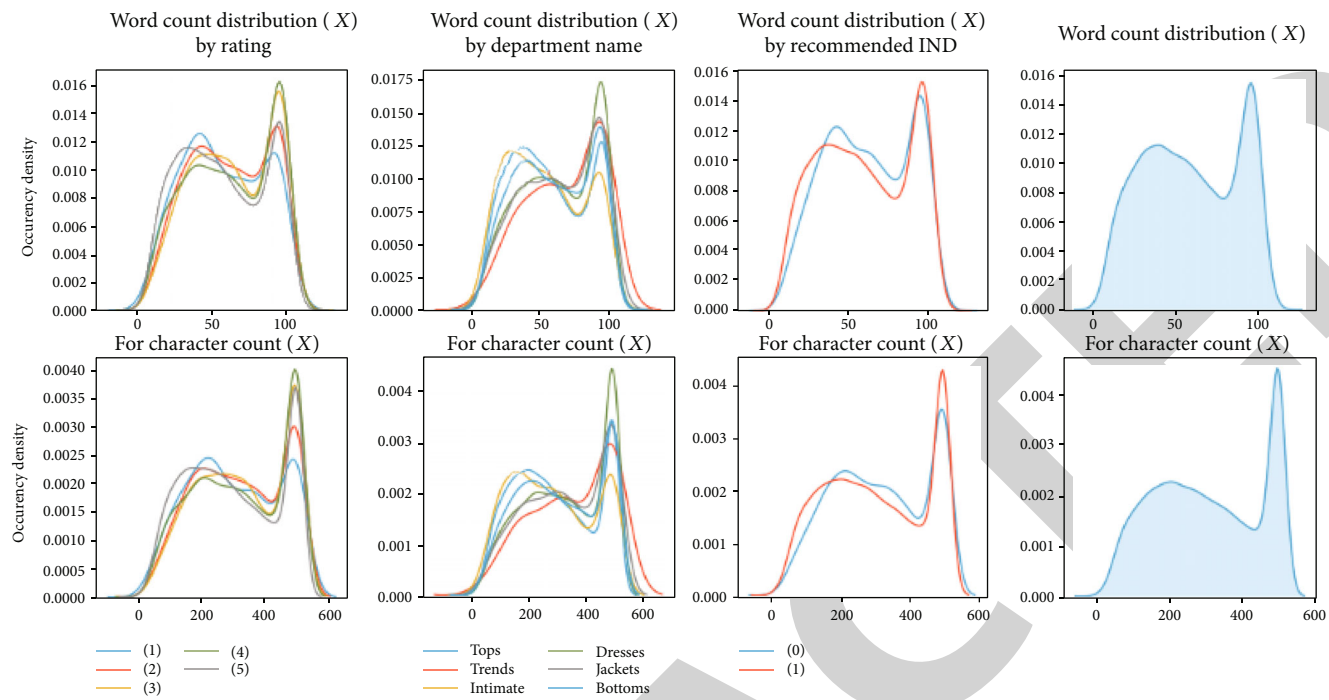

Figure 6: The distribution of count length and characters of the word.

Table 5: Character count of review vs. word counts of the women's clothing dataset.

Review	Count	Mean	Std	Min	25%	50%	75%	Max
Word counts	22,629.00	61.22	29.54	3.00	37.00	58.0	89.00	116.00
Character counts	22,629.00	309.77	144.94	8.00	187.00	303.0	458.00	509.00

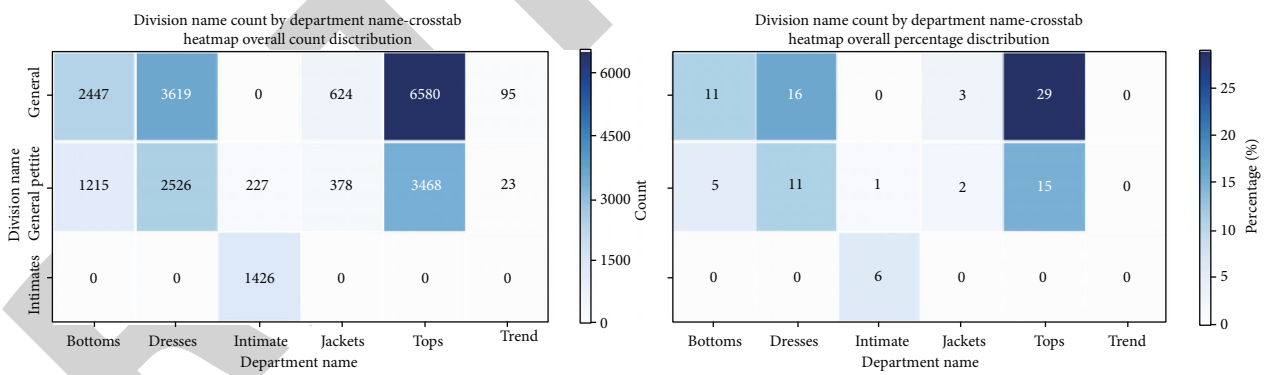

Figure 7: The cross-tab demonstrates the superiority of the general-sized top.

distributions, multivariate analysis, multivariate distributions, and descriptive analysis. Drawing the plot was done using the author's text in [34]. Table 3 describes the statistical detailed info of the datasets.

4.1.1. Analysis Univariate Distribution. Age and positive feedback count distribution: Figure 1 shows that most consumers aged 36-45 years had the most positive review of the products purchased. We also noticed two points from this analysis: (i) at the time of the analysis, e-commerce should include an emphasis on managing this section for the aged listed above, which remains with the utmost positive reviews, and (ii) electronic commerce will see that most of an age group remains quite pleased compared to more pleased age group of 36-45 years.

Division name and department distribution: Figure 2 indicates the frequency distributions of consumer ratings by division and department names.

Distributions of division name: the distribution of division names has three categories of standard, limited, and personal. This provided some perception into the size of the consumers' clothing sendoff comments.

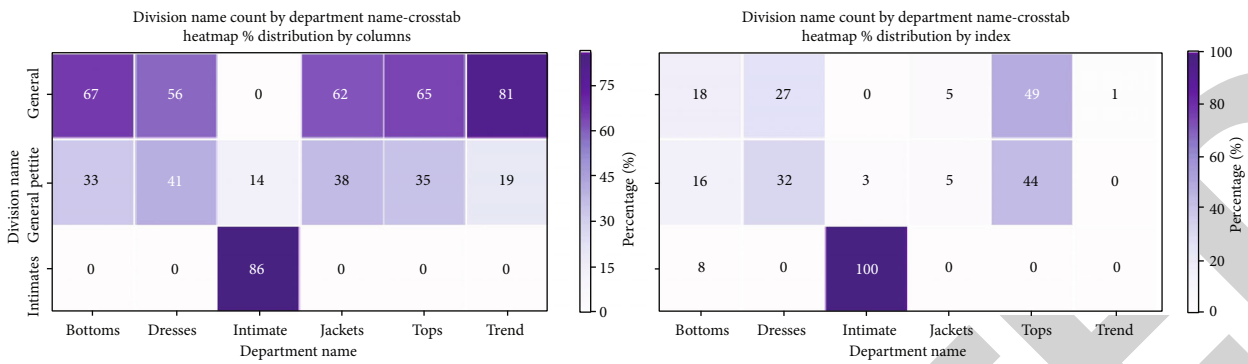

Figure 8: Standardized cross-tabulation of clothing by department and division.

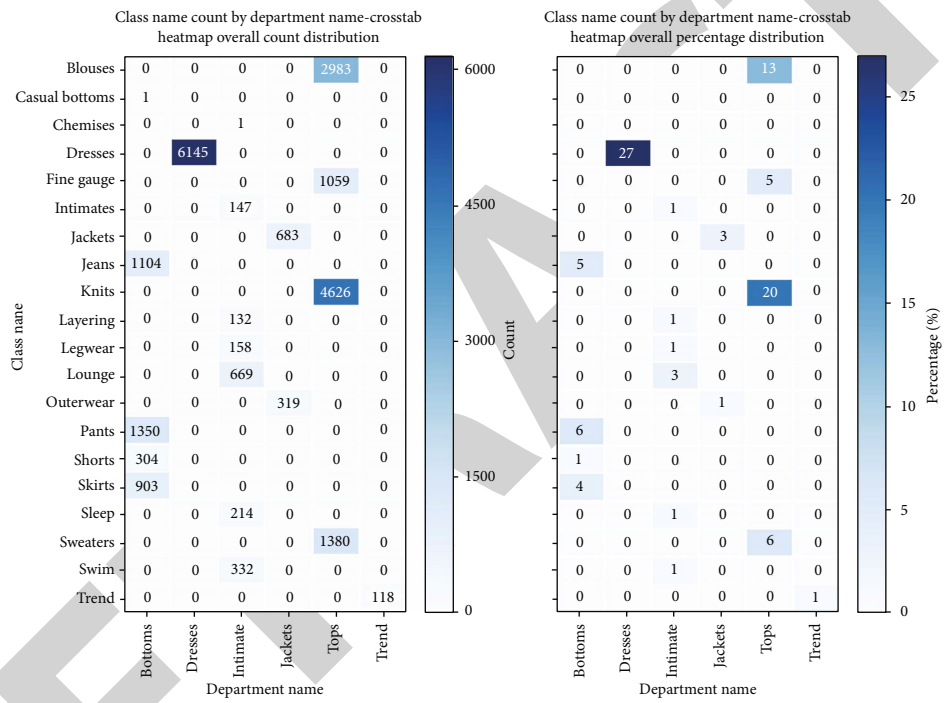

Figure 9: The domination of dress between clothe types.

Distribution of department name: this is important to remember that skirts and tops seem to be the most highly rated product. It will be fascinating to explore the motivation for leaving the analysis in the first place.

Clothing ID distribution: Figure 3 displays the top 60 IDs for clothes to identify the product's interest. Three dress IDs from 1079, 862, and 1095 have obtained considerably more ratings than others. As shown in Table 4, these products expected an average rating of 4/2 and an overall recommendation ratio of around 82%. They also observed that these products mainly were regular.

(1) Distributions of Rating, Recommendation, and Label. Rating distribution: the increasing number of ratings, with a score of five out of five, has been very positive. This proved that the department store was doing pretty well.

Recommended IND distribution: this factor represented the positivity of the rating distribution; however, as previously discussed, we assume that it produced the difference in positive thinking that had been societal rather than private.

Label distribution: we are surprised to find that the items were rated as three or better and recommended by the consumer. We predicted the relationship between rating and recommendation to be multivariate.

To figure out how customers express their hatred, we found these three variables especially promising. We based on the correlations between these variables in the multivariate section. The distribution of scores, recommendations, and labels is seen in Figure 5.

Length of word: Figure 6 indicates that the analysis's character and word counts are strongly correlated. They

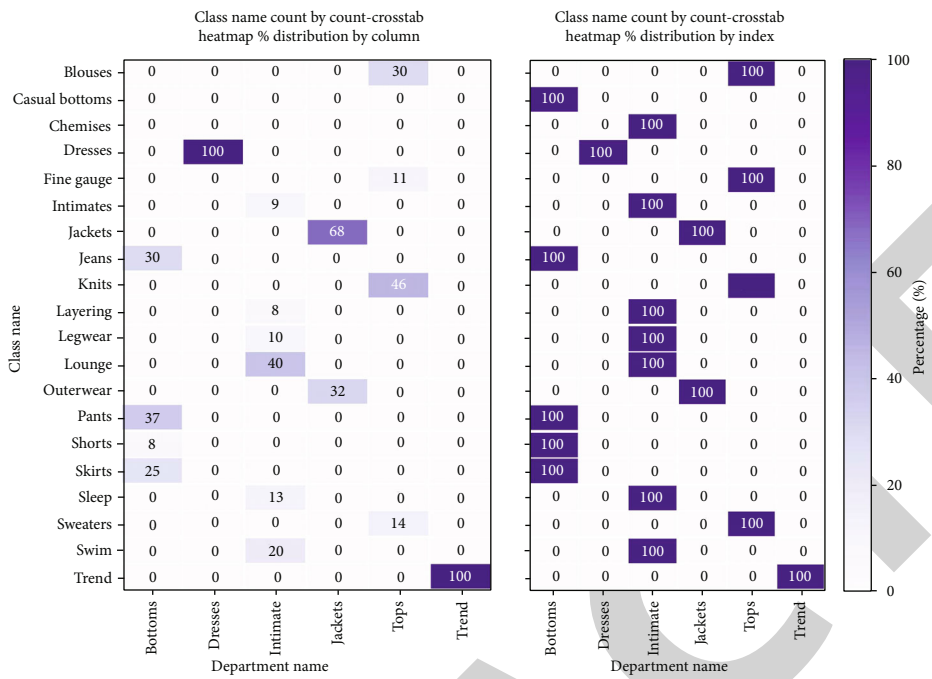

Figure 10: Dress supremacy between types of clothing (class name by division name).

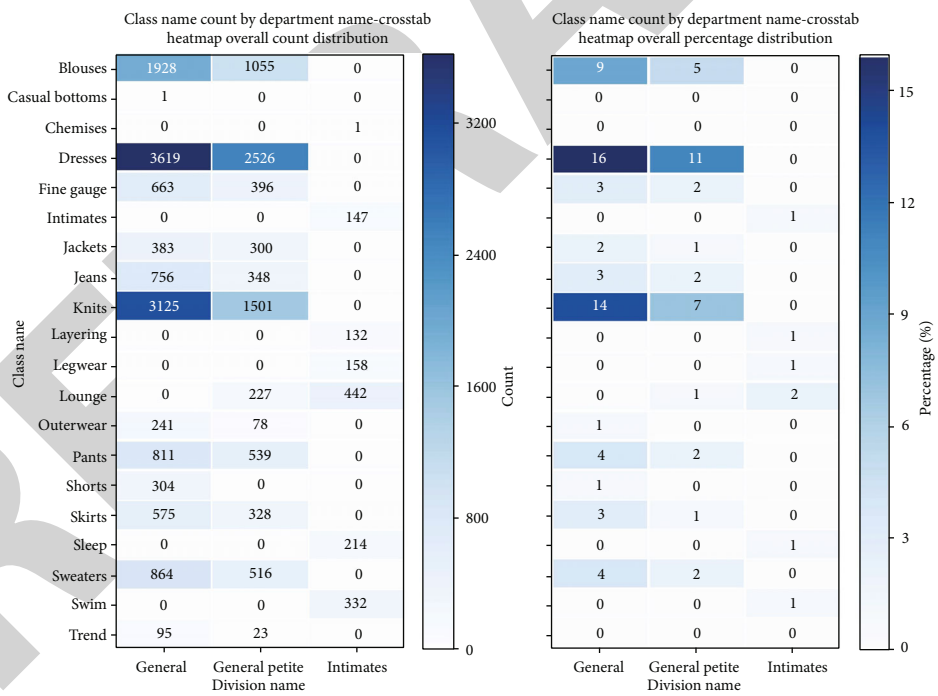

Figure 11: The types of clothing often reviewed, such as skirts, general-sized blouses, and knits.

were equal in length, as seen in Table 5. The term and character count correlation coefficient are 0.99.

4.1.2. Multivariate Distribution Analysis. Division name by the department: Figure 7 indicates that the general-sized top was the most dominant commodity. The dominance of general size within the department name was consistent across multiple categories, as seen in Figure 8. There had been a significant overall difference in the name of the general petite and the department.

Name of class by department name: Figure 9 provides a better look into the classification of multiple clothing types. As seen in Figure 10, the superiority of dress popularity was visible till now.

Figure 12: The most reviewed clothing are from a standard petite size.

Figure 11 indicates that the most reviewed clothing styles were general-sized blouses, skirts, and knits, and Figure 12 indicates that most reviews have stayed popular for dresses with general petite sizes.

Age as per positive feedback count: Figure 13 indicates that age was marginally correlated with positive feedback counts. Focusing on the textual anatomy of incredibly positive reviews will be fascinating.

Department and division naming recommendation: the same observations are shown in Figure 14 as those found in Figure 7.

Division and department rating names: Figure 15 indicates that the division and department are compatible with the overall rating distribution.

The positive response count is under 40 through recommended IND and rating. This plot offers still more nuance only as a follow-up to a previous review of the dominant strongly positive reviews recommended by consumers. The first was a bump to the lower left: cutoff = true and recommended IND = 0.0. This strategy interacted unexpectedly with criticism of individual items; that is why the second bump (rate = 1) of the lighter blue dominated the positive feedback range of ~110. In the bottom-right plot, later performance was identified, while standard ratings were recommended. The vast range of yellow distributions with a ranking of 3 was interesting to see. Positive reviews of constructive criticism were the most highly rated. Also, see Figure 16 for more visualization.

Rate by recommendation: Figure 17 shows that five-star ratings are not preferred, but some cases recommend low-quality items. The recommended portion of the feedback for the more real instance of recommended and nonrecommended items with three scores is interesting to listen to,

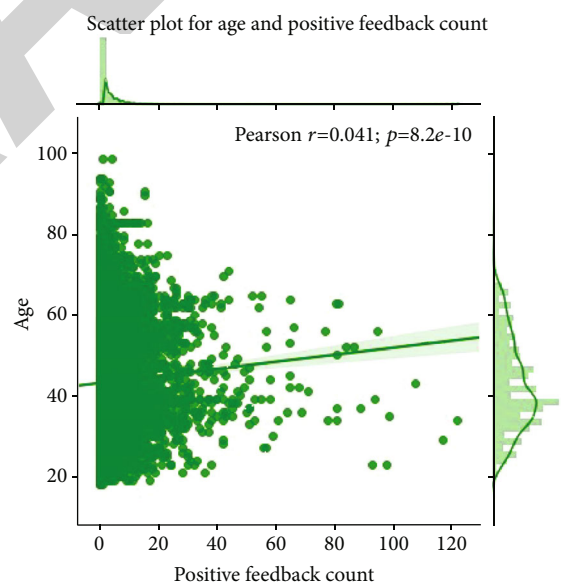

Figure 13: A slight relationship between ages and positive response cluster in a review.

which could shed light on the utmost essential constraints on the store manager and the consumer's apparel behaviour.

4.1.3. Descriptive Multivariate Analysis and Statistics. Classification average by recommendation: Figure 18 evaluates the rating recommendations. When recommended or reduced by the reviewer, the rating was below the maximum, so experimentation is not recommended. This process in the department and division has been persistent.

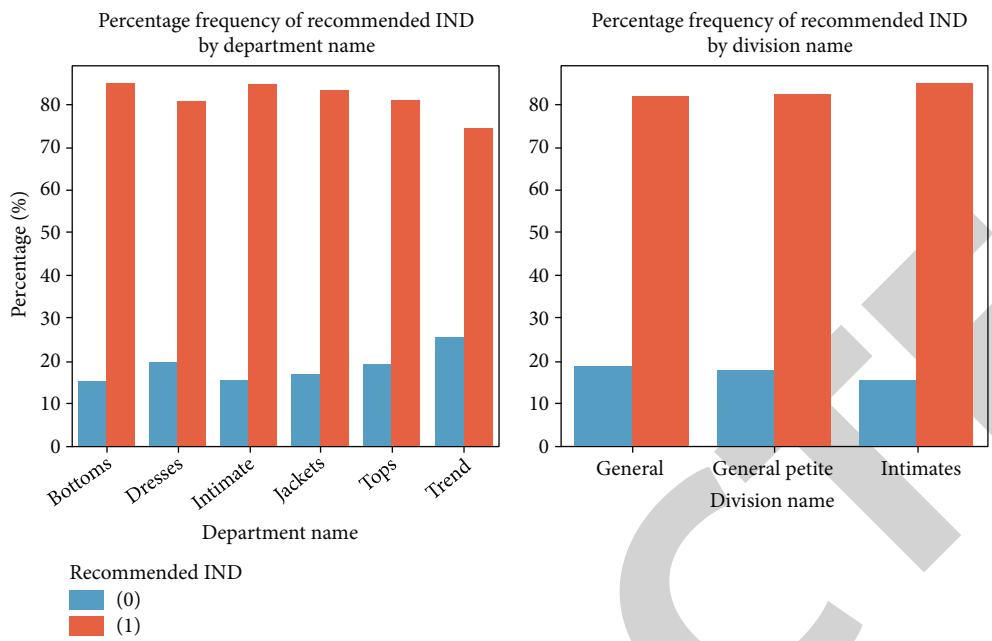

Figure 14: Percentage of recommendation metrics per analysis by division and department.

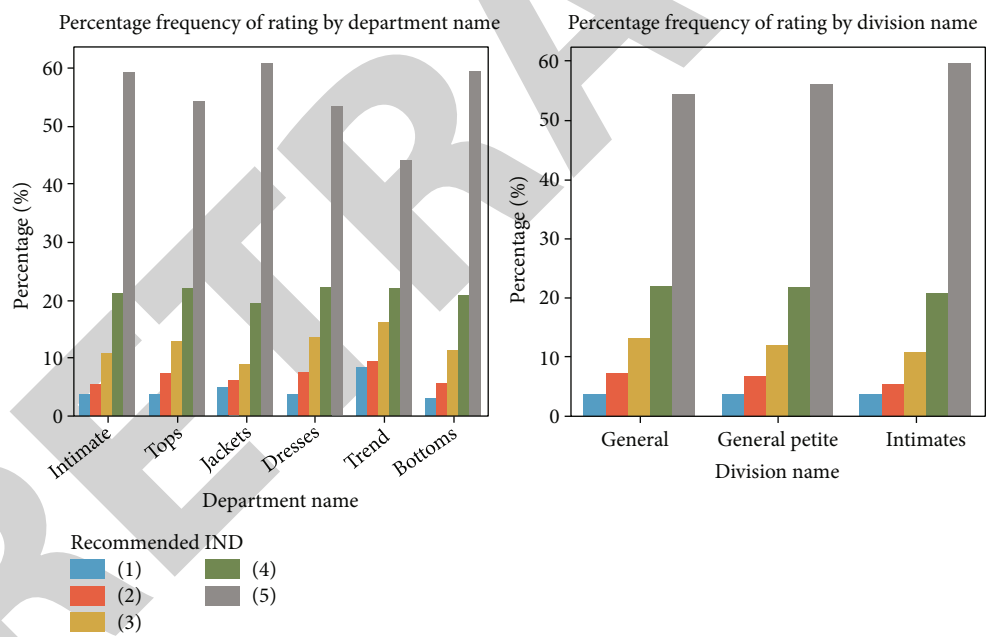

Figure 15: The continuity in the distribution of rating shows.

Average ranking and recommended IND correlated by clothing ID: Figure 19 shows the correlation between ratings and the dress ID recommended by IND. This heat map correlation indicates no relation between counts and average score, suggesting that the item's reputation did not contribute to special consideration once it came to average ratings. The age variables demonstrated similar behaviour.

However, there has been a high positive correlation of 80% between the recommended IND average and rating. A more quantitative view of the interest rate relationship is given in Figure 20 and focuses on the p value. The dots on the bottom left are the items that, in the expectation of maintaining the brand's reputation, definitely require attention from marketers.

Class name average rating and recommended IND correlation: in several class groups, Figure 21 shows significant relationships between average age and likelihood of recommendation.

4.2. Machine Learning Analysis. We use state-of-the-art machine learning classifiers for the role of emotion classification in this section, like naïve Bayes [35], KNN [12],

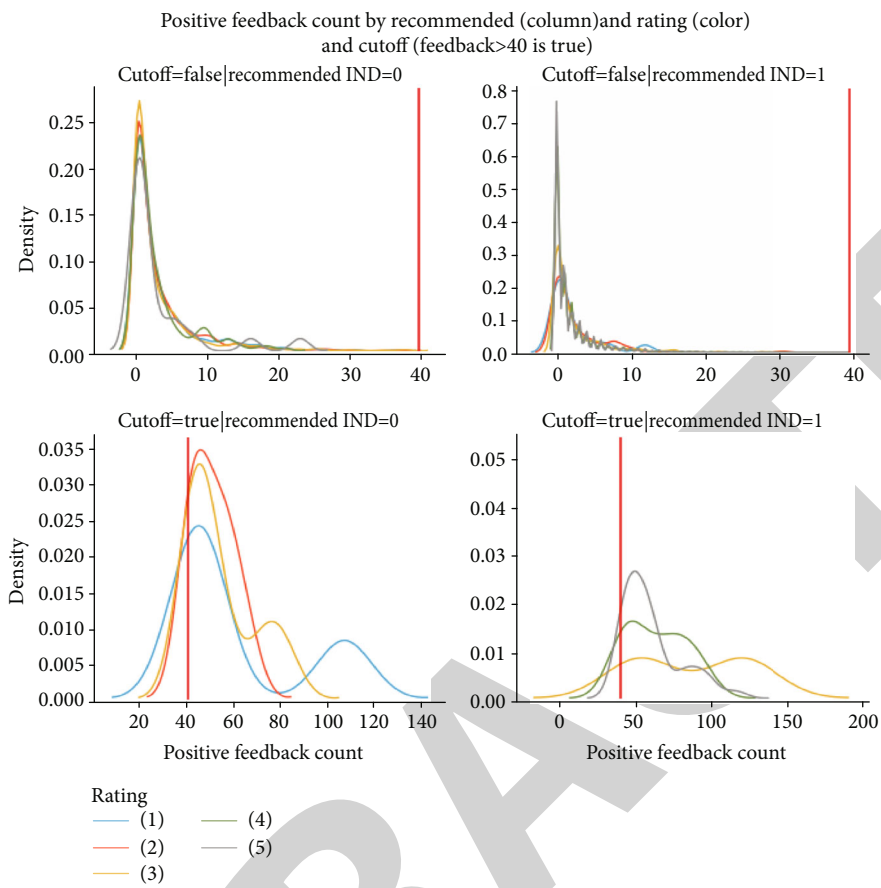

Figure 16: The positive opinion obtained by more than 40 reviews and ratings.

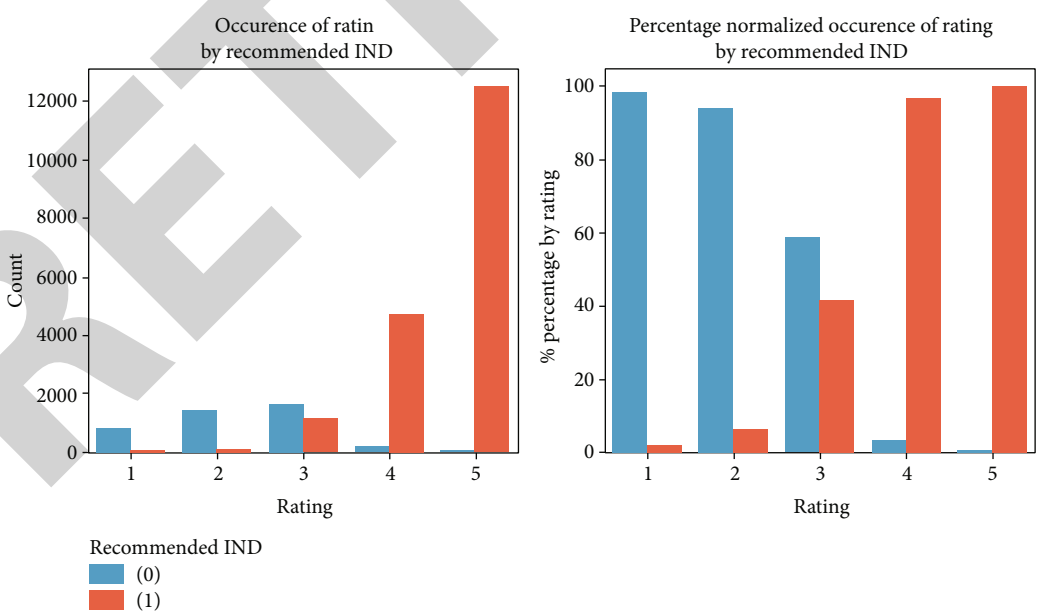

Figure 17: A review rating expresses the recommendation status.

support vector machine [36], random forest [37], logistic regression [38], decision tree [39], and multilayer perception [40]. We also considered both of these to be similar to the current DSC algorithm as simple classification methods.

The women's apparel dataset, which contains more than 23,000 user ratings with 9 attributes after preprocessing, was discussed during our first experiment (see Section 3). We reached an accuracy of 77.45% for KNN, 78.34% for RF,

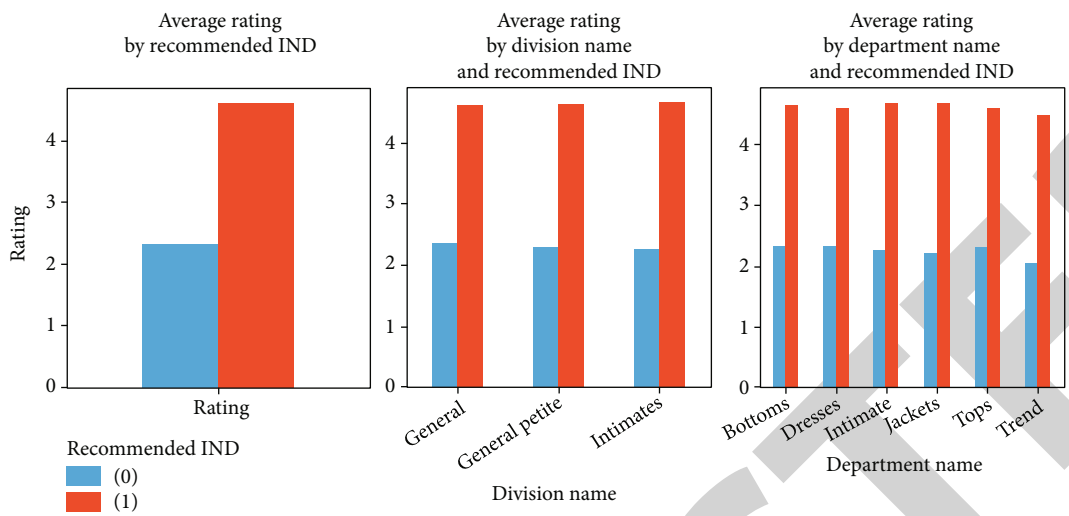

Figure 18: The improvement of recommendations and ratings.

73.34% for DTC (decision tree classifier) for this experiment, 77.25% for SVM (support vector machine), 82.80% for naïve Bayes, 82.75% for LR (logistic regression), and 82.80% for multilayer perceptron (MLP). The experimental findings show that the strongest classifiers for LR, naïve Baseline, and MLP remain with an accuracy of more than 80% across all these machine learning baseline classifiers. Table 6 summarizes the complete results.

Our next experiment discussed the IMDB dataset, containing 50,000 sentiments for movie reviews (see Section 3). For this study, DSC remains outstanding with an F1 score of 88.64% among the simple classification methods, including linear regression, random forest, decision trees, naive Bayes, multilayer perceptron, SVM classifiers, and KNN (see Table 7).

4.3. Deep Learning Analysis

4.3.1. Preprocessing. Embedding and tokenizer: for the analysis of documents, a fully convolutional neural network cannot be used directly; therefore, we must translate it somehow. There were two stages in the integration process. The first move was called a "tokenizer," which translated text analysis from word to integer and was performed on the datasets before a neural network input [41]. The 2nd phase had been an integral component of a neural network itself, called the "embedding" layer [42].

4.3.2. Dropout. Dropout layers offer an optimal process to prevent overfitting, which can be accomplished by arbitrary dropout to ignore these neurons in the training point [43]. Because this helps to minimize codependent neuronal learning, we boost DSC dropouts with linear and exponential growth.

4.3.3. Deep Sentiment Classifier. We introduced a deep sentiment classifier to extract a review text from the input series at numerous time phases. The recommended solution (DSC) is seen in Figure 22. The system was initially developed of the recurrent unit (RU) which has been internally

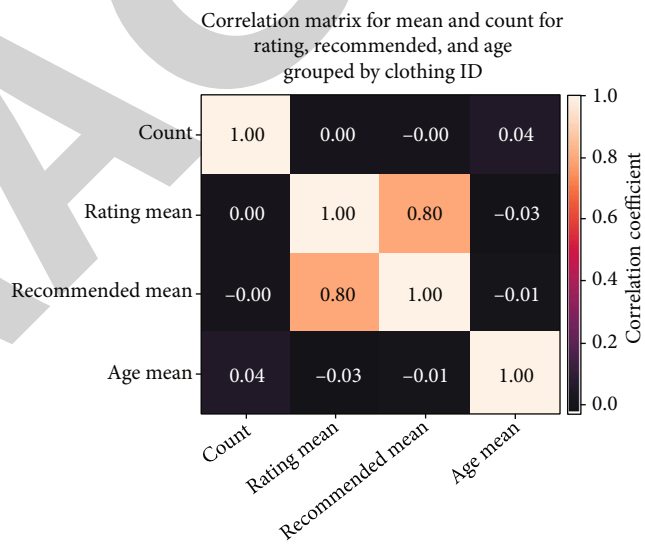

Figure 19: The heat map showing the correlation between recommended IND by clothing ID and rating.

set to 1 by TensorFlow each time a new series has begun. During the first phase, the word "this" is inserted into the RU that was used for its embedding layer (coded to zero) and also its gate to estimate a novel state. RU used another gate to measure the performance, but that was skipped since it simply included a description at the end of the series. In the 2nd phase, the expression "is" was introduced into the RU that used the embedding layer that had been shifted by seeing all previous words "this." There is no meaning in the term "this is" because by seeing these words, the RU probably did not save anything significant from its internal state.

Nevertheless, whenever the third word "not" was detected, RU discovered that the overall sentiment of input text could be valuable to calculate and therefore need to be recorded in the memory state of RU that can be used later once RU had seen the phrase "good" in step 6. Thirdly, RU

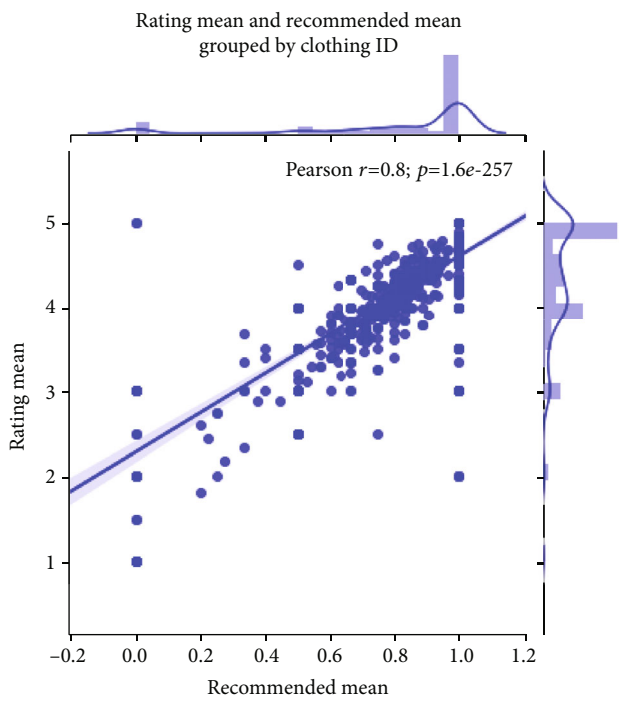

Figure 20: Rating and recommended mean by clothing ID.

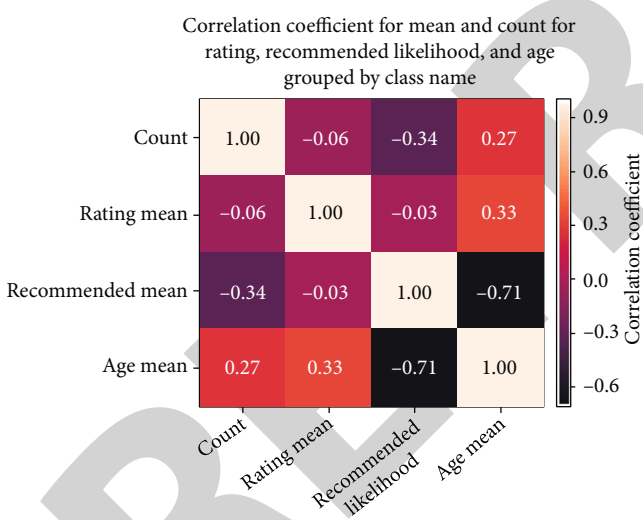

Figure 21: Good correlations between both the average age and the probability of recommendation in different class groups.

generated a vector of values after the entire series was evaluated, summarizing what it should have found in the time stage. To obtain a goal node between 0.0 and 1.0, which has been understood either negatively (values near to 0.0) or positively, we have used a fully associated layer with activation of a sigmoid (values relative to 1.0). Two types of text classification problems were applied to the recommended classification model.

Sentiment classification: sentiment on consumer ratings of the product purchased is classified. In this dataset, the product analysis has negative, positive, and neutral feeling states. As a multinomial classification problem, we considered this type of problem.

Classification by recommendation: this identifies whether the product reviewed is recommended by the customers' reviews. Here, the product evaluation in the datasets contains two recommended and not recommended approval states. We found these types of issues to be binary classification problems.

Table 6: A description of the success metrics compared to baseline classifiers using the women's clothing dataset for the proposed approach.

Method	Accuracy (%)	Precision (%)	Recall (%)	F1 score (%)
KNN	77.45	65	65	65
RF	78.34	80	80	80
DTC	73.34	73	73	73
LR	82.75	88	88	88
Naïve Bayes	82.80	81	80	80
SVM	77.25	75	75	75
MLP	82.80	87	87	87
DSC	80.01	80	80	80

Table 7: Deep sentiment classifier on average training and testing accuracy and loss.

Class	Train Acc (%)	Test Acc (%)	Train loss	Test loss
Recommended classification	97.48	89.33	0.03001	0.5068
Sentimental classification	99.99	94.56	0.0025	0.5326

5. Experimental Results and Discussion

5.1. Execution Environment. To evaluate our model in python3, we used TensorFlow [44], scikit-learn [45], and Keras [46]. Intel Core i5 2.67 GHz and 8 GB RAM are the computer systems used for this work. With the first learning rate of 0.0001, we used the Adam Optimizer. Table 8 shows the setup of the parameter method proposed. During the training and testing of the proposed deep sentiment classification model, 10 k cross-validations were applied. For both recommendation and sentiment classifications, the average preparation, consistency testing, and loss by the deep sentiment classifier are discussed in Table 7.

5.2. Evaluation Metrics. We use the usual metrics to measure the efficiency of the classifiers [12, 47–49]: true negative (TN) is the correct negative review analysis, true positive (TP) is the correct analysis of a positive review, and fake positive (FP) means the positive test's false positive interpretation. The accuracy, precision, recall, and F measurement are determined using the gauges set out directly above. Accuracy is calculated as the proportion of all forecasts to

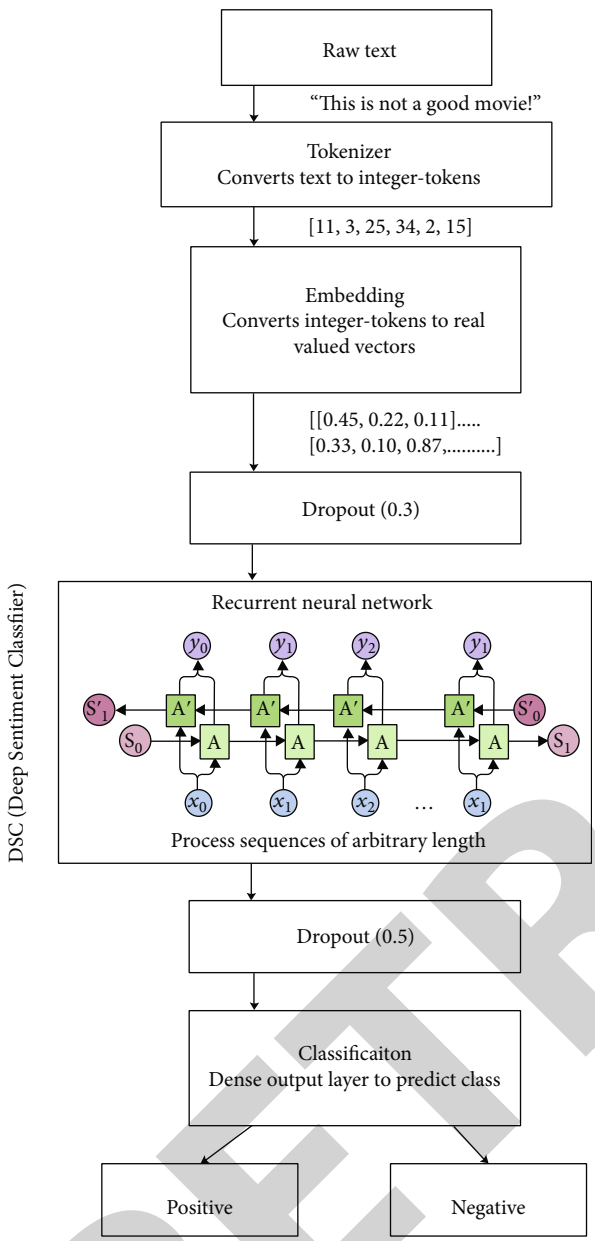

Figure 22: Deep sentiment classifier model.

Table 8: Hyperparameters for the deep sentiment classifier.

Hyperparameters	Values
Embedding size	8
Bidirectional gated recurrent unit	01
Batch size	64
Optimizer	Adam
Learning rate	0.0001
Epochs	50

the sum of the correct forecast results (see equation (1)). Precision indicates whether the model's positive predictions are accurate and are computed by dividing all positive predictions by the total number of true positives (shown in equation (2)). The recall is the positive described by the all feasible positive models and is accomplished by dividing the true positive by the actual positive total (shown in equation (3)). Its weighted average of recall and accuracy was F1-measurement. The controlled F score or F measure is now the precision and recall confusion matrix, as defined in equation (4).

Table 9: A description of the performance metrics similar to baseline IMDB dataset classifiers.

Method	Accuracy (%)	Precision (%)	Recall (%)	F1 score (%)
KNN	64.09	64	64	64
RF	79.61	80	80	80
DTC	72.79	73	73	73
LR	87.67	88	88	88
Naïve Bayes	83.37	83	82	82
SVM	75.58	75	75	75
MLP	83.37	87	87	87
DSC	88.01	88	88	88

Table 10: DSC method obtained an average accuracy.

Method	Accuracy (%)	Precision (%)	Recall (%)	F1 score (%)
KNN	25.53	40	40	40
RF	22.53	38	38	38
DTC	14.53	31	31	31
LR	13.53	29	29	29
Naïve Bayes	28.53	45	81	81
SVM	14.53	31	31	31
MLP	13.52	31	31	31
DSC	93.55	93	93	93

$$\text{Accuracy} = \frac{\text{TP} + \text{TN}}{\text{TP} + \text{TN} + \text{FP} + \text{FN}}, \tag{1}$$

$$\text{Precision} = \frac{\text{TP}}{\text{TP} + \text{FP}}, \tag{2}$$

$$\text{Recall} = \frac{\text{TP}}{\text{TP} + \text{FP}}, \tag{3}$$

$$\text{F1} = 2\text{X}\frac{\text{Pr cesion} * \text{Re call}}{\text{Pr cesion} + \text{Re call}}. \tag{4}$$

5.3. Experimental Setup. The efficiency of our proposed method (deep sentiment classifier) was compared in our experiment with 7 state-of-the-art machine learning methods:

(i) Trained classification algorithm with the training dataset and testing dataset

(ii) Trained decision tree (DT) classification model with the training dataset and testing dataset

Table 11: Summary of key performance indicators compared to existing methods based on sentiment classification.

Methods	Accuracy (%)	Precision (%)	Recall (%)	F1 score (%)
Data on merchant ratings [24]	93.62	92.22	94.80	93.49
Reviews on Tsukuba corpus [24]	84.62	90.18	88.18	89.17
Analysis of customer product SVM [46]	81.75	—	—	—
Consumer product review by naïve Bayes [46]	68.57	—	—	—
Decision tree of consumer product ratings [46]	81.25	—	—	—
Reviews from Amazon on unlock smartphone [48]	97	—	—	—
Info on women's clothe reviews [30]	92.84	93	93	93
DSC (deep sentiment analysis)	93.55	93.68	93.52	93.52

(iii) Trained random forest (RF) classification model with the training dataset and testing dataset

(iv) Trained SVM (support vector machine) machine learning algorithm with training data and analyzed by testing data

(v) Trained LR (logistic regression) classifier with the training dataset and testing dataset and trained computational modelling algorithm called multinomial (naïve Bayes) with training data and analyzed by the testing dataset

(vi) A neural network model called MLP (multilayer perceptron) has been trained with training data and analyzed with test data

We compared the performance of our proposed method to many current methods of computational intelligence based on problems of sentiment classification (see Table 9).

5.4. Result and Discussion. Our proposed DSC method obtained an average accuracy of 93.55% for sentiment classification tasks under the experiment described above. Table 10 shows the performance metrics of a new DSC methodology and other unique classifications based on the women's clothing databases for emotion detection tasks. It has been demonstrated that in terms of accuracy, precision, recall, and F1-measure, the method produced outperformed all other simple classifiers. In our DSC process, the F1 score is 25.53% more reliable than the KNN and RF baseline classifiers, 22.53% higher than the DTC baseline classifier, 14.53% higher than the LR baseline classifier, 13.53% higher than the Naïve Bayes baseline method, and 28.53 and 14.53% points higher than the SVM and MLP baseline classifiers, respectively.

With the other baseline IMDB dataset classifiers, Table 10 presents the experimental effects of the proposed DSC process. The experimental results show that DSC remained highly high among all baseline classification methods, with an F1 score of 88.01%.

Based on the sentiment classification analysis, Table 11 assesses the recommended method for existing techniques. It clearly shows that the approach proposed has remained extremely high compared to other approaches discussed.

It should, however, be stated that there was a variance in the distribution of frequencies between recommendation and sentiment groups. For example, more recommended reviews were done in the women's clothing database because there were more positive attitudes than potential and neutral ones. It can be a challenge for the model because it boosts the bias against a class of high-frequency propagation. Statistical analysis for the classification of recommendations is provided in Table 12. As shown in the table, comparatively, the deprecated class of the recommended classification problem gave worse predictions.

In addition, on the IMDB dataset, we tested DSC, which has a balanced sentiment for film reviews (25,000 for positive and 25,000 for negative). For the role of sentiment classification, which gained an average F1 score of 88.01% (see Table 13), our outcomes found that the deep sentimental classifier model was implemented well under the assumption that samples were spaced randomly and unevenly in the datasets.

Table 12: Recommended classification and result metric usage on women's apparel dataset (deep sentiment classifier).

Class	Precision (%)	Recall (%)	F1 score (%)
Recommended (1)	94.98	94.97	94.10
Not recommended (0)	71.83	68.91	70.41
Average/total	88	88	88

Table 13: Performance metrics using the IMDB dataset (DSC) on sentiment classification.

Class	Precision (%)	Recall (%)	F1 score (%)
Positively (1)	88	91	88
Negatively (0)	91	87	88
Average	88	88	88

Table 14: Metrics using DSC for sentiment classification results.

Class	Precision (%)	Recall (%)	F1 score (%)
Positive (0)	97.46	97.49	76.48
Negative (1)	49.41	51.16	50.39
Neutral (2)	33.47	21.95	26.04
Average/total	93	93	93

Table 14 describes our proposed DSC success metrics and reflects our observations on the stigma against the imbalanced community (the class with the maximum frequency distribution). The predictive utility of the proposed technique was moderately low for neutral and negative emotions, as stated in the tables.

Despite imbalances in the dataset, our empirical analysis provided the facts with relatively high predictive performance to support the recommendation and sentiment classifications. Our findings showed that the bidirectional gated recurrent unit (GRU) was acceptable and highly predictive for analyzing customer reviews. We also advocate employing the unidirectional RNN-LSTM and CNN for a fair comparison in the future work on the same classification problem to further validate this conclusion.

6. Conclusion and Future Work

Online reviews are becoming a forum for trust building-consumer buying trends and affecting them. There is a need to manage such a massive number of comments with such dependency and provide reliable reviews before the user. This article analyzed two different types of datasets to classify sentiments: "women clothing review" datasets, consisting of 22641 records and IMDB sample size, containing 50,000 sentiments from the movie reviews. Our study is aimed at exploring the correlation between the different variables in the statistical analysis datasets of the review and at constructing a deep learning algorithm for DSC (deep sentiment classifier). Our proposed method addresses two types of text classification problems: (ii) classification of sentiments by recommendation, which investigates whether customer ratings recommend the product reviewed, and (ii) classification of sentiment by calculating consumer reviews' sentiment values toward the purchased product. In our proposed model, there is no feature selection technique used. DSC, however, performed well in the emotional classification, with an F1 score of 93.52% in the recommended classification of the women's clothing dataset.

In addition, on the IMDB datasets, we tested DSC, which has a balanced sentiment for film reviews (25,000 for positive and 25,000 for negative), which obtained an average F1 score of 88.01% for the task of data mining (see Table 12). Our results demonstrated which the model DSC worked well under the situation that samples in the dataset were spread uniformly and unevenly.

Furthermore, our analyses have shown that the recommendation is a reliable indicator for studying positive sentiment. Based on statistically analyses and state-of-the-art classifiers, our extensively investigated findings of this study will provide businesses with ideas on how to develop their services and satisfy consumer demands accordingly. On this model, many possible studies can still be performed. The tuning of hyperparameters for further development may be used in future works. The hyperparameters of the recommended method were restricted to one randomly selected parameter because of the computational cost limit.

Data Availability

The datasets we used in this study are publicly available at the following links: (1) https://www.kaggle.com/nicapotato/womens-ecommerce-clothing-reviews and (2) https://www.kaggle.com/lakshmi25npathi/imdb-dataset-of-50k-movie-reviews.

Conflicts of Interest

The authors declare that they have no conflicts of interest.

Acknowledgments

The work was supported in part by the National Social Science Foundation of China under Grant No. 21ZDA033, by the National Natural Science Foundation of China under Grant Nos. 71771118 and 72071104, by the Humanities and Social Science Foundation of Ministry of Education of China under Grant No. 18YJCZH146, and by the Key Project of Jiangsu Social Science Foundation under Grant No. 20GLA007.

References

[1] M. S. Neethu and R. Rajasree, "Sentiment analysis in Twitter using machine learning techniques," in *2013 4th International Conference on Computing, Communications and Networking Technologies, ICCCNT 2013*, Tiruchengode, India, 2013.

[2] B. Pang and L. Lee, *Opinion Mining and Sentiment Analysis*, vol. 2, no. 1–2, 2008Foundations and Trends® in Information Retrieval, 2008.

[3] A. Kumar and T. M. Sebastian, "Sentiment analysis: a perspective on its past, present and future," *International Journal of Intelligent Systems and Applications*, vol. 4, no. 10, pp. 1–14, 2012.

[4] E. Cambria, B. Schuller, B. Liu, H. Wang, and C. Havasi, "Knowledge-based approaches to concept-level sentiment analysis," *IEEE Intelligent Systems*, vol. 28, no. 2, pp. 12–14, 2013.

[5] L. Maas, R. E. Daly, P. T. Pham, D. Huang, A. Y. Ng, and C. Potts, "Learning word vectors for sentiment analysis," in *Proceedings of the 49th Annual Meeting of the Association for Computational Linguistics (ACL-2011)*, Stanford, CA, 2011.

[6] G. Gezici, B. Yanikoglu, D. Tapucu, and Y. Saygin, "New features for sentiment analysis: do sentences matter?," in *CEUR Workshop Proceedings*, Bristol, UK, 2012.

[7] S. Sun and X. Gu, "Sentiment analysis using extreme learning machine with linear kernel," in *25th International Conference on Artificial Neural Networks and Machine Learning, ICANN 2016*, Barcelona, Spain, 2016.

[8] L. Nio and K. Murakami, "Japanese sentiment classification using bidirectional long short-term memory recurrent neural network," in *The Association for Natural Language Processing*, pp. 1119–1122, Okayama, Japan, 2018.

[9] P. Palanisamy, V. Yadav, and H. Elchuri, "Serendio: simple and practical lexicon-based approach to sentiment analysis," in *Second Joint Conference on Lexical and Computational Semantics (SEM), Volume 2: Proceedings of the Seventh International Workshop on Semantic Evaluation (SemEval 2013)*, India, 2013.

[10] M. J. Stefik, "Machine learning: An artificial intelligence approach," *Artificial Intelligence*, vol. 25, no. 2, pp. 236–238, 2003.

[11] S. B. Kotsiantis, I. D. Zaharakis, and P. E. Pintelas, "Machine learning: a review of classification and combining techniques," *Artificial Intelligence Review*, vol. 26, no. 3, pp. 159–190, 2006.

[12] D. Vasan, M. Alazab, S. Wassan, H. Naeem, B. Safaei, and Q. Zheng, "IMCFN: image-based malware classification using fine-tuned convolutional neural network architecture," *Computer Networks*, vol. 171, article 107138, 2020.

[13] D. Vasan, M. Alazab, S. Wassan, B. Safaei, and Q. Zheng, "Image-based malware classification using ensemble of CNN architectures (IMCEC)," *Computers & Security*, vol. 92, article 101748, 2020.

[14] H. Naeem, F. Ullah, M. R. Naeem et al., "Malware detection in industrial Internet of things based on hybrid image visualization and deep learning model," *Ad Hoc Networks*, vol. 105, article 102154, 2020.

[15] M. Qasem, R. Thulasiram, and P. Thulasiram, "Twitter sentiment classification using machine learning techniques for stock markets," in *2015 International Conference on Advances in Computing, Communications and Informatics (ICACCI)*, Kochi, India, 2015.

[16] Z. Ren, X. Wang, N. Zhang, X. Lv, and L.-J. Li, "Deep reinforcement learning-based image captioning with embedding reward," in *Proceedings of the IEEE conference on computer vision and pattern recognition*, pp. 290–298, Honolulu, HI, USA, 2017.

[17] N. Brooks, "No title," https://www.kaggle.com/.

[18] R. Jozefowicz, W. Zaremba, and I. Sutskever, "An empirical exploration of recurrent network architectures," in *International conference on machine learning*, Lille, France, 2015.

[19] S. de Kok, L. Punt, R. van den Puttelaar, K. Ranta, K. Schouten, and F. Frasincar, "Review-level aspect-based sentiment analysis using an ontology," in *Proceedings of the 33rd Annual ACM Symposium on Applied Computing*, pp. 315–322, New York, NY, USA, 2018.

[20] H. Nguyen, R. Al, and K. Academy, "Comparative study of sentiment analysis with product reviews using machine learning and lexicon-based approaches," *SMU Data Science Review*, vol. 1, no. 4, 2018.

[21] R. K. Roul and J. K. Sahoo, *Sentiment analysis and extractive summarization based recommendation system*, vol. 990, Springer, Singapore, 2020.

[22] K. Schouten and F. Frasincar, "Survey on aspect-level sentiment analysis," *IEEE Transactions on Knowledge and Data Engineering*, vol. 28, no. 3, pp. 813–830, 2016.

[23] T. Nakagawa, K. Inui, and S. Kurohashi, "Dependency tree-based sentiment classification using CRFs with hidden variables," in *Human Language Technologies: The 2010 Annual Conference of the North American Chapter of the Association for Computational Linguistics*, pp. 786–794, Los Angeles, California, 2010.

[24] P. Zhang and M. Komachi, "Japanese sentiment classification with stacked denoising auto-encoder using distributed word representation," in *Proceedings of the 29th Pacific Asia Conference on Language, Information and Computation*, pp. 150–159, Shanghai, China, 2015.

[25] D. Tang, F. Wei, N. Yang, M. Zhou, T. Liu, and B. Qin, "Learning sentiment-specific word embedding for Twitter sentiment Classification," in *Proceedings of the 52nd Annual Meeting of the Association for Computational Linguistics (Volume 1: Long Papers)*, Baltimore, Maryland, USA, 2015.

[26] D. Stojanovski, G. Strezoski, G. Madjarov, and I. Dimitrovski, "Twitter sentiment analysis using deep convolutional neural network," in *Lecture Notes in Artificial Intelligence (Subseries of Lecture Notes in Computer Science)*, Springer, 2015.

[27] W. Wang, M. Khalil-Ur-Rehman, J. Feng, J. Tao, and Y. Kim, *Convolutional neural networks for sentence classification*, EMNLP, 2014.

[28] R. Socher, J. Pennington, E. H. Huang, A. Y. Ng, and C. D. Manning, "Semi-supervised recursive autoencoders for predicting sentiment distributions," in *Proceedings of the 2011 conference on empirical methods in natural language processing*, pp. 151–161, Edinburgh, Scotland, UK, 2011.

[29] H. A. Schwartz, J. C. Eichstaedt, M. L. Kern et al., "Personality, gender, and age in the language of social media: the open-vocabulary approach," *PLoS One*, vol. 8, no. 9, 2013.

[30] F. Agarap and P. Grafilon, "Statistical analysis on E-commerce reviews, with sentiment classification using bidirectional recurrent neural network (RNN)," 2018, https://arxiv.org/abs/1805.03687.

[31] A. Mousa and B. Schuller, "Contextual bidirectional long short-term memory recurrent neural network language models," in *Proceedings of the 15th Conference of the European Chapter of the Association for Computational Linguistics: Volume 1, Long Papers*, pp. 1023–1032, Valencia, Spain, 2017.

[32] M. Song, X. Zhao, Y. Liu, and Z. Zhao, "Text sentiment analysis based on convolutional neural network and bidirectional LSTM model," in *International Conference of Pioneering Computer Scientists, Engineers and Educators*, pp. 55–68, Singapore, 2018.

[33] S. Calculations and S. Data, "Nag ranks and scores (G01Dhc) 1," *Analysis*, 1980.

[34] "No title," https://www.kaggle.com/nicapotato/womens-ecommerce-clothing-reviews.

[35] V. Kharde and P. Sonawane, "Sentiment analysis of Twitter data: a survey of techniques," *International Journal of Computers and Applications*, vol. 139, no. 11, pp. 5–15, 2016.

[36] S. Wang and C. D. Manning, "Baselines and bigrams: simple, good sentiment and topic classification," in *50th Annual Meeting of the Association for Computational Linguistics, ACL 2012- Proceedings of the Conference*, Jeju, Republic of Korea, 2012.

[37] K. S. Srujan, S. S. Nikhil, H. Raghav Rao, K. Karthik, B. S. Harish, and H. M. Keerthi Kumar, "Classification of amazon book reviews based on sentiment analysis," in *Advances in Intelligent Systems and Computing*, pp. 401–411, Springer, 2018.

[38] S. K. Onan and H. Bulut, "A multiobjective weighted voting ensemble classifier based on differential evolution algorithm for text sentiment classification," *Expert Systems with Applications*, vol. 62, pp. 1–16, 2016.

[39] T. K. Ho, "The random subspace method for constructing decision forests," *IEEE Transactions on Pattern Analysis and Machine Intelligence*, vol. 20, no. 8, pp. 832–844, 1998.

[40] N. Mohamed Ali, M. M. A. El Hamid, and A. Youssif, "Sentiment analysis for movies reviews dataset using deep learning models," *International Journal of Data Mining & Knowledge Management Process (IJDKP)*, vol. 9, no. 3, pp. 19–27, 2019.

[41] R. Mishra, *Deep learning using tensor flow and NLTK—analyzing corpus's sentiments part 1*, Medium, 2017.

Hindawi
Behavioural Neurology
Volume 2023, Article ID 9876194, 1 page
https://doi.org/10.1155/2023/9876194

Retraction

Retracted: A Rapid Artificial Intelligence-Based Computer-Aided Diagnosis System for COVID-19 Classification from CT Images

Behavioural Neurology

Received 8 August 2023; Accepted 8 August 2023; Published 9 August 2023

This article has been retracted by Hindawi following an investigation undertaken by the publisher [1]. This investigation has uncovered evidence of one or more of the following indicators of systematic manipulation of the publication process:

(1) Discrepancies in scope

(2) Discrepancies in the description of the research reported

(3) Discrepancies between the availability of data and the research described

(4) Inappropriate citations

(5) Incoherent, meaningless and/or irrelevant content included in the article

(6) Peer-review manipulation

The presence of these indicators undermines our confidence in the integrity of the article's content and we cannot, therefore, vouch for its reliability. Please note that this notice is intended solely to alert readers that the content of this article is unreliable. We have not investigated whether authors were aware of or involved in the systematic manipulation of the publication process.

In addition, our investigation has also shown that one or more of the following human-subject reporting requirements has not been met in this article: ethical approval by an Institutional Review Board (IRB) committee or equivalent, patient/participant consent to participate, and/or agreement to publish patient/participant details (where relevant).

Wiley and Hindawi regrets that the usual quality checks did not identify these issues before publication and have since put additional measures in place to safeguard research integrity.

We wish to credit our own Research Integrity and Research Publishing teams and anonymous and named external researchers and research integrity experts for contributing to this investigation.

The corresponding author, as the representative of all authors, has been given the opportunity to register their agreement or disagreement to this retraction. We have kept a record of any response received.

References

[1] H. H. Syed, M. A. Khan, U. Tariq et al., "A Rapid Artificial Intelligence-Based Computer-Aided Diagnosis System for COVID-19 Classification from CT Images," *Behavioural Neurology*, vol. 2021, Article ID 2560388, 13 pages, 2021.

Hindawi
Behavioural Neurology
Volume 2021, Article ID 2560388, 13 pages
https://doi.org/10.1155/2021/2560388

Research Article

A Rapid Artificial Intelligence-Based Computer-Aided Diagnosis System for COVID-19 Classification from CT Images

Hassaan Haider Syed,[1] Muhammad Attique Khan,[1] Usman Tariq,[2] Ammar Armghan,[3] Fayadh Alenezi,[3] Junaid Ali Khan,[1] Seungmin Rho,[4] Seifedine Kadry,[5] and Venkatesan Rajinikanth[6]

[1]*Department of Computer Science, HITEC University Taxila, Museum Road, Taxila, Pakistan*
[2]*College of Computer Engineering and Sciences, Prince Sattam Bin Abdulaziz University, Al-Kharj, Saudi Arabia*
[3]*Department of Electrical Engineering, Jouf University, Sakaka 75471, Saudi Arabia*
[4]*Department of Industrial Security, Chung-Ang University, Seoul, Republic of Korea (06974)*
[5]*Faculty of Applied Computing and Technology, Noroff University College, Kristiansand, Norway*
[6]*Department of Electronics and Instrumentation, St. Joseph's College of Engineering, Chennai 600119, India*

Correspondence should be addressed to Muhammad Attique Khan; attique.khan@hitecuni.edu.pk and Seungmin Rho; smrho@cau.ac.kr

Received 6 August 2021; Revised 16 September 2021; Accepted 17 November 2021; Published 27 December 2021

Academic Editor: Barbara Picconi

The excessive number of COVID-19 cases reported worldwide so far, supplemented by a high rate of false alarms in its diagnosis using the conventional polymerase chain reaction method, has led to an increased number of high-resolution computed tomography (CT) examinations conducted. The manual inspection of the latter, besides being slow, is susceptible to human errors, especially because of an uncanny resemblance between the CT scans of COVID-19 and those of pneumonia, and therefore demands a proportional increase in the number of expert radiologists. Artificial intelligence-based computer-aided diagnosis of COVID-19 using the CT scans has been recently coined, which has proven its effectiveness in terms of accuracy and computation time. In this work, a similar framework for classification of COVID-19 using CT scans is proposed. The proposed method includes four core steps: (i) preparing a database of three different classes such as COVID-19, pneumonia, and normal; (ii) modifying three pretrained deep learning models such as VGG16, ResNet50, and ResNet101 for the classification of COVID-19-positive scans; (iii) proposing an activation function and improving the firefly algorithm for feature selection; and (iv) fusing optimal selected features using descending order serial approach and classifying using multiclass supervised learning algorithms. We demonstrate that once this method is performed on a publicly available dataset, this system attains an improved accuracy of 97.9% and the computational time is almost 34 (sec).

1. Introduction

The novel Coronavirus Disease 2019 (COVID-19) has spread to at least 184 countries worldwide, with over one hundred seventeen million confirmed cases [1]. The number of deaths due to COVID-19 is over 5.3 million (http://worldometers.info). The timely diagnosis of COVID-19 has been a prime issue to be tackled. A test known as polymerase chain reaction (PCR) has proven relatively effective, but it generally takes around 6-8 hours to give results [2]. Since COVID-19 is a respiratory tract infection, chest X-ray images and high-resolution computed tomography (HRCT) or simply CT scans may also be used for its diagnosis [3, 4]. The manual inspection of CT images, however, becomes tedious when performed incessantly and requires expert radiologists to give the final verdict [5, 6]. Artificial intelligence (AI) can help in diagnosing COVID-19 at early stages using the CT images [7, 8], and several methods based on machine learning (ML) [9] have been recently proposed for identifying COVID-19 [8, 9]. The available literature

verifies that the diagnosis of COVID-19 using ML techniques is straightforward and time efficient [10, 11].

The ML techniques have shown great success in image processing applications during the last two decades [12–14]. In image processing, the input images are refined by a few filters (i.e., Gaussian filter and Weiner filter) and followed by segmentation of the object [15, 16]. The output of this step is utilized for feature extraction (i.e., texture, color, and point), which are classified using the ML algorithms like support vector machine (SVM) and to name a few more [17, 18]. This domain's development, especially deep learning, has shown great success in segmentation and classification tasks [19]. In a simple deep learning model, the automated features are extracted instead of handcrafted features [12].

Recently, deep learning has been applied to classify COVID-19 scans into infected or normal classes [20, 21]. The computer vision (CV) researchers have introduced many techniques using deep learning to classify COVID-19 using CT images [22]. Few CV researchers have also focused on fusing multiple features in one matrix for better classification accuracy [23, 24]. However, this fusion process increases the number of predictors, which eventually increases the computational time [25]. This problem is resolved by other researchers using feature selection (FS) techniques [26]. The FS techniques are most important in medical imaging and have recently received increased attention of the research community for better classification accuracy in minimal time, which they promise [27, 28].

Deep learning has played an important role in medical imaging during the last decade [29, 30]. The CV researchers have introduced many techniques for classifying medical infections like COVID-19, cancers of different types (skin, stomach, and lung), and brain tumors [31, 32]. Recently, Abbas et al. [33] implemented a deep Convolutional Neural Network (CNN) framework named DeTraC to diagnose the COVID-19 patients. In this approach, they focused on the chest X-ray scans and considered pretrained models. The training of the pretrained models was performed using shallow tuning, deep tuning, and fine-tuning [34]. Sun et al. [35] presented a computer-aided system using the deep forest learning. The main motive of this approach was to minimize the burdens of clinicians. The extraction of location-specific features was performed, and later, among them, the best features were chosen. Then, a deep forest learning model was employed for the learning. Ozturk et al. [36] proposed another technique intended to detect and diagnose COVID-19 in X-ray scans using deep learning. This method is implemented for binary class classification (COVID vs. no findings) and multiclass classification (COVID vs. no findings vs. pneumonia). In the learning process, the DarkNet model was employed, plus it attained enhanced performance. Apostolopoulosa and Mpesiana [37] described a multiclass framework for classifying COVID-19, pneumonia, and normal CT scans. In this framework, the authors compared the performance of pretrained models and evaluated the best one based on the accuracy.

Islam et al. [38] presented a combined framework for diagnosing COVID-19 with the help of X-ray images, called LSTM-CNN. The features were extracted from the CNN model, and LSTM performed the detection. The LSTM was employed as a classifier that was trained on the CNN features for the detection purpose. The experimental process was conducted on 4575 X-ray images and achieved an improved accuracy. Gianchandani et al. [39] presented an ensemble deep learning framework for classifying the COVID-19 patients from X-ray images. The presented framework was based on the pretrained models. The main functionality of this framework was that it was useful for both binary and multiclass classification. Shaban et al. [40] introduced a hybrid diagnosis strategy for detecting the COVID-19 patients. A feature connectivity graph approach was introduced for the selection of important features. Then, a hybrid model was employed for the final classification.

1.1. Problem Statement. This research is aimed at helping in early detection and analysis of COVID-19 using CT images. The significant challenges considered in this work are (i) there is extraction of irrelevant features from low-contrast chest CT images; (ii) a very common part of chest CT image is infected, and the rest is the same as healthy regions, so there exists a high chance of incorrect classification of the infected and the healthy images; and (iii) simple shape and texture features might not support the correct area of infected regions and, therefore, might result in extraction of the features from the whole image [41]. A deep learning-based framework has been presented in this research to classify the COVID-19 images. The proposed method is evaluated on a publically available dataset called SARS-CoV-2 CT scan. This dataset contains 1252 CT chest scans of COVID-19-infected patients and 1229 CT chest scans of non-COVID patients. Then, we also added around 1500 CT chest scans of patients affected with community-acquired pneumonia (CAP). By training our CNN-based models, we have obtained a detection accuracy of 93.7%.

1.2. Major Contributions. The key contributions presented in our work are listed as follows:

(i) We have collected a CT image database consisting of three classes, including COVID-19, normal, and pneumonia

(ii) Three deep learning models named VGG16, ResNet50, and ResNet101 are modified for the COVID-19 patients' classification. The modified models are trained using transfer learning

(iii) Features are fused using a new approach named descending order via serial fusion (DOvSF)

(iv) An enhanced firefly algorithm (EFA) is proposed for the best feature selection. Within this enhanced algorithm, a new activation function is also proposed

The rest of the manuscript is organized as follows. Section 2 presents the proposed methodology. Results and comparisons are discussed in Section 3. Finally, Section 4 presents the conclusion of this work.

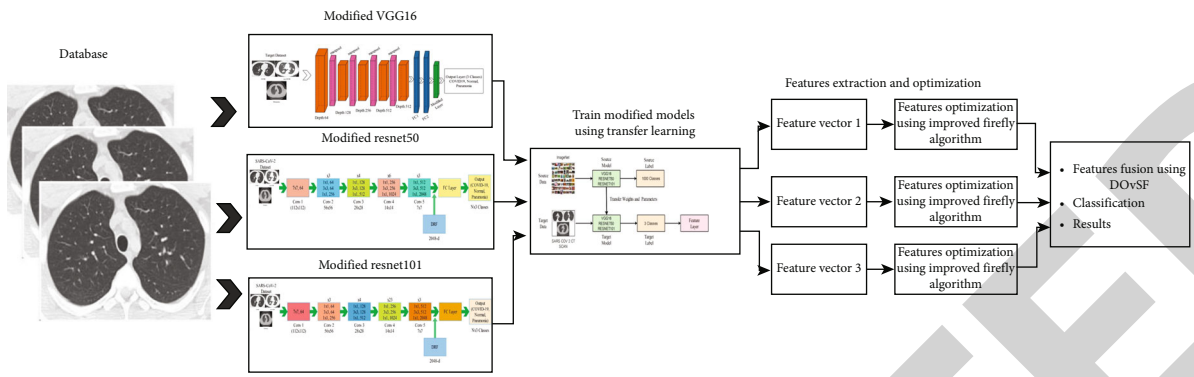

Figure 1: The proposed multiclass architecture of COVID-19 classification using deep learning feature selection and fusion.

2. Methodology

The proposed framework is intended for COVID-19 CT scan classification by using some unique deep learning features. The architecture of the framework is shown in Figure 1. This figure illustrates that the proposed framework consists of the following steps: (i) preparation of a CT image database composed of three classes, COVID-19, pneumonia, and normal; (ii) implementation followed by modification of three deep learning models (i.e., VGG16, ResNet50, and ResNet101); the modification is according to the prepared dataset; (iii) feature extraction from each model and optimization using an improved firefly algorithm. Later, the selected features are combined using the DOvSF technique. We have used supervised learning classifiers to classify the final features. The detail of every single step is described as follows.

2.1. Dataset Collection and Normalization. The publically available SARS-CoV-2 CT scan dataset is utilized in this work. This dataset includes actual patients of Brazilian hospitals. It comprises 1252 CT scans of COVID-19-infected patients, 1152 CT scans for healthy patients, and 1536 CT images of pneumonia-infected patients. Figure 2 presents some samples from the dataset. We have divided the dataset in the percentage ratio of 70 : 30 to use it for training and then testing purposes, respectively. In this figure, the given sample images correspond to COVID-19-infected, pneumonia, and normal. For the experimental process, this dataset is not enough; therefore, we perform data augmentation. In the data augmentation phase, two operations are performed: left flip and right flip. After the augmentation step, the images of each class are increased to 4000. The nature of each image is grayscale and of the dimension 512×512.

2.2. Convolutional Neural Networks (CNN). A Convolutional Neural Network (CNN) is a deep learning procedure in which we apply an image as input. Weights and biases are allocated in a layer called the convolutional layer [17, 42]. When working in this layer, the image pixels are initially considered weights and processed through a convolutional filter. Through the latter, the pixels are transformed into features. Mathematically, the equation of this operation is as follows:

$$x_{ij}^{l} = \sum_{a=0}^{n-1} \sum_{b=0}^{n-1} \omega_{ab} y_{(i+a)(j+b)}^{l-1}, \tag{1}$$

where x_{ij}^{l} represents output layer features and w represents weights. After employing this layer, the nonlinearity is defined as follows:

$$y_{ij}^{l} = \sigma\left(x_{ij}^{l}\right). \tag{2}$$

After the convolutional layer, a ReLu layer is employed. The ReLu layer is also known as activation layer. In this layer, the weights of the convolutional layer are quantized to zero or a positive integer. It means that if weights are positive values, they are considered as they are; otherwise, they are replaced with zero. Mathematically, this operation is defined as follows:

$$f(x) = \max\,(0, x), \tag{3}$$

$$f(x) = \left\{ \begin{array}{l} 0, \text{if } x < 0 \\ x, \text{if } x \geq 0 \end{array} \right\}. \tag{4}$$

A batch normalization layer is added in the neural network to adjust the input values, means, and variances of each layer. Then, a few irrelevant weights are removed using the pooling layer. Through the pooling layer, the spatial size of each layer (input data) is decreased. The pooling process depends on the filter size and stride. For example, in the CNN, the filter size is usually 3×2 and stride 2. Mathematically, this process is formulated as follows:

$$W^2 = \frac{\left(W^1 - F\right)}{S} + 1, \tag{5}$$

$$H^2 = \frac{\left(H^1 - F\right)}{S} + 1, \tag{6}$$

$$D^2 = D^1, \tag{7}$$

where W^1 represents the width of input data volume, H^1 is height, and depth is represented by D^1. Two major parameters such as filter size and stride are defined by F and stride

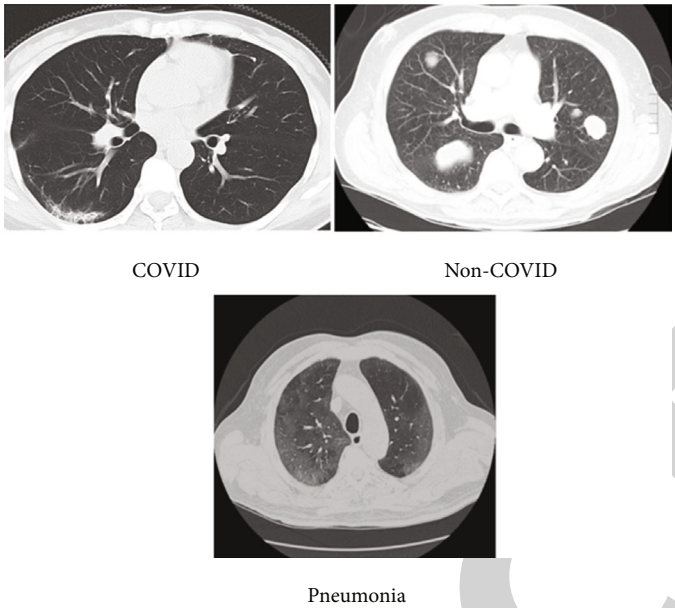

Figure 2: Sample CT images considered from the prepared dataset.

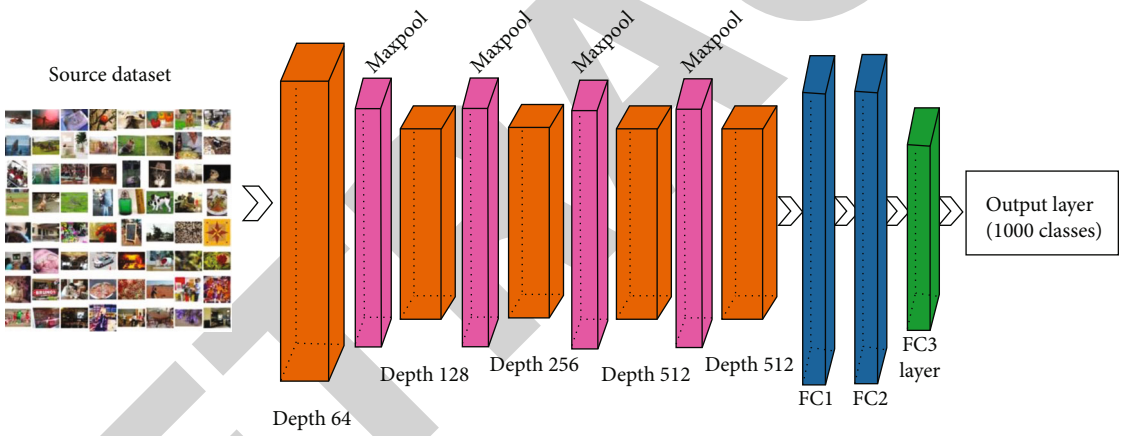

Figure 3: Original architecture of VGG16 CNN model.

S. The features are converted into 1D in the fully connected (FC) layer. In the FC layer, neurons consume complete links to all activations in the previous layer. Hence, their activations are calculated with a matrix multiplication and then the bias offset. In this layer, the features are extracted for the classification purpose. Softmax classifier is applied for the classification purpose.

2.3. Novelty 1: Modified VGG16 Network Features. A unique feature of the VGG16 is that rather than having numerous hyperparameters, it concentrates on using identical PL and MPL of 2×2 filter of stride two and a convolutional layer of 3×3 filter with stride 1. In this model, convolution layers and pooling layers are continuously followed by the fully connected layers. In this model, the total number of layers is 16, as indicated by its name, comprising 13 convolutional layers and three fully connected layers. The architecture of the VGG16 model is shown in Figure 3. This model was initially trained on the ImageNet dataset and of input size $224 \times 224 \times 3$.

In this work, we modify this network as follows. The last fully connected layer has been removed, and a new fully connected layer has been added, which includes only three classes as COVID-19, pneumonia, and normal. The modified model is trained on the selected COVID dataset using transfer learning (TL). The process of TL is described in Section 2.6. The features are extracted from FC layer seven and a vector of dimension $N \times 4096$ is obtained, where the output of the last layer is $N \times 3$. Visually, this network is illustrated in Figure 4.

2.4. Novelty 2: Modified ResNet50 Network Features. ResNet, also known as the Deep Residual Network (DRN), shows higher accuracy and efficiency for the image classification task. This model is also trained initially on 1000 object classes. This model is based on the extra straight pathway for the

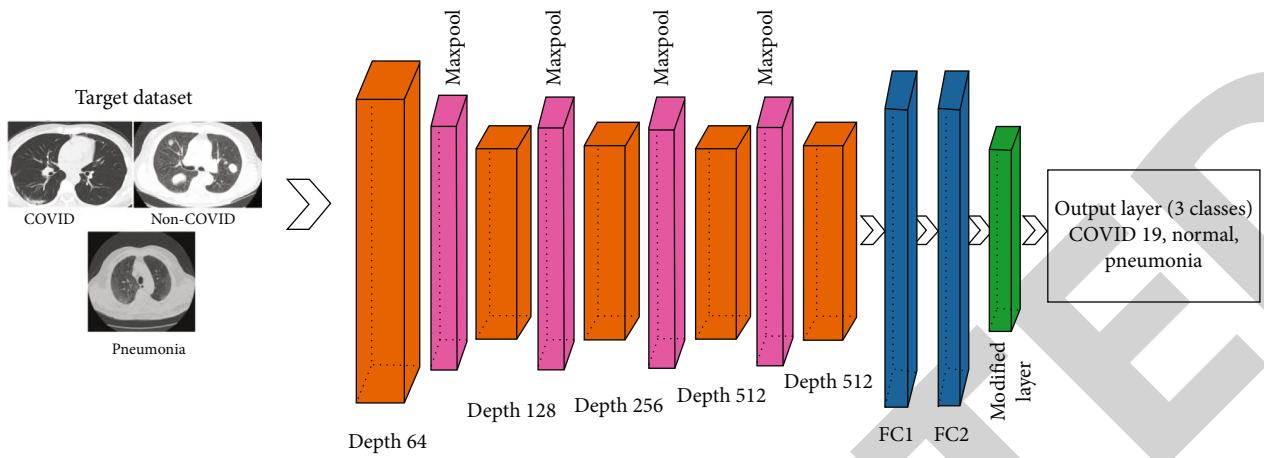

Figure 4: Architecture of modified VGG16 for COVID-19 classification using CT images.

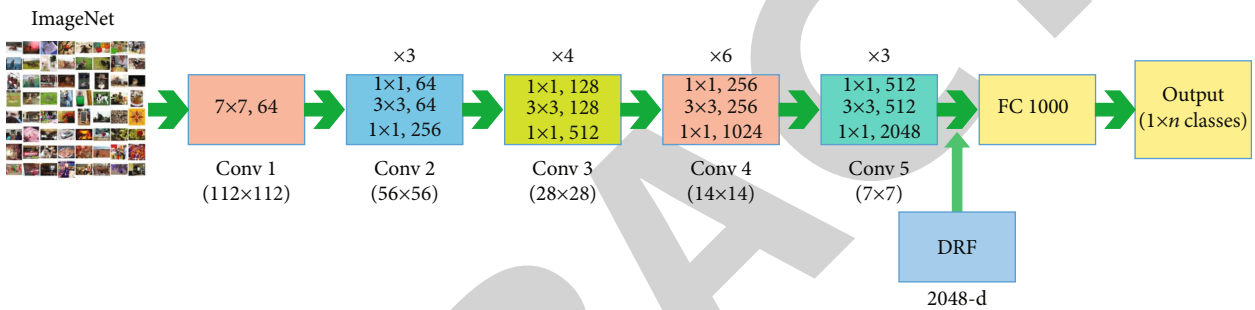

Figure 5: Architecture of ResNet50 for image classification.

transmission of data through a network. Backpropagation does not come across the vanishing gradient problem when working with ResNet. Therefore, the short connections are employed, also called Residual Blocks (RB). For this purpose, an input x has to be added for the output layer by adding the shortcut connection after some weight layers. The main functionality of the short connection is to avoid those layers that are not valuable for the training process. Hence, the output is achieved in rapid training. Mathematically, this process is formulated as follows:

$$H(x) = F(x) - x, \tag{8}$$

$$F(x) = H(x) - x. \tag{9}$$

Visually, this network is illustrated in Figure 5.

This network is modified in this work based on the fully connected layer. Only one fully connected layer has been added to this network, which includes 1000 classes. We remove this layer and change it by adding a new one, which includes only three classes as COVID-19, pneumonia, and normal. The modified model is later trained on the selected COVID dataset using transfer learning (TL). Section 2.6 describes the process of TL. Then, the vital step of feature extraction is performed on the global average pooling layer plus a vector with dimensions $N \times 2048$ is obtained. The output of the last layer is $N \times 3$. Figure 6 shows the architecture of the modified ResNet50 CNN model.

2.5. Novelty 3: Modified ResNet101 Network Features. This network consists of 104 convolutional layers, few batch normalization layers, many pooling layers of max function, one global average pool layer, and one FC layer. Similar to the ResNet50, this network is also trained on the ImageNet dataset, which consists of 1000 object classes. The input size of this network is 224-by-224-by-3. The original architecture is shown in Figure 7. This figure describes that the filter size of the first convolutional layer is 7-by-7, which is minimized for the subsequent layers.

In this work, this network is modified in terms of the FC layer. The FC layer is removed from the original network, and a new FC layer has been added, which includes only three classes, as demonstrated in Figure 8. This explains that the SARS-CoV-2 dataset is given as input to this model, where the same filters are considered, such as input size 224-by-224-by-3, the first layer filter size is 7-by-7. For the proceeding layers, the filter sizes are 1-by-1, 3-by-3, and 1-by-1, respectively. To train this modified network, transfer learning is employed. In the TL process, the learning rate, epochs, and batch size are 0.0001, 200, and 64, respectively. After training of the model, the feature extraction process is performed on the average pooling layer. Here, the dimensions of the extracted features are N-by-2048.

2.6. Transfer Learning. Transfer learning (TL) [43] can be described as the capability of a system to learn information and services while resolving one set of problems (source)

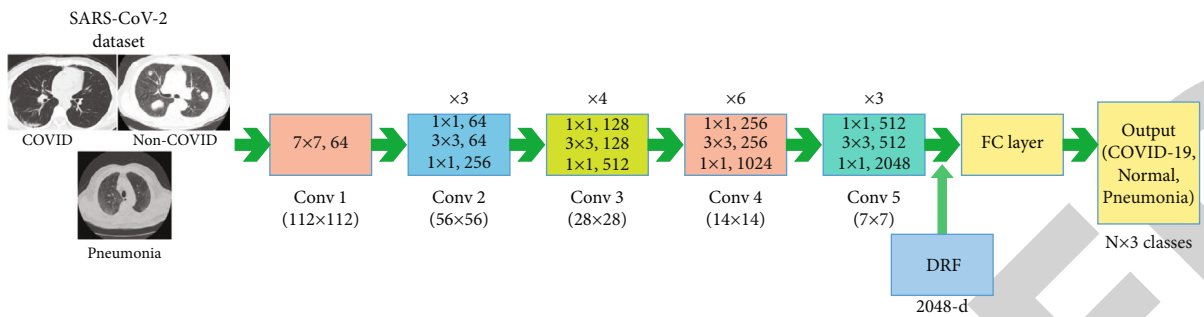

Figure 6: Architecture of modified ResNet50 for the classification of COVID-19 CT images.

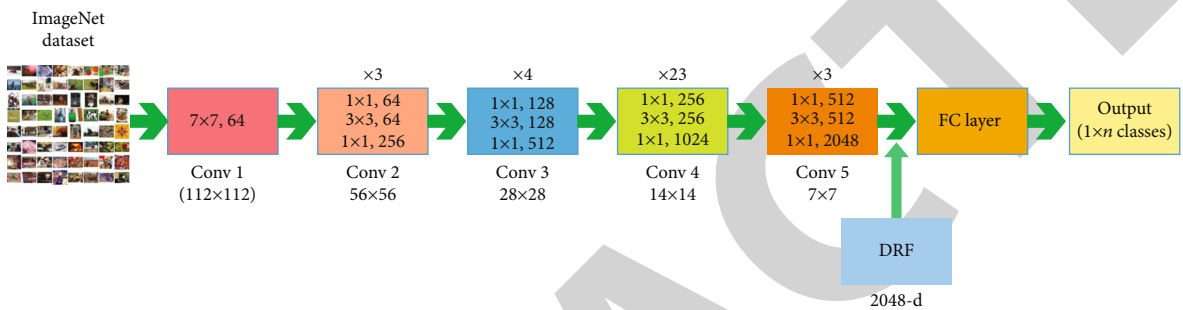

Figure 7: Architecture of Resnet101 for image classification.

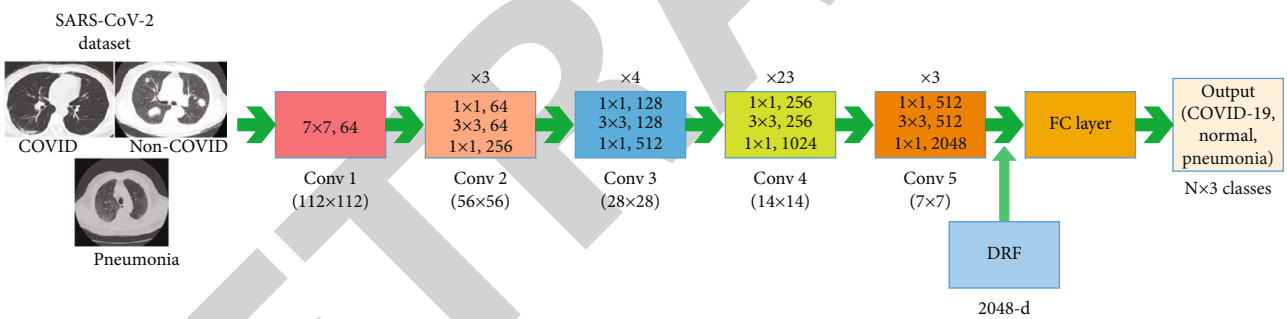

Figure 8: Architecture of modified ResNet101 for the classification of COVID-19 CT scans.

and applying to a different set of problems (target). The key objective of TL is to resolve the target domain with enhanced performance. TL can be a great instrument if the dataset of the target domain is considerably smaller than the dataset of the source domain. Given a source domain $D_S = \{(\alpha_1^S, \beta_1^S), \cdots, (\alpha_i^S, \beta_i^S), \cdots, (\alpha_n^S, \beta_n^S)\}$ with learning task $L_D, L_S, (\alpha_m^S, \beta_m^S) \epsilon \mathbb{R}$; target domain $D_T = \{(\alpha_1^T, \beta_1^T), \cdots, (\alpha_i^T, \beta_i^T), \cdots, (\alpha_m^T, \beta_m^T)\}$ with learning task $L_T, (\alpha_n^T, \beta_n^T) \epsilon \mathbb{R}$, (m, n) is the training data sizes where $n \ll m$ and β_1^D and β_1^T be the labels of training data, where $D_S \neq D_T$ and $L_S \neq L_T$. Visually, the transfer learning process is shown in Figure 9. This figure describes that the weights and parameters of source models (VGG16, ResNet50, and ResNet101) are transferred to modified models and then trained these models on the COVID dataset. At the end of the training, three classes are considered as an output.

2.7. Novelty 4: Enhanced Firefly Algorithm. In the area of CV, the feature selection techniques have shown great success in accuracy and computational time [44]. By maintaining the accuracy and, at the same time, decreasing the number of predictors, these feature selection techniques are really useful. The fewer the number of predictors, the minimal the computational time. Many techniques are introduced in the literature, and a few of them get notable performance. The metaheuristic techniques are more useful for the selection of the best features. In this work, we implement the firefly algorithm and improved its work based on a new activation function. This function is implemented to control the dimension of features and also to minimize the computational time. The basis of this function depends on entropy, kurtosis, and skewness values. This information is put into an activation function and then compared with the selected features of the firefly algorithm based on the fitness value. Hence, this approach is called as the enhanced firefly algorithm (EFA). This process can be mathematically represented as follows.

Consider an original vector $\varnothing(F)$ of dimension $N \times K$, and the selected vector is $\widetilde{\varnothing}(F)$ of dimension $N \times \tilde{K}$. As

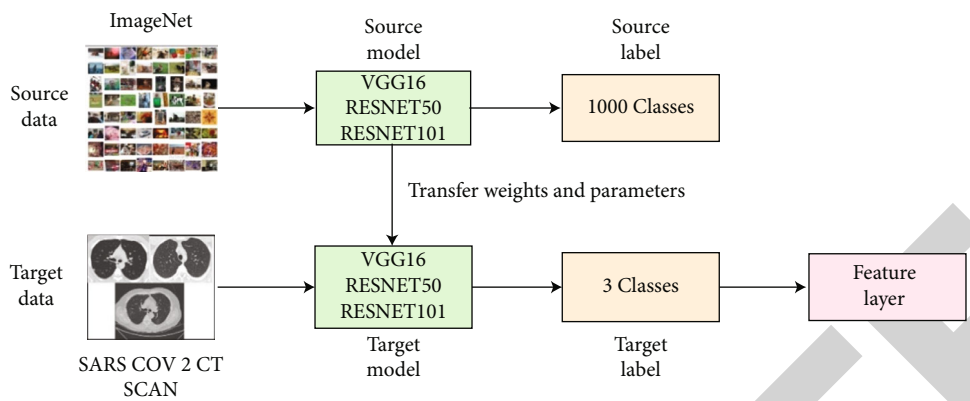

Figure 9: Transfer learning architecture.

Table 1: Classification output of the proposed method using VGG16 and EFA.

Classifier	Recall rate (%)	Precision rate (%)	FNR (%)	AUC	Accuracy (%)	Time (sec)
Linear SVM	95.26	95.33	4.74	0.993	95.3	**157.58**
Quadratic SVM	97.13	97.16	2.87	1.0	97.2	176.35
Cubic SVM	**97.63**	**97.63**	2.37	1.0	**97.6**	189.19
Medium Gaussian SVM	96.43	96.43	3.57	0.993	96.4	229.82
Fine KNN	96.96	96.96	3.04	0.976	97.0	247.06
Medium KNN	93.83	93.86	6.17	0.986	93.8	254.59
Cosine KNN	94.9	94.9	5.1	0.993	94.9	273.3
Cubic KNN	92.86	92.93	7.14	0.986	92.19	1471.3
Weighted SVM	94.86	94.86	5.14	0.993	94.8	305.36
Subspace KNN	96.83	96.83	3.17	0.993	96.8	975.05

mentioned, we have an original feature vector $\varnothing(F)$ having G_1 features and N number of training features.

$$\varnothing(F) = \{\varnothing(F_1), \varnothing(F_2), \cdots, \varnothing(F_K)\}_{G_1}, \tag{10}$$

where $\varnothing(F_K)$ represent input features up to the kth term. There are two significant properties of the firefly algorithm, namely, brightness variation and attractiveness. We have used the distance formula between two fireflies i and j to measure their attractiveness. When we have calculated the distance, the brightness depends on it. The brightness is decreased when the distance between the two fireflies i and j is increased. The brightness is calculated in mathematical form as follows:

$$\partial(D) = \partial_0 e^{-lD}. \tag{11}$$

In the above equation, D is the distance between the two fireflies i and j, ∂_0 denotes original brightness, and l denotes the light absorption coefficient. As we have explained before, brightness ∂ and attractiveness ∂_A between i and j are relational to each other. Hence, this equation can be written as

$$\partial_A(D) = \partial_0 e^{-lD}. \tag{12}$$

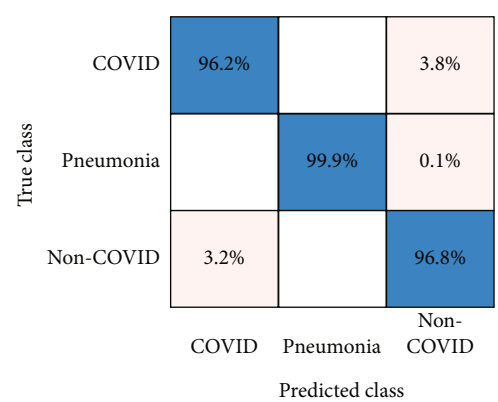

Figure 10: Confusion matrix of Cubic SVM for experiment 1.

By moving to the next destination, the firefly algorithm achieves its goal. This motion is equated as follows, as it depends on the previous and current firefly:

$$\alpha_i^{t+1} = \partial_A e^{-lD_{ij}^2}\left(\alpha_j^t - \alpha_i^t\right) + p_1(r_1 - 0.5). \tag{13}$$

As written in the above equation, p_1 represents the randomization parameter, t denotes the current iteration, and r_1 is the current feature value. Also, in this equation, α_i^{t+1}

Table 2: Classification output of the proposed method using ResNet50 and EFA.

Classifier	Recall rate (%)	Precision rate (%)	FNR (%)	AUC	Accuracy (%)	Time (sec)
Linear SVM	95.96	96.06	3.04	0.993	96.0	95.626
Quadratic SVM	96.93	97	3.07	0.996	96.9	107.41
Cubic SVM	97.20	97.23	2.8	1	97.2	121.81
Medium Gaussian SVM	95.0	95.0	5.0	0.993	95.0	140.97
Fine KNN	93.03	93.13	6.97	0.95	93.1	143.19
Medium KNN	89.9	90.86	10.1	0.98	89.9	151.14
Cosine KNN	93.36	93.33	6.64	0.986	93.4	162.94
Cubic KNN	89.9	90.43	10.1	0.976	89.9	609.23
Weighted SVM	89.76	91.1	10.24	8.986	89.8	178.37
Subspace KNN	94.13	94.1	5.87	0.986	94.1	440.78

represents current firefly, α_i^t represents preceding firefly, and D_{ij} represents the distance between the fireflies i and j. The following equation can calculate the distance:

$$D_{ij} = \sum_{\varnothing=1}^{G_1} \left[\alpha_{i\varnothing} - \alpha_{j\varnothing}\right]^2. \tag{14}$$

In the above equation, $\varnothing \in \varnothing(F)_{G_1}$. When these weights move, the weights are updated every time. The weights are changed according to the following function:

$$\alpha_{i\varnothing}^{t+1} = \left\{ \begin{matrix} M, & \text{if } \dfrac{1}{1+e_{i\varnothing}^{\alpha^t}} \\ 0, & \text{Otherwise} \end{matrix} \right\}. \tag{15}$$

In the above equation, the KNN fitness function is applied for the selected features denoted by M in one iteration. We apply the Manhattan distance formula in KNN as follows:

$$\Delta_m(M) = \sum_{u=1}^{M} |\alpha_u - L_u|. \tag{16}$$

In the above equation, α_u represents the selected features that are updated and L_u denotes the labels of the class. Until the best solution is achieved, we continue this process. After this process, we get an optimal feature vector of dimension $N \times V_1$. This resultant vector is further refined using a new activation function. Mathematically, the activation function is formulated as follows:

$$\text{act} = \frac{\text{Entropy} + \text{Skew}}{\text{Kurt} + C}, \tag{17}$$

$$\text{Entropy} = -\sum_{i=1}^{n} p(\lambda_f) \log(\lambda_f), \tag{18}$$

$$\text{Skew}(\lambda_f) = \frac{\sum_{i=1}^{N} (\lambda_{fi} - \mu)^3 / N}{(N-1) \times \sigma^3}, \tag{19}$$

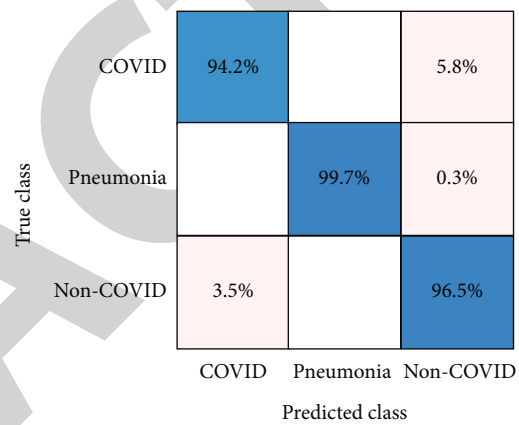

Figure 11: Confusion matrix of Cubic SVM for experiment 2.

$$\text{Kurt}(\lambda_f) = \frac{\sum_{i=1}^{N} (\lambda_{fi} - \mu)/N}{\sigma^4}, \tag{20}$$

$$\text{Act}_{(\text{Fn})} = \begin{cases} S_1(i) \text{ for } V_1(i) \geq \text{act}, \\ \text{Ignore, Elsewhere}, \end{cases} \tag{21}$$

where act represents the activation formula, $\text{Act}_{(\text{Fn})}$ represents the activation function, and $S_1(i)$ is a final selected feature vector. This function is applied for all three deep feature vectors, and as a result, three last optimal vectors are attained with dimensions $N \times 1620$, $N \times 760$, and $N \times 750$. The main purpose of this activation function is to select the most appropriate features for the final classification. In the end, all these features are sorted into descending order and serially fused in one vector. Mathematically, this process is formulated as follows:

$$\text{Fused} = \begin{pmatrix} S_1(i) \\ S_2(i) \\ S_3(i) \end{pmatrix}_{N \times K}. \tag{22}$$

This fused vector of dimension $N \times 3130$ is finally classified using multiclass classification algorithms such as SVM, KNN, and names a few more.

Table 3: Classification output of the proposed method using ResNet101 and EFA.

Classifier	Recall rate (%)	Precision rate (%)	FNR (%)	AUC	Accuracy (%)	Time (sec)
Linear SVM	95.0	95.1	5	0.993	95.0	31.799
Quadratic SVM	97.0	97.06	3	1	97.0	33.323
Cubic SVM	97.5	97.5	2.5	1	**97.5**	35.945
Medium Gaussian SVM	95.56	95.56	4.44	0.993	95.6	42.995
Fine KNN	95.36	95.4	4.64	0.963	95.4	21.224
Medium KNN	90.83	91.43	9.17	0.983	90.8	20.741
Cosine KNN	95.06	95.1	4.94	0.993	95.1	22.4
Cubic KNN	90.36	90.6	9.64	0.98	90.4	146.63
Weighted SVM	91.6	92.66	8.4	0.986	91.6	20.812
Subspace KNN	95.56	95.56	4.44	0.99	95.6	92.172

3. Experimental Results

The experiment was performed on the SARS-CoV-2 CT scan dataset, containing 1252 CT images of COVID-infected patients, 1152 CT images of non-COVID patients, and 1536 CT images of pneumonia-infected patients. 70% of the data is used for training purposes, while 30% of the information is used for testing purposes. The following measures are utilized to analyze the proposed technique's performance: sensitivity, precision, $F1$ score, accuracy, FPR, and FNR. The coding was done in MATLAB 2020a. The experiments are done on Core-i7 7700 CPU, 8 GB of memory, and Intel HD 630 GPU.

3.1. Experiment 1: Modified VGG16 and EFA. In this experiment, the modified VGG16 process of feature extraction is performed, and they are given to EFA for the optimal feature selection. The results are presented in Table 1. In this table, it is described that the best accuracy is 97.6% achieved by the Cubic SVM classifier. The recall rate and precision rate are 97.63%. The Cubic SVM accuracy is also validated in Figure 10. The exact prediction rate shown by this figure for COVID-19 is 96.2%, whereas the pneumonia and normal classes' prediction rates are 99.9% and 96.8%, respectively. The accuracy of the remaining classifiers such as LSVM, MGSVM, MKNN, CKNN, Cubic KNN, WSVM, and Subspace KNN is 95.3%, 96.4%, 93.8%, 94.9%, 92.19%, 94.8%, and 96.8%, respectively. The computational time is also noted during the testing process and shows the minimum computational time of 157.58 (sec) for the Linear SVM. The computational time of the Cubic SVM is 189.9 (sec). Based on the accuracy value, however, the Cubic SVM has performed better.

3.2. Experiment 2: Modified ResNet50 and EFA. The modified ResNet50 features are extracted and passed in EFA for the optimal feature selection in this experiment. The results are presented in Table 2. The best accuracy of 97.2% is achieved by the Cubic SVM classifier. The recall rate and precision rates are 97.2% and 97.23%, respectively. The Cubic SVM accuracy is also validated in Figure 11. The exact prediction rate shown by this figure for COVID-19 is 94.2%, whereas the pneumonia and normal classes' prediction rates are 99.7% and 96.5%, respectively. In Table 2, each classifier is shown with its computational time and accuracy during the testing phase. The minimum computational time is approximately 95 (sec) for Linear SVM, whereas the computational time of Cubic SVM is 121.81 (sec). The difference among Linear SVM, Quadratic SVM, and Cubic SVM accuracy is approximately 1% and the time difference is around 15-20 (sec). Hence, the performance of Cubic SVM is overall better for this experiment.

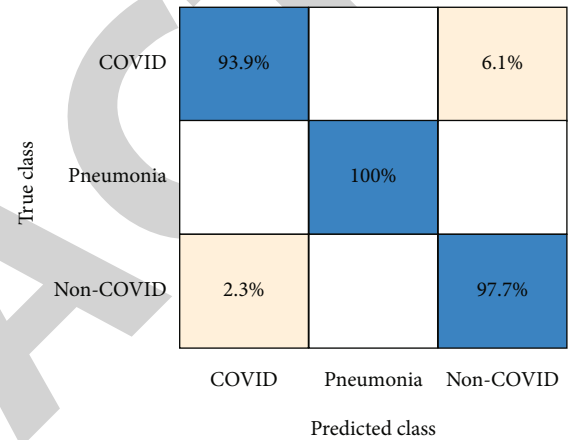

Figure 12: Confusion matrix of Cubic SVM for experiment 3.

3.3. Experiment 3: Modified ResNet101 and EFA. The modified ResNet101- and EFA-based selected feature results are discussed in this experiment. The results are presented in Table 3. This table shows that the best accuracy is 97.5% achieved by the Cubic SVM. Figure 12 illustrates the confusion matrix of Cubic SVM. As shown in this figure, the exact prediction accuracy of COVID-19 is almost 93%, whereas the normal and pneumonia classes' accuracy is 97.7% and 100%, respectively. Few other classifiers are also implemented, and their accuracies are noted in this table. Based on the accuracy, the Cubic SVM showed better performance. The computational time of Cubic SVM during the testing process was approximately 35 (sec); however, the minimum noted time is 31.799 (sec) for the Linear SVM. Compared to experiment 1 and experiment 2, the performance of this experiment is significantly better in both accuracy and

Table 4: Classification output of the proposed method using fusion of all optimal features.

Classifier	Recall rate (%)	Precision rate (%)	FNR (%)	AUC	Accuracy (%)	Time (sec)
Linear SVM	95.2	95.3	4.8	0.993	95.2	30.564
Quadratic SVM	97.2	97.26	2.8	1	97.2	34.323
Cubic SVM	97.9	97.9	2.1	1	**97.9**	34.323
Medium Gaussian SVM	95.86	95.9	4.14	0.993	95.9	49.809
Fine KNN	95.26	95.23	4.77	0.96	95.3	22.065
Medium KNN	90.73	91.36	9.27	0.98	90.8	22.441
Cosine KNN	94.8	94.83	5.2	2.98	94.8	27.401
Cubic KNN	89.9	90.3	10.1	0.97	89.9	163.2
Weighted SVM	91.7	92.7	8.3	0.986	91.7	26.045
Subspace KNN	95.16	95.2	4.84	0.986	95.2	93.763

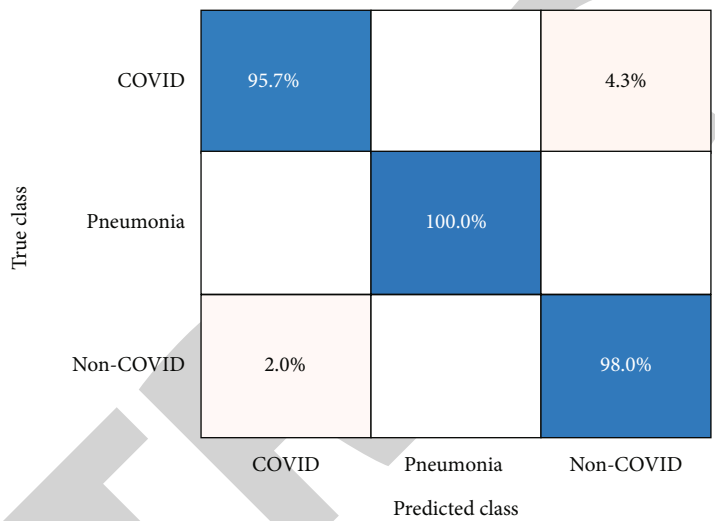

Figure 13: Confusion matrix of Cubic SVM for experiment 4.

Table 5: Confidence interval-based analysis of proposed classification results.

Classifier	Min Acc	Avg Acc	Max Acc	σ	$\sigma_{\bar{x}}$	CI
L-SVM	94.1	94.65	95.2	0.55	0.38	94.65 ± 0.762 (±0.81%)
SKNN	94.3	94.75	95.2	0.45	0.31	94.75 ± 0.624 (±0.66%)
F-KNN	93.7	94.50	95.3	0.80	0.56	94.5 ± 1.109 (±1.17%)
MG-SVM	93.9	94.90	95.9	1.0	0.70	94.9 ± 1.386 (±1.46%)
QSVM	96.4	96.80	97.2	0.4	0.28	96.8 ± 0.554 (±0.57%)
CSVM	97.2	97.55	97.9	0.35	0.24	97.55 ± 0.485 (±0.50%)

computational time. However, this performance is essential to enhance further; therefore, we have fused features of all three experiments.

3.4. Experiment 4: Final Fused Features. In this experiment, we fuse all optimal features of three networks using descending order serial approach. The results of this experiment are presented in Table 4. Cubic SVM achieves the highest accuracy of 97.9%, which is further confirmed by Figure 13. This figure presents the confusion matrix of Cubic SVM. The exact prediction accuracy, according to this figure, of COVID-19 is 95.7%. In the previous experiments (experiment 1, experiment 2, and experiment 3), this rate was approximately 93%.

Similarly, the prediction accuracy of normal and pneumonia classes is also increased. The performance of other classifiers is also increased by approximately 2%. However, the time is slightly increased. Based on the results, the Cubic SVM manages to produce the highest accuracy after the fusion is performed on all optimal features.

The confidence interval-based analysis is also conducted for the final classification results (Table 5). The CI is computed for confidence level 95%, $1.960\sigma_{\bar{x}}$. Based on the

Table 6: Comparison of the proposed method and other techniques in terms of accuracy.

Reference	Year	Accuracy (%)
[45]	2020	95.7
[33]	2020	93.1
[46]	2020	91.6
Proposed	**2021**	**97.9**

results of this table, it can be seen that the Cubic SVM (CSVM) outcomes are more consistent and accurate. Lastly, we compare the proposed method accuracy (after fusion) with some recent techniques, as presented in Table 6. This table shows that our proposed method has obtained far better results than recent techniques.

4. Conclusion

This research offers a unique combination of deep learning feature-based framework to classify COVID-19, pneumonia, and normal patients using CT images. This framework's main steps are preparing a database, modifying pretrained deep learning models, enhancing the firefly algorithm for feature selection, and final fusion, followed by the classification. The core forte of this research is the choice of pretrained models to extract features. Several pretrained models are implemented in this work, and three of them are chosen based on their better performance, like minimum error rate. The second strong point of this research is the enhanced firefly algorithm to select the best features. By the use of this algorithm, the features are first selected into two phases. We propose an activation function based on entropy, skewness, and kurtosis for the second phase's more rich features. The number of predictors is further minimized by minimizing the computational time and improving the accuracy. The fusion of these optimal features shows the limitation of this research. This process increases computational time, but the advantage is gained in improving accuracy. In the future, we will focus on two key steps: (i) increase the size of the database and design a CNN model from scratch for COVID-19 classification and (ii) focus on new feature fusion approach that does not affect the computational time.

Data Availability

The entire dataset was collected from the following publically open link: https://www.kaggle.com/tawsifurrahman/covid19-radiography-database.

Conflicts of Interest

All authors declare that they have no conflict of interest in this work.

Acknowledgments

This work was supported by the National Research Foundation of Korea (NRF) grant funded by the Korea government (MSIT) (NRF-2019R1F1A1060668) and also supported by the MSIT (Ministry of Science and ICT), Korea, under the ITRC (Information Technology Research Center) support program (IITP-2021-2018-0-01799) supervised by the IITP (Institute for Information & Communications Technology Planning & Evaluation).

References

[1] U. Özkaya, Ş. Öztürk, and M. Barstugan, "Coronavirus (covid-19) classification using deep features fusion and ranking technique," in *Big Data Analytics and Artificial Intelligence Against COVID-19: Innovation Vision and Approach*, Springer, 2020.

[2] I. Floriano, A. Silvinato, W. M. Bernardo, J. C. Reis, and G. Soledade, "Accuracy of the polymerase chain reaction (PCR) test in the diagnosis of acute respiratory syndrome due to coronavirus: a systematic review and meta-analysis," *Revista da Associação Médica Brasileira*, vol. 66, no. 7, pp. 880–888, 2020.

[3] H. Panwar, P. Gupta, M. K. Siddiqui, R. Morales-Menendez, P. Bhardwaj, and V. Singh, "A deep learning and grad-CAM based color visualization approach for fast detection of COVID-19 cases using chest X-ray and CT-scan images," *Chaos, Solitons & Fractals*, vol. 140, article 110190, 2020.

[4] A. S. Alghamdi, K. Polat, A. Alghoson, A. A. Alshdadi, and A. A. Abd el-Latif, "Gaussian process regression (GPR) based non-invasive continuous blood pressure prediction method from cuff oscillometric signals," *Applied Acoustics*, vol. 164, article 107256, 2020.

[5] M. Turkoglu, "COVIDetectioNet: COVID-19 diagnosis system based on X-ray images using features selected from pre-learned deep features ensemble," *Applied Intelligence*, vol. 51, no. 3, pp. 1213–1226, 2021.

[6] H. Kaushik, D. Singh, S. Tiwari et al., "Screening of COVID-19 patients using deep learning and IoT framework," *Computers Materials & Continua*, vol. 69, no. 3, pp. 3459–3475, 2021.

[7] A. Sedik, M. Hammad, F. E. Abd El-Samie, B. B. Gupta, and A. A. Abd El-Latif, "Efficient deep learning approach for augmented detection of Coronavirus disease," *Neural Computing and Applications*, pp. 1–18, 2021.

[8] M. A. Khan, M. Alhaisoni, U. Tariq et al., "COVID-19 case recognition from chest CT images by deep learning, entropy-controlled firefly optimization, and parallel feature fusion," *Sensors*, vol. 21, no. 21, p. 7286, 2021.

[9] A. A. Abdulmunem, Z. A. Abutiheen, and H. J. Aleqabie, "Recognition of corona virus disease (COVID-19) using deep learning network," *International Journal of Electrical and Computer Engineering (IJECE)*, vol. 11, no. 1, pp. 365–374, 2021.

[10] T. Akram, M. Attique, S. Gul et al., "A novel framework for rapid diagnosis of COVID-19 on computed tomography scans," *Pattern Analysis and Applications*, vol. 24, no. 3, pp. 951–964, 2021.

[11] H. T. Rauf, M. I. U. Lali, M. A. Khan et al., "Time series forecasting of COVID-19 transmission in Asia Pacific countries using deep neural networks," *Personal and Ubiquitous Computing*, pp. 1–18, 2021.

[12] A. Majid, M. A. Khan, Y. Nam et al., "COVID19 classification using CT images via ensembles of deep learning models," *Computers, Materials & Continua*, vol. 69, no. 1, pp. 319–337, 2021.

[13] M. Hammad, R. N. V. P. S. Kandala, A. Abdelatey et al., "Automated detection of shockable ECG signals: a review," *Information Sciences*, vol. 571, pp. 580–604, 2021.

[14] M. Hammad, A. M. Iliyasu, A. Subasi, E. S. Ho, and A. A. A. el-Latif, "A multitier deep learning model for arrhythmia Detection," *IEEE Transactions on Instrumentation and Measurement*, vol. 70, pp. 1–9, 2020.

[15] Y.-D. Zhang, M. A. Khan, Z. Zhu, and S.-H. Wang, "Pseudo zernike moment and deep stacked sparse autoencoder for COVID-19 diagnosis," *Cmc-Computers Materials & Continua*, vol. 69, no. 3, pp. 3145–3162, 2021.

[16] J. Naz, M. A. Khan, M. Alhaisoni, O.-Y. Song, U. Tariq, and S. Kadry, "Segmentation and classification of stomach abnormalities using deep learning," *CMC-COMPUTERS MATERIALS & CONTINUA*, vol. 69, no. 1, pp. 607–625, 2021.

[17] M. A. Khan, M. I. Sharif, M. Raza, A. Anjum, T. Saba, and S. A. Shad, "Skin lesion segmentation and classification: A unified framework of deep neural network features fusion and selection," *Expert Systems*, p. e12497, 2019.

[18] K. S. Manic, R. Biju, W. Patel, M. A. Khan, N. Raja, and S. Uma, "Extraction and evaluation of corpus callosum from 2D brain MRI slice: a study with cuckoo search algorithm," *Computational and Mathematical Methods in Medicine*, vol. 2021, 15 pages, 2021.

[19] M. A. Khan, S. Kadry, Y.-D. Zhang, T. Akram, M. Sharif, and A. Rehman, "Prediction of COVID-19-pneumonia based on selected deep features and one class kernel extreme learning machine," *Computers & Electrical Engineering*, 2020.

[20] M. A. Khan, N. Hussain, A. Majid et al., "Classification of positive COVID-19 CT scans using deep learning," *Computers, Materials and Continua*, vol. 66, no. 3, pp. 2923–2938, 2021.

[21] W. Shui-Hua, M. A. Khan, V. Govindaraj, S. L. Fernandes, Z. Zhu, and Z. Yu-Dong, "Deep rank-based average pooling network for COVID-19 recognition," *Computers, Materials, & Continua*, pp. 2797–2813, 2022.

[22] A. Sedik, A. M. Iliyasu, B. A. El-Rahiem et al., "Deploying machine and deep learning models for efficient data-augmented detection of COVID-19 infections," *Viruses*, vol. 12, no. 7, p. 769, 2020.

[23] A. Majid, M. A. Khan, M. Yasmin, A. Rehman, A. Yousafzai, and U. Tariq, "Classification of stomach infections: a paradigm of convolutional neural network along with classical features fusion and selection," *Microscopy Research and Technique*, vol. 83, no. 5, pp. 562–576, 2020.

[24] M. A. Khan, K. Muhammad, M. Sharif, T. Akram, and S. Kadry, "Intelligent fusion-assisted skin lesion localization and classification for smart healthcare," *Neural Computing and Applications*, pp. 1–16, 2021.

[25] M. Attique Khan, M. Sharif, T. Akram, S. Kadry, and C. H. Hsu, "A two-stream deep neural network-based intelligent system for complex skin cancer types classification," *International Journal of Intelligent Systems*, 2021.

[26] M. A. Khan, M. Sharif, T. Akram, S. A. C. Bukhari, and R. S. Nayak, "Developed Newton-Raphson based deep features selection framework for skin lesion recognition," *Pattern Recognition Letters*, vol. 129, pp. 293–303, 2020.

[27] M. A. Khan, S. Kadry, M. Alhaisoni et al., "Computer-aided gastrointestinal diseases analysis from wireless capsule endoscopy: a framework of best features selection," *IEEE Access*, vol. 8, pp. 132850–132859, 2020.

[28] N. Naheed, M. Shaheen, S. A. Khan, M. Alawairdhi, and M. A. Khan, "Importance of features selection, attributes selection, challenges and future directions for medical imaging data: a review," *Computer Modeling in Engineering & Sciences*, vol. 125, no. 1, pp. 315–344, 2020.

[29] A. U. Ibrahim, M. Ozsoz, S. Serte, F. Al-Turjman, and P. S. Yakoi, "Pneumonia classification using deep learning from chest X-ray images during COVID-19," *Cognitive Computation*, pp. 1–13, 2021.

[30] M. A. Khan, T. Akram, Y.-D. Zhang, and M. Sharif, "Attributes based skin lesion detection and recognition: a mask RCNN and transfer learning-based deep learning framework," *Pattern Recognition Letters*, vol. 143, pp. 58–66, 2021.

[31] W. Saad, W. A. Shalaby, M. Shokair, F. Abd El-Samie, M. Dessouky, and E. Abdellatef, "COVID-19 classification using deep feature concatenation technique," *Computing*, pp. 1–19, 2021.

[32] K. Kamal, Z. Yin, M. Wu, and Z. Wu, "Evaluation of deep learning-based approaches for COVID-19 classification based on chest X-ray images," *Signal, Image and Video Processing*, vol. 15, no. 5, pp. 959–966, 2021.

[33] A. Abbas, M. M. Abdelsamea, and M. M. Gaber, "Classification of COVID-19 in chest X-ray images using DeTraC deep convolutional neural network," 2020, arXiv preprint arXiv:2003.13815.

[34] M. A. Khan, S. Kadry, Y.-D. Zhang et al., "Prediction of COVID-19 - pneumonia based on selected deep features and one class kernel extreme learning machine," *Computers & Electrical Engineering*, vol. 90, article 106960, 2021.

[35] L. Sun, Z. Mo, F. Yan et al., "Adaptive feature selection guided deep forest for covid-19 classification with chest ct," *IEEE Journal of Biomedical and Health Informatics*, vol. 24, no. 10, pp. 2798–2805, 2020.

[36] T. Ozturk, M. Talo, E. A. Yildirim, U. B. Baloglu, O. Yildirim, and U. R. Acharya, "Automated detection of COVID-19 cases using deep neural networks with X-ray images," *Computers in Biology and Medicine*, vol. 121, p. 103792, 2020.

[37] I. D. Apostolopoulos and T. A. Mpesiana, "Covid-19: automatic detection from x-ray images utilizing transfer learning with convolutional neural networks," *Physical and Engineering Sciences in Medicine*, vol. 43, no. 2, pp. 635–640, 2020.

[38] M. Z. Islam, M. M. Islam, and A. Asraf, "A combined deep CNN-LSTM network for the detection of novel coronavirus (COVID-19) using X-ray images," *Informatics in medicine unlocked*, vol. 20, article 100412, 2020.

[39] N. Gianchandani, A. Jaiswal, D. Singh, V. Kumar, and M. Kaur, "Rapid COVID-19 diagnosis using ensemble deep transfer learning models from chest radiographic images," *Journal of Ambient Intelligence and Humanized Computing*, pp. 1–13, 2020.

[40] W. M. Shaban, A. H. Rabie, A. I. Saleh, and M. Abo-Elsoud, "Detecting COVID-19 patients based on fuzzy inference engine and deep neural network," *Applied Soft Computing*, vol. 99, article 106906, 2021.

[41] S. A. Khan, M. A. Khan, O.-Y. Song, and M. Nazir, "Medical imaging fusion techniques: a survey benchmark analysis, open challenges and recommendations," *Journal of Medical Imaging and Health Informatics*, vol. 10, no. 11, pp. 2523–2531, 2020.

[42] M. A. Khan, M. S. Sarfraz, M. Alhaisoni, A. A. Albesher, S. Wang, and I. Ashraf, "StomachNet: optimal deep learning

Hindawi
Behavioural Neurology
Volume 2023, Article ID 9820206, 1 page
https://doi.org/10.1155/2023/9820206

Retraction

Retracted: Ensemble Classification Approach for Sarcasm Detection

Behavioural Neurology

Received 8 August 2023; Accepted 8 August 2023; Published 9 August 2023

This article has been retracted by Hindawi following an investigation undertaken by the publisher [1]. This investigation has uncovered evidence of one or more of the following indicators of systematic manipulation of the publication process:

(1) Discrepancies in scope

(2) Discrepancies in the description of the research reported

(3) Discrepancies between the availability of data and the research described

(4) Inappropriate citations

(5) Incoherent, meaningless and/or irrelevant content included in the article

(6) Peer-review manipulation

The presence of these indicators undermines our confidence in the integrity of the article's content and we cannot, therefore, vouch for its reliability. Please note that this notice is intended solely to alert readers that the content of this article is unreliable. We have not investigated whether authors were aware of or involved in the systematic manipulation of the publication process.

Wiley and Hindawi regrets that the usual quality checks did not identify these issues before publication and have since put additional measures in place to safeguard research integrity.

We wish to credit our own Research Integrity and Research Publishing teams and anonymous and named external researchers and research integrity experts for contributing to this investigation.

The corresponding author, as the representative of all authors, has been given the opportunity to register their agreement or disagreement to this retraction. We have kept a record of any response received.

References

[1] J. Godara, I. Batra, R. Aron, and M. Shabaz, "Ensemble Classification Approach for Sarcasm Detection," *Behavioural Neurology*, vol. 2021, Article ID 9731519, 13 pages, 2021.

Hindawi
Behavioural Neurology
Volume 2021, Article ID 9731519, 13 pages
https://doi.org/10.1155/2021/9731519

Research Article

Ensemble Classification Approach for Sarcasm Detection

Jyoti Godara,[1] **Isha Batra**,[1] **Rajni Aron**,[2] **and Mohammad Shabaz**[3,4]

[1]*Department of Computer Science and Engineering, Lovely Professional University, Punjab, India*
[2]*SVKM's Narsee Monjee Institute of Management Studies (NMIMS), Mumbai, India*
[3]*Department of Computer Science Engineering, Chandigarh University, Punjab, India*
[4]*Arba Minch University, Ethiopia*

Correspondence should be addressed to Jyoti Godara; jyotipoonia6@gmail.com
and Mohammad Shabaz; mohammad.shabaz@amu.edu.et

Received 4 October 2021; Revised 25 October 2021; Accepted 1 November 2021; Published 22 November 2021

Academic Editor: Hong Lin

Cognitive science is a technology which focuses on analyzing the human brain using the application of DM. The databases are utilized to gather and store the large volume of data. The authenticated information is extracted using measures. This research work is based on detecting the sarcasm from the text data. This research work introduces a scheme to detect sarcasm based on PCA algorithm, *K*-means algorithm, and ensemble classification. The four ensemble classifiers are designed with the objective of detecting the sarcasm. The first ensemble classification algorithm (SKD) is the combination of SVM, KNN, and decision tree. In the second ensemble classifier (SLD), SVM, logistic regression, and decision tree classifiers are combined for the sarcasm detection. In the third ensemble model (MLD), MLP, logistic regression, and decision tree are combined, and the last one (SLM) is the combination of MLP, logistic regression, and SVM. The proposed model is implemented in Python and tested on five datasets of different sizes. The performance of the models is tested with regard to various metrics.

1. Introduction

Microblogging sites provide an open stage to a common individual to convey their thoughts, views, and opinions on different subjects and episodes. Sarcasm is a complex version of irony generally observed in social media and microblogging websites, as these media usually promote trolling and/or condemnation of others. Irony and sarcasm have a minor difference. Sarcasm, as a word, usually expresses verbal irony. Sarcasm has drawn considerable research interest in cognitive science, semantics, and psychology. Opinion mining and reputation management find automatic sarcasm detection quite advantageous. Therefore, ASD (automatic sarcasm detection) has got much attention from the NLP (natural language processing) group [1]. It is a daunting task to deal with text on social network. Its distinguishing features are as follows: it is casual and uses the distorted language. To express themselves, people use unstructured content in a defensive way. Typically, text available on social networking sites is misspelled and contained abbreviations, slang, etc. The number of characters of a text on Twitter is limited to 140. Hence, figurative linguistic is conveyed very briefly, which generates one more issue. Individuals expressing their opinions with sarcastic words are free to select the language form to meet their interaction objectives. A special structure is not present there for constructing sarcastic statements. As such, the major goal of the work of detecting sarcasm is to find the characteristics that enable people to distinguish satirical texts from nonsatirical texts [2].

1.1. Sarcasm Detection from Twitter Data. Detecting sarcasm from tweets can be modeled as a binary text classification function. Sarcasm detection in text classification is a vital mechanism with multiple implications for many sectors, such as safety, marketing, and fitness. Sarcasm detection methods may help companies to analyze customer sentiments about their goods. It leverages those companies to promote the quality of their product. In sentiment analysis, classification of sentiments is a vital subfunction, especially to classify tweets, containing latent information within the message that an individual shares with others. Besides this, one can also use the composition of the tweet to predict

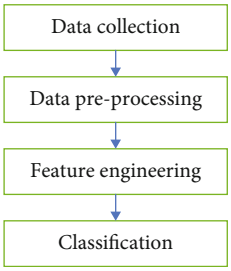

Figure 1: Sarcasm detection process.

sarcasm. Implementing machine learning algorithms can yield successful results for sarcasm detection. Building an effective classification model depends on many aspects. The main aspects are the attributes used and the sovereign attributes in the learning algorithm which are easily combined with the class example [3]. Figure 1 illustrates the sarcasm detection process based on machine learning.

The stages in the above can be summarized as below:

(a) Data collection: acquisition of a suitable dataset is the first step towards sarcasm detection. Dataset plays an important role in any data mining study. Dataset is generally acquired from the Twitter Streaming API for both collections having sarcasm and nonsarcasm. Each tweet derived using the API contains comprehensive information of users, including user identity, URL, and username of tweets. The text in tweets is the key text data for analysis as it includes diverse information and ideas. This information is used to build a feature set so that Twitter data can be classified successfully

(b) Data preprocessing: a major shortcoming of getting datasets from Twitter is the noise present in the data. Tweets can be simple text, mentions of users, and references to URLs or content tags, also called hashtags (#). This step involves preprocessing of satirical and nonsarcastic data in order to get them ready before subsequent tasks. Multiple operations are performed in this step to wipe out noise from the satirical dataset which includes retweets, duplicates, numbers, different language tweets, and tweets with a single URL [4]. These noises do not facilitate to increasing the data classification accuracy and are hence wiped out. Many fundamental preprocessing methods such as to eliminate the stop word, stream, and lemmatize the spell check are implemented after converting data text data to the lower case

(i) Tokenization: the main purpose of this process is to break words or sentences into small pieces known as tokens, for example, words, phrases, and symbols which are beneficial in their own right. The procedure of tokenization also removes blank whitespace characters present in text documents. A token denotes a series of characters obtained in a certain document that join to form a suitable semantic component beneficial later in the analysis. Thus, the output of this process is an input for future study. NLP Toolkit is a well-known mechanism for tokenization process [5]

(ii) Stop word removal: these are general words that include articles and prepositions which have no effect on the context of the expression and are unable to contribute in analyzing the text. The NLTK corpus is a commonly used mechanism to eliminate stop words from the dataset. In turn, in order to improve the classification output, stop words are removed. The preprocessing stage is used as an input to the subsequent stage called the feature engineering stage

(iii) Spell correction: this step is aimed at verifying the spelling of text to correct misspelled text. A common tool to correct all misspelled words is PyEnchant (the spell checker Python library) [6]

(iv) Stemming: it is the restoration of extracted words to their original form or the removal of prefixes and suffixes from the word to obtain a root word called a stem. This process emphasizes on alleviating the number of keyword spaces. It increases classification efficiency when a keyword is derived from a dissimilar kind of keywords

(v) Lemmatizing: an extracted word can sometime lose its meaning when prefixes and suffixes are removed from this [7]. Lemmatization is a kind of normalization that uses morphological and lexical analysis of a word to reduce the inflection of a word to a dictionary form. This process generalizes the word to its root forms. Different from earlier, lemmatization is unable to generate a word stem; however, it creates the normalized form of the input word by replacing its suffix with an alternate word

(vi) Part-of-speech (POS) tagging: its tagger is utilized to read the text documents and assigns POS to every token according to its meaning. It assigns dissimilar POS like adjective, conjunction, and interjection. Fine-grained POS tagging is the main requirement for maximum computational science applications

(c) Feature engineering: feature extraction is important in determining the result of a machine learning operation. Feature engineering is a crucial process in the text classification [8]. The quality of the classification is contingent upon the chosen characteristics. The feature engineering phase is aimed at extracting features with discriminatory ability from the processed data so as to separate sarcastic and nonsarcastic text

(d) Classification: this step is about machine learning algorithms, known as the classification models.

Machine learning analyzes the algorithm from which it can learn and make predictions on the data. This is commonly known as the model training phase post the feature extraction phase. This stage builds machine learning algorithms using features derived from the dataset. The built models are further used for sarcasm classification. In other words, machine learning algorithms classify tweets into sarcastic and nonsarcastic. The most optimal classifier is selected by analyzing numerous classifiers through various tests for sarcasm prediction. The most used classifiers for sarcasm prediction are DT, RF, LR, SVM etc. [9]

(i) Decision tree (DT): being a ML technique, decision tree uses a tree-shaped algorithm for decision making. This model has no parameter; however, it is quite easy to manage the interaction of features. The classifier is contingent upon the rule that represents the DT obtained from a disorganize class in an asymmetrical case. It depends on the feature value, for example, classification through a sorting algorithm. The tree is composed of routes, leaf and decision nodes, and branch. Instance classification begins from the root node and depends on its feature value for categorization. The main shortcoming of this classifier is overfitting which arises due to its capability to fit all sections of the data along with noise, and hence, its performance may be lacking. The issue of overfitting can be resolved by using a multiclassifier model such as random forest [10]

(ii) Random forest (RF): unlike single classifier, ensemble classifiers become more popular due to their strength and accuracy to noise. RF is a strong ensemble of DTs that combines numerous DTs. The idea of unifying numerous classification algorithms gives a RF better attributes which set it apart to a large extent from classic tree classifier models. Similar to one DT algorithm with outliers or noise, which can influence the general performance of a model, RF classifiers provide randomness to address such issues. Random forest gives randomness both the data and the features. This classifier uses the same notions obtained in bootstrapping and bagging algorithms. This is done by making the trees more diverse, whereby they grow from various training data subsets created through bagging

(iii) Support vector machine (SVM): it is a binary linear classification algorithm [11]. It makes use of larger size space to generate a group of hyperplanes. The main aim here is to divide the data into several classes using training data. However, the target value is predicted by constructing the model with the help of training data. This data contains only the features of the test data. SVM is one of the most employed text classification algorithms. It selects the best hyperplane for the appropriate classification of problem cases

(iv) Logistic regression (LR): this algorithm emphasizes on classifying the probability of an event as a linear function of a class of predictor variables. This algorithm generally uses a linear function of the attributes for creating the decision boundaries. The purpose of LR is that the probability function was extended to identify document class labels. The selection of parameters is performed to get the highest conditional probability. In spite of the satisfactory results of LR, typically, the class created is outside the variable [12]

(v) K-nearest neighbor (KNN): it is an example-based ML framework. The identity of the class label for every instance in this algorithm relies upon KNN of that example. Therefore, the class label in the nearby example is determined using the majority voting concept

1.1.1. Common Features of Sarcasm Detection. In text mining, deriving data attributes is an important task for classification algorithms to make ultimate decisions. One can use certain attributes of social media posts as a crucial aspect for sarcasm detection while classifying text messages [13]. Therefore, preparing a dataset with appropriate features will make a significant contribution to the general productivity of machine learning. Implementing various text mining methods can have different characteristics. The important attributes employed to detect sarcastic tweets for every classification algorithm include the following features:

(a) Sentiment-related feature: Whisper is the widely used sarcasm type available on social media. In Whisper, composers of sarcastic accents use positive emotion to define a negative case. Incidentally, the sarcasm utilizes the contradictory emotion which is seen in the expression of a negative case through positive emotion

(b) Pragmatic features: symbolic and figurative texts correspond to practical attributes. These attributes are most common in tweets, particularly because of the limited length of tweets. Practical features are a strong sign of sarcasm detection in Twitter. Hence, many researchers have derived these features to use them in the sarcasm classification operation [14]

(c) Frequency-related features: these are the most utilized features in a document or a corpus. It shows the significance of a word in a document or collection. It is a crucial job to extract frequency-related features. There are many ways to apply these features for classifying sarcasm

(d) TF-IDF: it is a numerical statistic representing the significance of a word (period) for a document in the corpus. A comparison must be made between the frequencies of a word in a document against its number in other documents. TF-IDF is commonly employed to prevent filtering of words in text summarization and classification applications. This assists in maximizing the number of times a word seems in a document in proportional way

(e) Hashtag features: users sometime use hashtags in the tweets to convey their emotions. The hashtags are utilized to express the emotional content. Hashtags are used to illustrate the true purpose of a Twitter user to convey the message. In this statement, the hashtag "#i hate you" suggests that the user is expressing thanks for nothing in fact [15] wanting, but hating it so much for not helping when needed. The above expression is a negative hashtag tweet. Hashtag features can be positive or negative hashtags

(f) Lexical features: lexical features are frequently used in text mining. Lexical attributes include unique words, phrases, noun phrases, or named objects related to a score to display the range of polarity. The use of these attributes for emotion mining can help decide the level of emotion in a text

2. Literature Review

Porwal et al. projected a RNN to detect the sarcasm. This technique was capable of extracting the attributes in an automatic manner to be fed in ML (machine learning) methods [16]. Moreover, LSTM cells were utilized on tensor flow for capturing the syntactic and semantic information over Twitter tweets while detecting the sarcasm. At last, an overview of dataset was presented statistically. The outcomes generated from the suggested approach were also defined. An approach to detect the sarcasm automatically was introduced by Gupta et al. [17]. The initial stage focused on extracting attributes regarding sentiments and punctuation. The chi-square test was adopted to select the effective attributes. The subsequent phase was aimed at extracting and integrating 200 top TF-IDF attributes with sentiment-related and punctuation-related features for recognizing the sarcastic content in the tweet. The SVM (support vector machine) algorithm provided the highest accuracy around 74.59% in an initial technique. The second technique provided the accuracy of 83.53% using voting classification algorithm. A system was developed by Arifuddin et al. with the objective of recognizing the sarcastic sentence in the text [18]. The data have 480 train data and 120 test data taken from Twitter. Afterward, the data was preprocessed and the attributes were extracted. The SVM (support vector machine) algorithm was implemented for classifying the sentences as having sarcasm or normal. The accuracy of N-gram, POS Tag, Punctuation, and Pragmatic was compared in the experimentation. The experimental results indicated that the developed system provided the accuracy up to 91.6% and precision up to 92% after integrating all the attributes. A hyperbolic feature-based sarcasm detector was projected by Santosh et al. for Twitter data [19]. In the hyperbolic attributes, intensifiers and interjections of the text were comprised. Various ML techniques, namely, NB, DT, SVM, RF, and AdaBoost, had been employed for the analysis of projected detector. The projected detector obtained the accuracy of 75.12% from NB, 80.27% from DT, 80.67%% from SVM, 80.79% from RF, and 80.07% from AdaBoost. Ren et al. emphasized on implementing NN (neural network) models in order to detect the sarcasm in Twitter [20]. For this purpose, two diverse context-augmented neural algorithms were put forward on the basis of CNN (convolutional neural network). The outcomes acquired on datasets confirmed the supremacy of suggested models over the traditional techniques. In the meantime, the presented context-augmented neural models were proved adaptable for decoding the sarcastic clues from contextual information and enhancing the detection performance. A hybrid framework BiLSTM-CNN was designed by Jain et al. in which BiLSTM was integrated with a softmax attention layer and CNN in detecting the sarcasm in real-time [21]. The designed framework was quantified by extracting the real-time tweets on the trending political and entertainment posts on Twitter. The performance was analyzed for comparing and authenticating the designed framework. The results exhibited that the designed framework provided 92.71% accuracy and 89.05% F-measure which was found superior in comparison with traditional techniques. Pawar and Bhingarkar discussed that the sarcastic reorganization system was effective to enhance the process of analyzing the sentiment automatically from diverse social networks and microblogging sites [22]. The sarcasm was detected using a pattern-based method on the basis of Twitter data. Four sets of attributes, in which specific sarcasm was comprised, were adopted, and the classification of tweets was done as sarcasm and nonsarcasm. The suggested feature sets were analyzed and its additional cost classifications were computed. A LSTM-RNN model and word embeddings were established by Salim et al. in order to detect the sarcasm efficiently and classify the statements taken from Twitter in an easy manner [23]. The pretrained embedding was completed, and the next work in sequence was predicted by training the established model. The data of tweets was streamed. The established model classified the tweet as sarcastic or normal. The established model was quantified on test dataset containing 1500 tweets. A new self-deprecating sarcasm detection model was formulated by Abulaish and Kamal in which the rule-based methods were integrated with ML (machine learning) methods [24]. The initial methods focused on recognizing the candidate self-around tweets, and the latter methods assisted in extracting the attributes and classifying the tweets. Three algorithms such as DT (decision tree), NB (Naïve Bayes), and bagging were trained by recognizing 11 attributes. A Twitter dataset consisting of 107536 tweets was employed to compute and compare the formulated model against the existing technique for detecting the sarcasm. A new MAQ (multidimension question answering) network was recommended by Diao et al.

for detecting the sarcasm [25]. This technique was efficient to provide the plentiful semantic information for analyzing the ambiguity of sarcasm with the help of multidimension representations. The deep memory QA network was deployed to construct the conversation context information depending upon the BiLSTM for detecting the sarcasm. The experimental outcomes indicated that the recommended approach performed more effectively against traditional schemes. The recommended approach was proved efficient to detect the sarcasm. A Weka classification approach was suggested by Al-Ghadhban et al. with the objective of detecting Arabic sarcasm in Twitter. This approach was generated when the NB (Naïve Bayes) multinomial text algorithm was trained [26]. Various Saudi trending hashtags were utilized to gather the tweets in a manual way. Thereafter, some attributes were set for presenting the sarcastic tweets. The suggested approach yielded the precision of0.659, recall of 0.710, and f-score of 0.676 in comparison with other methods. An MHA-BiLSTM model was constructed by Kumar et al. in order to detect the sarcasm [27]. Two major layers were contained in this model. The initial layer summarized the contextual information taken from diverse directions in a comment to offer a novel representation for each word. The constructed model was capable of making the BiLSTM model more effective. The experimental results revealed that the constructed model was more applicable in contrast to others. An IWAN (incongruity-aware attention network) model was devised by Wu et al. for detecting the sarcasm in which word-level incongruity was considered among modalities through a scoring approach [28]. This approach was capable of assigning the larger weights to words with incongruent modalities. The outcomes of experiments confirmed that the devised model was more adaptable as compared to existing models on the MUStARD dataset and provided interpretability. A CFN (complex-valued fuzzy network) was introduced by Zhang et al. that employed the mathematical formalisms of QT and FL for detecting the sarcasm [29]. Generally, the identified target utterance was taken in account as a quantum superposition of a set of separate words. The probabilistic results of detecting the sarcasm were obtained by conducting a QF measurement on the density matrix of each utterance. MUStARD and Reddit track datasets were utilized for performing experiments. The results depicted the superiority of the introduced approach over others. The CANs (Coupled-Attention Networks) were projected by Zhao et al. for integrating the information related to the text and image into a unified model so that the sarcasm was detected [30]. Hence, the fusion of dissimilar forms of resources was realized. A real-world dataset was applied in the experimentation. The experimental results revealed that the projected approach had generated promising results.

3. Proposed Methodology

This research work designed a hybrid classifier in the sarcasm detection. The sarcasm detection has various phases which include preprocessing, feature reduction, clustering, and classification. The features are reduced using the PCA algorithm. The K-means clustering is deployed for clustering similar and different kinds of information. To classify the data, various voting classifier models are designed. The four voting classification models (SKD, SLD, MLD, and SLM) are designed in the first model; SVM, KNN, and decision tree classifiers are combined through a voting process. The second model integrates SVM, LR, and DT. The third model is an ensemble of MLP, LR, and DT. The last model is a hybrid of MLP, LR, and SVM. The phase of the proposed is explained below:

(1) Dataset collection and preprocessing: the database is collected through the twippy API. The dataset contains date of the tweet and tweet. The dataset is preprocessed in which single words, link, and other not required information is removed which leads to clean dataset. The dataset is further processed in which strings are converted to tokens for the classification

(2) Feature extraction and reduction: the random forest model is applied which can extract useful features from the dataset. The PCA algorithm is applied on the extracted features for the feature reduction. The PCA algorithm is utilized to build a low-dimensional representation of the data which defines the efficient amount of variance in the data. Mathematically, this algorithm focuses on investigating a linear mapping M to increase $M^T \operatorname{cov}(X)M$ in which $\operatorname{cov}(X)$ denotes the covariance matrix of the data X as shown in Equation (1). It is demonstrated that the d principal eigenvectors of the covariance matrix of the zero-mean data generate this linear mapping. Thus, the issue of Eigen is resolved using principal component analysis as

$$\operatorname{cov}(X)M = \lambda \searrow M \tag{1}$$

The Eigen problem is tackled for the d principal eigenvalues $\searrow$.The low-dimensional data representations y_i of the data points x_i are calculated for which these values are mapped onto the linear basis M, i.e., $Y = (X - \bar{X})M$. Principal component analysis (PCA) is implemented in several domains to recognize the face, classify the coin, and analyze the seismic series. The major limitation of this algorithm is the proportionality of the size of the covariance matrix to the dimensionality of the data points.

(3) Clustering of similar information: the phase of clustering deploys KMC for the same kind of information clustering. The K-means algorithm first chooses K points from the data patterns as the initial clustering center. Second, it computes the distance from each sample to the cluster's center. The classification of sample is performed into the class nearest to the cluster's center. Third, the new clustering center is obtained by computing the average value of every recently created clustering data object. Eventually,

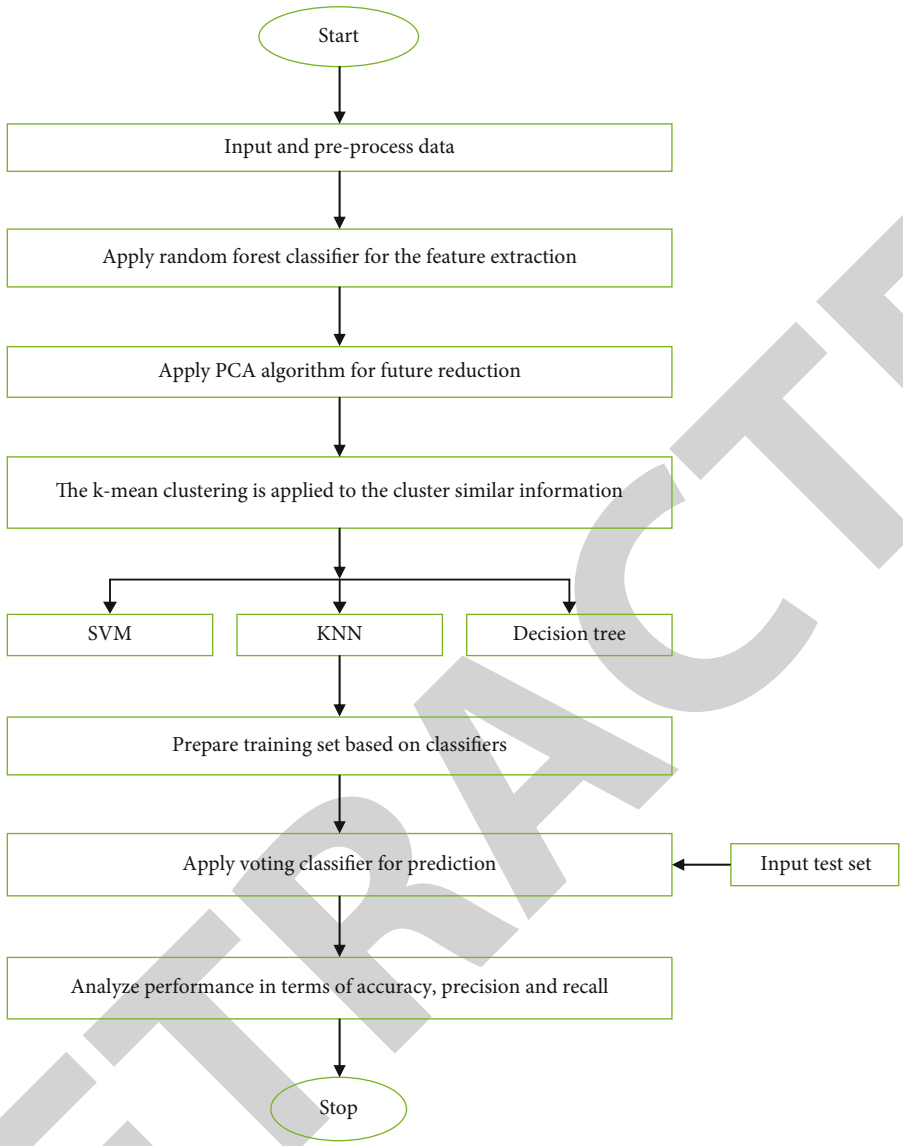

Figure 2: Ensemble classifier 1 (SKD).

all these steps are iterated until there is no change in the clustering center of two adjacent times, which depicts that the change in sampling is complete and the clustering principal function has reached the highest value. To execute the algorithm, the distance among data samples is computed using Euclidean distance, and the clustering performance is estimated using the error square sum criterion function. In a sample set $D = \{x_1, x_2, \cdots .x_m\}$, K-means algorithm splits the clusters into $C = \{C_1, C_2, \cdots .C_k\}$ to make the squared error minimum, just like the equation shown in the following:

$$E = \sum_{i=1}^{k} \sum_{x \in c_i} \|x - \mu_i\|_2^2, \tag{2}$$

where $\mu_i = (1/|c_i|)\sum_{x \in C_i} x$ as per Equation (2) denotes the mean vector of the C_i cluster

(4) Classification: the four classification models are designed for the classification. The first models are based on the various machine learning algorithms which are SVM, KNN, MLP, logistic regression, and decision tree. The SVM algorithm is emphasized on generating a hyperplane for expanding the margin, the distance from the hyperplane to the nearest data from a class. When the margin is large and the error is least, this is known as generalization. The initial optimization issue is expressed as

$$\begin{aligned} &\min \frac{1}{2}\|w\|^2 + C\sum_{i=1}^{N} \xi_i \\ &\text{s.t.} \quad y_i(w \bullet x_i + b) \geq 1 - \xi_i, \quad i = 1, 2, \cdots N, \\ &\xi_i \geq 0, \quad \mathrm{i} = 1, 2, \cdots N, \end{aligned} \tag{3}$$

in which $w \bullet x_i + b$ denotes a hyperplane with weight

parameter w and bias parameter b, $C > 0$ denotes a regulation metric that assists in controlling the balance amid the least misclassification and highest hyperplane margin, and the slack variable is represented with ξ_i. The slack variable is utilized to perform misclassification at some distances. In this case, $\xi_i = 0$, this illustrates that the ith data is located right at the margin or on the right side of the margin. In this case, $0 < \xi_i \leq 1$, this represents that the ith data is present in the margin at the right side. When $\xi_i > 1$, this implies that the ith data is available at the wrong side and misclassified. This issue can be expressed as a dual problem (Equation (4)) as

$$\min \frac{1}{2}\sum_{i=1}^{N}\sum_{j=1}^{N}\alpha_i\alpha_j y_i y_j \left(x_i \bullet x_j\right) - \sum_{i=1}^{N}\alpha_i \tag{4}$$

$$\text{s.t.} \sum_{i=1}^{N} y_i\alpha_i = 0, \quad 0 \leq \alpha_i \leq C, i = 1, 2, \cdots, N, \tag{5}$$

in which the Lagrange multiplier is defined with α_i. The weight vector is represented as $w = \sum_{i=0}^{N}\alpha_i y_i x_i$.

KNN is a simple and principal classification algorithm which assists in recording all the categories in correspondence with the training data. In case of matching of features of the test object exactly with the features consisted in a training object, the classification is performed. The KNN algorithm is generated on the basis of defined situations. This algorithm emphasizes on computing the distance among the nodes as a nonsimilarity index among nodes for avoiding the matching problem among nodes in which Euclidean distance or Manhattan distance is executed as

$$\begin{aligned} d_{ij} &= \sqrt{\sum_{k=1}^{d}\left(x_{ik} - x_{jk}\right)^2}, \\ d_{ij} &= \sum_{k=1}^{d}\left|x_{ik} - x_{jk}\right|. \end{aligned} \tag{6}$$

Simultaneously, K-nearest neighbor is aimed at making the decisions on the basis of dominant categories of k objects instead of on a single object category.

Logistic regression has y as a dependent variable which takes only two values 0 and 1. The hypothesis is that the probability$p$for$y = 1$which is defined in the presence of independent variable$x$is

$$p = P(y = 1 \mid x). \tag{7}$$

Afterward, odds ratio of the event can be expressed as

$$\text{Odds} = \frac{p}{1 - p}. \tag{8}$$

The LR model is a linear regression model amid the logarithm in odds and independent variable which generates the odds ratio, such as

$$\text{In odds} = \beta_0 + \beta_1 x, \tag{9}$$

in which β_0 and β_1 denote the regression coefficients. At the moment, the association of probability p with the independent variable is defined as

$$p = \frac{1}{1 + e^{-(\beta_0 + \beta_1 x)}}. \tag{10}$$

This is recognized as the logistic function.

Decision tree common classification algorithm is adopted in various applications in real world. This symbolic learning method focuses on correlating the information taken from a training dataset in a stratified structure obtained. The nodes and ramifications are comprised in this dataset. Decision tree concentrates on alleviating the least squares error for the next split of a node in the tree so that the average of the dependent variable comprised in all training instances covered for unseen instances in a leaf can be predicted. A DT model $T(x; \{R_j\}_{j=1}^{J})$ is capable of partitioning the x-space into J disjoint regions $\{R_j\}$ and predicting a separate constant value in each one as

$$x \in R_j \Rightarrow T\left(x; \{R_j\}_{j=1}^{J}\right) = \hat{y}_j, \tag{11}$$

or equivalently

$$T\left(x; \{R_j\}_{j=1}^{N}\right) = \sum_{j=1}^{J}\hat{y}_j I\left(x \in R_j\right), \tag{12}$$

in which $\hat{y}_j = (1/a_j)\sum_{i=1}^{a_j} y_i$ denotes the mean of the response y in each region R_j, $y_i \in R_j$, and a_j represents the size of region R_j. Hence, a tree assists in predicting a constant value y_j in each region R_j. The top-down iterative splitting is implemented on the basis of a least squares fitting criterion to construct the trees. In this algorithm, the identities of the predictor variables that are useful to perform splitting and their corresponding split points are utilized to resolve the regions $\{R_j\}_{j=1}^{J}$of the partition.

MLP is an effective FFNN (feed-forward neural network) in which common and popular classes of NNs are comprised to process an image and recognize the pattern. A number of subsequent layers having perceptron type are included in this algorithm such as an input layer which assists in acquiring the external inputs, a set of hidden layers, and one output layer.

Assuming x_l as the input signals to multilayer perceptron, the output value obtained from the jth hidden neuron

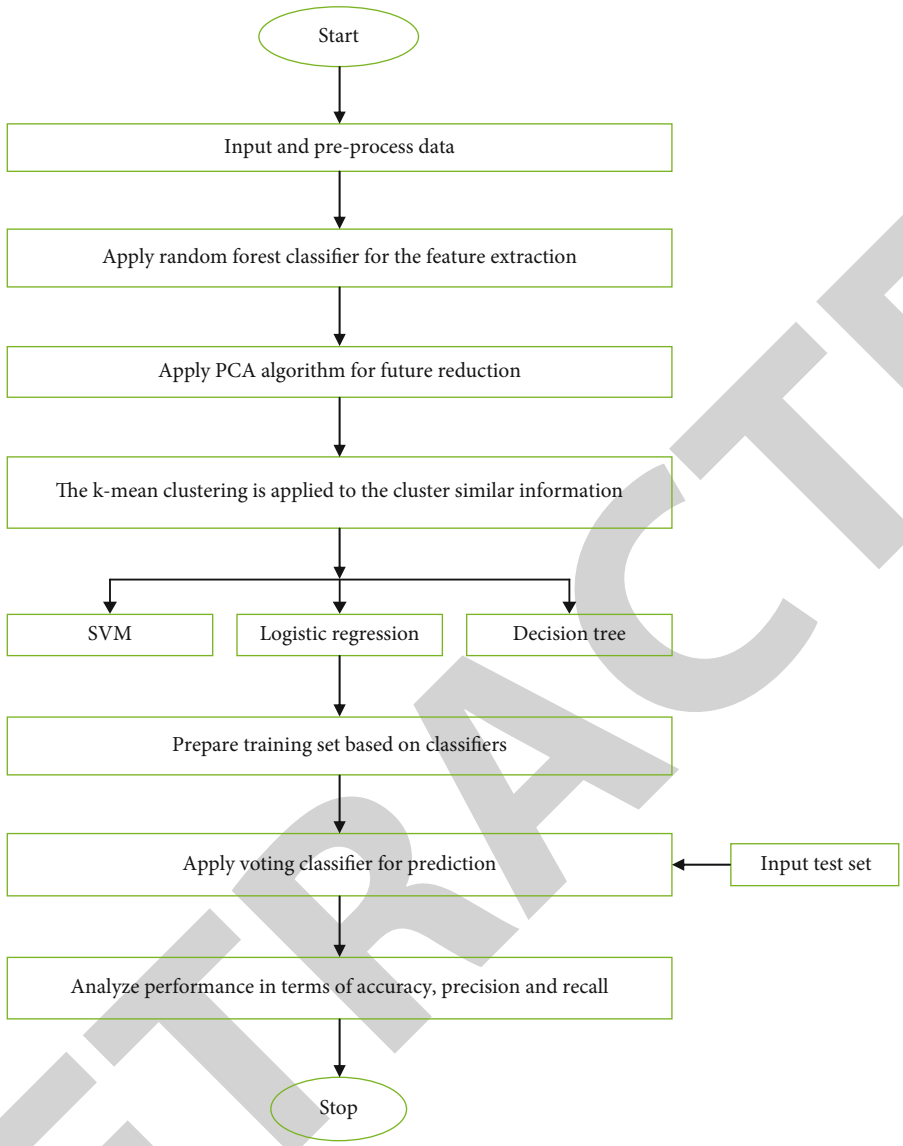

Figure 3: Ensemble 2 classifier (SLD).

is defined as

$$y_{lj=}f\left(\sum_{i=1}^{n} x_{li}w_{ij}\right), \tag{13}$$

in which f is the activation function and considered as the connection weight from the ith input neuron to the jth hidden neuron. Afterward, the evaluation of final output value from the output neuron is done as

$$y^{\text{out}} = f\left(\sum_{j=1}^{k} y_{lj}w_j\right), \tag{14}$$

in which k is utilized to denote the number of hidden neurons and w_j defines the connection weight from the jth hidden neuron to the output neuron.

The first ensemble classification model is the combination of SVM, KNN, and decision tree. The detailed model is explained in Figure 2.

The second ensemble classification model integrates SVM, LR, and DT. The detailed model is explained in Figure 3.

The third ensemble classification model integrates MLP, LR, and DT. The detailed model is explained in Figure 4.

The fourth ensemble classification model is the combination of MLP, logistic regression, and SVM. The detailed model is explained in Figure 5.

4. Result and Discussion

This research is based on the sarcasm detection based on the machine learning algorithms. The four ensemble classifiers are designed for the sarcasm detection. The ensemble classifiers are a combination of multiple classifiers. The first ensemble classifier (SKD) is the combination of SVM,

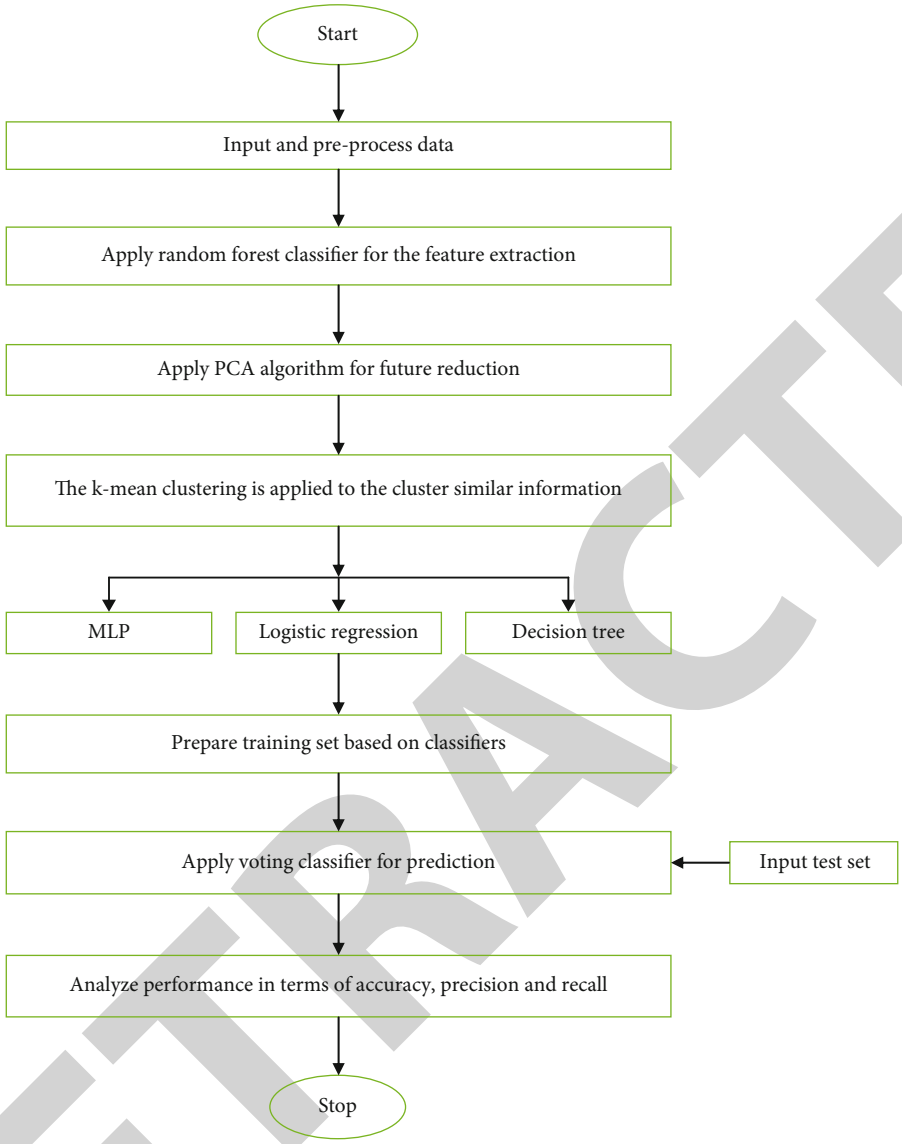

Figure 4: Ensemble 3 classifier (MLD).

KNN, and decision tree. In the second ensemble classifier (SLD), SVM, logistic regression, and decision tree classifiers are combined for the sarcasm detection. The third ensemble model (MLD), MLP, logistic regression, and decision tree are combined and the last one (SLM) is the combination of MLP, logistic regression, and SVM. All the four ensemble models are tested on five datasets. Each dataset number of instances gets varied for the sarcasm detection. In dataset 1, the number of instances is 1964; in second dataset, the number of instances is 6439; in the third dataset, the number of instances is 1960; in the fourth dataset, the number of instances is 2976; and in the fifth dataset, the number of instances is 4621. The performance of each ensemble classifier is measured in terms of accuracy, precision, and recall. Table 1 denotes the efficacy of four ensemble classification models on dataset 1 which contains 1964 numbers of instances. Table 2 represents the efficacy of all ensemble classification algorithms on dataset 2 which contains 6439 instances. Table 3 exhibits the performance of all classification models on dataset 3 which contains 1960 instances. Table 4 displays the efficiency of all ensemble classification algorithms on dataset 4 which contains 2976 instances. Table 5 indicates the efficiency of all ensemble classification algorithms on dataset 5 which contains 4621 instances.

As shown in Figure 6, all four ensemble classification models are tested on dataset 1. Dataset 1 contains 1964 numbers of instances. The performance is tested with regard to accuracy, precision, recall, and F1 score. The ensemble classification model 2 gives a maximum accuracy of 90.43 percent on dataset 1 for the sarcasm detection.

As shown in Figure 7, all four classification models are tested on dataset 2. Dataset 2 contains 6439 numbers of instances. The performance is tested concerning accuracy, precision, recall, and F1 score. The ensemble classification algorithm gives a maximum accuracy of 99.17 percent on dataset 2 for the sarcasm detection.

As shown in Figure 8, all four ensemble classification algorithms are tested on dataset 3. Dataset 3 contains 1960

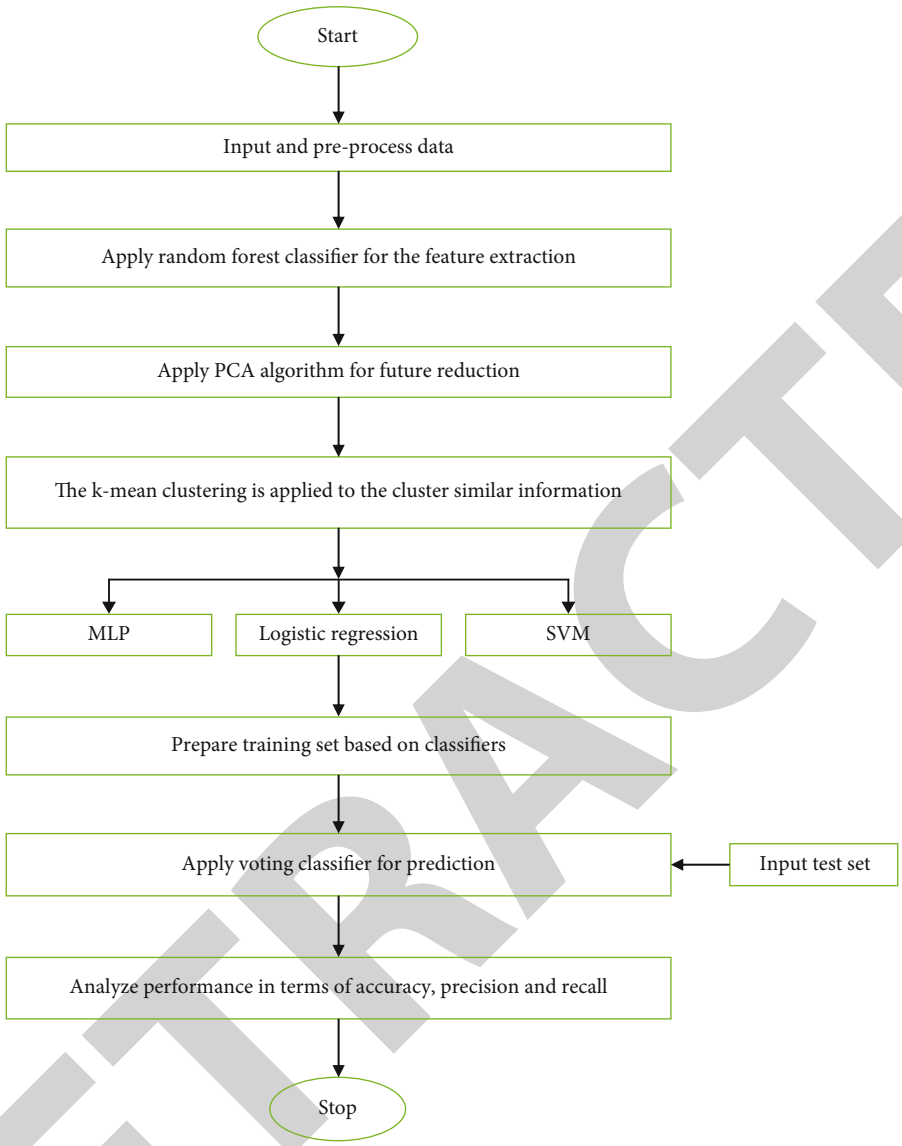

Figure 5: Ensemble 4 classifier (SLM).

Table 1: Performance of ensemble classifiers on dataset 1.

Performance parameters	Ensemble 1 (SKD)	Ensemble 2 (SLD)	Ensemble 3 (MLD)	Ensemble 4 (SLM)
Accuracy	87.71%	90.43%	88.71%	88.00%
Precision	78%	80%	79%	78%
Recall	78%	81%	79%	79%
F1-score	78%	80%	79%	78%

Table 2: Performance of ensemble classifiers on dataset 2.

Performance parameters	Ensemble 1 (SKD)	Ensemble 2 (SLD)	Ensemble 3 (MLD)	Ensemble 4 (SLM)
Accuracy	99.17%	98.09%	98.87%	98.78%
Precision	90%	88%	88%	88%
Recall	89%	88%	88%	88%
F1-score	89%	87%	88%	88%

Table 3: Performance of ensemble classifiers on dataset 3.

Performance parameters	Ensemble 1 (SKD)	Ensemble 2 (SLD)	Ensemble 3 (MLD)	Ensemble 4 (SLM)
Accuracy	88.43%	91.57%	91.00%	90.71%
Precision	79%	82%	81%	81%
Recall	79%	82%	81%	81%
F1-score	79%	82%	81%	81%

Table 4: Performance of ensemble classifiers on dataset 4.

Performance parameters	Ensemble 1 (SKD)	Ensemble 2 (SLD)	Ensemble 3 (MLD)	Ensemble 4 (SLM)
Accuracy	97.53%	98.56%	94.64%	94.45%
Precision	86%	88%	86%	86%
Recall	87%	88%	84%	84%
F1-score	86%	86%	80%	79%

Table 5: Performance of ensemble classifiers on dataset 5.

Performance parameters	Ensemble 1 (SKD)	Ensemble 2 (SLD)	Ensemble 3 (MLD)	Ensemble 4 (SLM)
Accuracy	95.72%	95.48	69.74	69.74
Precision	86%	85%	39%	39%
Recall	85%	85%	62%	62%
F1-score	85%	85%	48%	48%

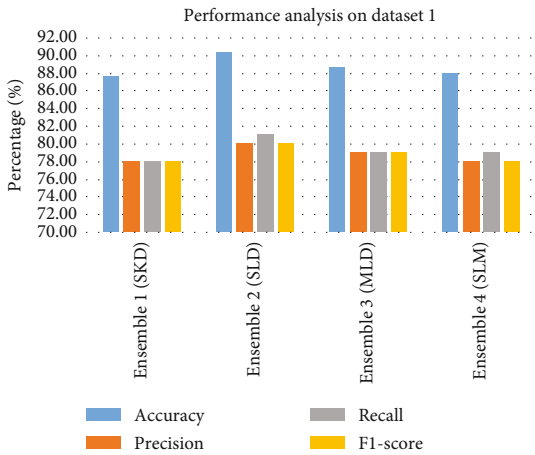

Figure 6: Performance analysis on dataset 1.

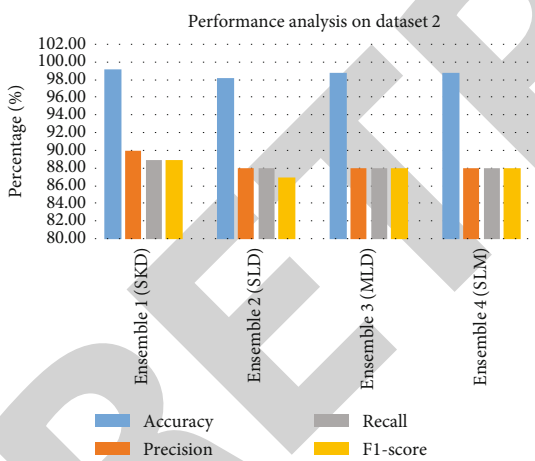

Figure 7: Performance analysis on dataset 2.

numbers of instances. The performance is tested with regard to accuracy, precision, recall, and F1 score. The ensemble classification algorithm gives a maximum accuracy of 91.57 percent on dataset 3 for the sarcasm detection.

As shown in Figure 9, all four ensemble classification algorithms are tested on dataset 4. Dataset 4 contains 2976 numbers of instances. The performance is tested concerning accuracy, precision, recall, and F1 score. The ensemble classification algorithm gives a maximum accuracy of 98.56 percent on dataset 4 for the sarcasm detection.

As shown in Figure 10, four ensemble classification models are tested on dataset 5. Dataset 5 contains 4621

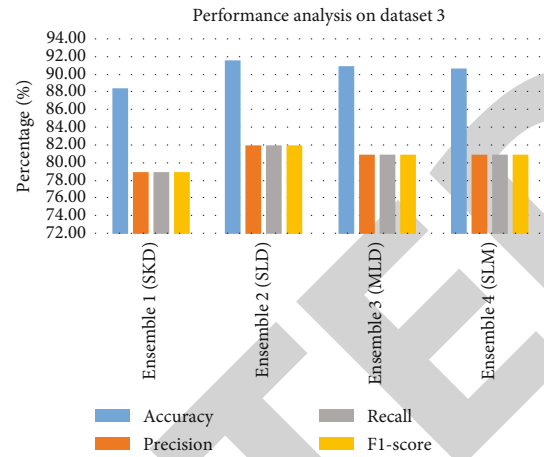

Figure 8: Performance analysis on dataset 3.

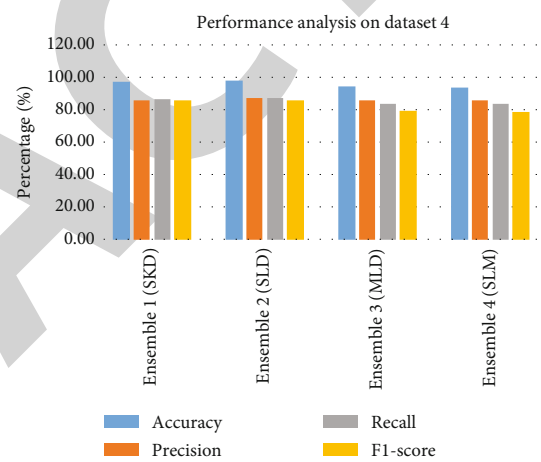

Figure 9: Performance analysis on dataset 4.

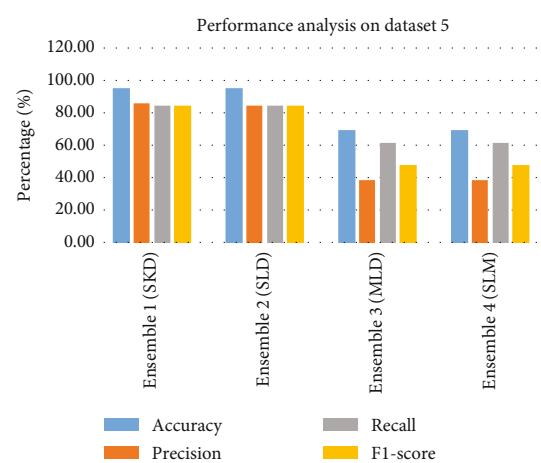

Figure 10: Performance analysis on dataset 5.

numbers of instances. The performance is tested with regard to accuracy, precision, recall, and F1 score. The ensemble classification algorithm gives a maximum accuracy of 95.72 percent on dataset 5 for the sarcasm detection.

5. Conclusion

In this paper, it is concluded that sarcasm is a kind of verbal irony which emphasizes on expressing ridicule. Sarcasm has a negative implied sentiment. However, it is free of negative surface sentiment. A sarcastic sentence may carry positive, negative, or no surface sentiment. There are 4 kinds of techniques to detect the sarcasm. The sarcasm detection techniques have various phases in which data is preprocessed; attributes are extracted and reduced, clustered, and classified. The data is preprocessed using approach of tokenization; the features are extracted using random forest algorithm; PCA algorithm is applied for the feature reduction; K-means is used for the data clustering; and in the phase of classification, four different ensemble classifiers are designed which are a combination of multiple classifiers. The first ensemble classifier is the combination of SVM, KNN, and decision tree. In the second ensemble classifier, SVM, logistic regression, and decision tree classifiers are combined for the sarcasm detection. In the third ensemble model, MLP, logistic regression, and decision tree are combined and the last one is the combination of MLP, logistic regression, and SVM. The performance of each ensemble models is tested on five different types of datasets, and each dataset has different sizes. The performance of the ensemble models is tested with regard to accuracy, precision, recall, and F1 score. It is analyzed that ensemble 2 classifier (SLD), in which SVM, LR, and DT algorithms were comprised, had performed well in comparison with other ensemble algorithms concerning various metrics for sarcasm detection.

Data Availability

The data shall be made available on request.

Conflicts of Interest

The authors declare that they have no conflicts of interest.

References

[1] A. Srivastava, V. Singh, and G. Singh, "Sentiment analysis of Twitter data: sarcasm detection survey," in *4th International Conference on "Computing for Sustainable Global Development*, New Delhi, India, 2017.

[2] B. D. Dharmavarapu and J. Bayana, "Sarcasm detection in Twitter using sentiment analysis," *International Journal of Recent Technology and Engineering (IJRTE)*, vol. 8, no. 1, 2018.

[3] M. Athira, C. Chithra, G. Anil, and E. S. Smitha, "Sentiment analysis-sarcasm detection in Twitter," *IOSR Journal of Computer Engineering*, vol. 22, 2020.

[4] K. H. Wandra and M. Baro, "Sarcasm detection in sentiment analysis," *International Journalof Current Engineering and Scientific Research*, vol. 4, 2017.

[5] A. Dwi, "P. Rahayu, Soveatin Kuntur, Nur HayatinSarcasm detection on Indonesian Twitter feeds," in *2018 5th International Conference on Electrical Engineering, Computer Science and Informatics (EECSI)*, Malang, Indonesia, 2018.

[6] K. Sundararajan, J. V. Saravana, and A. Palanisamy, "Textual feature ensemble-based sarcasm detection in Twitter data," in *Intelligence in Big Data Technologies—Beyond the Hype*, J. Peter, S. Fernandes, and A. Alavi, Eds., vol. 1167 of Advances in Intelligent Systems and Computing, Springer, Singapore, 2021.

[7] E. Lunando and A. Purwarianti, "Indonesian social media sentiment analysis with sarcasm detection," in *2013 International Conference on Advanced Computer Science and Information Systems (ICACSIS)*, pp. 195–198, Sanur Bali, Indonesia, 2013.

[8] M. Bouazizi and T. Otsuki Ohtsuki, "A pattern-based approach for sarcasm detection on Twitter," *IEEE Access*, vol. 4, pp. 5477–5488, 2016.

[9] S. Hiai and K. Shimada, "A sarcasm extraction method based on patterns of evaluation expressions," in *2016 5th IIAI International Congress on Advanced Applied Informatics (IIAI-AAI)*, pp. 31–36, Kumamoto, Japan, 2016.

[10] A. D. Dave and N. P. Desai, "A comprehensive study of classification techniques for sarcasm detection on textual data," in *2016 International Conference on Electrical, Electronics, and Optimization Techniques (ICEEOT)*, pp. 1985–1991, Chennai, India, 2016.

[11] S. K. Bharti, K. S. Babu, and S. K. Jena, "Parsing-based sarcasm sentiment recognition in Twitter data," in *2015 IEEE/ACM International Conference on Advances in Social Networks Analysis and Mining (ASONAM)*, pp. 1373–1380, Paris, France, 2015.

[12] E. Fersini, F. A. Pozzi, and E. Messina, "Detecting irony and sarcasm in microblogs: the role of expressive signals and ensemble classifiers," in *2015 IEEE International Conference on Data Science and Advanced Analytics (DSAA)*, pp. 1–8, Paris, France, 2015.

[13] T. Ahmad, H. Akhtar, A. Chopra, and M. W. Akhtar, "Satire detection from web documents using machine learning methods," in *2014 International Conference on Soft Computing and Machine Intelligence*, pp. 102–105, New Delhi, India, 2014.

[14] M. Khokhlova, V. Patti, and P. Rosso, "Distinguishing between irony and sarcasm in social media texts: linguistic observations," in *2016 International FRUCT Conference on Intelligence, Social Media and Web (ISMW FRUCT)*, pp. 1–6, St. Petersburg, Russia, 2016.

[15] D. K. Tayal, S. Yadav, K. Gupta, B. Rajput, and K. Kumari, "Polarity detection of sarcastic political tweets," in *2014 International Conference on Computing for Sustainable Global Development (INDIACom)*, pp. 625–628, New Delhi, India, 2014.

[16] S. Porwal, G. Ostwal, A. Phadtare, M. Pandey, and M. V. Marathe, "Sarcasm detection using recurrent neural network," in *2018 Second International Conference on Intelligent Computing and Control Systems (ICICCS)*, Madurai, India, 2018.

[17] R. Gupta, J. Kumar, and H. Agrawal, "A statistical approach for sarcasm detection using Twitter data," in *2020 4th International Conference on Intelligent Computing and Control Systems (ICICCS)*, Madurai, India, 2020.

[18] N. A. Arifuddin and I. S. A. Indrabayu, "Comparison of feature extraction for sarcasm on Twitter in Bahasa," in *2019 Fourth International Conference on Informatics and Computing (ICIC)*, Semarang, Indonesia, 2019.

[19] S. K. Bharti, R. Naidu, and K. S. Babu, "Hyperbolic feature-based sarcasm detection in tweets: a machine learning

Hindawi
Behavioural Neurology
Volume 2023, Article ID 9879352, 1 page
https://doi.org/10.1155/2023/9879352

Retraction

Retracted: Transcranial Electrical Motor Evoked Potential in Predicting Positive Functional Outcome of Patients after Decompressive Spine Surgery: Review on Challenges and Recommendations towards Objective Interpretation

Behavioural Neurology

Received 19 December 2023; Accepted 19 December 2023; Published 20 December 2023

This article has been retracted by Hindawi following an investigation undertaken by the publisher [1]. This investigation has uncovered evidence of one or more of the following indicators of systematic manipulation of the publication process:

(1) Discrepancies in scope

(2) Discrepancies in the description of the research reported

(3) Discrepancies between the availability of data and the research described

(4) Inappropriate citations

(5) Incoherent, meaningless and/or irrelevant content included in the article

(6) Manipulated or compromised peer review

The presence of these indicators undermines our confidence in the integrity of the article's content and we cannot, therefore, vouch for its reliability. Please note that this notice is intended solely to alert readers that the content of this article is unreliable. We have not investigated whether authors were aware of or involved in the systematic manipulation of the publication process.

In addition, our investigation has also shown that one or more of the following human-subject reporting requirements has not been met in this article: ethical approval by an Institutional Review Board (IRB) committee or equivalent, patient/participant consent to participate, and/or agreement to publish patient/participant details (where relevant).

Wiley and Hindawi regrets that the usual quality checks did not identify these issues before publication and have since put additional measures in place to safeguard research integrity.

We wish to credit our own Research Integrity and Research Publishing teams and anonymous and named external researchers and research integrity experts for contributing to this investigation.

The corresponding author, as the representative of all authors, has been given the opportunity to register their agreement or disagreement to this retraction. We have kept a record of any response received.

References

[1] M. R. Jamaludin, K. W. Lai, J. H. Chuah et al., "Transcranial Electrical Motor Evoked Potential in Predicting Positive Functional Outcome of Patients after Decompressive Spine Surgery: Review on Challenges and Recommendations towards Objective Interpretation," *Behavioural Neurology*, vol. 2021, Article ID 2684855, 16 pages, 2021.

Hindawi
Behavioural Neurology
Volume 2021, Article ID 2684855, 16 pages
https://doi.org/10.1155/2021/2684855

Review Article

Transcranial Electrical Motor Evoked Potential in Predicting Positive Functional Outcome of Patients after Decompressive Spine Surgery: Review on Challenges and Recommendations towards Objective Interpretation

Mohd Redzuan Jamaludin,[1] **Khin Wee Lai**,[1] **Joon Huang Chuah**,[2] **Muhammad Afiq Zaki**,[3] **Yan Chai Hum**,[4] **Yee Kai Tee**,[4] **Maheza Irna Mohd Salim**,[5] **and Lim Beng Saw**[6]

[1]*Department of Biomedical Engineering, Faculty of Engineering, Universiti Malaya, 50603 Kuala Lumpur, Malaysia*
[2]*Department of Electrical Engineering, Faculty of Engineering, Universiti Malaya, 50603 Kuala Lumpur, Malaysia*
[3]*Center of Environmental Health and Safety, Faculty of Health Sciences, Universiti Teknologi Mara Selangor, Puncak Alam Campus, 42300 Bandar Puncak Alam, Selangor Darul Ehsan, Malaysia*
[4]*Centre for Healthcare Science & Technology, Department of Mechatronics and Biomedical Engineering, Lee Kong Chian Faculty of Engineering and Science, Universiti Tunku Abdul Rahman, Malaysia*
[5]*Bioinspired Device and Tissue Engineering Research Group, School of Biomedical Engineering and Health Sciences, Faculty of Engineering, Universiti Teknologi Malaysia, 81300 Skudai, Johor, Malaysia*
[6]*Department of Orthopaedic Surgery, Sunway Medical Centre, Malaysia*

Correspondence should be addressed to Khin Wee Lai; lai.khinwee@um.edu.my and Yan Chai Hum; humyc@utar.edu.my

Received 4 August 2021; Accepted 18 October 2021; Published 3 November 2021

Academic Editor: Hong Lin

Spine surgeries impose risk to the spine's surrounding anatomical and physiological structures especially the spinal cord and the nerve roots. Intraoperative neuromonitoring (IONM) is a technology developed to monitor the integrity of the spinal cord and the nerve roots via the surgery. Transcranial motor evoked potential (TcMEP) (one of the IONM modalities) is adopted to monitor the integrity of the motor pathway of the spinal cord and the motor nerve roots. Recent research suggested that the IONM is conducive as a prognostic tool towards the patient's functional outcome. This paper summarizes the researches of IONM being adopted as a prognostic tool. In addition, this paper highlights the problems associated with the signal parameters as the improvement criteria in the previous researches. Lastly, we review the challenges of TcMEP to achieve a prognostic tool focusing on the factors that could interfere with the generation of a stable TcMEP response. The final section will discuss recommendations for IONM technology to achieve an objective prognostic tool.

1. Introduction

Spine surgeries (such as posterior spinal instrumentation and fusion, discectomy, and laminectomy) are usually conducted along the spine vertebra that is surrounded by the spinal cord, the nerve roots, and other relevant vascular supply to these elements; thus, spine surgeries pose high risk to the patient concerning the motor and sensory functions [1, 2]. Intraoperative neuromonitoring (IONM) refers to a technology to provide information on the dorsal column somatosensory and corticospinal motor pathway integrity during the surgery [1, 3]. IONM consists of several tests (such

as motor evoked potential (MEP), somatosensory evoked potential (SSEP), and other descending neurogenic evoked potentials) which can be utilized to monitor neurologic activities. Benefited from these modalities, surgeons can be notified in a timely manner allowing the possibility or reversing neurologic deficits before these deficits further deteriorate [2–5].

Ideally, IONM is applied on a patient that has no neurologic impairment to acquire a meaningful baseline so that any signal deterioration induced by surgical intervention during the surgery could be detected and reversed [6]. IONM is possible to be applied on patients who have neurological deficit preoperatively (due to structural compression to the spinal cord or nerve roots) despite reduced or no response to the IONM. However, when a decompression is performed, the conductivity of the neural structure can be indicated by an improved IONM response; this response holds potential to be valuable information for the surgeon [6]. This paper focuses on reviewing the findings that indicate the prognostic value of improved MEP signals after surgical interventions were conducted.

1.1. Brief Introduction to Motor Evoked Potential (MEP). Motor evoked potential (MEP) functions to monitor the motor function of a patient [7]. Spinal and brainstem motor neurons together with the corresponding peripheral axons constitute a system known as Lower Motor Neurons (LMNs) [8]. The MEP, generated by the firing of LMNs, excites muscle response. To produce the firing of LMNs through external stimulation, pulse train stimulation is utilized to evoke a series of *D*-waves and *I*-waves; a sequential excitatory postsynaptic potential (EPSP) is thus produced. The accumulation of EPSPs, if the firing threshold is achieved, induces the firing of LMNs which in turn results in muscle contraction permitting the acquisition of muscle's MEP. In summary, electrical stimulation from the motor cortex of the brain and muscles will respond to the stimulation by contraction thus producing recordable MEP signals [7, 9, 10].

2. The Significance of MEP Improvement

The main purpose of intraoperative monitoring is to prevent nonreversible damage to the neural structure of a patient during surgery. Usually, the most ideal situation to apply IONM is to apply it on patients without neurologic impairment in order to acquire ideal MEP's baseline; thus, any surgical intervention that induces signal deterioration during the surgery can be compared to this baseline and interpreted efficiently [6]. However, MEP can also be applied to patients with neurological deficit preoperatively due to structural compression to the spinal cord or nerve roots, but these could lead to reduced or no response at all to the MEP. Thus, when a decompression is performed, the conductivity of the neural structure could be indicated by an improved MEP response and hence it is conducive to the surgeon [6].

The comparison between TcMEP outcomes and pain visual analogue scale (VAS) was shown by Voulgaris et al. [11] on 25 patients' data that have undergone lumbar spinal stenosis surgery for decompressive laminectomy. The patients were evaluated preoperatively with the VAS scale and again postoperatively at a third month and 12th month interval. The IONM modalities adopted were the TcMEP and EMG monitoring. The corkscrew electrodes for MEP were placed at C1–C2 with multipulse current stimulation ranging from 0 mA to 200 mA. Each of the stimulus duration was set from 0.2 ms to 0.5 ms. The muscles' electrodes for MEP and EMG were put according to the level of operations. The MEP improvement criteria were set to exceed 50% of amplitude increment. The Wilcoxon signed-rank test was used as the statistical analysis to compare the presurgery and postsurgery VAS score. Result shows that the mean VAS score demonstrated improvement at the third month follow-up and further improved at the 12th month follow-up as compared to the preoperative score. No patient experienced transient or permanent motor deficit after the surgeries. Among the 25 patients, 17 patients had more than 50% improvement to the MEP response postdecompression and 6 patients exhibited slightly increased response or no changed response, while the remaining 2 were not accommodated with IONM during their surgeries because of the application of an inhalational agent by the anaesthetists. The patients with more than 50% MEP response improvement showed a better VAS score at the 12th month follow-up as compared to the remaining patients.

Visser et al. [6] presented a study of 8 patients out of 74 patients with spinal canal stenosis ($n = 2$), extradural meningioma ($n = 3$), or a herniated nucleus polposus ($n = 2$) that showed significant improvement on MEP responses after decompression of the spinal cord or cauda equina. Out of the 74 patients, 44 patients experienced the onset of neurological symptoms for more than 6 months before the surgery date and 30 patients experienced neurological symptoms for less than 6 months before the surgery date. The stimulus parameter adopted were transcranial voltage stimulation using either Cz–Fz montage with a monophasic pulse train or C3–C4 montage with a biphasic pulse train. Muscle groups without responses remained under monitoring to detect improvement on MEP response after the surgical decompression. Three of the 4 lower limb muscles (quadriceps (L2–L4), tibialis anterior (L4–L5), hamstrings (L5–S1), and gastrocnemius (S1–S2)) were selected depending on the thoracolumbar surgical levels. As a control, the abductor digiti minimi or abductor pollicis brevis was selected. For cervical procedures, the trapezius (C2–C4), the biceps (C5–C6), the triceps (C7–C8), and the extensor of the forearm (C6–C7) or the abductor digiti minimi (C6–C8) were adopted for monitoring. The control for cervical procedures was selected from either the trapezius muscle or orbicularis oris muscle. There was no SSEP modality applied on all the patients. Anaesthetic-wise, a short-acting muscle relaxant was used during intubation together with propofol (4–8 $mg \cdot kg^{-1} \cdot h^{-1}$), ketamine (2.5 $\mu g \cdot kg^{-1} \cdot min^{-1}$), and remifentanil (0.05–0.5 $\mu g \cdot kg^{-1} \cdot min^{-1}$). MEP responses were recorded at the start and at the end of the procedures. If the baseline MEP amplitude exceeds 10 μV, the changes of MEP amplitude were computed in percentage. If the baseline MEP amplitude is less than 10 μV or no response at all, the increment of the MEP amplitude (if any) was stated as "response appearance after absence." A

significant improvement to the MEP signal was defined as exceeding 200% increment of amplitude to factor out other factors that affected the MEP amplitudes. Patients' age, gender, medical history, onset of neurologic symptoms, neurologic function before surgery, neurologic function 3 months after surgery, pathology, type of surgery, anaesthetic details during the surgeries, and postoperative blood loss were recorded and analyzed. The muscle motor function (muscle strength, sensory function, neurogenic pain, and walking distance) was analyzed based on the Medical Research Council with a scale from 0 to 5. Any sign of relief from the stated symptoms was defined as neurologic improvement. Out of the 44 patients with more than 6 months of neurologic symptoms, 24 of them showed no improvement of symptoms 3 months after the surgery despite having more than 100% of MEP amplitude increment. Meanwhile, 20 patients from the same group had improvement of symptoms 3 months after the surgery, but none of them had an increment of MEP amplitude for more than 100%. The other 30 patients had neurological symptoms for less than 6 months, and 13 of them had no improvements of symptoms 3 months after surgery and no improvement on MEP amplitude, while 17 of them had improvement of symptoms 3 months after surgery and 6 of them had more than 100% improvement on MEP amplitude. Even though the 8 patients had improvement of MEP amplitude postdecompression, 2 of them had no improvement to their neurological symptoms. A relation (by Visser et al. [6]) was found between the duration of the neurological deficit onset prior to the surgery date; these 2 patients had more than 6 months of neurological deficit as compared to the other 6 patients who had MEP improvement and symptom improvement with only less than 6 months of neurological deficit.

Another study by Raynor et al. [12] of 12375 spinal surgeries over 25 years presented the efficacy of multimodality IOM in relation to the outcome of the surgeries. Out of the 12375 patients, IOM signals were spotted to have changes whether the changes were improvements or degradations in 386 patients. The multimodality IOM included descending neurogenic evoked potentials (DNEP), transcranial electrical motor evoked potentials (TcMEP), spontaneous electromyography (EMG), triggered electromyography (TrigEMG), and dermatomal SSEP (dSSEP). The anaesthetic protocol was applied according to the conditions of surgeries, patients, and anaesthetic guidelines, although certain anaesthetic criteria were followed to ensure that the IOM could be performed effectively: halogenated agents were applied not more than 0.5 MAC, NO_2 usage should be applied less than 50% of the end tidal volume, and no muscle relaxant was used when TcMEP was utilized. The TcMEP used C3–C4 motor cortex scalp electrode montage. The TcMEP was mostly used on upper extremity surgeries and only some on lumbar cases requested by the surgeons. The result showed that of all the changes from the 386 patients with 406 IOM signals' significant events or true positive events, 360 patients' events indicated signal improvement after surgical interventions were conducted. One patient from the 360 improved IOM signals had permanent neurological deficit. The balance 46 events had no improvement to the IOM signals despite the fact that surgical interventions were applied, and out of these instances, 14 patients were confirmed with permanent neurological deficits. The comparison between one patient with the improved IOM signal but permanent neurological deficit and 14 patients that had no signal improvement with true permanent neurological deficit was still statistically significant. However, this study did not specify the improvement criteria and which modalities exactly were indicated to have IOM signal improvement by the authors.

Wang et al. [13] presented a finding from degenerative cervical compressive myelopathy (CCM) cases from 59 patients that went through laminoplasty or laminectomy procedures with reliable MEP baseline from December 2013 until April 2015. Patients with no reliable or no MEP readings at all were secluded from the study. The selected 59 patient's data were categorized into a group with more than 50% of MEP improvement, a group with less than 50% MEP improvement or considered not significant, and a group with MEP degradation. Patients were assessed preoperatively with the mJOA scale and postoperative evaluation of motor, sensory, and pain a week after and 6 months after surgery with the mJOA scale. Both MEP and SSEP modalities were used for monitoring. Information regarding the MEP settings adopted for monitoring, and the muscles used to monitor the MEP responses, was absent from the research. The MEP responses were recorded predecompression, postdecompression, and throughout the surgery. The anaesthesia protocol adopted was TIVA without muscle relaxant or inhalation agents with the use of propofol ($5–8\,mg{\cdot}kg^{-1}{\cdot}h^{-1}$), remifentanil ($0.05–2\,\mu g{\cdot}kg^{-1}\,min^{-1}$), and fentanyl ($5–6\,\mu g{\cdot}kg^{-1}$). One-way ANOVA using SPSS 19.0 (SPSS, Inc., Chicago, IL, USA) software was used for statistical comparison analysis with $p < 0.05$ as the statistical difference. The results showed that 21 patients had MEP improvement postdecompression with a mean MEP improvement rate at $140 \pm 76\%$, 32 patients had no significant MEP changes, and six patients had deteriorated MEP signals. The mJOA improvement rate was significantly better for patients that had MEP improvement compared to the group that had no significant changes to the MEP response ($59.5 \pm 4.2\%$ vs. $48.9 \pm 3.9\%$, $p < 0.05$) and the improved MEP group against the deteriorated MEP response group ($59.5 \pm 4.2\%$ vs. $40.6 \pm 7.4\%$, $p < 0.05$). The authors also highlighted that MEP amplitude was more effective compared to the MEP latency or SSEP modality in predicting the outcome of the surgery.

Another study was made by Wi et al. [14] on 29 improved IONM of spine cases compared to the baselines out of 317 cases with IONM of spine cases and their clinical significance. The surgeries' IONM data were chosen between January 2013 and May 2017. The modalities that were used as monitoring tools were MEP and SSEP. The spine cases of the 29 patients included cervical myelopathy (22 patients), neurofibroma C1 (1 patient), thoracic myelopathy (5 patients), and neurogenic tumour L5–S1 (1 patient). The MEP monitoring was performed bilaterally from the deltoid, triceps, and thenar muscles for the upper extremities, while for the lower extremities, the tibialis anterior and abductor

hallucis were used. Meanwhile, the SSEP was stimulated from the median nerve for upper limbs and posterior tibial nerves for the lower limbs. No specific MEP stimulation parameters were mentioned, and only the stimulation was given accordingly for each patient to obtain acceptable responses. The IONM events were recorded at the beginning of the surgeries as the baseline, before change, during change, after change, and throughout the main procedure. The anaesthesia protocol utilized the TIVA protocol with propofol (4.5 μg/mL) and/or remifentanil (1.7 ng/mL) with the usage of a short-acting muscle relaxant during intubation. Patients' data for analysis were selected preoperatively and 3 months postoperatively. The data included the measurement of Motor Index Scoring System (MISS), the Short-Form 36 Health Survey Questionnaire (SF-36), the Japanese Orthopaedic Association (JOA) Cervical Myelopathy Evaluation Questionnaire (JOACMEQ), and Neck Disability Index (NDI) for cervical myelopathy patients, the JOA for thoracic myelopathy patients, and the JOA Back Pain Evaluation Questionnaire and Oswestry Disability Index for lumbar disorder patients. The statistical analysis was performed by using IBM SPSS software version 23.0 (IBM Corp., Armonk, NY, USA) by comparing the preoperation and postoperation by using the Wilcoxon rank-sum test while the improvement rate of MISS and SF-36 was compared by using the Kruskal-Wallis test given the threshold for significance at $p < 0.05$. It was found that 29 patients exhibited improvement to the IONM signals from the recorded data. Two patients with early death (which was unrelated to the surgery) were excluded from the analysis. Ten patients had MEP-only improvement with 8 of them exceeding 100% increment in amplitude, one of them having a response appearance, and one of them having both 100% amplitude increment and response appearance. Twelve patients had SSEP-only improvement with 10 of them having an increase more than 100% increase in amplitude, one of them having more than 6% of decrement of latency, and one of them having both 100% of amplitude increment and 6% of latency decrement. Five patients had both MEP and SSEP improvement. It was found that the MISS improvement rate was significantly better in the group that had MEP improvement only compared to the other two groups while the SF-36 improvement rate was significantly better in the group that had SSEP improvement only compared to the other two groups. It was concluded by the authors that the improvement of IONM signals was conclusive to show that the decompression of the spinal cord is successful and can be valuable information to the surgeon. However, several limitations were mentioned; for example, the study did not compare the group which had no IONM improvement and the group with IONM improvement and the sample size was relatively small and included one lumbar case.

Barley et al. [15] reported a case of a 15-month-old boy with a tethered spinal cord extending through the entire cord and a worsening scoliosis. The patient had greater motor weakness on the left upper extremities than on the right upper extremities and weak lower extremities. The tethered cord release and spine correction procedures were performed with the assistance of NIOM. The baseline of TcMEP and SSEP of posterior tibial nerves and ulnar nerves was obtained. TcMEP was stimulated on C1 and C2, and monitoring was performed bilaterally on the quadriceps femoris, tibialis anterior, gastrocnemius, sphincter, abductor pollicis brevis (APB), and abductor hallucis. The stimulation for TcMEP was set from 145 mA to 187 mA for the left extremities and from 175 mA to 200 mA for the right extremities. The only TcMEP response obtained during baseline was on the right-side APB, and the SSEP showed no response during baseline acquisition. It was found that the TcMEP signal on the left APB appeared immediately with increased amplitude after the completion of the cord untethering. Furthermore, the right-side APB also had increment in amplitude, but no SSEP changes were obtained after the detethering procedure. Afterwards, the patient exhibited observable left upper extremity improvement notified by the family and the physicians which supported the outcome of the TcMEP response obtained after the cord detethering procedure.

The next study that researched on the usefulness of the MEP response as a prognostic tool for spine surgeries was conducted by Dhall et al. [16]. The 32 patients' data that were selected had decompression and instrumented stabilization surgeries. The IONM modalities that were used for the surgeries were EMG, TcMEP, and SSEP. The TcMEP stimulation parameters used were double train with a total of 9 pulses, 50 ms pulse width, 1.7 ms interstimulus, 13.1 ms ISI, and constant voltage with intensity that ranged from 100 V to 1000 V. The authors used anodal stimulation that stimulates C1 to acquire responses on the right side and C2 to obtain responses on the left side. For the anaesthetic protocol, the centre where the data were collected used propofol 120 mcg/kg/min, fentanyl 100 mcg/h, and 1.0% or 0.5 MAC sevoflurane with the aim of obtaining more than 85 mmHg of mean arterial pressure (MAP). The baselines were obtained before the patients were positioned and after the patients were positioned prior to surgeries. The end results of the MEP responses were compared with the axial Magnetic Resonance Imaging (MRI) grade of the Brain and Spinal Injury Centre (BASIC) score. The BASIC score basically ranged from grade 0 that indicates no injury to the spinal cord to grade 4 with more severe spine injury. The American Spinal Injury Association Impairment Scale (AIS) grading was performed before and after surgeries upon discharge, and this was compared with the MEP outcome with the Mann-Whitney U test. It was found that the presence of MEP was highly correlated with the AIS at discharge that showed that the patients with present MEP had a higher AIS grade as compared to the patients with absent MEP. The correlation of MEP and BASIC scores was implemented by using the Spearman correlation, and it was found that patients that had absent MEP had higher BASIC scores significantly compared to the patients that had present MEP.

Piasecki et al. [17] did a prospective study of the predictive value of the MEP outcome of patients that had lumbar spinal stenosis decompression surgeries. As much as 24 consecutive patients' data were used for the study, which were

collected within a 28-month period, and all of them had central spinal stenosis without lateral recess stenosis. But only 18 patients' data were selected since they were the only patients that had complete follow-up records. The adopted IONM modalities were TcMEP and lower limb SSEP. The SSEP data were not adopted for the study as the stimulation of the posterior tibial nerve only concerned one nerve root which was the S1 nerve root. The TcMEP stimulation used 50 V to 150 V intensity, biphasic stimulation, 500 Hz of 5 to 7 train pulses, and 1 ms intertrain. The TcMEP corkscrew electrodes were placed at C1–C2. The anaesthetic protocol adopted mainly TIVA with sufentanil and propofol, while a muscle relaxant was only used during intubation. The patients were assessed by using the Zurich Claudication Questionnaire (ZCQ) which was a self-assessment score before surgery (baseline) and after surgery (at 8 months after surgery and 29 months after surgery). The ZCQ scores were obtained by dividing the relative change scores (obtained by patients answering self-assessment questionnaire after surgery) with the baseline scores, and if the score was more than 0.5, it indicated significance for the study. The ZCQ scores were used to be compared with the outcome of the MEPs. The muscles used were dependent upon the level of the surgeries with the bilateral tibialis anterior and abductor hallucis as considerations. One upper limb muscle was used as the reference. The area under the curve of the MEP was used as the measurement tool to compare between the baseline value and after the full decompression value. It was mentioned that 20% of improvement was significant. The outcome of the MEP values showed that eight patients had improvement of more than 20%, three patients had MEP improvement of less than 20%, and 7 patients showed no MEP improvement. Fisher's exact test and the linear Pearson correlation were the statistical analysis tools used accordingly. It was found that by dichotomizing the data, the MEP improvement correlates with the ZCQ score at the early follow-up, while there was only a minor correlation between the 2 at the latest follow-up.

He et al. [18] presented a case report of a 60-year-old male patient that had a percutaneous endoscopic lumbar discectomy with the aid of IONM of MEP and free-running EMG modalities. The patient had more than 10 years of low back pain symptom with progressive left lower limb radicular pain and numbness a week before the procedure was done. The muscle strength evaluation of the quadriceps and first toe was 4/5 grades. The diagnosis of the patient imaging showed that the lumbar L2/L3 nerve roots on the left had been compressed by the herniated disc. The IONM recording electrodes were placed at the iliopsoas, rectus femoris, tibialis anterior, and medial gastrocnemius muscles bilaterally. There were no fluctuations of free-running EMG signals during the procedure. However, the MEP amplitude was increased after decompression was done. The patient presented a relieved pain of the low back and leg immediately after he was awake. This case report showed that the MEP could provide immediate feedback on the nerve root decompression effectiveness.

Another case report was presented by Rodrigues et al. [19] of a 22-year-old male athlete who had a decompression surgery after having lumbar pain symptom over 6 months. The patient was examined for muscle strength and showed grade 4/5 of the dorsiflexion of the right foot and hypoesthesia in L5 and S1. The surgery was done with the help of IONM of lower limb SSEP, TcMEP, free-running EMG, and stimulated EMG. The lower limb SSEP monitoring was done by stimulating the bilateral tibial nerve and recorded on the Cz–Fz on the scalp, while the stimulation for the MEP was done on the C3–C4 on the scalp and the recording was done on L3, L4, L5, S1, and S2 myotomes. The anaesthetic protocol utilized was the TIVA protocol with propofol and remifentanil. It was then found that an increment of MEP response amplitude was as much as 30% from the baseline value right after the discectomy procedure. The patient was able to return to a competitive level after a month of surgery.

Table 1 summarizes the findings of studies that proved IONM signal improvement which is correlated with the patients' positive outcome after surgery. If IONM signal improvement can be used as a guidance to indicate actual improvement, it will be valuable to the surgeons during the surgery to determine the depth of decompression which could help to reduce the surgery time and hence lower the risk of nerve injury.

It is difficult to measure the exact success rate for TcMEP as a prognosis tool because different studies used different improvement thresholds to show significant improvement. Some papers presented that the TcMEP amplitude after the decompression needs to be more than 50% than the baseline reading to imply actual clinical improvement [11]. Another study showed that the TcMEP amplitude needs to have more than 200% for improvement to happen to overcome the influence of anaesthesia that is used during intubation which could dampen the baseline TcMEP response and hence mislead the surgical team into thinking that there is improvement even though there is not any [6]. Improvement of more than 20% on the area under the curve (AUC) of the TcMEP signal is another indicator used by Piasecki et al. [17], while other studies only mentioned that the improvement of the TcMEP signal is correlated with the postsurgery clinical outcome without mentioning the parameters and the improvement criteria that they used [12, 13, 15, 16, 18, 19].

There are several research questions that can be derived from the previous paragraph. Since there are either 50% or 200% amplitude improvement criteria or 20% of AUC increment, it shows that there are no single universal criteria established that can be used to inform the surgeons that improvement has been achieved intraoperatively. This phenomenon was also presented by [20] that the rate of trial-to-trial variability of MEP is high from one response to another. Visser et al. [6] mentioned that the establishment of a good baseline reading is crucial and yet difficult to generate because of anaesthetic factors with the use of a short-acting muscle relaxant during intubation. The initial responses could be perceived as baseline reading even though it is still under anaesthetic influence and hence could cloud the judgement of whether the final TcMEP response obtained has improved or not.

Table 1: Summary for the reviews of the significance and the prognostic values of the MEP response improvement intraoperatively.

No.	Reference	No. of samples	IONM modalities used	Stimulation parameters	Muscles used to monitor MEP	Improvement criteria	Results
1	Barley et al. (2010)	One (15 months old boy)	TcMEP and SSEP	C1.-C2 scalp electrode positioning, current stimulation (145 mA to 187 mA for the left extremities and 175 mA to 200 mA for the right extremities)	Bilateral quadriceps femoris, tibialis anterior, gastrocnemius, sphincter, abductor pollicis brevis, abductor hallucis	Not mentioned	TcMEP response of the left APB had increment in amplitude. The patient had observable left upper extremity improvement
2	Voulgaris et al. (2010)	25 (2 had no IONM results)	TcMEP, EMG	C1–C2 with multipulse current stimulation, 0 mA to 200 mA, stimulus duration 0.2 ms to 0.5 ms	Not mentioned	>50% MEP amplitude improvement	17 patients with >50% improvement had better VAS score improvement
3	Rodrigues et al. (2011)	One (case report)	SSEP, MEP, and free-running EMG	C3-C4 stimulation	Not mentioned muscles' names specifically but monitoring covered L3-S2 myotomes	Not mentioned	MEP improved as much as 30%, and patient had returned to sports
4	Raynor et al. (2013)	386 patients had IOM signal improvement out of 12375 patients that had spinal surgeries over 25 years	DNEP, TcMEP, spontaneous EMG, triggered EMG, dermatomal SSEP	C3-C4 TcMEP scalp electrode stimulation montage	Upper extremity TcMEP was recorded from the deltoid, flexor/extensor carpi radialis, and/or abductor digiti minimi/abductor pollicis brevis. Lower extremity TcMEP was recorded from the anterior tibialis, medial gastrocnemius, and/or extensor hallucis longus	Not mentioned	The results did not mention specifically TcMEP improvement, but out of the modalities used, 88.7% patients had IOM signal improvement but one patient out of this percentage had permanent neurological deficit
5	Visser et al. (2014)	74 patients	TcMEP	Cz–Fz with monophasic stimulation and C3–C4 with biphasic stimulation	For the lower limbs: the quadriceps muscle (L2-L4), the tibialis anterior muscle (L4-L5), the hamstrings (L5-S1), or the gastrocnemius muscle (S1-S2). For cervical: the bilateral trapezoid muscle (C2-C4), the biceps (C5-C6), and the triceps muscle (C7-C8) of the arm; the extensor muscles of the forearm (C6-C7); or the abductor digitus V muscle (C6-C8)	>200% of amplitude increment	There is a correlation between the duration of symptom onset and the MEP improvement. MEP improvement can be accurate if the symptom onset duration is less than half a year
6	Wang et al. (2016)	59 patients that had cervical myelopathy underwent laminoplasty or laminectomy	MEP and SSEP	Not mentioned	Not mentioned	Not mentioned	Patients that had MEP signal improvement had a significant mJOA improvement rate. MEP amplitude was found to be a more accurate parameter compared to MEP latency in predicting surgery outcome

Table 1: Continued.

No.	Reference	No. of samples	IONM modalities used	Stimulation parameters	Muscles used to monitor MEP	Improvement criteria	Results
7	Dhall et al. (2017)	32	EMG, MEP, SSEP (not used for the study)	100 V–1000 V constant voltage stimulation, C1–C2 anodal stimulation, double train with a total of 9 pulses, 50 ms pulse width, 1.7 ms interstimulus, 13.1 ms ISI	Not mentioned	Comparison with the AIS grade and BASIC score of MRI images	MEP outcome (present) highly correlated with the better AIS grade and BASIC grade
8	Piasecki et al. (2018)	18	MEP, SSEP (not used for the study)	50 V–150 V C1–C2 biphasic stimulation, 5 to 7 train pulses, 500 Hz, 1 ms interstimulus pulse	1 upper limb muscle (control), bilateral tibialis anterior/bilateral abductor hallucis	>20% of AUC MEP, >50% of ZCQ score	The MEP improvement was related to the early follow-up functional outcome
9	Wi et al. (2019)	29 patients had improvement of IONM signals out of 317 cases	MEP and SSEP	Not mentioned	Upper extremity TcMEP was recorded from the deltoid, triceps, and thenar muscles. Lower extremity TcMEP was recorded from the anterior tibialis and abductor halluces	Comparison with MISS, SF-36, JOA, NDI, and Oswestry Disability Index	The patients with MEP improvement had a better MISS improvement rate while the patients with SSEP improvement only had a better SF-36 improvement rate
10	He et al. (2020)	One (case report)	MEP and free-running EMG	Not mentioned	Bilateral iliopsoas, rectus femoris, tibialis anterior, and medial gastrocnemius	Not mentioned	MEP improvement aligned with the patient's relieved symptoms

In the next section, we will review the factors that could influence MEP response so that we could make a suggestion on the utilization of MEP response as a prognostic tool intraoperatively.

2.1. Factors Influencing MEP Response. MEP is influenced by various factors, and it is important to identify these factors because if these factors are believed to be affecting the reliability of MEP response readings, the study of the MEP response improvement might not produce accurate favourable results. The factors influencing MEP are generally anaesthesia, the stimulation parameters used by the IONM personnel, electrode placements, surgical interventions, anatomy, physiology, and the technical specialist handling the IONM machine.

2.1.1. Anaesthesia. Since the MEP signal is generated by the contraction of muscles when the motor cortex is stimulated, the usage of neuromuscular blockade or muscle relaxant which blocks the transmission of the neurotransmitter causing the patients' reflex movements to be paralyzed should be avoided [8, 21].

Although inhalational anaesthetic agents such as desflurane and isoflurane have advantages such as rapid induction for sedation and recovery with low solubility, Malcharek et al. [22], Lo et al. [23], Pechstein et al. [24], and Tamkus et al. [25] had presented that the failing effects towards MEP response were correlated with the use of inhalational anaesthetic agents. Malcharek et al. [22] found out in their study to compare the effect of anaesthesia particularly between the combination of propofol/remifentanil and the combination of desflurane/remifentanil that the desflurane had a dampening effect on the amplitude of the MEP responses.

On the other hand, Lo et al. [23] reported that the MEP was plausible to be obtained within a suitable desflurane "concentration window" which was 0.5 maximum alveolar concentration (MAC) with 60% of NO_2 even though there was one patient that had nonreadable MEP response. Pechstein et al. [24] had only one successful MEP signal outcome when isoflurane and NO_2 were used together with alfentanil compared to the group that had the TIVA protocol with the combination of propofol and alfentanil with the outcome of 15 out 17 successful MEP signals. When they applied only the NO_2 to the TIVA group 10 minutes before all the tests were completed, they found that the MEP amplitudes were dropped to more than 40% compared to the baseline.

A study conducted by Tamkus et al. [25] involved a large number of samples which were 1814 patients mixed with patients that had preoperative motor deficits and patients with no preoperative motor deficits. They studied the false positive rates for MEP recordings by using inhalational agents and TIVA. False positive was defined as the MEP recording which is observed to be abnormal but not associated with intraoperative or postoperative motor deficits [25]. It turned out that the false positive rates were higher in the inhalational agent group compared to the TIVA group.

Meanwhile, Ubags et al. [26] conducted a study on different concentrations of propofol usage and the effects on the MEP responses had showed that the higher the dosage of propofol used, the more dampening it will impose on the MEP responses as compared to the effect of using NO_2. Furthermore, a study by Kawaguchi et al. [27] also supported the claim that MEP response excitability is dependent upon propofol dosage in which they showed that MEP response latency had not been significantly influenced by the propofol concentration, but the MEP response amplitude was increasing with the decrement of the propofol infusion rate.

Total intravenous anaesthesia (TIVA) using propofol is the common anaesthesia protocol for a successful MEP monitoring [22]. Even though inhalational agents are possible to be used for MEP monitoring, the TIVA protocol is still advisable to be used because various studies have shown that inhalational agents cause a more suppressive effect on the MEP responses compared to the TIVA protocol [22, 24, 25, 28, 29]. Higher concentrations of propofol were shown to suppress the MEP responses, but it goes with the rule that the deeper the anaesthesia is, the lower the MEP responses will be and the lighter the anaesthesia is, the higher the MEP responses will be [8]. With certain stimulus parameter adjustments which will be presented in the following section of this paper, MEP can be obtainable by using propofol even though it was shown that propofol also has some suppressive effects on the MEP responses [24, 26]. A summary of anaesthetic consideration done by Leppanen [30] is shown as follows:

(1) $NO_2 \leq 50\%$

(2) Isoflurane: not to be used or 0.2 to 0.5%

(3) Propofol: less than 200 μg/kg/min

(4) Fentanyl: continuous infusion

(5) Muscle relaxant: not to be used

2.1.2. Stimulation Parameters. There is no standardized protocol for stimulation to obtain MEP [8]. Stimulation parameters include stimulation intensity, number of pulses, pulse duration, single or train stimulation, constant-current or constant-voltage stimulation, anodal or biphasic stimulation, and other stimulation parameters [1, 8, 24, 26, 31–33].

The number of stimulation pulses was shown to have significant contribution to lowering or increasing the stimulus threshold to ignite MEP response [34]. Ubags et al. [26] tested the obtainability of MEP response by using two-pulse MEP stimulation, and the result showed that the MEP responses were obtainable 100% by using two pulses with the propofol-induced protocol. Pechstein et al. [24] applied different numbers of stimulation pulses (1–5 pulses), and it was presented that the amplitude of the MEP responses increased with the increasing number of pulses. However, latencies were not affected significantly by the number of pulses [24].

As a summary from combined authors, if more stimulation pulses are used:

(1) The latency threshold to obtain the MEP response will be reduced which means that the MEP response will appear sooner on the recording graph [8, 10, 35]

(2) The MEP response amplitude will become larger [8]

(3) There will be more polyphasic parameters produced on the MEP response signal, thus prolonging the duration of response [8]

(4) There will be increased likelihood of achieving the stimulation threshold [1]

Increasing stimulation intensity enhances the current field size and activates the subcortical white matter motor tracts at the bend of the axon exiting the grey matter [8]. This situation is acceptable if the monitored structures are below the foramen magnum such as the spine [1]. If the monitored structures are within the pyramidal tract in the white matter, it is advisable to use minimum MEP stimulus intensity so that any changes within these structures during, for example, brain tumour excision surgeries could be identified [36]. Response duration would also be increasing when stimulation intensity is increased [35].

Shigematsu et al. [32] introduced a method to increase the MEP response recording by using tetanic stimulation at single and multiple peripheral nerve sites. The tetanic stimulation at the posterior tibial nerve, for example, shown in the study a second before the MEP stimulation was evoked enhanced the MEP response at the abductor hallucis muscle which is the muscle innervated from the tibial nerve. It was mentioned by Shigematsu et al. [32] that this technique is suitable for patients with preoperative neurological deficit and patients with neuromuscular anaesthesia blockade.

2.1.3. Electrode Placements. The specific muscles correspond to specific spinal cord levels for efficient MEP monitoring purposes; for example, if the surgery takes place in the lumbar region, generally electrode placement of the leg muscles takes place at TA and AH [37]. The distance between recording electrodes (between active and reference electrodes) and the positioning of the recording electrodes on the muscle could also influence on the amplitude size and latency of the MEP response [38]. MEP response latency was found to be more delayed when the different electrodes were placed at a more distal location of the muscle. It was also recommended by Chomiak et al. [38] to position the recording MEP electrodes at the motor end plate zone and at the distal myotendinous junction to obtain significant MEP response.

The common scalp electrode montage to elicit MEP is C3–C4, but different montages could also lead to different outcomes to the MEP response [39]. Ryosuke et al. [39] simulated the scalp electrode montage from three different montages which were C3–C4, C1–C2, Cz–inion, and Cz–forehead in order to find out the best montage to elicit lower extremity MEP efficiently. The test was conducted on the 3D model of the head, and with finite element analysis, the tests were conducted. It was found that the Cz–inion scalp electrode montage produced MEP for lower extremities with a lower stimulus threshold. These findings are correlated with the homunculus representation of the cortex.

The homunculus was developed by Penfield et al. [40] through a lengthy experiment of electrical stimulation to the brains of their patients in order to identify or map the location of which part of the muscles or sensations responded to which part of the brain that was stimulated. Catani [41] had simplified the findings by Penfield et al. [40] with representation of the motor stimulations for different body parts with colour coded. The homunculus shows that the primary motor cortex area of the brain that controls the lower limbs is located towards the medial side of the brain, while the control of the upper limbs is located towards the lateral side of the primary motor cortex [42]. The more complex the movement of the muscle is, the larger the area of the motor cortex involved to control it: just to exemplify, the hand consists of a larger motor cortex area than the legs because of the complex movement it can produce.

Insulation such as a fat layer between the stimulating electrodes on the scalp affects the depth of electrical penetration towards the motor cortex thus influencing the recorded MEP response [43]. The use of peg screw electrodes for stimulation on the scalp could reduce the stimulus threshold because the current passes through the scalp more effectively rather than using corkscrew electrodes where the stimulation current spreads laterally because of the high resistivity of the skull [44–46]. However, the peg screw requires microdrilling before its insertion; this drilling has to be conducted with care to prevent the drilling from penetrating the skull even though the risk is minimal [45].

2.1.4. Surgical Interventions, Anatomy, and Physiology. Temperature affects the MEP response: low temperature increases the latency of the response while higher temperature reduces the latency of the response [8]. The source of temperature changes might stem from the patient's body temperature, or specific muscles' or limbs' temperature, or the temperature of the exposed spinal cord during the surgery [8]. Temperature can also affect MEP indirectly by changing the pharmacokinetics and pharmacodynamics of anaesthetic agents where a study showed that decreased temperature can cause increased concentration of propofol and reduce the bispectral (BIS) index value thus reducing the amplitudes of MEP responses [47]. Other effect of temperature on MEP response is that low temperature could obliterate MEP response while increasing the temperature could revive the MEP response [37].

In the study conducted by Kanemaru et al. [48] whereby MEP was performed on patients that underwent descending aortic replacement (DAR) and thoracoabdominal aortic replacement (TAAR) surgeries, they showed that when the patients were put through deep hypothermic circulatory arrest (DHCA) (12°C-22°C), the MEP response disappeared. The MEP amplitude was then increased to more than 50% during the rewarming process when the body temperature reached approximately 34°C. Another similar study was made by Shinzawa et al. [49] that the MEP latencies in both the abductor pollicis brevis (APB) and abductor hallucis (AH) muscles which were tested were inversely proportional

to the temperature. It was also found that the AH muscles or the leg muscles had a slower rate of MEP amplitudes' increment during the rewarming process compared to the hand muscles or APB muscles. These studies indicated that the body temperature of the patient should be kept close to the normal human body temperature for MEP monitoring to function well.

MEP response is also subjected to surgical manipulations [50]. MacDonald et al. [51] had elaborately presented the surgical interventions that affected the MEP responses during their study which were as follows:

(1) Hypotension:

(i) It is defined as the mean arterial pressure that fells below 60 mmHg

(ii) Any reduction to MEP responses in the study had considered raising the blood pressure. If there were no other interventions involved in the deterioration of MEP responses, raising blood pressure had shown to bring restoration to MEP responses

(2) Ischemia:

(i) Leg ischemia was shown in one of the cases in the presented study which was caused by femoral artery pressure to deteriorate the leg MEP responses. Pelvic support was repositioned and MEP responses gradually returned except the protracted right TA's MEP

(3) Spinal cord contusion:

(i) Spinal cord contusion due to instrumentation could cause MEP response deficit

(ii) As shown by MacDonald et al. [51], placement of the hook into one thoracic vertebra in one of the cases caused disappearance of bilateral leg MEP. Removal of the hook afterwards brought back the MEP responses

(iii) Another case presented with an overcorrection done had bilateral leg MEP disappearance. The rod was released and the MEP response was returned

(iv) An idiopathic scoliosis case had disappearance of MEP after discectomy during anterior release. The patient was positioned in lateral flexion. After the patient was straightened, the MEP reappeared

Anatomical factors of the patients could also affect the MEP response. One of the most important practices to perform before any surgical interventions are made is to obtain the best MEP response baseline, and failure to obtain this important information can be caused by preoperative motor function or motor power deficit [52]. This means that the lower the motor power is, the less chance it is to obtain a successful reading of MEP response.

Age is also a factor that could affect MEP response as studies showed that a paediatric patient at the age below 7 years has a lower successful rate of producing reliable MEP readings due to the electrophysiologic immaturity of the corticospinal tract which is considered fully developed generally at the age of 10 years old [33, 53].

The number of nerve innervations towards the target muscle represents the sensitivity of the MEP readings as shown in various studies [52, 54]. As shown by Kim et al. [52], the AH muscle is reported to achieve a higher successful rate in producing MEP response as the baseline than the AT muscle, while Yue et al. [54] presented that the event of foot drop postoperatively could be determined from the monitoring of the AT muscle rather than the AH muscle. These two events were deducted as there are more nerves that innervate towards the AH muscle, making it less sensitive to motor power deficit or nerve injury than the AT muscle which has a lower number of nerves that innervate towards it [52].

2.1.5. Technical Specialist Handling the IONM Technology. The team that handles IONM during the surgery plays an integral role in providing reliable interpretation of signals to the entire IONM team even though it is not a direct factor that affects the MEP signal characteristics. The IONM team as defined in Kim et al. [55] consists of the surgeon, clinical neurophysiologist, anaesthesiologist, and monitoring technologist.

Kim et al. [55] claimed that the majority of the IONM signals' changes primarily stem from faulty machine, inappropriate IONM machine settings, changes in the anaesthetic regime, and inconsistent hemodynamic state and are not entirely due to neural damage. These factors could be minimized or eliminated by the expert evaluation and analysis of the experienced neurophysiologist resulting in the reduction of false positive and false negative rates.

In order to prevent neural damage, the neurophysiologist or the monitoring technologist has to interpret the changes or the drop of the signal. The variety of alarm criteria to the MEP signal alone within the literature has led the neurophysiologist to identify the best alarm criteria to suit the situation of the surgery. For instance, Weinzierl et al. [50] proposed to use 50% drop of MEP response amplitude if the surgery is considered less risky and less aggressive by the surgical team and 80% drop of MEP response amplitude if the surgery is more complicated. However, the authors highlighted that if 80% drop of MEP response amplitude was used as their alarm criteria in their studies, 2 of the patients that developed postsurgery motor deficit will be missed out.

Another example that requires the neurophysiologist or the monitoring technologist to be equipped with new findings and knowledge in the IONM research area is the usability of certain IONM modalities for certain procedures. For example, Pajewski et al. [56] recommended that no MEP and SSEP monitoring should be used in simple lumbar discectomy or decompression as the modalities would slow down the operation time and prevent muscle relaxation. Meanwhile, He et al. [18] presented that the MEP is

beneficial in detecting improvement in MEP intraoperatively which correlated with the relief of symptoms postoperatively. The MEP could also be useful in lumbar procedures with the appropriate MEP monitoring on the tibialis anterior and extensor hallucis longus to prevent foot drop [57]. The researches from He et al. [18] and Lieberman et al. [57] seem contradicting to the proposal made by Pajewski et al. [56], but in the end, it is up to the IONM team to decide on how they would approach the surgeries based on these recommendations from the literatures.

2.1.6. Summary for Factors Influencing MEP Response. Most of the factors influencing MEP response presented in Section 2.1 are already well known and standardized. However, IONM personnel (surgeon, anaesthetist, and technician) acceptance and interpretations towards the standardized knowledge on MEP might vary. Communication within the team is the key to maintain the parameters as steady as possible, so that the IONM can be used solely to analyze the condition of the neural integrity. If communication fails, the IONM technician will have to try to adapt with the patient's physiological changes due to, for example, the anaesthesia fluctuations by adjusting the stimulation parameters, and the adjustment requires skills and experience from the technician himself/herself. These show how each factor is interrelated with one another. We summarized that in order for MEP to be used successfully as an indicator of positive outcome postsurgery, these influencing factors should be maintained to keep the nonsurgical factor from interfering with the interpretation of the MEP.

3. Discussion

In Malaysia, IONM is usually conducted by IONM technicians from companies that distribute medical devices to the hospitals. There are no specialized neurophysiologists behind every IONM technician to give advices and analyze the IONM signals in depth. The IONM technicians in Malaysia do not necessarily have the specific certificate or qualification in IONM. The companies rely on training for product use conducted by their respective IONM technology supplier or manufacturer, and some may go further by attending IONM conferences conducted worldwide. The IONM technicians in Malaysia need to cope with the technology and become the interpreter or intermediary between the IONM technology and the medical practitioners such as the surgeon and the anaesthetist inside the operation theatre during surgery. It is already challenging to alarm the surgeons and at the same time not limit the surgeons conducting their task. At the same time, apart from inspecting whether the patient's spine integrity is still intact, the surgeons desire to know if they can expect any positive functional outcome to their patients during the surgery through IONM.

Figures 1 and 2 show MEP baseline and after decompression, respectively, of a patient that underwent microendoscopic discectomy of L4/L5. The patient complained of back pain and left leg pain, with no motor weakness, and was diagnosed with lumbar disc prolapse at L4/L5. The percentages of signal peak-to-peak amplitude increments are circled in Figure 2. The amplitude increments are shown to be more than 200% in seven channels and 24% in channel LM4. It is difficult to suggest that the patient will incur positive functional outcome from these signals.

Unlike the alarm criteria, the literatures have established alarm criteria that can be used by the neuromonitoring technologist in live surgery even though there are differences between the studies, whether it is 50% MEP signal drop [50] or 80% MEP signal drop [58], or even with all-or-nothing criteria [1], the IONM technicians can choose the criteria based on their interpretations and situations during the surgery. Alarm criteria can be established since the signal drop can only range from 0% to 100% from the baseline reading.

The increment of the MEP signal can be more than 100% as shown in Figure 2. Based on Table 1, if improvement criteria such as 50% [11] are used, all of the channels in Figure 2 will be noted as improved, even though the only focus is on L4/L5 since that is where the disc prolapse and the patient experience pain only on the left leg. Another example based on Table 1, if 200% increment [6] is chosen as the improvement criteria, all channels will be presumed as having improvement except for channel LM4 that only exhibits 24% of increment. In Sunway Medical Centre, we have experienced many IONM events which were similar to what is shown in Figures 1 and 2, which is why the current literatures' recommendations on the improvement criteria cannot be used for all of the cases.

This phenomenon of having all channels to have increment was mainly due to the unreliable baseline establishment. The baseline establishment was affected by the use of a muscle relaxant for intubation, which had not worn off fully by the time the MEP baseline is established. Some of the anaesthetists even use inhalational agents during intubation, and this will interfere with stable MEP baseline establishment. In Sunway Medical Centre, a one-level lumbar discectomy decompression procedure takes about 2 hours. The most ideal baseline should be established before decompression is done. But the problem is that, as shown in the example in Figures 1 and 2, the actual response was only obtained after the decompression is done, indicated by the global increments throughout all channels.

However, MEP can still be considered a prognostic tool by considering the following recommendations by the authors of this paper:

(a) Identify the problematic myotome based on presurgery clinical evaluation

(b) The TIVA protocol is the preferred anaesthesia throughout the surgery. If possible, the anaesthetist should intubate the patient without using inhalational gas

(c) Use higher stimulus intensity and number of trains if it is difficult to obtain observable MEP response, and lower down the stimulus intensity once the response amplitude is increasing when the surgery is progressing and the muscle relaxant effect is fading

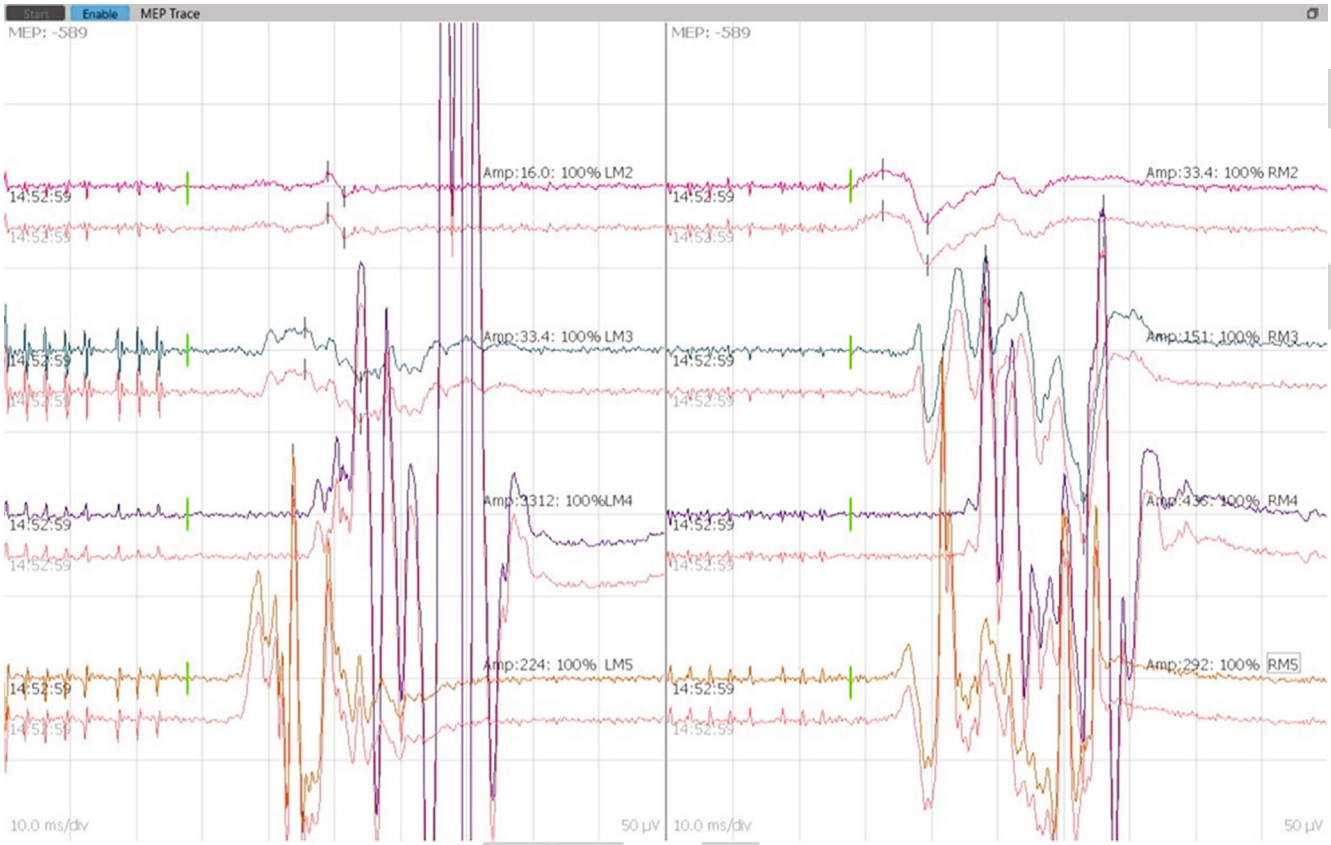

Figure 1: Baseline MEP response of a patient from microendoscopic discectomy of the L4/L5 procedure. LM2 and RM2: bilateral vastus lateralis. LM3 and RM3: bilateral tibialis anterior. LM4 and RM4: bilateral abductor hallucis. LM5 and RM5: bilateral medial gastrocnemius.

(d) Request to stimulate MEP before decompression starts

(e) Observe the global behaviour of the MEP responses. Even if there are amplitude increment on the control channels (channels which are not the problematic myotome), the increment on the symptomatic myotome should be in higher percentage compared to that on the control channels. This may indicate improvement to the functional outcome of the patient

(f) Point (e) above should consider that all of the factors that could affect the MEP response as presented in Section 2.1 are not the cause of the assumption on improvement

Once we know the symptomatic myotome as stated in point (a) above and monitor it through MEP, we can observe visually the difference between the final reading and the initial baseline reading. If the initial and the final response makes prediction difficult as shown in Figures 1 and 2 as the responses heightened globally, we can still visually compare the symptomatic myotome against the other controlled channels. This means that the symptomatic myotome's improvement should be more significant compared to that of the other asymptomatic channels hence suggesting actual functional improvement.

Point (b) is almost true for all of the surgeries that require IONM in Malaysia because of the increasing awareness among the anaesthetists of the need of TIVA for stable monitoring. However, the anaesthetists still have their own techniques used during intubation. Some of the anaesthetists are comfortable of using inhalational agents during intubation and will only switch to TIVA once the patient is positioned and draped. This will prolong the establishment of a reliable MEP baseline. A monitoring technician can only advice, but the anaesthetists will make their own decisions on what suits them and the patients best.

Point (c) is proposed because the adjustment of stimulus parameters as mentioned in Section 2.1.2 could help to establish a proper baseline if the MEP is affected by the muscle relaxant and inhalational agents used during intubation. Point (d) emphasizes on the important of communication between the IONM technician and the surgeon. If the surgeon is honest in utilizing the feedback from the IONM technology, the IONM technician should be allowed to request to do their tests (MEP more importantly because MEP stimulation causes the patient's body movement) at the times that suit their needs. Sometimes, requesting to test MEP just before the decompression starts will help to prolong the time needed for the anaesthesia from intubation to wear off, hence producing a stable MEP baseline. This will help the comparison between before and after decompression more reliable.

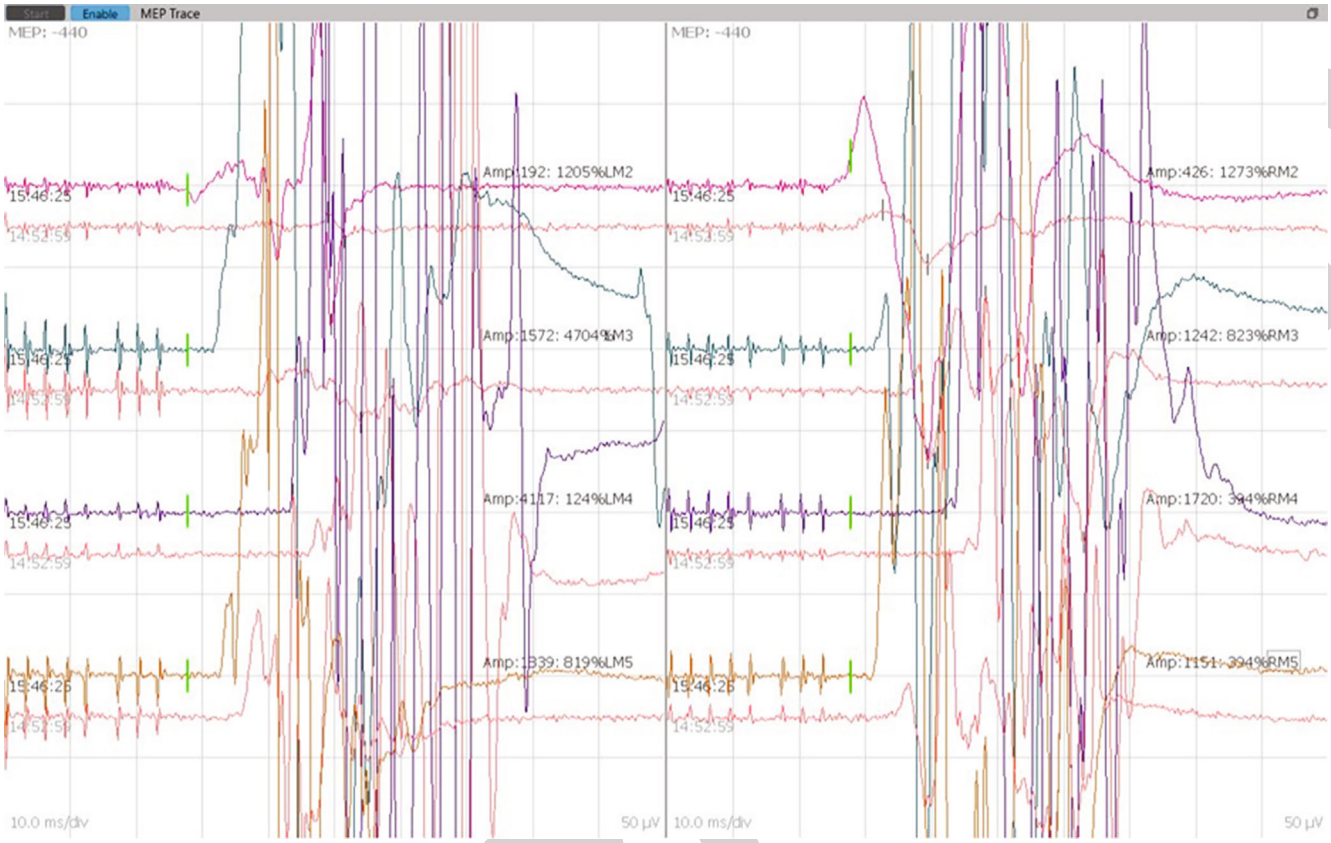

Figure 2: MEP response of a patient from microendoscopic discectomy of the L4/L5 procedure after decompression is performed. LM2 and RM2: bilateral vastus lateralis. LM3 and RM3: bilateral tibialis anterior. LM4 and RM4: bilateral abductor hallucis. LM5 and RM5: bilateral medial gastrocnemius.

We propose that point (e) in the recommendations above should be assisted with signal processing and algorithm that could identify the global MEP response pattern of a patient during surgery, allowing the identification of significant improvement pattern on the problematic myotome. This can be done if more MEP parameters can be extracted and calculated compared to just relying on peak-to-peak amplitude or AUC as presented in studies mentioned in Section 2.

4. Conclusions

In this study, improvement to the MEP responses after surgical manipulation to the affected surgical sites from various levels of the spinal cord is shown in Section 2 to be highly corresponded to the positive functional outcome of the patients. This indicates that improvement to the MEP responses intraoperatively is reliable to be used as a prognostic tool and a valuable indicator to the surgeons during the surgery.

However, there was no specific indicator for improvement that could be used to replicate the same result as the authors in Table 1 did in their studies. We highlighted in Discussion an example problem that prolonged anaesthetic muscle relaxant fading causes unknown suppression to the MEP baseline, causing wrong justification of improvement postdecompression. In order to make use MEP indications as a prognostic tool, we propose that the factors affecting MEP as presented in Section 2.1 should be maintained without huge variability throughout the surgery in the best way possible.

As we presented in Section 3, these improvement criteria need to distinguish between the global MEP behaviour and the symptomatic myotome MEP behaviour. We reviewed in Section 2.1 various factors that could affect MEP parameters such as the polyphase of the signal, latency of the response's starting point, and the duration or the length of the response. Some of these parameters are also presented in the reviews as the alarm criteria. These parameters can be further studied to be used as improvement criteria. A machine learning algorithm can also be used to make use of the combination of the MEP parameters as a pattern that signifies improvement rather than just relying on a single parameter.

Although significant work has been made in addressing such issue, there is much more room for the development of MEP improvement and its prognostic value correlation by taking into account the MEP signal's parameters and the justification of choosing the improvement criteria in the future.

Data Availability

All the data are available from the list of references. Data presented in Figures 1 and 2 were collected from Sunway Medical Centre, Malaysia, upon medical ethics approval.

Ethical Approval

The data collection is approved by the medical ethics committee of SunMed Clinical Research Centre (SMRR No. SMRR/IIR/SMC/21/002, SRB Approval No. SRB/NF/21/002).

Conflicts of Interest

The authors declare that the research was conducted in the absence of any commercial or financial relationships that could be construed as a potential conflict of interest.

Acknowledgments

This work was supported in part by FRGS, Ministry of Higher Education Malaysia, and Universiti Malaya (FRGS/1/2018/TK04/UM/02/9) and Universiti Tunku Abdul Rahman Research Fund (IPSR/RMC/U-TARRF/2020-C1/H02).

References

[1] A. A. Gonzalez, D. Jeyanandarajan, C. Hansen, G. Zada, and P. C. Hsieh, "Intraoperative neurophysiological monitoring during spine surgery: a review," *Neurosurgical Focus*, vol. 27, no. 4, article E6, 2009.

[2] F. Rabai, R. Sessions, and C. N. Seubert, "Neurophysiological monitoring and spinal cord integrity," *Best Practice & Research. Clinical Anaesthesiology*, vol. 30, no. 1, pp. 53–68, 2016.

[3] R. N. Holdefer, D. B. MacDonald, and S. A. Skinner, "Somatosensory and motor evoked potentials as biomarkers for postoperative neurological status," *Clinical Neurophysiology*, vol. 126, pp. 857–865, 2015.

[4] M.-K. Oh, H.-R. Kim, W.-S. Kim, and H. I. Shin, "Relationship between motor evoked potential response and the severity of paralysis in spinal cord injury patients," *Annals of Rehabilitation Medicine*, vol. 41, no. 2, pp. 211–217, 2017.

[5] M. G. Vitale, D. L. Skaggs, G. I. Pace et al., "Best practices in intraoperative neuromonitoring in spine deformity surgery: development of an intraoperative checklist to optimize response," *Spine Deformity*, vol. 2, no. 5, pp. 333–339, 2014.

[6] J. Visser, W. C. Verra, J. M. Kuijlen, P. P. Horsting, and H. L. Journee, "Recovery of TES-MEPs during surgical decompression of the Spine," *Journal of Clinical Neurophysiology*, vol. 31, no. 6, pp. 568–574, 2014.

[7] G. Agrawal, S. Iyer, and A. H. All, "A comparative study of recording procedures for motor evoked potential signals," *Conference Proceedings: Annual International Conference of the IEEE Engineering in Medicine and Biology Society*, vol. 2009, pp. 2086–2089, 2009.

[8] D. B. MacDonald, S. Skinner, J. Shils, and C. Yingling, "Intraoperative motor evoked potential monitoring - A position statement by the American Society of Neurophysiological Monitoring," *Clinical Neurophysiology*, vol. 124, no. 12, pp. 2291–2316, 2013.

[9] A. Farajidavar, J. L. Seifert, M. R. Delgado, S. Sparagana, M. I. Romero-Ortega, and J. C. Chiao, "Electromagnetic interference in intraoperative monitoring of motor evoked potentials and a wireless solution," *Medical Engineering & Physics*, vol. 38, no. 2, pp. 87–96, 2016.

[10] M. Watson, N. Dancause, and M. Sawan, "Intracortical microstimulation parameters dictate the amplitude and latency of evoked responses," *Brain Stimulation*, vol. 9, no. 2, pp. 276–284, 2016.

[11] S. Voulgaris, D. Karagiorgiadis, G. A. Alexiou et al., "Continuous intraoperative electromyographic and transcranial motor evoked potential recordings in spinal stenosis surgery," *Journal of Clinical Neuroscience*, vol. 17, no. 2, pp. 274–276, 2010.

[12] B. L. Raynor, J. D. Bright, L. G. Lenke et al., "Significant change or loss of intraoperative monitoring Data," *Spine (Phila Pa 1976)*, vol. 38, no. 2, pp. E101–E108, 2013.

[13] S. Wang, Y. Tian, C. Wang et al., "Prognostic value of intraoperative MEP signal improvement during surgical treatment of cervical compressive myelopathy," *European Spine Journal*, vol. 25, no. 6, pp. 1875–1880, 2016.

[14] S. Wi, H.-J. Lee, T. Kang et al., "Clinical significance of improved intraoperative neurophysiological monitoring signal during spine surgery: a retrospective study of a single-institution prospective cohort," *Asian Spine Journal*, vol. 14, 2020.

[15] J. L. Barley, J. F. Mooney, S. S. Glazier et al., "Sudden appearance of new upper extremity motor function while performing neurophysiologic intraoperative monitoring during tethered cord Release," *Journal of Pediatric Orthopedics*, vol. 30, no. 6, pp. 624–628, 2010.

[16] S. S. Dhall, J. Haefeli, J. F. Talbott et al., "Motor evoked potentials correlate with magnetic resonance imaging and early recovery after acute spinal cord injury," *Neurosurgery*, vol. 82, pp. 870–876, 2018.

[17] K. Piasecki, G. Kulik, K. Pierzchala, E. Pralong, P. J. Rao, and C. Schizas, "Do intra-operative neurophysiological changes predict functional outcome following decompressive surgery for lumbar spinal stenosis? A prospective study," *Journal of Spine Surgery*, vol. 4, no. 1, pp. 86–92, 2018.

[18] S. He, Z. Ren, X. Zhang, and J. Li, "Neurophysiologic monitoring for treatment of upper lumbar disc herniation with percutaneous endoscopic lumbar discectomy: a case report on the significance of an increase in the amplitude of motor evoked potential responses after decompression and literature review," *International Journal of Surgery Case Reports*, vol. 67, pp. 271–276, 2020.

[19] L. M. Rodrigues, F. W. Rosa, R. J. Ferreira, F. Ueno, and C. Milani, "Herniated lumbar disc surgery in triathlon athletes with intraoperative neurophysiologic monitoring," *Einstein (São Paulo)*, vol. 9, no. 4, pp. 530–533, 2011.

[20] K. F. Kothbauer, "The interpretation of muscle motor evoked potentials for spinal cord monitoring," *Journal of Clinical Neurophysiology*, vol. 34, no. 1, pp. 32–37, 2017.

[21] W. C. Bowman, "Neuromuscular block," *British Journal of Pharmacology*, vol. 147, Supplement 1, pp. S277–S286, 2006.

[22] M. J. Malcharek, S. Loeffler, D. Schiefer et al., "Transcranial motor evoked potentials during anesthesia with desflurane versus propofol - A prospective randomized trial," *Clinical Neurophysiology*, vol. 126, no. 9, pp. 1825–1832, 2015.

[23] Y. L. Lo, Y. F. Dan, Y. E. Tan et al., "Intra-operative monitoring in scoliosis surgery with multi-pulse cortical stimuli and desflurane anesthesia," *Spinal Cord*, vol. 42, no. 6, pp. 342–345, 2004.

[24] U. Pechstein, J. Nadstawek, J. Zentner, and J. Schramm, "Isoflurane plus nitrous oxide versus propofol for recording of motor evoked potentials after high frequency repetitive electrical stimulation," *Electroencephalography and Clinical Neurophysiology/Evoked Potentials Section*, vol. 108, no. 2, pp. 175–181, 1998.

[25] A. A. Tamkus, K. S. Rice, and H. L. Kim, "Differential rates of false-positive findings in transcranial electric motor evoked potential monitoring when using inhalational anesthesia versus total intravenous anesthesia during spine surgeries," *The Spine Journal*, vol. 14, no. 8, pp. 1440–1446, 2014.

[26] L. H. Ubags, C. J. Kalkman, H. D. Been, and J. C. Drummond, "Differential effects of nitrous oxide and propofol on myogenic transcranial motor evoked responses during sufentanil anaesthesia," *British Journal of Anaesthesia*, vol. 79, no. 5, pp. 590–594, 1997.

[27] M. Kawaguchi, T. Sakamoto, S. Inoue et al., "Low dose propofol as a supplement to ketamine-based anesthesia during intraoperative monitoring of motor-evoked potentials," *Spine*, vol. 25, no. 8, pp. 974–979, 2000.

[28] T. Kerz, H. J. Hennes, A. Feve, P. Decq, P. Filipetti, and P. Duvaldestin, "Effects of propofol on H-reflex in humans," *Anesthesiology*, vol. 94, no. 1, pp. 32–37, 2001.

[29] J. Zentner, T. Albrecht, and D. Heuser, "Influence of halothane, enflurane, and isoflurane on motor evoked potentials," *Neurosurgery*, vol. 31, no. 2, pp. 298–305, 1992.

[30] R. E. Leppanen, "Intraoperative applications of the H-reflex and F-response: a tutorial," *Journal of Clinical Monitoring and Computing*, vol. 20, no. 4, pp. 267–304, 2006.

[31] E. Okamoto, E. Ishikawa, T. Yamamoto et al., "Variability in amplitude and stimulation threshold values in motor evoked potential (MEP) monitoring during the resection of brain lesions," *Clinical Neurophysiology*, vol. 126, no. 6, pp. 1271–1278, 2015.

[32] H. Shigematsu, M. Kawaguchi, H. Hayashi et al., "Post-tetanic transcranial motor evoked potentials augment the amplitude of compound muscle action potentials recorded from innervated and non-innervated muscles," *The Spine Journal*, vol. 18, no. 5, pp. 740–746, 2018.

[33] T. B. Sloan, D. Janik, and L. Jameson, "Multimodality monitoring of the central nervous system using motor-evoked potentials," *Current Opinion in Anaesthesiology*, vol. 21, no. 5, pp. 560–564, 2008.

[34] A. Szelényi, K. Kothbauer, and V. Deletis, "Transcranial electric stimulation for intraoperative motor evoked potential monitoring: stimulation parameters and electrode montages," *Clinical Neurophysiology: Official Journal of the International Federation of Clinical Neurophysiology*, vol. 118, no. 7, pp. 1586–1595, 2007.

[35] M. Watson, M. Sawan, and N. Dancause, "The duration of motor responses evoked with intracortical microstimulation in rats is primarily modulated by stimulus amplitude and train duration," *PLoS One*, vol. 11, no. 7, article e0159441, 2016.

[36] T. Umemura, S. Nishizawa, Y. Nakano et al., "Intraoperative monitoring of motor-evoked potential for parenchymal brain tumor removal: an analysis of false-negative cases," *Journal of Clinical Neuroscience*, vol. 57, pp. 105–110, 2018.

[37] J.-H. Park and S.-J. Hyun, "Intraoperative neurophysiological monitoring in spinal surgery," *World Journal of Clinical Cases: WJCC*, vol. 3, no. 9, pp. 765–773, 2015.

[38] J. Chomiak, J. Dvorak, J. Antinnes, and A. Sandler, "Motor evoked potentials: appropriate positioning of recording electrodes for diagnosis of spinal disorders," *European Spine Journal*, vol. 4, no. 3, pp. 180–185, 1995.

[39] R. Tomio, T. Akiyama, T. Ohira, and K. Yoshida, "Effects of transcranial stimulating electrode montages over the head for lower-extremity transcranial motor evoked potential monitoring," *Journal of Neurosurgery*, vol. 126, no. 6, pp. 1951–1958, 2016.

[40] W. Penfield and E. Boldrey, "Somatic motor and sensory representation in the cerebral cortex of man as studied by electrical stimulation," *Brain*, vol. 60, no. 4, pp. 389–443, 1937.

[41] M. Catani, "A little man of some importance," *Brain*, vol. 140, no. 11, pp. 3055–3061, 2017.

[42] T. Dewolf and C. Eliasmith, *NOCH: a framework for biologically plausible models of neural motor control, [M.S. thesis]*, University of Waterloo, 2010.

[43] R. Tomio, "Effects of electrodes length and insulation for transcranial electric stimulation," *Surg Neurol Int*, vol. 10, 2019.

[44] T. Goto, H. Muraoka, K. Kodama, Y. Hara, T. Yako, and K. Hongo, "Intraoperative monitoring of motor evoked potential for the facial nerve using a cranial peg-screw electrode and a "threshold-level" stimulation method," *Skull Base*, vol. 20, no. 6, pp. 429–434, 2010.

[45] R. Tomio, T. Akiyama, T. Ohira, and K. Yoshida, "Comparison of effectiveness between cork-screw and peg-screw electrodes for transcranial motor evoked potential monitoring using the finite element method," *Surgical Neurology International*, vol. 7, no. 33, 2016.

[46] K. Watanabe, T. Watanabe, A. Takahashi, N. Saito, M. Hirato, and T. Sasaki, "Transcranial electrical stimulation through screw electrodes for intraoperative monitoring of motor evoked potentials," *Journal of Neurosurgery*, vol. 100, no. 1, pp. 155–160, 2004.

[47] M. Kawaguchi, M. Kawamata, and Y. Yamada, "Improvement of motor evoked potentials monitoring is required during thoracic or thoracoabdominal aortic aneurysm surgery under hypothermic cardiopulmonary bypass," *Journal of Anesthesia*, vol. 26, no. 2, pp. 157–159, 2012.

[48] E. Kanemaru, K. Yoshitani, S. Kato, Y. Tanaka, and Y. Ohnishi, "Reappearance of motor-evoked potentials during the rewarming phase after deep hypothermic circulatory arrest," *Journal of Cardiothoracic and Vascular Anesthesia*, vol. 32, no. 2, pp. 709–714, 2018.

[49] M. Shinzawa, K. Yoshitani, K. Minatoya, T. Irie, H. Ogino, and Y. Ohnishi, "Changes of motor evoked potentials during descending thoracic and thoracoabdominal aortic surgery with deep hypothermic circulatory arrest," *Journal of Anesthesia*, vol. 26, no. 2, pp. 160–167, 2012.

[50] M. R. Weinzierl, P. Reinacher, J. M. Gilsbach, and V. Rohde, "Combined motor and somatosensory evoked potentials for intraoperative monitoring: intra- and postoperative data in a series of 69 operations," *Neurosurgical Review*, vol. 30, no. 2, pp. 109–116, 2007, discussion 116.

[51] D. B. MacDonald, Z. al Zayed, and A. al Saddigi, "Four-limb muscle motor evoked potential and optimized somatosensory evoked potential monitoring with decussation assessment: results in 206 thoracolumbar spine surgeries," *European Spine Journal*, vol. 16, no. S2, pp. 171–S187, 2007.

Hindawi
Behavioural Neurology
Volume 2021, Article ID 4028761, 9 pages
https://doi.org/10.1155/2021/4028761

Research Article

Patient Behavioral Analysis with Smart Healthcare and IoT

Anurag Tiwari,[1] **Viney Dhiman**,[2] **Mohamed A. M. Iesa**,[3] **Haider Alsarhan**,[4] **Abolfazl Mehbodniya**,[5] **and Mohammad Shabaz**[6,7]

[1]*Babu Banarasi Das Institute of Technology & Management, Lucknow, India*
[2]*Department of Cardiology, PGIMER, Chandigarh, India*
[3]*Department of Physiology, Al Qunfudah Medical College, Umm Al Qura University, Mecca, Saudi Arabia*
[4]*Mustansiriyah University, College of Medicine, Baghdad, Iraq*
[5]*Department of Electronics and Communications Engineering, Kuwait College of Science and Technology (KCST), Doha Area, 7th Ring Road, Kuwait*
[6]*Arba Minch University, Ethiopia*
[7]*Department of Computer Science Engineering, Chandigarh University, Punjab, India*

Correspondence should be addressed to Anurag Tiwari; anuragrktiwari@gmail.com

Received 4 September 2021; Revised 29 September 2021; Accepted 1 October 2021; Published 3 November 2021

Academic Editor: Hong Lin

Patient behavioral analysis is the key factor for providing treatment to patients who may suffer from various difficulties including neurological disease, head trauma, and mental disease. Analyzing the patient's behavior helps in determining the root cause of the disease. In traditional healthcare, patient behavioral analysis has lots of challenges that were much more difficult. The patient behavior can be easily analyzed with the development of smart healthcare. Information technology plays a key role in understanding the concept of smart healthcare. A new generation of information technologies including IoT and cloud computing is used for changing the traditional healthcare system in all ways. Using Internet of Things in the healthcare institution enhances the effectiveness as well as makes it more personalized and convenient to the patients. The first thing that will be discussed in the article is the technologies that have been used to support the smart class, and further, there will be a discussion on the existing problems with the smart healthcare system and how these problems can be solved. This study can provide essential information about the role of smart healthcare and IoT in maintaining behavior of patent. Various biomarkers are maintained properly with the help of these technologies. This study can provide effective information about importance of smart health system. This smart healthcare is conducted with the involvement of proper architecture. This is treated as effective energy efficiency architecture. Artificial intelligence is used increasingly in healthcare to maintain diagnosis and other important factors of healthcare. This application is also used to maintain patient engagement, which is also included in this study. Major hardware components are also included in this technology such as CO sensor and CO_2 sensor.

1. Introduction

This article is about the importance of smart healthcare inpatient behavioral analysis. In the digital world, everything is getting transformed and becoming informative. The advancement and the rapid growth of technology allow traditional biotechnology as well as medicine to get digital and become more informed. New information technology has emerged by the incorporation of smart healthcare. The smart care health system is a multilevel change. The changes involved in the smart healthcare system for analyzing the patient behavioral include disease-centered to patient-centered, changed concept of management and prevention, and changing of information construction to the regional medical transformation to clinical informatization.

These changes are based on the current needs of the patients by improving the efficiency and performance of the healthcare system. The implementation of IoT will help in developing a smart healthcare system. The challenges in the traditional medical system will be overcome through

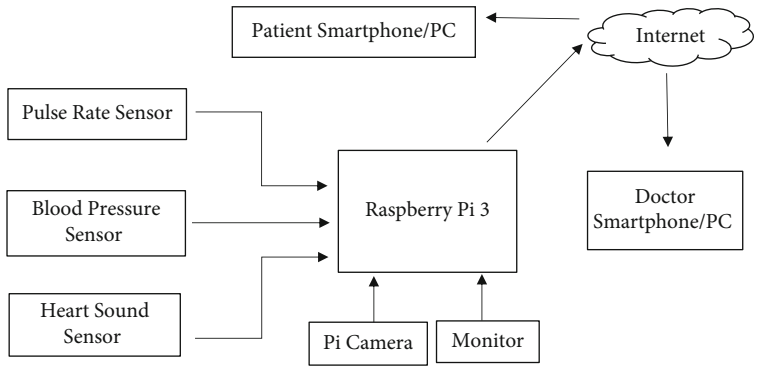

Figure 1: Block diagram.

Table 1: List of future and available sensors and their applications for detecting patient behavioral analysis.

Biomarker	CVD	COPD	PD/HD	Diabetes
Respiratory rate	True	True	True	?
ECG	True	True	True	True
Surface EMG	True	True	True	/?
Gait (posture)	True	True	True	?
Skin temperature	True	True	True	True
Blood pressure	True	True	True	True
Oxygenation	True	True	?	?
Heart sound	True	True	?	?
Title volume	True	True	True	?

the smart healthcare system. In this article, the concept of smart healthcare will be discussed as well and the features and challenges of smart healthcare have been also discussed. The key technology is IoT that is used in the smart healthcare system, and it will be also discussed, and how effectively it can analyze the patient behavior will be discussed in the article. IoT is implemented successfully to maintain smart health monitoring system, which is represented in block diagram. Raspberry Pi 3 is used to maintain pulse rate sensor, blood pressure sensor, and heart sound sensor. Figure 1 shows the block diagram for the same, and Table 1 shows the list of future and available sensors and their applications for detecting patient behavioral analysis.

1.1. Literature Review. Internet of Things has a major contribution in the healthcare sector and improves the lives of various people throughout the world. From the literature review, it has been cleared that using IoT in the healthcare institution can enhance the quality of the medical facilities as well as enhance the efficiency of healthcare management [1]. This article is focusing on the challenges and difficulties faced by people in treatment as well as how a smart healthcare system allows doctors to track the disease and provide digital medicine to their patients [2]. Cloud computing, artificial intelligence, big data, and soft computing are the advanced technologies of the IoT that are used for monitoring patients' health and blood pressure as well as body temperature. Electrocardiograms, monitoring, glucose level sensing, and emergency healthcare as well as wheelchair management are connected through these devices. This facilitates the doctor to check the patient's status from any corner of the world. The article will highlight the automated wheelchair, warfarin, wearables, wireless transmission, and receivers [3].

1.2. Importance of Smart Healthcare System. Healthcare system consists of multiple participants including hospitals, patients, doctors, and research organizations. The cornerstone of smart healthcare consists of various information technologies that include IoT, cloud computing, mobile Internet, 5G, artificial intelligence, and big data together with biotechnology [4]. Smart healthcare uses these technologies for the healthcare system. Wearable gadgets are used by patients with wearable gadgets to keep track of their health every time, provide medical care by virtual helpers, and use remote places to implement remote services; a variety of sophisticated clinical decisions are employed by doctors to support systems to improve diagnosis. According to Baker et al., integrated information platforms are handled by doctor's form that incorporates tools like picture archiving, communication systems and information management system of laboratory, and the electronic medical record [5]. Surgical robots and mixed reality technology can help with more precise surgery.

People materials, as well as the supply chain of the hospitals, are maintained through radiofrequency identification (RFID), with integrated management platforms, collecting data and assisting decision-making. Mobile medical platforms are widely used for improving mobile medical platforms [6]. At the scientific research institutes, instead of manual drug screening, machine learning is widely used as well as big data may be used to discover suitable participants. The cost and risk of medical procedures can be effectively reduced with the help of smart healthcare. The utilization efficiency of medical resources as well as self-service medical care as well as promotion of regional exchange and cooperation provides personalized medical services by implementing IoT in the smart healthcare system [7].

1.3. The Architecture of the Smart Healthcare System. The smart healthcare institute that has been developed in this article is capable of making decisions according to the observed conditions of the patient's pulse rate and heartbeat

Table 2: Healthcare case studies with the description.

Parameter	Company	Description
Remote patient monitoring	Vivity	Monitor and management of remote heart failure
	CardioMEMS	The implantable device is used for monitoring the remote heart failure monitoring as well as management
	AliveCor	Arrhythmia diagnosis and monitoring through ECG
	Dexcom	Glucose monitoring continuously, linked to a smartphone app and social media network
Behavior modification	Omada	Preventing from diabetes by providing weight loss coaching
Telehealth	Doctor on demand	The meeting is conducted between patients and doctor through virtual mode

as well as body temperature. The given architecture is also an energy-efficient solution as it does not turn on the senior management every time. The sensors and the cost and lifetime of the system are handled through the used algorithm in the architecture. The issues faced by the remote monitoring of the patients help in providing them a necessary treatment through expert doctors in the hospital. Communication channels and embedded internal as well as external sensors consist in the monitoring of the smart healthcare monitoring system as well as patient management system. Different levels of refinement are used for performing these activities including the management layer, device layer, and network layer. The working performance of telemedicine in rural areas gets improved through telemedicine. IoT has helped in implementing the device in a rural clinic. All data of the patients are taken by the device then sent to the doctor concerned in the hospital. These data get analyzed by the doctors and suggest some necessary steps for the patient best treatment.

1.4. Diagnosis and Treatment Based on Artificial Intelligence. Various healthcare institutions are overcome by the challenges of AI implementation. Rule-based system includes NHS11 and lacks the accuracy of more algorithm; machine learning-based systems are embedded in the EHR system that is used. Maintenance of these clinical decision support systems is quite challenging due to the evolvement of medical knowledge. The knowledge generated through metabolic and other genomic proteomic approaches is difficult to cope by the support system. Compared to clinical practice, they are more used in research labs as well as by tech companies. These clinical decision support systems are difficult to maintain as medical knowledge evolves, and they are unable to cope with the sources of data and knowledge generated by metabolic and other genomic proteomic approaches to care. It is more prevalent in research labs and tech companies than in clinical practice to analyze the behavior of patients [8].

1.5. Patient Engagement and Adherence Applications. Adherence and involvement of the patient are considered a last mile challenge for the healthcare industry. It acts as a challenge between the good health results. The participation of the patients increased through the better outcome. Better outcomes will also lead to good utilization as well as provide better member experience and financial results. These issues can be addressed through big data and AI. Hospitals and providers used clinical experience for establishing a care plan for the patients that helps in knowing the improvement of acute or chronic patients [9, 10]. That does not matter if the patient does not make the necessary behavioral changes, such as arranging a follow-up visit, losing weight, filling medicines, or adhering to a treatment plan. When a patient fails to follow a treatment plan or take prescription medications as directed, this is a big issue.

1.6. IoT-Enabled Healthcare. Highly creative linked health technolines are driven by the positioning of the healthcare business that includes services of IoT and IoT apps, as well as solutions. Improvisation of healthcare services is the main objective of digital health by reducing the cost [11]. In smart healthcare, all remote patients are allowed to get diagnosis and treatment by using wearable devices. The patient's status is analyzed with the help of devices that are embedded with the sensor. Wearable devices collect the heart rate and blood glucose as well as oxygen saturation and transfer them to the caregiver through the smartphone of the patients [12]. Telehealth allows doctors to consult with patients without having to travel to a clinic or hospital. Behavior modification is a technique that can assist patients in changing poor behaviors and adopting healthier lifestyles to better control their health. Table 2 below describes a few healthcare case studies.

2. Materials and Methods

The materials and method used in the article for analyzing the behaviour of patients with smart healthcare are based on the advancement of the technology. A comprehensive survey has been done on IoT-enabled healthcare. IoT-enabled healthcare involves IoT healthcare network (IoThNet) that is the most important element in the smart healthcare system [13]. IoThNet consist of IoThNet platform, IoThNet architecture, and IoThNet topology. In various services and applications, IoT-enabled healthcare gets divided, and each service gets one potential vertical. More than 300 clinical leaders and healthcare staffs were present. More than 70% of the respondents claimed that less than half of their

patients were highly involved, and 42% stated that less than a quarter of their patients were extremely in an IoT network; a health management system can observe a patient's basic symptoms such as oxygen saturation percentage, heart rate, and body temperature [14].

SpO_2, heartbeat, eye blink, and temperature sensors were provided as capturing elements, while an Arduino UNO was used as a processing device. The system was sent; there are no defined performances for patients. In an IoT ecosystem, a healthcare monitoring kit, heartbeat, body temperature, ECG, and respiration were among the basic characteristics determined by the designed system. Temperature sensor, blood pressure sensor, ECG sensor, pulse sensor, and Raspberry Pi are the hardware components used here [15]. The data was gathered from the sensors and transferred to a Raspberry Pi to process before being delivered back to the IoT network.

The system's main flaw is that no data visualization interfaces have been created. In the survey, as a noninvasive method, a pulse rate detection system was used. A system was proposed that utilized the plethysmography method and digitally presented the results, making it a real-time monitoring gadget. In comparison to other intrusive treatments, the procedure has proven to be safe for the patient. The finger blood flow can be tracked through mobile light and cameras for calculating the blood flow-based cardiac output [16]. Integrated gadgets are developed through the developed system that was sent to the computer through the person's pulse. It allows users to check the heart rate by just looking in the phone not thoroughly by the person's hand. This is an awesome way; however, it requires constant heart monitoring that completely works with the cardiovascular disease sensing system for the smartphone and has the goal of discovering the tool that is created through the given time and phones [17].

The prototype produced only captured coronary rhythm, but not heart rate, and failed to detect any cardiovascular disease. Arduino-based health parameter surveillance framework managed through a mobile device Arduino Uno gets delivery of the captured analog sensor data board. The captured values of analog get transformed into digital information through inbuilt analog to digital converter. The physical properties were exchanged with the designed device through Bluetooth [18]. The Bluetooth gadget had an area that did not cover a large area. An IoT safety monitoring device that adapts the framework's setup is divided into three layers: the control layer, the transport layer, and the device layer. In the control section, a pulse sensor was employed to detect a pulse and DS18B20 sensor was utilized to measure. The data from the Arduino into the cloud gets loaded with the help of Wi-Fi module and Ethernet shield on the transport layer. However, because an Arduino Uno was utilized, several sensors were unable to be appropriately processed [19]. To track smart houses and heartbeats, a wireless sensor network (WSN) was created. There is a parallel data processing; Spartan3 is used with FPGA architecture. On the LCD, results of the MCU are shown and through the microcontroller, the sensors get linked.

3. Major Hardware Components

Various hardware has been used in the smart healthcare system. Body temperature sensor, ESP32 processor, room-temperature sensor, heartbeat sensor, CO sensor, and CO_2 sensor have been used for developing the smart care system for healthcare. The I2C/UART and SPI/SDIO interfaces on the EPS32 allow it to have communication with other Wi-Fi and Bluetooth devices. The sensitivity of the sensor can be adjusted using the potentiometer. The detection and quantification of NH_3, smoke, nicotine, benzene, and CO_2 are done through the MQ-135 gas sensors used in the air quality control. The MQ-135 sensor module has a digital pin that allows it to work without the use of a microcontroller, which is useful for detecting specific gases. The analog pins are used to determine the gases in PPM.

The plethysmography principle was used to design the heartbeat sensor. The changing in the blood volume can be easily detected by it in any organ that is responsible for the intensity of light to travel through that organ. The pulse timings are even more important in systems that track the heart rate [20] .When light is devoured by the blood, the rate of heartbeat affects the blood volume distribution, and the signal pulses are equivalent to the heartbeat pulses. ESP32 is used as an IoT tool that offers a Linux system at a cheap price. GPIO pins are used by ESP32 for connecting actuators to the device sensors [21]. Acquisition of IoT with ESP32 brings new creativity to the healthcare system. With integrated antenna switches, control amplification, RF balloon, low-noise amplifier, and filters, as well as power management modules, the ESP32 is particularly well designed. It can work as a slave to a host MCU or a stand-alone scheme, reducing the amount of time spent interacting with the main application processor [22]. Compared to Kelvin's linear temperature sensors, LM35 has more advantages in that realistic centigrade scaling prevents the consumer from deleting the great constant voltage from the display. MQ-9 is suitable for detecting LPG, CO, and CH4 [23]. Measurements can be taken quickly because of their high sensitivity and quick reaction time [24]. Researchers are also providing security protocols for exchanging information among clients and servers and to maintain the confidentiality of the shared information as in Figure 2 [25].

4. Discussion and Results

A smart healthcare system allows doctors to analyze the patient's behaviour that helps in providing a proper diagnosis to them [26]. Monitoring of the smart health management system allows patients to check their health status according to their comfort at any place [27]. Smart healthcare systems allow by providing this status on a digital platform that can be visible from any corner of the world. The real-time value of the health system is allowed by the smart healthcare system as well as it shows how it can be implemented in the real-life world [28]. The disease of the patients can be easily identified with the smart healthcare system, and diagnosis can be easily made by observing the various symptoms. The smart healthcare system allows the doctors

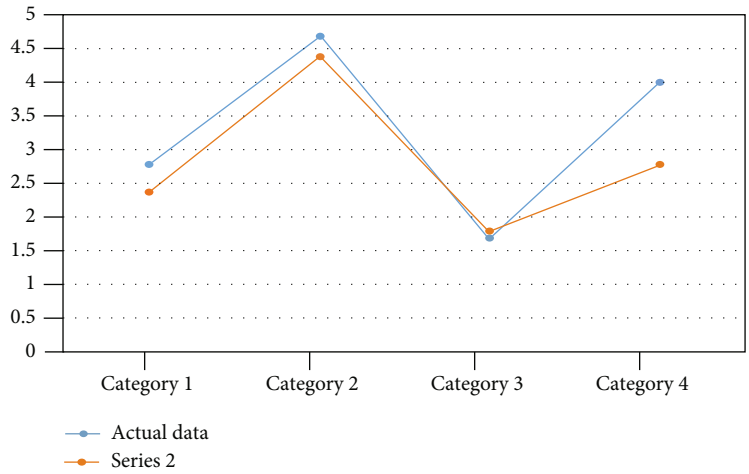

Figure 2: Deviation of data in room humidity.

Table 3: Smart healthcare monitoring system using IoT.

Subjects	Actual data (bpm)	Observed data (bpm)	Error (%)
S1	65	67	1.47
S2	69	72	4.25
S3	75	76	4.03
S4	74	74	2.63
S5	72	71	1.32
S6	79	80	3.70

Table 4: Using of the analog machine (actual) for collecting data for body temperature.

Subjects	Actual data (F degree)	Observed data (F)	Error (%)
S1	96.3	98.7	0.50
S2	97.4	98.7	0.70
S3	98.2	97.6	0.50
S4	96.7	97.1	0.61
S5	97.4	97.0	0.40
S6	98.1	97.5	0.79

to use the log of the patient's body conditions for analyzing the medicine effect on other things.

The devised methodology was put to the test with a variety of participants of varying ages in a variety of situations. The real value and observed value have been manually determined from the built system in the test scenarios for a body temperature, heartbeat, and room temperature sensors [29]. Room temperature sensor is only used for measuring the humidity; in this case, the error rate based on the data has been calculated to demonstrate the system's effectiveness. The data of MQ-9 and MQ-135 on the web server has been observed because there are no other means to measure the harmful gas level [30]. In Tables 3, 4, and 5 given below, the body temperature and room temperature, as well as the error rate for heartbeat, have been provided [31].

Table 5: Collection of room humidity through the actuarial machine and the observed system.

Experiments	Actual data (%)	Observed data (%)	Error (%)
1	64	62	3.05
2	67	68	1.45
3	62	61	1.56
4	69	70	2.80
5	65	63	3.01
6	60	59	1.59

In Figure 3, the deviation of the data has been obtained through the developed system. A clear deviation can be shown between actual and observed data showing the heart rate data that has been collected from various patients of different ages in healthcare. The movement that is caused by the patients during the treatment was responsible for causing the deviation. There is a chance of error due to motion artifacts that create deviation. This can lead to inaccurate data. Light scattering from other sources is also responsible for causing deviation. The mispositioning of the system is responsible for the deviation of the body temperature. PPM units are used for measuring the toxic gases including CO and CO_2 levels. The room condition as well as the specific patient can be monitored by the medical staff. The data can be accessed through the password only, which protects the data of the patients. The system can be monitored only by the authorized staff. From the remote location, the doctor can easily monitor the status of the patient. The level has been specified for the threshold for these measurements. The medical staff is allowed to take necessary steps for healthcare in the case when the data crosses its level [32]. In Figure 4, the developed system for the room humidity measurement, body temperature, heart rate, and error rate has been found, which has been shown in Figure 5 and Figures 6(a)–6(c). In the cases, the highest rate of error has been found about 4.28%, 3.07%, and 0.81%. An error rate of more than 5% is not acceptable in all cases.

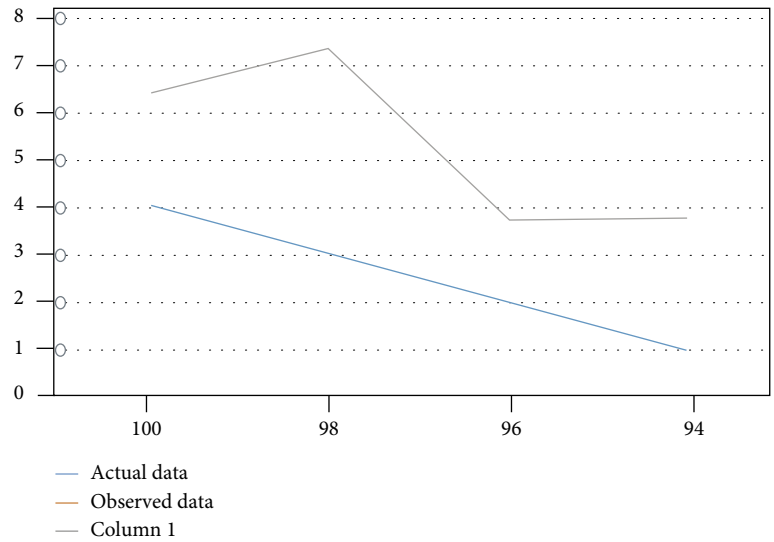

Figure 3: Data collected for measuring the body temperature of patients.

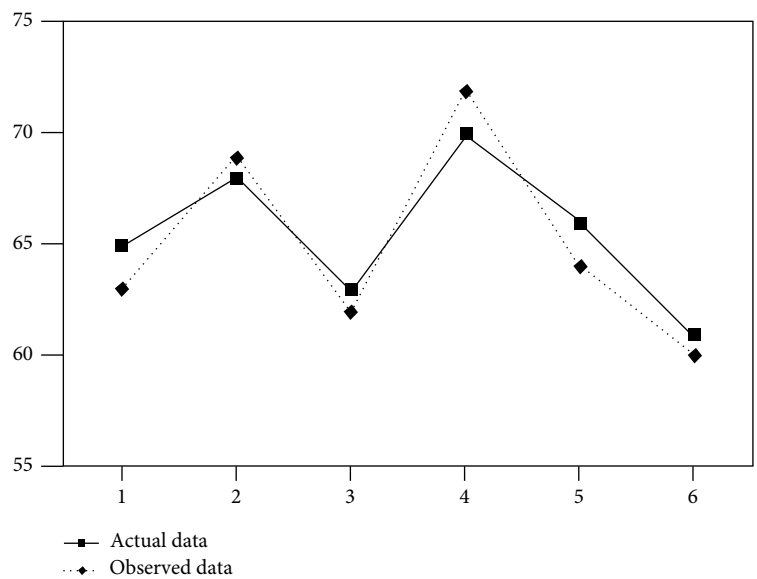

Figure 4: Data collected for room humidity.

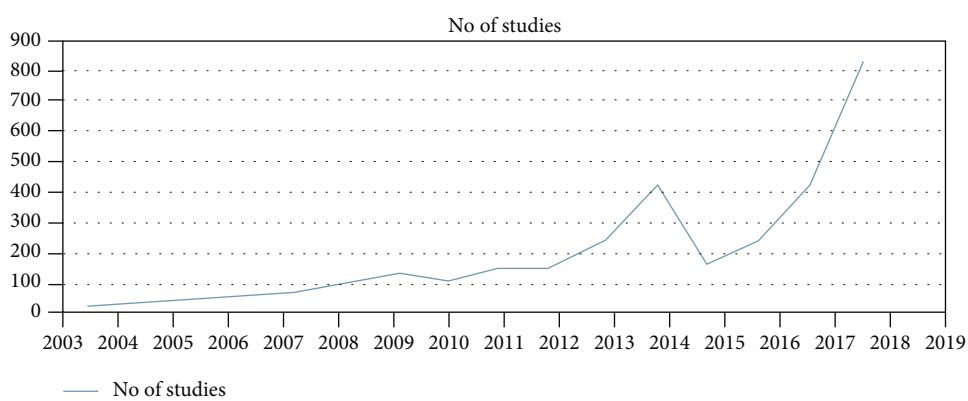

Figure 5: No. of studies regarding smart healthcare.

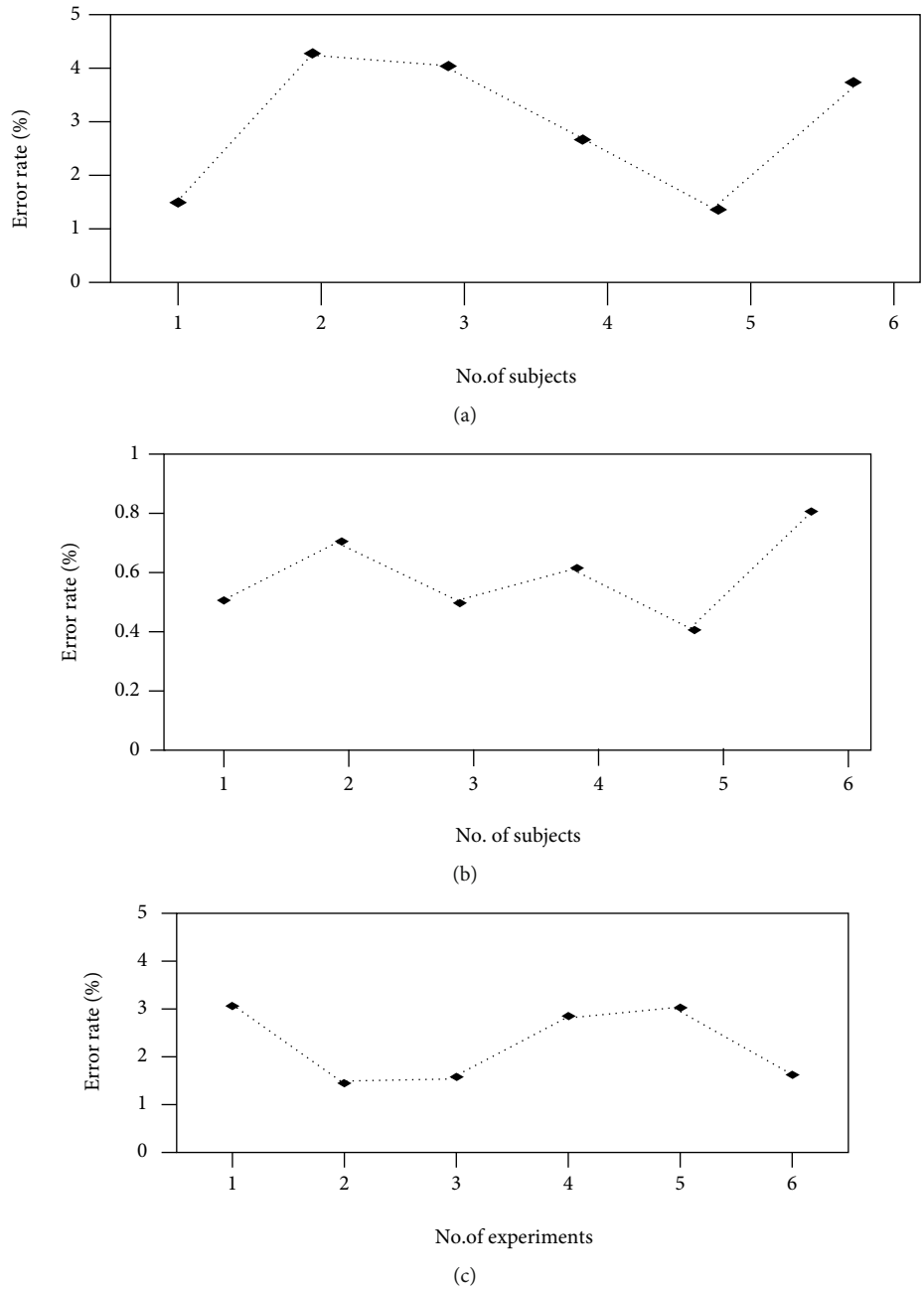

Figure 6: (a–c) Error rate for a developed system for (a) heart rate, (b) body temperature, and (c) room humidity.

5. Conclusion

Based on this study, it is concluded that the use of Internet of Things can play a crucial role in maintaining the development of smart healthcare. The use of analog machine in maintaining body temperature is evaluated properly in this study. Actuarial machine is also used to maintain body temperature of patients, which is concluded in this study. Flexibility of healthcare system is improved with the help of Internet of Things. To provide proper diagnosis towards patients, it is important to implement Internet of Things. Based on this study, it is noticed that proper architecture is present in maintaining growth and development of smart healthcare system. It has been concluded that smart healthcare has key contribution in analyzing the patient's behavior. Better health self-management can be enjoyed by the patients by smart healthcare. As compared to the traditional healthcare, smart healthcare system can reduce personnel pressure, relieve costs, and improve the patient's medical experience. The status of medical resources can be enhanced with the help of smart healthcare. Implementation of IoT in the development of smart healthcare allows the healthcare staff to easily detect the types of diseases as well as the diagnosis can be done properly in smart healthcare systems as compared to traditional medical facilities. Results shows that the developed system monitors the room humidity measurement, body temperature, and heart rate; also, error rate has been found. The highest rate of error has been found about

4.28%, 3.07%, and 0.81%, respectively. An error rate of more than 5% is not acceptable in all cases. With several advantages, some problems in the smart healthcare system still exist that can be overcome with the development of the technologies as well as with joint effort of the doctors, healthcare staff, and patients as well as medical institutes.

Data Availability

The data captured to support the findings of this study are available from the corresponding author upon request.

Conflicts of Interest

The authors declare that there is no conflict of interest regarding the publication of this paper.

References

[1] P. Sundaravadivel, E. Kougianos, S. P. Mohanty, and M. K. Ganapathiraju, "Everything you wanted to know about smart health care: evaluating the different technologies and components of the internet of things for better health," *IEEE Consumer Electronics Magazine*, vol. 7, no. 1, pp. 18–28, 2018.

[2] D. He, R. Ye, S. Chan, M. Guizani, and Y. Xu, "Privacy in the internet of things for smart healthcare," *IEEE Communications Magazine*, vol. 56, no. 4, pp. 38–44, 2018.

[3] C. Moore, "Medical internet of things-based healthcare systems: wearable sensor-based devices, patient-generated big data, and real-time clinical monitoring," *American Journal of Medical Research*, vol. 7, no. 1, pp. 41–47, 2020.

[4] L. Chen, V. Jagota, and A. Kumar, "Research on optimization of scientific research performance management based on BP neural network," *International Journal of System Assurance Engineering and Management*, vol. 12, 2021.

[5] S. B. Baker, W. Xiang, and I. Atkinson, "Internet of things for smart healthcare: technologies, challenges, and opportunities," *IEEE Access*, vol. 5, pp. 26521–26544, 2017.

[6] D. Pal, S. Funilkul, N. Charoenkitkarn, and P. Kanthamanon, "Internet-of-things and smart homes for elderly healthcare: an End User perspective," *IEEE Access*, vol. 6, pp. 10483–10496, 2018.

[7] R. Dantu, I. Dissanayake, and S. Nerur, *Exploratory analysis of Internet of Things (IoT) in healthcare: a topic modeling approach*, AIS eLibrary, 2019.

[8] R. Bharti, A. Khamparia, M. Shabaz, G. Dhiman, S. Pande, and P. Singh, "Prediction of heart disease using a combination of machine learning and deep learning," *Computational Intelligence and Neuroscience*, vol. 2021, Article ID 8387680, 11 pages, 2021.

[9] S. Zeadally and O. Bello, *Harnessing the power of the Internet of Things-based connectivity to improve healthcare*, Internet of Things, 2019.

[10] G. Strobel and J. Perl, "Farming in the era of Internet of Things: An information system architecture for Smart Farming," *Health*, vol. 6, pp. 208–223, 2020.

[11] V. Jagadeeswari, V. Subramaniyaswamy, R. Logesh, and V. Vijayakumar, "A study on medical Internet of Things and Big Data in personalized healthcare system," *Health Information Science and Systems*, vol. 6, no. 1, pp. 1–20, 2018.

[12] A. I. Newaz, A. K. Sikder, M. A. Rahman, and A. S. Uluagac, "HealthGuard: a machine learning-based security framework for smart healthcare systems," in *2019 Sixth International Conference on Social Networks Analysis, Management and Security (SNAMS)*, pp. 389–396, Granada, Spain, 2019.

[13] S. Ahmed, M. Ilyas, and M. Y. A. Raja, "Internet of Things: application in smart healthcare," in *Proceedings of the 9th International Conference on Society and Information Technology (IICSIT 2018)*, pp. 19–24, Orlando, Florida, 2018.

[14] S. Banka, I. Madan, and S. S. Saranya, "Smart healthcare monitoring using IoT," *International Journal of Applied Engineering Research*, vol. 13, no. 15, pp. 11984–11989, 2018.

[15] P. Ratta, A. Kaur, S. Sharma, M. Shabaz, and G. Dhiman, "Application of blockchain and Internet of Things in healthcare and medical sector: applications, challenges, and future perspectives," *Journal of Food Quality*, vol. 2021, Article ID 7608296, 20 pages, 2021.

[16] J. Qi, P. Yang, A. Waraich, Z. Deng, Y. Zhao, and Y. Yang, "Examining sensor-based physical activity recognition and monitoring for healthcare using Internet of Things: a systematic review," *Journal of Biomedical Informatics*, vol. 87, pp. 138–153, 2018.

[17] M. Z. Uddin, "A wearable sensor-based activity prediction system to facilitate edge computing in smart healthcare system," *Journal of Parallel and Distributed Computing*, vol. 123, pp. 46–53, 2019.

[18] Z. Alansari, S. Soomro, M. R. Belgaum, and S. Shamshirband, "The rise of Internet of Things (IoT) in big healthcare data: review and open research issues," in *Progress in Advanced Computing and Intelligent Engineering*, Advances in Intelligent Systems and Computing, pp. 675–685, Springer Singapore, 2018.

[19] K. J. Chung, J. Kim, T. K. Whangbo, and K. H. Kim, "The prospect of a new smart healthcare system: a wearable device-based complex structure of position detecting and location recognition system," *International Neurourology Journal*, vol. 23, no. 3, pp. 180–184, 2019.

[20] I. Jayatilleka and M. N. Halgamuge, "Internet of things in healthcare: smart devices, sensors, and systems related to diseases and health conditions," in *Real-Time Data Analytics for Large Scale Sensor Data*, Academic Press, 2020.

[21] S. A. Butt, J. L. Diaz-Martinez, T. Jamal, A. Ali, E. De-La-Hoz-Franco, and M. Shoaib, "IoT smart health security threats," in *2019 19th International Conference on Computational Science and Its Applications (ICCSA)*, pp. 26–31, St. Petersburg, Russia, 2019, July.

[22] J. Qi, P. Yang, G. Min, O. Amft, F. Dong, and L. Xu, "Advanced internet of things for personalised healthcare systems: A survey," *Pervasive and Mobile Computing*, vol. 41, pp. 132–149, 2017.

[23] S. U. Amin, M. S. Hossain, G. Muhammad, M. Alhussein, and M. A. Rahman, "Cognitive smart healthcare for pathology detection and monitoring," *IEEE Access*, vol. 7, pp. 10745–10753, 2019.

[24] R. Dantu, I. Dissanayake, and S. Nerur, "Exploratory analysis of internet of things (IoT) in healthcare: a topic Modelling & co-citation approaches," *Information Systems Management*, vol. 38, no. 1, pp. 62–78, 2021.

[25] M. Soni and D. K. Singh, "LAKA: lightweight authentication and key agreement protocol for Internet of Things based wireless body area network," in *Wireless Personal Communication*, Springer, 2021.

[26] M. Soni and D. K. Singh, "Blockchain implementation for privacy preserving and securing the healthcare data," in *2021 10th IEEE International Conference on Communication Systems and Network Technologies (CSNT)*, pp. 729–734, Bhopal, India, 2021.

[27] N. Gavrilović and A. Mishra, "software architecture of the internet of things (IoT) for smart city, healthcare and agriculture: analysis and improvement directions," *Journal of Ambient Intelligence and Humanized Computing*, vol. 12, no. 1, pp. 1315–1336, 2021.

[28] F. Ajaz, M. Naseem, S. Sharma, M. Shabaz, and G. Dhiman, "COVID-19: challenges and its technological solutions using IoT," Current Medical Imaging: Current Medical Imaging Reviews, 2021.

[29] D. A. M. Budida and R. S. Mangrulkar, "Design and implementation of smart healthcare system using IoT," in *2017 International Conference on Innovations in Information, Embedded and Communication Systems (ICIIECS)*, pp. 1–7, Coimbatore, India, 2017, March.

[30] A. Ahad, M. Tahir, and K. L. A. Yau, "5G-based smart healthcare network: architecture, taxonomy, challenges and future research directions," *IEEE Access*, vol. 7, pp. 100747–100762, 2019.

[31] J. Wang, C. Xia, A. Sharma, G. S. Gaba, and M. Shabaz, "Chest CT findings and differential diagnosis of Mycoplasma pneumoniae pneumonia and mycoplasma pneumoniae combined with streptococcal pneumonia in children," *Journal of Healthcare Engineering*, vol. 2021, Article ID 8085530, 10 pages, 2021.

[32] K. Zhan, "Sports and health big data system based on 5G network and Internet of Things system," *Microprocessors and Microsystems*, vol. 80, article 103363, 2020.